STUDY OF MECHANISM OF GENETIC DEATH IN *ESCHERICHIA COLI* IN RESPONSE TO A) dTTP STARVATION AND B) COMBINATION OF TEMPERATURE SENSITIVE DEFECTS IN REPLICATION INITIATION AND DOUBLE STRAND BREAK REPAIR

BY

PRITHA RAO

DISSERTATION

Submitted in partial fulfillment of the requirements
for the degree of Doctor of Philosophy in Microbiology
in the Graduate College of the
University of Illinois Urbana-Champaign, 2021

Urbana, Illinois

Doctoral Committee:

Professor Andrei Kuzminov, Chair
Professor Steven R. Blanke
Professor James A. Imlay
Professor Rachel J. Whitaker

ABSTRACT

At the cellular level life can be described as replication of metabolism. Cells first grow by continuous synthesis of RNA, protein and lipids. Once they reach a certain dimension, they duplicate their genomes, which is followed by division of the mother cell into two daughter cells, capable of repeating this growth – duplication – division cycle again. Because of its dual nature, this cycle can be stopped by either inhibiting the period of continuous cellular growth (i.e. preventing the synthesis of RNA, proteins, lipids), which can be classified as metabolic death of the cell, or by blocking the process of DNA replication and segregation (without affecting protein/RNA/lipid metabolism) – which we classify as genetic death of the cell. Irreparable DNA lesions therefore inflict genetic death on the cells, and we are interested in identifying such DNA lesions or conditions that lead to them, providing future effective strategies to get rid of cancerous or infecting cells.

In this thesis, I present our investigation of two distinct examples of genetic death in *E. coli*. The main story is about death in response to dTTP starvation known as Thymineless Death (TLD). This phenomenon has been subject to decades of investigation since its discovery in 1954, and I present our recent efforts to further understand the consequences of dTTP starvation in prokaryotic cells. The other example of genetic death that I studied is the synthetic lethality of the combination of two partial defects in *E. coli* – *dnaA* in replication initiation and *recBC*, in double-strand-break repair. This lethality was discovered by Sharik Kahn, a Post-Doctoral researcher in this lab, and I continued to investigate this mysterious synthetic lethal combination.

The first chapter presents a review of the phenomenon of TLD, history of its investigation and a summary of recent progress in elucidation of its complicated mechanism. The second chapter presents my work on TLD which clarifies the role of non-canonical nucleotide incorporation-excision cycles on DNA stability and viability of *E. coli* cells. Additionally, we explore some possible sources of endogenous dT *E. coli* cells utilize in the later stages of dTTP starvation. We also report detection and accumulation of persistent single strand gaps that happens concurrently with viability loss due to dTTP starvation.

In the third chapter, I report novel mutants that experience hyper-TLD and cell lysis when *E. coli* cannot utilize an overlooked internal source of dTTP. We show that *E. coli* relies on this internal reserve of dT to maintain its viability early during dTTP starvation. We also confirm the (discovered earlier) replication-independence of TLD and propose a possible mechanism of replication-independent chromosome fragmentation observed in hyper-TLD mutants. The fourth chapter is a compilation of TEM images of *E. coli* cells undergoing TLD. As a comparison, we have also imaged *E. coli* cells treated with nalidixic acid, which kills the cells by chromosome damage unrelated to TLD.

The fifth chapter presents my investigation on the synthetic lethal combination *dnaA recBC* and another known colethal combination *dnaN recBC*. We find that *dnaA* mutants require DNA degradation activity of RecBCD for viability, while *dnaN* relies more on recombinational repair for its viability. We show that replication is stalled in the *dnaA recBC* mutant, while it is inhibited but continues in the *dnaN recBC* mutant. We are yet to identify the DNA lesion responsible for fork stalling in the *dnaA recBC* mutant.

In the final chapter, I summarize my overall findings and propose specific questions to pursue in the future, to further explore the phenomena of TLD and *dnaA recBC* colethality.

Dedicated to the past, present and future members of the Kuzminov lab

ACKNOWLEDGEMENTS

This milestone was achieved in large part due to the constant guidance and efforts of Dr. Andrei Kuzminov. I am very grateful to him for introducing me to the interesting research projects I have worked on during my stay in the lab. He has been very generous with his time to educate me through each step of my scientific training over the years, right from how to think about a problem to, designing experiments and interpreting their outcomes, to presenting our findings and reporting the results in a concise scientific language. The dedication and honesty he brings to his duties have been a great source of inspiration for me to do better as a student.

I am grateful for the guidance of my committee members Dr. Blanke, Dr. Imlay and Dr. Whitaker for their active interest in my research progress and professional success. Dr. Imlay especially has often helped us with his scientific insights and steered our experiments into new and interesting directions. I am also thankful to Deb Lebaugh and Diane Tsevelekos in the Microbiology office for helping me with all the paperwork required and keeping track of my visa status, program requirements and for always welcoming me with a smile to their office.

I have spent some the best times with my lab mates – Lenna, Sharik, Glen, Tulip, Pooja and Sneha over the years in the lab, at the micro conferences, our yearly lab gatherings and every Friday afternoon for our lab meetings. They have been the best colleagues and have been supportive through all the little upheavals I have had during my stay in Urbana-Champaign. Coming to the lab and meeting my friends has always cheered me up on a bad day.

Lastly, I would like to thank my family members for all the emotional support they have given me over the years. I would like to thank my mother for keeping me updated with all the news in the extended family and showing by her example how one can live a richer life even with limited means. I would like to thank my older brother to leading me to think about the purpose of life and how to get back towards a goal even after many failures. I would like to thank my sister-in-law for becoming my best friend over the years and showing me what a responsible and confident woman looks like.

TABLE OF CONTENTS

CHAPTER 1: INTRODUCTION

1.1 Prokaryotic Nucleotide Metabolism

Nucleic acid polymers form the informational basis of life. Deoxyribose nucleic acid (DNA) is used to encode genome information in all cellular organisms; at the same time, many viruses are known to use ribonucleic acid (RNA) as their genome medium. DNA structure based on the deoxyribose sugar is more chemically stable and physically flexible (as a duplex) than the RNA structure based on the ribose sugar and hence has been used as a preferred conduit for carrying the hereditary information in the much larger genomes of cellular organisms. The instability of RNA, on the other hand, makes it a perfect medium for temporary copies of the genomic information in the form of mRNA, which can be translated into proteins by ribosomes.

1.1.1 Synthesis of NTPs

The information-transfer capacity of the nucleic acids is based on two complementary pairs of four bases. The three bases shared between DNA and RNA are Adenine (A), Cytosine (C) and Guanine (G). But one base out of the four is variable: Thymine (T) is exclusively used in DNA, while RNA uses Uracil (U) instead of T. These bases are associated with the ribose or deoxyribose sugars making them either ribonucleotide or deoxyribonucleotides. The synthesis of both purine (A, G) and pyrimidine (U, T, C) nucleotides converges at the metabolite PRPP, which is derived from ribose-5-phosphate, an intermediate generated in the pentose phosphate pathway (93). In the purine biosynthesis pathway, PRPP is converted into inosine monophosphate

(IMP), which is a precursor for both GTP and ATP (Fig. 1). The pyrimidine ring of U is derived from dihydro-orotate (obtained from condensation of aspartate and carbamoyl phosphate), which is then modified by PRPP and decarboxylated to give UMP, which is also a precursor for CMP (Fig. 1). Apart from the *de novo* synthesis of these nucleotides, salvage pathways also contribute to the nucleotide pools by recycling free bases, nucleosides or nucleic acid degradation intermediates into (d)NTPs (93).

1.1.2 Synthesis of dNTPs

DNA synthesis precursors, dNTPs, are derived from conversion of the ribonucleotide diphosphates (NDPs) into deoxyribonucleotide diphosphates by the enzyme ribonucleotide-diphosphate reductase (in *E. coli*, NrdAB or NrdEF during aerobic growth)(31) (Fig. 2). This generates dADP, dCDP, dGDP and dUDP. The dNDPs are then phosphorylated by nucleotide diphosphate kinase to dATP, dCTP, dGTP and dUTP (3). *E. coli* also has NrdD, which can reduce NTPs to dNTPs during anaerobic growth (34). Additional steps are required to produce dTTP – hydrolysis of dUTP to dUMP by Dut followed by methylation of dUMP to dTMP by ThyA, (thymidylate synthase) (Fig. 2)(127, 134). dTMP is then phosphorylated by kinases to make dTTP.

Because of the unique methylation step required for generating dTMP, *de novo* synthesis of dTTP can be blocked by inactivation of the *thyA* gene. The *thyA* mutants can be maintained in culture by adding T or thymidine (dT) in the growth medium, which the *thyA* mutants convert to dTTP for use in their DNA synthesis (2). After importing, T is covalently linked to deoxyribose 1-phosphate to become dT by thymidine phosphorylase (DeoA) (121). A recent metabolomic screen has identified another enzyme PpnP which

can attach the deoxy sugar to all nucleobases *in vitro* (126). dT is phosphorylated to dTTP by thymidine kinase (*tdk*)(118), thymidine monophosphate kinase (*tmk*)(28, 113) and nucleotide diphosphate kinase (*ndk*) (3) successively before used in DNA synthesis. In the absence of a steady source of (d)T, an actively growing *thyA* culture go into thymine/thymidine(T)-starvation and succumbs to Thymineless Death (TLD) (23). TLD was first described in *E. coli* in 1954; since then it was confirmed in bacteriophages, several gram-positive and gram-negative bacteria, eukaryotes like yeast, mouse and even in human cells (2). As the pathway for dUMP methylation to dTMP is conserved in all free-living organisms, TLD is predicted to be a universal phenomenon.

1.2 Phenomenon of Thymine Starvation

Our current understanding of the events in TLD come from decades of research in *E. coli* (2, 43, 58). During T-starvation, *E. coli* cells become bacteriostatic for a limited period, called the lag or the resistance phase, and then undergo a sudden rapid exponential death (RED) phase, losing viability by about 2-3 orders of magnitude (Fig. 3) (67). The cultures then enter the survival phase with very few viable cells left, perhaps mostly represented by persisters. It is universally agreed that TLD is caused by formation of irreparable DNA lesions, although the exact nature of these lesions is still unclear (2, 43, 58). Active DNA replication with dU in the absence of T, followed by DNA-uracil excision, repeated multiple times, is considered the primary source of the mysterious irreparable chromosomal lesions that cause TLD.

Important cellular functions that protect from or escalate TLD have been identified. The role of recombinational repair is extensively studied – the RecF pathway

for repair of persistent single strand gaps (SSG) contributes to T-starvation toxicity, while the RecBCD pathway for repairing double strand breaks (DSB) delays viability loss during T-starvation (36, 67, 90). For a while, *mazEF* toxin-antitoxin function was also implicated in TLD, but this could not be reproduced (120). More recent research suggests that *oriC* disappearance, SOS induction and oxidative damage also contribute to TLD (35, 50, 68, 119).Thus, there are several factors identified as important for TLD, but none of these ideas offered a mechanistic explanation of how T-starvation leads to DSBs, or SSG, or *oriC* disappearance. This chapter is an attempt to summarize our current understanding of TLD and propose some new avenues for future investigations.

1.3 Enzymatic Features of Thymidylate Synthase

The enzyme thymidylate synthase encoded by the *thyA* gene in *E. coli* catalyzes the essential conversion of dUMP to dTMP using 5,10-methylene tetrahydrofolate (5,10-CH_2-THF) as a cofactor, which supplies the methyl group and hydrogen to modify dUMP to dTMP (134). Apart from thymidylate, THF conjugated with carbons at different oxidation states is a C1 donor for the biosynthesis of purines, serine, methionine, N-formyl-methionyl-tRNA and pantothenic acid (123). After C1 transfer, THF gets converted to dihydrofolate (DHF) which is recharged back to TFH by Dihydrofolate reductase (DHFR) enzyme, a step required for continuation of DNA/RNA and protein synthesis (42). The ThyA-DHFR couple is found conserved in several prokaryotes and eukaryotes, including humans. Because of its important function in dTMP synthesis and essentiality of T for growing cells, DHFR and folate synthesis is a target of several antibacterial and antiprotozoan drugs like trimethoprim and proguanil that treat

bacterial/fungal infections in humans (19, 109). Drugs used in chemotherapeutic cocktails, like 5FU, FdUMP and tomudex, also inactivate the thymidylate synthase function to induce TLD in cancerous cells, making TLD a medically relevant phenomenon (74, 123).

However, about a third of sequenced bacteria do not carry DHFR; instead, these organisms use an alternative flavin-dependent thymidylate synthase called ThyX (89). This enzyme uses 5,10 CH_2-THF as a methyl donor only and NADPH as the hydride donor and generate THF as a byproduct. Crystal structure studies of ThyX from *T. maritima* suggest that the flavin group accepts the -CH_2 group from CH_2-THF and transfers it onto dUMP; the oxidized flavin is then reduced by NADPH (86). Several human pathogens, like *H. pylori*, *B. anthrasis* and *Ricketssia*, only have the flavin dependent ThyX enzyme, while *M. tuberculosis* has both ThyA and ThyX (89). Thus, inhibitors targeting ThyX are being actively developed as antibiotics, as they would induce TLD in these pathogenic bacteria without affecting the human host that only contains the ThyA-type enzyme (86).

1.4 Nutrient Starvation Response in Bacteria

E. coli routinely encounters nutrient starvation when outside its vertebrate host. Nutrient starvation under laboratory conditions induces the starvation response in *E. coli*. The well-studied starvation for carbon, nitrogen or phosphorous leads to the induction of the alternative sigma factor σ^{38} (RpoS) which is also functional during the stationary phase (growth saturation) (105). RpoS is degraded in exponentially growing cells by the ClpXP protease, but it is either induced or becomes more stable under various starvation

regimens (122). RpoS is also induced and stabilized by (p)ppGpp messenger molecule, which accumulates in starving cells (38, 48). (p)ppGpp accumulation has been linked to a rise in the population of persisters, that escape antibiotic killing and form a reservoir for recurring infections in hosts (44). Because of its key role in mediating starvation response, the function of RpoS is regulated at the level of its transcription, translation, activity and protein stability (105). Apart from starvation, RpoS promotes the expression of several genes that increase survival of other insults, like hydrogen peroxide, high temperatures, salt stress and low pH, etc. (46, 82). RpoS expression changes *E. coli* cell shape from longitudinal to more spherical and smaller, increases osmoprotectants in the periplasm and redirects metabolism to use accumulated storage compounds, like glycogen and polyphosphates (105). In other words, nutrient starvation or entry into stationary phase prepares *E. coli* cells to tolerate various stresses in a RpoS-dependent manner.

Amino acid starvation response is another well-studied phenomenon, triggered in *E. coli* by the presence of an uncharged tRNA in the ribosome A site. In response, the RelA protein in *E. coli* synthesizes (p)ppGpp which upregulates amino acid biosynthesis pathways (108). Absence of the required amino acid during the growth of an auxotroph shuts down the metabolic growth of the cell immediately (8). In the absence of protein synthesis, ongoing DNA synthesis continues, but no new rounds of DNA replication are initiated, as new protein synthesis is required for replication initiation (75). Amino acid deprivation again mimics entry into stationary phase. Pathogenic bacteria also encounter "nutritional immunity" — starvation for essential metal ions like Fe, Mn, Zn inside the host organism — which can slow down their growth and make them susceptible to host

immune system (24, 56). This immunity is countered by pathogens by upregulating expression of siderophores and high affinity metal importers (56).

Thus, once an essential nutrient is used up, *E. coli* stops growing with no loss in the ability to form colonies on nutrient-supplemented plates. In contrast to this standard response of *E. coli* to starvation for essential metabolites, during T-starvation Barner and Cohen saw a dramatic loss in titer (7, 23). To explain this unexpected death, they proposed the idea of an unbalanced growth (explained in a later section). T-starvation does not stop general metabolism, as evident from filamentation of the cells, but only impedes DNA replication (67, 140).This imbalance in biomolecular synthesis was postulated to be somehow lethal for the cell.

In bacteria like *Bacillus* and *Clostridia*, nutrient starvation can activate spore formation. Bacterial spores have been found to resist extreme temperatures, desiccation, DNA damaging agents and hydrolytic enzymes (125). Apart from forming spores to survive during nutrient limitation, *Bacillus* is known to become competent and accept foreign DNA, secrete antibiotics to kill its neighbors to alleviate competition for resources, increase scavenging for extracellular proteins and polysaccharides, induce flagellar motility to search for nutrient-rich environment or create biofilms (49, 129, 136). Yet, with all these tricks to deal with starvation, *Bacillus* still succumbs to TLD (2).

Indeed, in the light of the various ways in which bacteria can respond to starvation, by either inducing the stress response, virulence factors of by forming spores, it is a puzzle why T-starvation should be lethal. Still T-starvation is not unique in this respect, as two more conditions of nutrient starvation leading to death have been identified in *E. coli*. One of them is starvation for diaminopimelic acid (DAP), which is a

constituent of the peptidoglycan (PG) layer. PG is made up of alternating N-acetyl muramic acid (MurNAc) and N acetyl glucosamine (GlcNAc) molecules. MurNAc is linked to a pentapeptide chain composed of L-alanine, D-glutamate, meso-diaminopimelic acid (m-A_2pm) and didpeptide D-alanyl-alanine (137). At the inner membrane the GlcNAc is joined to MurNAc pentapeptide to form the monomer constituent of PG - disaccharide pentapeptide, which is translocated to the periplasmic space. Transpeptidase catalyzes the 4-3 linking of a D-alanine in the fourth position of one monomer to m-A_2pm in the third position of a separate monomer or the 3-3 joining of two m-A_2pm from separate monomers to create the PG mesh around the inner membrane (137). Starvation for DAP in growing culture can thus compromise the mesh-like structure of the PG layer. When DAP auxotrophs of *E. coli* are deprived of DAP in its growth medium, cells form spheroplasts and eventually lyse (11). DAP is found in the PG layer of almost all gram-negative and some gram-positive bacteria and has been a target for antibiotic development to prevent bacterial growth (71, 107).

The other (potentially) lethal nutrient starvation is the recently discovered dGTP starvation in *E. coli* (see a separate section later).

1.5 TLD as the Chromosomal Damage Phenomenon

1.5.1 Role of DNA repair enzymes in TLD

Since dTTP is a DNA precursor and, besides chromosomal DNA synthesis, was not considered to be involved in any other major cellular process, irreparable chromosome damage was always assumed to be the primary cause of TLD. To identify the nature of irreparable chromosomal lesions, various DNA repair pathways have been

removed to identify their role in TLD. Of importance are the two recombinational repair pathways in *E. coli*:double-strand break (DSB) repair by the RecBCD pathway and persistent single-strand gap (SSG) repair by the RecFOR pathway (Fig. 4) (69).

Double-strand ends are recognized by the heterotrimeric RecBCD complex, in which RecB is the nuclease as well as a 3' to 5' helicase (15, 106, 139), RecD is a 5' to 3' helicase, and RecC recognizes the χ sequence on the DNA, the signal that modifies the nuclease activity of RecB (128). When RecBCD enzyme binds to a double strand DNA end, it degrades both DNA strands until a properly oriented χ site, which prevents further degradation of the 3'-ending strand, while degradation continues of the 5'-ending strand (4). This generates the 3' overhang, which is the substrate for RecA polymerization, required for the subsequent strand invasion into an intact sister duplex (5, 22). Repair of single-strand gaps begins with the RecFR complex sensing the gap, which attracts the RecO protein. The RecOR protein then displaces SSB, allowing RecA to polymerize on the ss-gap for subsequent strand invasion into an intact sister duplex (135). After homologous strand invasion, the invading 3' end is extended by the Dna pol I using the intact complementary strand as the template and ligated with the cognate 5' end, also annealed with the same template strand. This generates two Holliday Junctions, the points at which the two complementary-aligned DNA duplexes exchange strands. These junctions are removed by the RuvABC resolvase or the RecG DNA pump (69).

An early intriguing finding was the ~10-fold better survival of a *recF thyA* mutant subjected to T-starvation compared to the *thyA* mutant, suggesting that repair of persistent SSG contributes to TLD pathology (90). Later on, Nakayama *et. al* reported single strand gaps in the chromosomal DNA by electron microscopy studies, although no

quantification was provided (91). In contrast, the RecBCD pathway is essential for the resistance phase and also prevents deeper exponential death (36, 67, 90). Sub-chromosomal fragments were indeed found to accumulate during TLD, and to accumulate more in *recBCD* mutants, supporting the role of RecBCD in fixing double-strand DNA breaks for avoiding a steeper TLD (67). Inactivation of RecA, which is required for both RecFOR- and RecBCD-initiated repair pathways, leads to a hybrid TLD curve, with no resistance phase, but ~10-fold better survival during the exponential death phase (35, 67). It seems like RecA assists in the DSB repair pathway early on, but later, during the RED phase, switches to promoting RecF-mediated toxicity. Epistatic analysis shows that the 10-fold better viability in the *recF thyA* double mutant compared to the *recA thyA* double mutant is due to protective RecA function, as this difference disappears in the *recF recA thyA* triple mutant, which overlaps with the *recA thyA* curve (67).

Inactivation of the late steps of recombinational repair — RecA filament dispersal and Holliday junction (HJ) resolution — also affects TLD kinetics (67). Loss of *ruv* results in shorter resistance phase and deeper RED phase in *thyA* mutants, suggesting that Ruv HJ-resolution activity is important throughout T-starvation (36, 67). The *ruv* mutants still retain some HJ resolution activities, as further inactivation of *recG* function has an additive effect on TLD kinetics (67). The *recG thyA* mutant is more sensitive early on in T-starvation, but eventually survives better than *thyA*, suggesting that RecG like RecA promotes the RecF toxicity (67).

The SOS response induces expression of some 40 genes in bacteria in response to a diminished DNA synthesis rates on damaged DNA templates (33). T-starvation leads to a strong SOS activation in *E. coli* (67, 119). The *lexA*(IND) *thyA* mutant, defective in

mounting the SOS response, phenocopies the *recA thyA* mutant (35, 67). It was found that inactivation of *sulA*, one of the genes overexpressed during the SOS response, mimics an SOS null strain during TLD, suggesting that continuous SOS response and particularly SulA activity as cell division inhibitor, is one of the causes for TLD (35). RecF is epistatic to SOS inactivation, suggesting that the better survival of *recF thyA* is due to its inability to induce the SOS response (35).

One of the isolated suppressors of TLD was inactivation of *recQ*. RecQ is a helicase that prevents illegitimate recombination and is required for SOS activation in some cases. RecJ is a ssDNA exonuclease that assists RecQ in unwinding and degrading new DNA at stalled forks. Inactivation of *recJ* was found to alleviate TLD in some studies, but not in others (35, 67, 92). Combining SOS inactivation with *recQ*/*J* inactivation improved viability additively during TLD suggesting that RecQ/J partly contribute to TLD independently of SOS inductions (35).

Another function alleviating T-starvation is the UvrD helicase, as the *uvrD thyA* double mutant has a steeper RED phase compared to *thyA* (36, 67). This helicase has been found to curb excessive recombination by RecA, while survival during TLD of *uvrD thyA* improves if *recA* is also inactivated (36, 67, 69). This alleviation of *uvrD thyA* *recA* is epistatic to the loss of SOS response, as *lexA uvrD thyA* behaves the same as *uvrD thyA*. The hyper TLD of *uvrD thyA* is also suppressed by *recF/Q/J* inactivation which work in the same pathway in *uvrD*- condition to promote TLD (36).

The study of various DNA repair activities identified TLD-promoting functions (RecF, RecQ(J), SulA) and TLD alleviating functions (RecBCD, UvrD, Ruv). Certain functions, like the SOS response, RecA and RecG, have dual roles — they are important

for the early resistance to TLD, but later contribute to TLD pathology. Unfortunately, this incisive genetic analysis still leaves uncertain the irreparable chromosomal lesions and how they develop during T-starvation.

Based upon the above behaviors of DNA repair mutants during TLD, the following scheme has been proposed to outline TLD pathways (Fig. 5): Due to the absence of T, SSG accumulate behind the replication fork across A rich template sequence. Attempted repair of these SSG by RecFOR + RecA is toxic, and in parallel continues to increase the SOS signal, which also contributes to lethality. It is possible that RecA/F functions entangle DNA in non-productive structures, which cannot be repaired due to lack of T. RecQ may assist in cell killing by unravelling the DNA strands at the gaps and elongating them, while RecJ degrades the interrupted DNA strand supporting more RecF-dependent toxic repair. Additionally, DNA behind the replication fork is actively segregated into independent nucleoids in bacteria and the force of this separation could convert ss-gaps into DSB during T-starvation. This would initiate DNA degradation and DSB repair in the chromosome by RecBCD. Bacterial chromosomes have χ sites oriented in such a way that DNA ends going toward *oriC* are repaired but the DNA ends going towards the terminus are often degraded. An unrepaired DSB is lethal by itself, explaining the deeper viability loss in *recBCD thyA* conditions. This model depends on active replication during T-starvation to generate toxic events. In the next section I will discuss the nature of DNA replication during TLD.

1.5.2 TLD as "the tragedy of nascent replication bubbles"

Since the discovery of TLD, researchers have postulated that unbalanced growth is common denominator of all the problems in T-starved cultures (23). Unbalanced growth refers to the scenario when the cell continues to synthesize all the necessary biomolecules except one, leading to the overall disbalance and death. In the case of T-starvation, the unbalanced growth can be imagined due to the inhibited DNA synthesis, but normal protein/RNA/cell envelope synthesis.

In growing cells, 30 minutes of T-starvation reduces the rate of replication to 10% of the one in an actively growing culture, which further decreases to 5% 3 hours into starvation (68). Replication forks also become progressively non-functional, as determined by their inability to use ^{3}H dT for replication (68). Several reports suggest no significant change in the DNA amounts during starvation, but a recent study reports ~ 1.5-fold initial increase in the amount of DNA during the resistance phase, which is consistent with measured replication rates (9, 17, 37, 68). Furthermore, during the RED phase, the accumulated DNA is lost by an unknown mechanism (57, 68, 119).

Measuring the amount of origin to follow the initiation potential of the T-starved culture shows a single round of initiation during the resistance phase (68). Not all existing rounds of replication can reach the terminus, as the absolute amount of terminus increases by only 1.5 times in the resistance phase (68).

Marker frequency analysis on T-starved cultures also show a profound origin region loss by 4 hours into T- starvation, leaving only 1 copy of the origin (out of the initiated 2.5-3), which supports the physical measurements of the *oriC* amounts (68, 119). This massive loss of DNA within the *ori* macrodomain seemed to finally explain TLD,

although it was still not clear how T-starvation promotes *ori* loss. When recombinational repair mutants were tested by marker frequency analysis, it was found that *recF thyA*, *recQ thyA* and *recO thyA* mutants had minimal loss in the *ori* signal, correlating with their better survival (119). It was expected that *recBCD thyA* would have a more dramatic *oriC* loss explaining its deeper death, — yet surprisingly, even after an extended period of starvation in this strain, a narrow peak was found at the origin, flanked by DNA loss on either side, suggesting initial DNA breaks away from *oriC*, and RecBCD-dependence of the origin degradation (68). Interestingly the *recA thyA* mutant had a higher peak at the origin relative to normally-growing cells, suggesting overinitiation of replication with no detectable DNA damage (68). These observations ruled out origin loss as being essential for TLD, suggesting it is an independent event that may worsen TLD.

How does *ori* destruction happen during TLD? It is suggested that DSB during T-starvation can come from breaks at SSG structure (68). Additionally, inhibition of DNA synthesis in T-starved cells should be able to cause fork regress-split, as has been shown in other slow replication conditions (41). DSBs from either source should be repaired by the RecBCD and RecA. The restored fork could again fall apart, as T is still limiting, only to be repaired again – forming the futile fork breakage-repair cycle (Fig. 6). Because of the significant linear DNA degradation associated with DSB repair in prokaryotes, repeated cycles of DSB and replication fork restoration close to *oriC* should eventually lead to origin loss.

The *recF thyA* phenotype suggest a critical role of ss-gaps in T-starvation toxicity, but the question remains as to how these gaps form. SSG accumulation in T-starved cultures could be via an active process of T-analog excision repair, which prevents

synthesis across As on the template DNA. These gaps should be relatively short. Alternatively, ss-gaps may be much longer (= daughter-strand gaps), if they form as a result of the replisome skipping 'A rich' tracks of the DNA template and resuming DNA synthesis downstream. The former idea, which was proposed multiple times, is discussed in the next section; but the latter idea is yet to be tested (Fig. 7).

1.5.3 Proposed mechanism of lethality: the futile incorporation - excision cycle

Since TLD was observed in cells capable of active replication, attempted erroneous replication in the absence of dT is a general explanation for lethality. An obvious idea proposed by multiple researchers in the TLD field posits that in the absence of dT, dUTP is utilized for DNA synthesis (Fig. 7) (2, 17, 58, 70). When dU is found in the DNA, it is excised by the base excision repair (BER) pathway. Specifically, uracil DNA glycosylase (UDG), which is the product of the *ung* gene, removes the dU base, leaving an abasic site behind, which is nicked by ExoIII (or Endo IV) (26, 72, 132). Using the generated 3'-OH, Dna Pol I replaces the abasic site with T (in WT or T-supplemented medium), and DNA ligase seals the gap. In the absence of T, the gap will be repaired using dUTP again, only to be subjected to another round of excision repair, fueling a futile cycle of dU insertion and excision (Fig. 8).

An analogous possibility that has not been considered before is the use of rUTP instead of dTTP/dUTP for DNA synthesis (Fig. 7). This is a reasonable expectation, as the cellular rNTP concentrations are at least 10 times higher than the dNTP concentrations (14, 20). Also, recent studies on fidelity of DNA polymerases report detectable incorporations of rNTPs *in vivo* in the DNA (25, 63); such single DNA-rNs are

then excised by the ribonucleotide excision repair pathway (RER), initiated by RNase HII, which attacks the phosphodiester bond one nucleotide upstream of the junction between 5' rN and 3' dN in the DNA (45, 131). From here, ExoIII, DNA pol I and ligase activity can fix the gap again using the wrong base in the absence of T, which would require another round of RER or BER to repair.

This futile cycle of BER is postulated to irreversibly damage the chromosome, either by itself, or by creating some irreparable DNA lesions in T-starved cells. Repeated excision of T-analogs can explain the slow replication, instability of replication forks due to repeated fork collapse-reassembly cycle and DSBs due to approach and collapse of a new replication fork at the site of excision repair — all proposed and identified phenotypes of TLD.

Surprisingly there is little evidence in the literature to support the idea of futile incorporation-excision cycles. Although DNA polymerases efficiently utilize dUTP for replication, they are effectively prevented from doing so as the concentration of dUTP in the cell is limited by the action of dUTPase (Dut), which hydrolyses dUTP to dUMP, an important intermediate in dTMP synthesis (114, 127). In *E. coli*, Dut is an essential function and cannot be completely inactivated (32), although mutant alleles, like *dut-1* and *dut-11*, which under some conditions have undetectable Dut activity, are nevertheless fully viable (64). In WT *E. coli*, dUTP levels are estimated to be around 0.5 µM and their incorporation in the DNA can be detected upon inactivation of the UDG function (32, 62, 127, 138). Measurements detect 1 uracil incorporated from every 16 kbp to every 7 kbp in the *E. coli* genome (62, 110). This level of uracil incorporation may be enough to trigger the events of TLD. But interestingly, preventing uracil excision in *thyA* strains

does not affect TLD in *E. coli* at all (2, 67). This suggests that the uracil insertion events, if they happen in the *thyA* mutant during TLD, are so rare, that they cannot contribute to TLD. However, one study in *B. subtilis* reports slightly longer resistance phase and overall ~ 3 fold better survival in *ung* $^{-}$ condition, which still supports the idea that cells can undergo TLD in the absence of uracil-DNA BER (77).

In *E. coli* dUTP levels in the absence of dTTP could rise due to the de-repression of deoxycytidine deaminase (Dcd) enzyme. 75% of dUTP in *E. coli* is derived from deamination of dCTP by Dcd (13, 96). As mentioned above, dUTP is all channeled to the dTTP production; *in vitro* dTTP has been shown to inhibit the Dcd function (13). Thus, in *E. coli thyA* mutant during T-starvation, dUTP levels can rise due to increased function of Dcd. The active Dut enzyme could still intercept and hydrolyze all the excess dUTP before its incorporation into DNA. The effect of dUTP pool fluctuation in *dut* or *dcd* strains hasn't been studied in TLD. *dut thyA* should have an exacerbated TLD due to increased incidence of dU incorporation and excision, while *dcd thyA* should have lower dUTP incorporation in the DNA, alleviating TLD (Fig. 9).

Conversely, more frequent stable uracil incorporation can happen when both *dut* and *ung* genes are inactivated (Fig. 9). In one study, researchers studying a *dut ung* (*thyA*$^{+}$) strain report 19% of Ts as being replaced by Us in the DNA (138). A study designed to maximize DNA-dT replacement with DNA-dU, in the strain *dut ung thyA dcd deo*, reported replacement of about 93-96% of Ts with Us under thymineless condition, but this strain died within one generation of such growth (32). It is unclear whether the cells become bacteriostatic at this stage or succumb to toxicity of excessive stable uracil in the DNA or develop TLD of a *thyA* mutant. A more recent study describes

evolution of a *thyA* mutant of *E. coli* after about 1,000 generations to a condition where they can grow equally well in the presence of either dT or chlorouracil. These evolved strains accumulated deletions, inversions and base substitutions, have slower doubling time, but remain viable even upon replacement of almost 99% of its Ts with the analog (78). Thus, it is possible that an increased incidence of stable U incorporation could alleviate TLD, but this hasn't been formally tested. If DNA-dU BER is a true cause of TLD then, the *dut ung thyA* strain should avoid TLD completely, as the increased dUTP concentrations due to the *dut* defect will lead to stable DNA-dU incorporation due to the *ung* defect. In a similar vein, the role of RER in TLD can be probed by inactivating RNase HII, which initiates removal of ribonucleotides. It would be also interesting to examine the *dut ung thyA* strain by marker frequency analysis to follow the *oriC* degradation, if any, in this mutant.

Studies in eukaryotic systems provide conflicting views about the importance of uracil incorporation in TLD. In yeast, inactivation of abasic site processing (the late step in uracil BER pathway) is more debilitating during treatment with aminopterin (an anti-DHFR activity drug), suggesting frequent formation of abasic sites upon drug treatment (30).This sensitivity can be blocked by inactivation of UDG, which forms abasic site and initiates DNA-dU BER. Goulian *et. al* report that in human lymphoid cells upon treatment with methotrexate, which is an inhibitor for ThyA, dTMP levels fall, while dUMP levels increase by 1,000-fold (39). Normally dUTP is undetectable in the cell due to its rapid hydrolysis, but upon methotrexate treatment dUTP becomes detectable at 0.2 pmol/10^6 cell. In a later study dUMP was also found in the DNA at concentrations of 0.8 pmol/ µmol of DNA nucleotides (40). Other antifolates, like FUdR, trimethoprim, FUdR

and piritrexim also led to uracil misincorporation in mammalian cells (52, 116, 124). Similar studies in yeast report rise in the dUTP/dTTP ratio upon treatment with DHFR inhibitors aminopterin or sulfamethaxazole, with loss in viability (133). This lethality could be rescued by overexpression of Dut, which keeps the level of dUTP low. However, opposing results were presented in other studies, which didn't detect uracil in the DNA upon thymidylate synthase inhibition in HeLa cell lines or only trace accumulation of dUTP, even after extended treatments with ThyA inhibitors in a mouse lymphoid cell lines, where dTTP levels fell, while dUMP levels were inflated (55). One reason for the discrepancies could be variation in the expression of the mammalian Dut and UDG enzymes between various cell cycle stages and tissues. T-starvation also leads to an increase in dATP levels, and it has been argued in some studies that it is the imbalance of dATP: dTTP ratio that causes TLD, since dUTP levels were undetectable (1).

Despite conflicting reports, uracil incorporation and excision events are still assumed to be the primary cause of TLD. Therefore, a systematic study of this pathway in *E. coli* should verify its role in TLD, at least in prokaryotes.

1.6 Guanineless Death

The additional enzymatic steps involved in dTTP production allow us to prevent thymidine synthesis without affecting RNA synthesis or even the overall DNA replication in the cells. It is also possible to inhibit the overall DNA synthesis without affecting RNA synthesis, — by targeting ribonucleotide-diphosphate-reductase, the enzyme that makes all four DNA precursors. Such inhibition of DNA synthesis with

hydroxyurea is only bacteriostatic at least for several hours (66, 88), suggesting that it is the "unbalanced DNA replication", rather than "unbalanced general growth", that kills the cell during TLD. However, this general idea is hard to test, as any block to production of either dGTP, dATP or dCTP also affects RNA synthesis and therefore cannot generate the situation of "unbalanced DNA synthesis". This constraint left the long-standing question, whether starvation for any single DNA precursor would lead to similar events as seen in T-starvation, unanswered.

The question was eventually answered with the discovery of dGTP starvation in the *gpt optA* mutant (53). The Dgt protein hydrolyzes dGTP to deoxyguanine (dG) and a triphosphate; the *optA* mutation is a promoter-up mutation of the *dgt* gene increasing its transcription by 50-fold and consequently dGTP hydrolysis (12, 60, 85). Gpt acts in the salvage pathway to convert guanine to guanine monophosphate. Inactivating *gpt* in the *optA* background induces dGTP starvation for a while until other salvage pathway enzymes take over (93). The *gpt optA* mutant can be maintained by adding hypoxanthine (Hx) in the media which is converted into dGTP in Gpt-independent manner (53).

Upon removal of Hx, dGTP levels become undetectable within 30 minutes, but start to recover in the next 30 minutes, although the dGTP levels don't reach the pre-starvation level (53). Despite the immediate disappearance of dGTP, death in the starving cultures is seen after initial period of normal growth followed by a long lag phase. The cultures lose titer by ~100-fold and then recover due to appearance of spontaneous suppressors which are resistant to future exposure to dGTP starvation – making Guanineless Death (GLD) a temporary/reversible phenomenon (54). Most of these isolated suppressors were either deleted for *dgt* gene or were upregulated for purine

biosynthesis pathway (54). Overall GLD shares some features with T-starvation, but the phenomenon is weaker compared to TLD and is easily suppressed.

Like TLD, GLD happens in exponentially growing cultures and leads to SOS induction and cell filamentation. Also, like in TLD, over-initiation is observed at *oriC*, probably to compensate for the lower replication rates. RecA function is required for the initial stages of CFU increase and plateauing seen after Hx removal. Because of the late appearance of cell death, the *gpt optA* cultures must be maintained in exponential phase through repeated dilutions in fresh starvation media (53). The repeated dilutions, induction of alternate salvage pathways and ready suppression makes studying the phenomenon difficult. Still a few parallels can be drawn with TLD – removal of a single DNA precursor can dramatically reduce replication rates, lead to over-initiation and make recombinational repair essential to maintain viability early in starvation.

The mechanism of GLD is also currently unclear. The popular idea of futile cycles of incorporation and excision, used to explain TLD, seems an unreasonable mechanism to explain GLD, as hypoxanthine is a guanine analog and instead of contributing to death, it prevents GLD and allows normal growth. By extension, this argues for the existence of a cell death pathway upon starvation for a lone DNA precursor, that is independent of futile base excision repair events. Hx-starved cells, apart from filamenting, also show bloating (irregular diameter), suggesting that extra chromosomal events may also play a role in GLD (53).

1.7 Is DNA Replication Essential for TLD?

All models used to explain TLD – the futile cycle of fork breakage and repair, creation of gaps on DNA by skipping of sequences or by futile cycles of dU/rU incorporation and excision events, segregation-induced DSB or entangled DNA structures due to RecF/A repair, — depend on active replication during TLD. INhibition of protein synthesis with chloramphenicol suppress TLD completely, which could be interpreted in 2 ways: either suppression due to prevention of unbalanced growth or suppression due to block of initiation of the new replication rounds (which depends on protein synthesis) (75, 99). Initial work by Bouvier and Sicard addressed this dilemma by investigating TLD in replication initiation-defective *dnaA*(Ts) and *dnaC*(Ts) strains (16). The corresponding *thyA dna*(Ts) strains, when grown at the non-permissive temperatures, escaped TLD with only minor loss of viability. This was reinvestigated by the more recent works by Mata Martin *et. al*, which showed that block of replication initiation by rifampicin during T-starvation prevents stalling of replication forks and TLD (81). Rifampicin is a transcription inhibitor and is thought to prevent replication initiation at *oriC* by inhibiting transcription of neighboring genes that aid in formation of the replication bubble at the *oriC* (6, 84). Stalled replication forks have been detected around *oriC* during T-starvation (81) providing a possible reason behind *oriC* loss detected by the marker frequency analysis (68, 119). It has also been found that the extent of death during T-starvation is proportional to the number of active replication forks, establishing another link between death and active replication in the absence of a required DNA precursor (80).

Currently, the role of active replication forks in TLD has become debatable, as a recent study shows that addition of *seqA* or *rep* defects to *thyA* mutants, which cause extra initiation events (*ori*/*ter* ~ 5 as opposed to 2 in *seqA*+ or *rep*+ strains) and hence more replication forks, do not exacerbate TLD (57). The study further increased the *ori*/*ter* ratio in *thyA* mutant by HU treatment (ori/ter= 16) or by using inducible origins (ori/ter= 32) which still didn't lead to a more severe TLD. It could still be argued that, although the *ori/ter* ratios are high, the number of functional replication forks stays the same due to limitation of one of the components of the replisome. However, more seriously, this study also couldn't confirm the protection from TLD observed previously in the *dnaA*(Ts) mutants. The researchers argue that the protection seen in the *dnaA*(Ts) mutants in the previous studies was because those cultures reached saturation soon upon shift to 42°C and therefore escaped TLD (saturated cultures do not experience TLD). In contrast, this study clearly showed that, if the *dnaA*(Ts) *thyA* mutants are maintained in the exponential phase, yet are unable to initiate replication successfully, they still experience a similar loss in viability as the *thyA* mutant (57). The authors also ruled out the possibility of existing rounds of replication killing the *dnaA*(Ts) *thyA* mutant by employing a novel T-starvation protocol, ensuring that the chromosomes are completely aligned before the cultures shift to the non-permissive temperature. However, it cannot be ruled out that unsuccessful replication initiation in the *dnaA*(Ts) *thyA* (undetectable by physical assays) is sufficient to kill the strains. Overall, the recent developments suggest that a replication-independent mechanism can also lead to TLD (57). Although this recent study has been done in specialized conditions to accommodate the (Ts) phenotypes of the

dna mutants, it still demonstrates the fact that TLD can happen in complete absence of replication forks.

1.8 Oxidative Damage in TLD

A recent publication by Hong *et. al* proposed that damage from reactive oxygen species (ROS) also contributes to TLD (50). The evidence presented in support of this assertion includes the following: 1) inactivation of one of the catalases (enzymes that scavenge intracellular peroxide) causes a deeper death during TLD; 2) inhibition of respiration allows better survival during TLD; 3) ROS indicator accumulates in T-starved cells; 4) some conditions/mutations that alleviate TLD also reduce ROS accumulation. The study also claims that ssDNA is converted to DSB by ROS. The authors suggest that the process of respiration creates enough ROS that it can attack the ssDNA regions generated under T-starvation to create DSBs.

The idea in the recent years that ROS accumulation explains antibiotic-mediated killing of bacterial cells has become a controversy (59, 73). So, links between oxidative damage and TLD must be carefully examined before they can be accepted. Some of the concerns that need to be addressed are: 1) The study was done in a growth medium that produces more ROS than M9CAA/MOPSCAA, which have been traditionally used for TLD studies. The role of oxidative damage in death observed in M9CAA/MOPS media needs testing. 2) The authors show a shallow TLD for *thyA* strain in M9CAA condition and extra sensitivity of catalase mutants in this condition, which is not consistent with the extent of TLD in *thyA* strain in other studies (35, 81). 3) Their measurements of ROS levels per cell using fluorescent dye have not been normalized to cell lengths or OD

during starvation, so their current measurements may just reflect the increase in cell volume due to filamentation (104, 111). 4) They argue that a better survival in anerobic media is due to lack of ROS production, but slower growth in general is known to improve survival during TLD. Additionally, they still show rescue of lethality in anaerobic condition by adding metal chelators, suggesting production of ROS in anaerobic growth conditions, which makes no sense. 5) They document visible SSB foci – a marker for ssDNA, in the T-starved cells, but not in non-starved cells. But SSB foci marking the replisome are usually visible in exponentially growing cells as well in other studies (21, 112). 6) Finally, they use fluorescent RecN foci as a marker for DSBs, although it has not been conclusively shown that RecN functions in DSB repair. In summary, more work is required to understand the (possible) relationship between TLD and ROS.

1.9 The Dilemma of the Resistance Phase

The resistance/lag phase preceding lethality in T-starved culture has long puzzled researchers in the TLD field. In the early studies, the resistance phase in bacteria was often altogether missing due to use of lysogenic strains which would be immediately lysed by prophage induction. Eventually, when prophage-free strains were developed, they consistently showed a lag period before the exponential death characteristic of T-starvation (2). As mentioned previously, recombinational repair supports the resistance phase, as *recBCD* mutants lack the resistance phase, while *recA*, *ruv recG* and *uvrD* mutants have a shorter resistance phase. No mutations have been identified so far that extend this resistance period. Cellular metabolism continues during the resistance phase –

RNA, protein and lipid synthesis all go normally, allowing the cells to induce the SOS response and filament. Unlike during carbon/nitrogen/phosphate starvation stress response, RpoS is not induced during T-starvation, nor any accumulation of (p)ppGpp has been reported (119). There are extra initiation events at *oriC*, and DSBs accumulate, while the rate of DNA synthesis decreases. From the known size of the dTTP pool, which is ~1% of the chromosomal dT content (94), it can be estimated that the cells should run out of dTTP within minutes of T-starvation, predicting that chromosomal DNA levels should remain constant during T-starvation.

Blocking protein synthesis by chloramphenicol or rifampicin at the beginning of starvation prevents TLD, implicating either new rounds of DNA replication, or synthesis of specific proteins as the cause of subsequent death. Based on all these futile damage-repair cycle ideas of TLD, it was always assumed that replication-dependent DNA damage accumulates during the resistance phase, and once it reaches a threshold, it becomes irreparable, ushering the RED phase. But since the role of replication in TLD was challenged, a new explanation for the resistance phase has to be explored.

1.10 Potential Endogenous HMW Sources of Thymine

A possible reason for the resistance phase that has not been considered before is that there is an internal source of dT available in the cell, and while this pool lasts, it supports some DNA synthesis, maintaining constant viability. An obvious significant source of dT is the chromosomal DNA itself. The chromosomal fragments detected during the resistance phase can be a significant source of dT. One of the proposed mechanisms of TLD is the futile replication fork breakage-repair cycle, proposed to

happen at slow-moving forks in T-starved cells. If, instead of repair, the broken DNA is degraded, the cells may derive enough dTMP that can allow surviving forks to continue and finish replication, maintaining the resistance phase. This scenario can be tested by inactivating the DNA degradation function to see if the resistance phase disappears.

Another possible source of T in starving cells is the pool of stable RNAs. Bases found in certain positions in tRNA and rRNA are post-transcriptionally modified to assist in the RNA molecule function. In all tRNAs, U54 is methylated by TrmA to become T54 (95). Similarly, in 23S rRNA, U747 and U1939 are methylated to T by RumB and RumA respectively (76). Even human tRNAs carry the T54 modification, and the increased activity of the enzyme responsible for this modification, TRMT2A, has been implicated in recurrence of HER2+ breast cancer in patients (29, 47). These Ts found in tRNA and rRNA are not essential in *E. coli*, as deletions of the corresponding genes have no phenotype (at least in the lab). In rapidly-growing *E. coli*, with ~ 50,000 ribosomes and 10-times as many tRNA molecules (18), if all of them are degraded during T-starvation, they can collectively provide ~600,000 Ts, enough to synthesize ~2.4 mbp of DNA. The contribution of these rT to the resistance phase can be tested by inactivating the respective modification enzyme and investigating the resulting TLD kinetics.

1.11 Involvement of dTTP in Processes Other than DNA Replication

Apart from these two high molecular weight sources of T – the chromosome and the stable RNAs, a long-ago found and now mostly forgotten low molecular weight source of dT exists in prokaryotic cells. Another major role of dT in prokaryotic cells is related to the surface polysaccharide biosynthesis. These polysaccharide antigens are

made up of repeated units – each unit composed of a defined set of covalently attached sugars (65, 117). During antigen synthesis, nucleotide diphosphate handles, like UDP, GDP, CDP, ADP and dTDP, are attached to hexose sugars, while the sugar moieties are modified in several steps to convert them to precursors of the surface antigen.

A complete review of how the various NDP-glucose complexes are used in antigen synthesis is beyond the scope of this review, but I will briefly discuss the use of dTDP-glucose in the synthesis of exopolysaccharide (EPS) capsule in *E. coli*. dTTP is first conjugated to glucose -1-phosphate to form dTDP-glucose. This reaction is catalyzed by thymidine glucose pyrophosphorylases RfbA and RffH (79). This glucose is modified sequentially by the RfbB, RfbC, RfbD enzymes to L-rhamnose, which is one of the sugars specific to O-antigen; or by the RffG, WecE, RffC enzymes to 4-acetamido, 4,6-dideoxy-αD-galactose, one of the sugars found in the repeating unit that makes up the Enterobacter Common Antigen (ECA) (65, 83, 117, 130). These sugars are then deposited onto the undecaprenol handle, that extends into the cytoplasm from the inner membrane, while the nucleotide diphosphates are released back into the cytoplasm. Once a tri-saccharide unit is assembled, the undecaprenol moiety is flipped across the inner membrane into the periplasmic space, where the tri-saccharides are further polymerized, before being transported to the outer membrane, while the undecaprenol is recycled. On the *E. coli* surface, O-antigens contain an average of 30-40 repeating units, and the ECA chains are composed of on average of 7 repeating units (10, 117). *E. coli* K12 strains lack O-antigens because of a mutation, but still have the ECA. The EPS capsule is required for bile salt resistance, virulence, membrane integrity, and is also useful for serotype classification (27, 87, 115).

Although NDPs are recycled back into the cytoplasm after sugar deposition in the inner membrane, a significant population of NDP-sugar complex exists inside the cell. Evidence for dTDP-sugar comes from early studies by Okazaki who stumbled upon them while studying the mechanism of *in vivo* DNA replication with the help of tritiated thymidine (101). He found that, apart from thymidine in DNA and dTTP, an even bigger fraction of ^{3}H-dT label incorporates into dTDP-rhamnose and its precursor, dTDP-glucose. Moreover, the labelled dT present in this complex can be (slowly) chased into DNA, suggesting that dTDP-hexoses can be a potential DNA precursor under some conditions (100, 102). Subsequent studies identified the dTDP-glucose pyrophosphorylase activity in *E. coli* cell extracts (61). A study by the group of Ohkawa *et. al* show disappearance of the dTDP-sugar pool during T-starvation and reduction of the resistance phase due to an uncharacterized mutation in the pathway that creates the dTDP-sugar pools in the Ter 15 strain of *E. coli* (97). A later study by Ohkawa *et. al* also showed evidence of smaller or larger than normal pools of dTDP-sugars in various dTDP-glucose pyrophosphorylase-deficient and -overexpressing strains, respectively (98). The intracellular estimates for the dTDP-glucose and its derivatives is about 250 µM, which is thought to primarily reflect the pool of dTDP-rhamnose (14). This is about 3 times more than the pool of dTTP in the same cells. The existence of the ECA intermediate dTDP- 4-acetamido-4,6- dideoxy-α-D-galactose was completely missed in these earlier studies, although Okazaki's studies mention unidentified dTDP-sugar complexes (51, 103). It was much later that the alternate dTDP-glucose pyrophosphorylase— RffH of the ECA pathway — was discovered and characterized.

The dTDP-sugars thus make up another modest pool of internal LMW-dT (in addition to dTTP), but its role as a source of dT during T-starvation is not known. Also, does the presence or absence of the surface antigens affect filamentation in T-starving cultures in any way? With better understanding of processes involved in dTDP-sugar pool synthesis we can now explore this pathway genetically, to reveal its possible effect on the TLD kinetics.

1.12 Summary

The anomalous feature of T-starvation induced death has been puzzling researchers for more than 6 decades. Even though the mechanism of the lethality is far from being understood, efforts in the recent decade have systematized the various events happening in T-starved cells. Most of these events can be explained by ongoing faulty replication or abortive initiation in the absence of a required DNA precursor. But the recent developments that show TLD even in the absence of ongoing or new rounds of replication argue that a replication-independent mechanism also contributes to TLD. It seems that multiple different mechanisms/DNA lesions can contribute to TLD, and although some of the lethal pathways can be inactivated in some mutants, other mechanisms still kill T-starved cells. The complete avoidance of TLD upon chloramphenicol treatment encourages us to entertain the possibility that T-starvation may express a still unknown protein, which is toxic for the cell, or that dT may be required for some other essential function in the cell.

Living cells have somehow avoided developing a coping strategy to deal with T-starvation, maybe because in natural environments cells have never encountered T-

starvation. Alternatively, TLD is one of several deliberately placed vulnerabilities in the cellular design (like GLD, DAPless death) whose physiological purpose as of yet is unclear to us.

In the subsequent chapters of this thesis regarding TLD we will be experimenting in the following areas:

1. The role of DNA-dU BER in TLD
2. The role of DNA-rU RER in TLD
3. Detect SSG in DNA isolated from T-starved cultures
4. Is the chromosomal DNA or the stable RNA species a source of endogenous dT during TLD?
5. Is the dTDP-sugar species a source of endogenous dT during TLD?

1.13 Figures

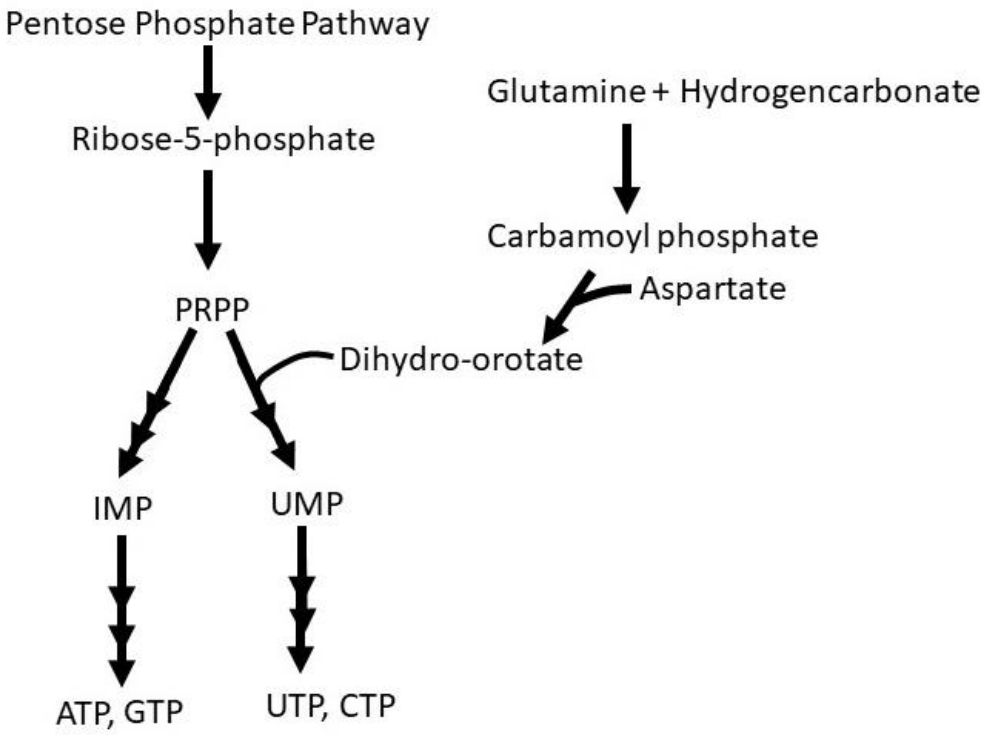

Figure 1.1. Schematic of NTP synthesis in *E. coli*.

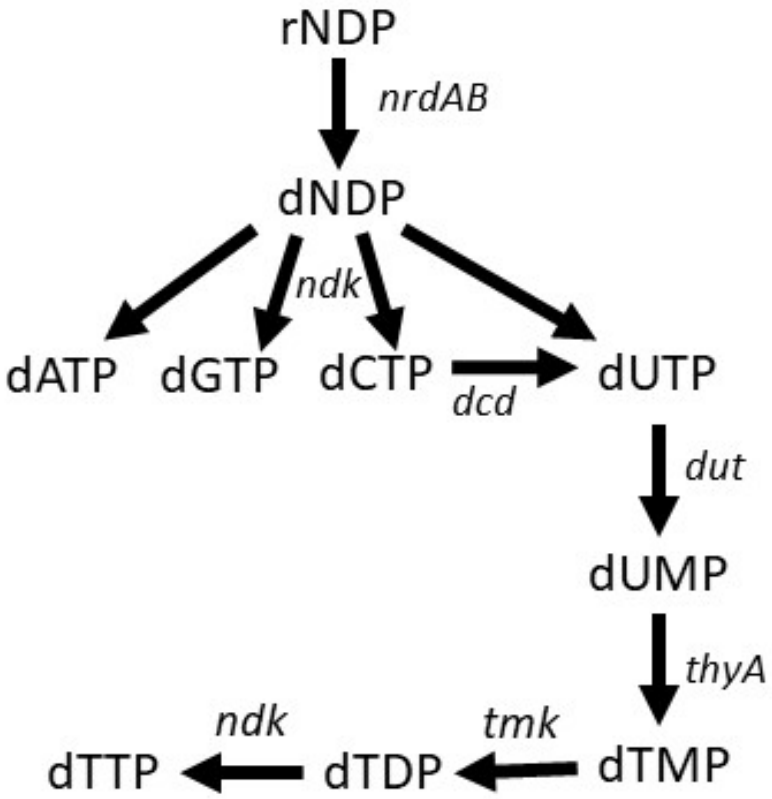

Figure 1.2. Scheme for dNTP synthesis in *E. coli*.

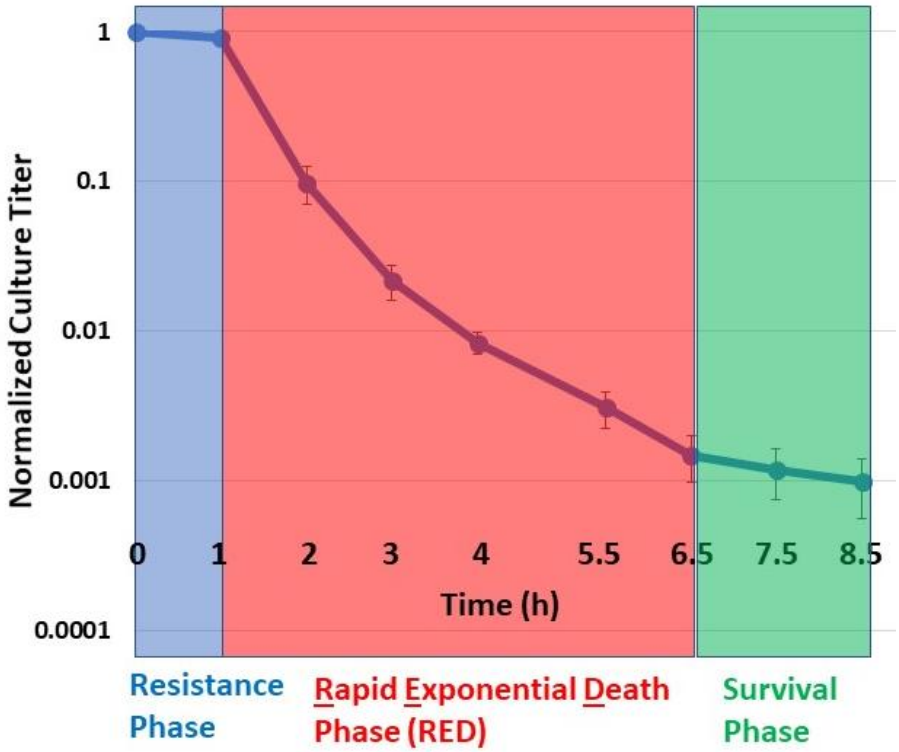

Figure 1.3. Graph depicting 3 stages of TLD in *thyA* mutants at 37°C. Resistance phase lasts for an hour, Rapid Exponential Death (RED) phase – characterized by fast decline of viability and Survival phase – viability stabilizes at a lower level.

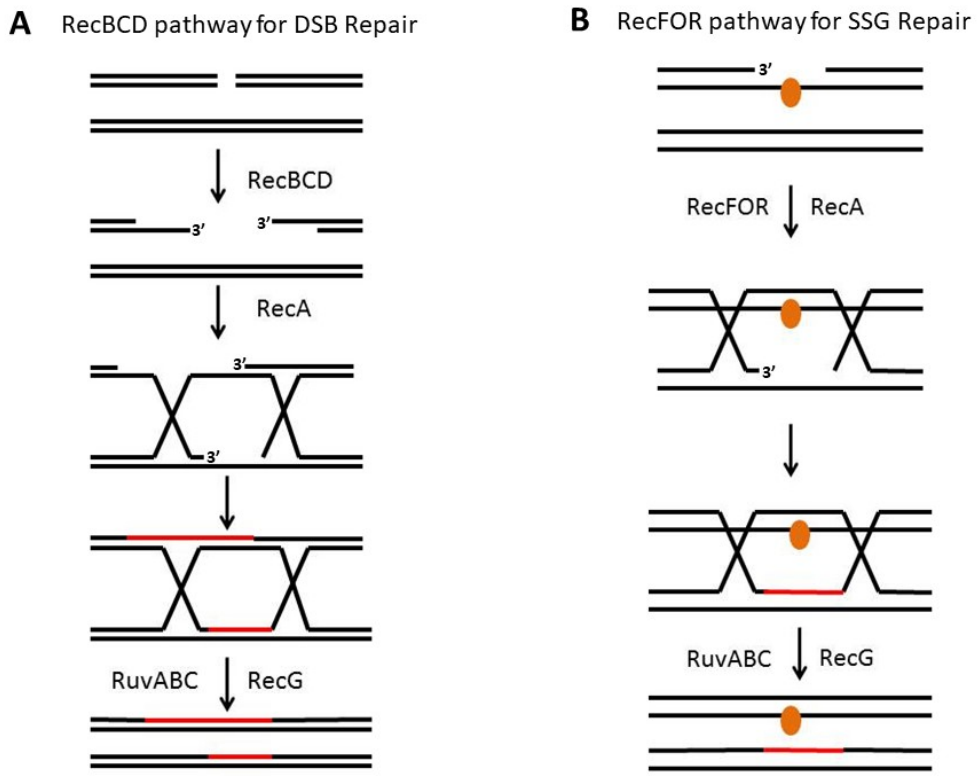

Figure 1.4. Recombinational repair pathways in *E. coli*. A. Double Strand break repair in *E. coli* is initiated by RecBCD, which degrades DNA ends to generate 3' overhang. **B.** Persistent single strand gaps are recognized by RecFOR complex which allow RecA to polymerize on the gapped DNA. The RecA polymerized strand invades homologous duplex DNA. Strand invasion is followed by repair synthesis resulting in Holliday junctions which are resolved or removed by RuvABC and RecG respectively.

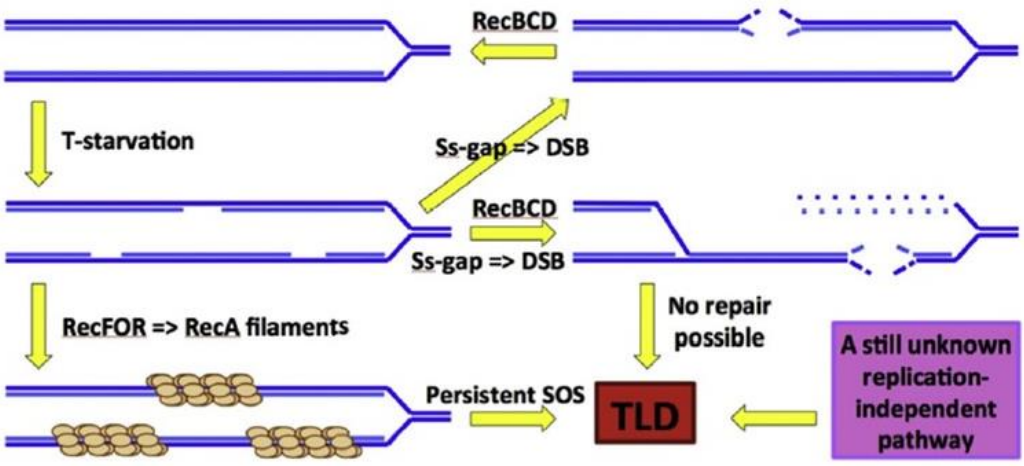

Figure 1.5. Role of DNA repair pathways in preventing or promoting as described in recent studies. RecBCD functions repairs double strand breaks that occur early during TLD. RecBCD could also degrade linear DNA which can leave some DNA breaks unrepaired. Attempted single strand gap repair by RecF induces persistent SOS promoting TLD. An unknown replication independent mechanism also promotes TLD.

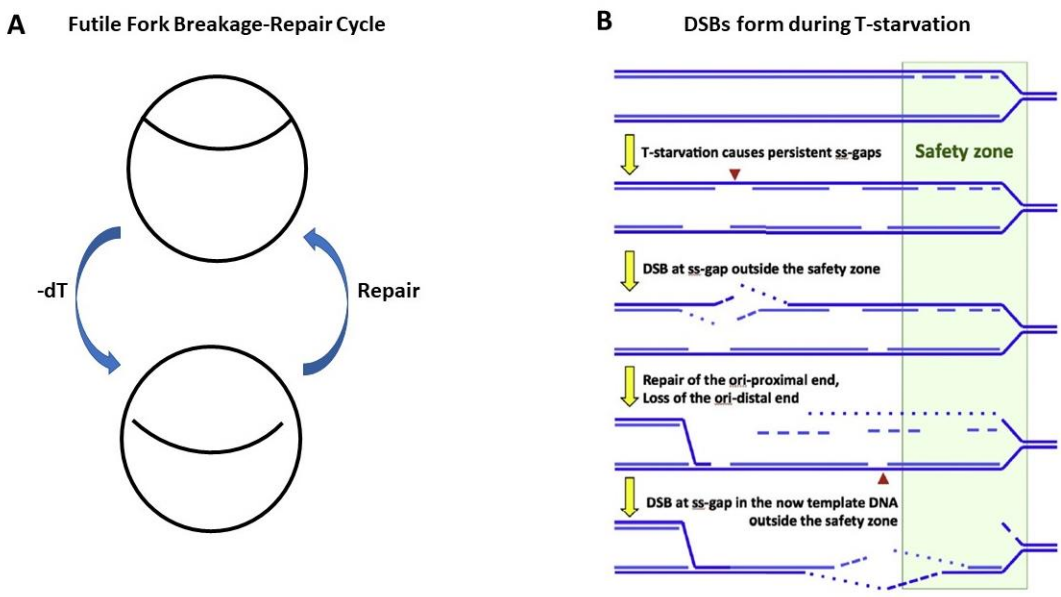

Figure. 1.6. A. Fork stalling due to dTTP deprivation can lead to fork collapse. Such collapsed forks can be reassembled by recombinational repair but will still be inhibited for replication due to continued dTTP deprivation. **B.** In the absence of dTTP A rich sequences may be skipped by replication to resume DNA synthesis downstream. These gapped DNA structures may be broken by the force of chromosomal segregation. Gapped DNA is in the safety zone before it encounters the segregation forces.

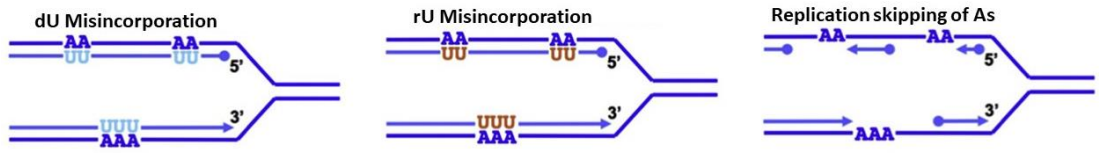

Figure 1.7. Possible nature of replication in the absence of dTTP. dUTP or rUTP may be used to synthesize DNA across A-rich sequences in the template or the A-rich sequences are skipped altogether with replication resuming downstream.

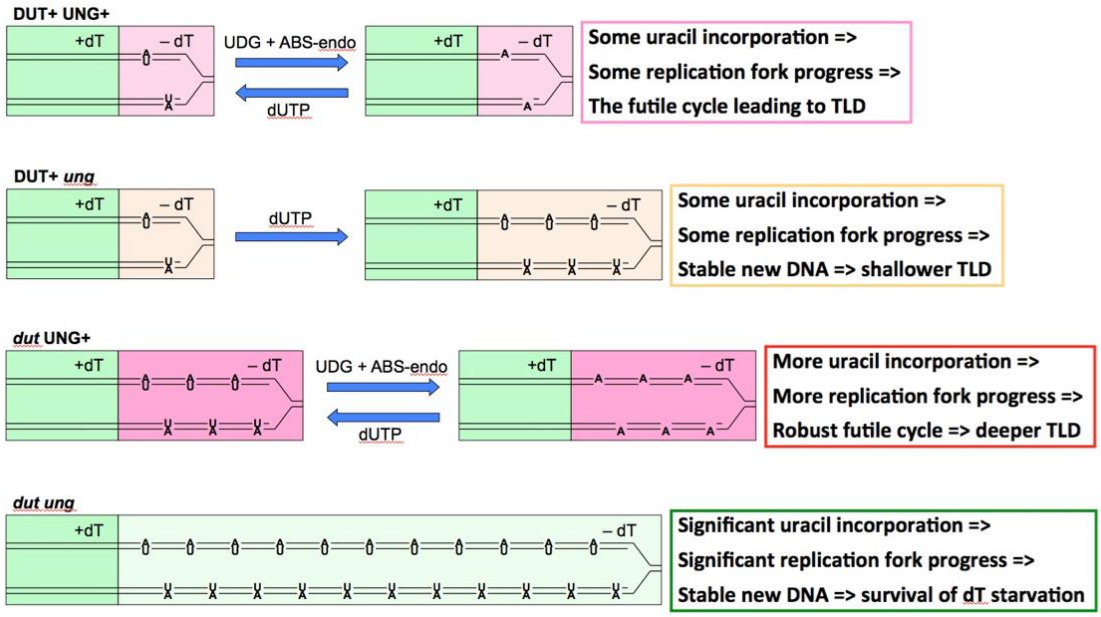

Figure 1.8. The futile uracil incorporation-excision cycle proposed to lead to TLD. In dT replete conditions dUTP is not used for replication in WT cells and it is not detected in the DNA unless Uracil DNA glycosylase (product of *ung* gene) is blocked. During TLD if uracil excision is blocked such as in *ung*- background, there should be an increase in density of dU incorporation in the DNA. In the *dut*- background where dUTP pools have expanded, there should be more frequent uracil incorporation followed by its excision leading to a more severe TLD. In *dut ung* background, an increased density of uracils should be stable incorporated and such strains should escape TLD completely.

1.14 References

1. Aherne GW, Brown S. 1999. The role of uracil misincorporation in thymineless death. *Antifolate Drugs Cancer Ther.*, pp. 409–21.

2. Ahmad SI, Kirk SH, Eisenstark A. 1998. Thymine metabolism and thymineless death in prokaryotes and eukaryotes. *Annu. Rev. Microbiol.* 52:591–625.

3. Alamula N, Lu Q, Delgado J, Belki S, Inouye M. 1995. Nucleoside diphosphate kinase from *Escherichia coli*. *J. Bacteriol.* 177(9):2524–29.

4. Anderson DG, Kowalczykowski SC. 1997. The recombination hot spot chi is a regulatory element that switches the polarity of DNA degradation by the RecBCD enzyme. *Genes Dev.* 11(5):571–81.

5. Anderson DG, Kowalczykowski SC. 1997. The translocation RecBCD enzyme stimulates recombination by directing RecA protein onto ssDNA in a x-regulated manner. *Cell*. 90:77–86.

6. Baker TA, Kornberg A. 1988. Transcriptional activation of initiation of replication from the *E. coli* chromosomal origin: An RNA-DNA hybrid near oriC. *Cell*. 55(1):113–23.

7. Barner HD, Cohen SS. 1954. The induction of thymine synthesis by T2 infection of a thymine requiring mutant of *Escherichia coli*. *J. Bacteriol.* 68(1):80–88.

8. Barner HD, Cohen SS. 1957. The isolation and properties of amino acid requiring mutants of a thymineless bacterium. *J. Bacteriol.* 74(3):350–55.

9. Barner HD, Cohen SS. 1958. Protein synthesis and RNA turnover in a pyrimidine deficient bacterium. *Biochim. Biophys. Acta*. 30:12–20.

10. Barr K, Klena J, Rick PD. 1999. The modality of enterobacterial common antigen polysaccharide chain lengths is regulated by o349 of the *wec* gene cluster of *Escherichia coli* K-12. *J. Bacteriol.* 181(20):6564–68.

11. Bayer E. 1967. The cell wall of Escherichia coli early: Effects of penicillin treatment and deprivation of diaminopimelic acid. *J. Gen. Microbiol.* 46(2):237–46.

12. Beauchamp B, Richardson C. 1988. A unique deoxyguanosine triphosphatase is responsible for the *optA1* phenotype of *Escherichia coli*. *Proc Natl Acad Sci USA.* 85:2563–67.

13. Beck CF, Eisenhardt AR, Neuhard J. 1975. Deoxycytidine triphosphate deaminase of *Salmonella typhimurium*. *J. Biol. Chem.* 250(2):609–16.

14. Bochner BR, Ames BN. 1982. Complete analysis of cellular nucleotides by two-dimensional thin layer chromatography. *J. Biol. Chem.* 257(16):9759–69.

15. Boehmer PE, Emmerson PT. 1992. The RecB subunit of the *Escherichia coli* RecBCD enzyme couples ATP hydrolysis to DNA unwinding. *J. Biol. Chem.* 267(7):4981–87.

16. Bouvier F, Sicard N. 1975. Interference of dna ts mutations of *Escherichia coli* with thymineless death. *J. Bacteriol.* 124(3):1198–1204.

17. Breitman TR, Maury PB, Toal JN. 1972. Loss of deoxyribonucleic acid-thymine during thymine starvation of *Escherichia coli*. *J. Bacteriol.* 112(1):646–48.

18. Bremer H, Dennis PP, Neidhardt FC. 1996. Modulation of Chemical Composition and Other Parametrs of the Cell by Growth Rate. *Escherichia coli* and *Salmonella typhimurium.* ASM Press, Washington D.C. 1553–1569 pp.

19. Brogden R, Carmine A, Heel R, Speight T, Avery G. 1982. Trimethoprim: A review of its antibacterial activity, pharmacokinetics and therapeutic use in urinary tract infections. *Drugs*. 23(6):40–30.

20. Buckstein MH, He J, Rubin H. 2008. Characterization of nucleotide pools as a function of physiological state in *Escherichia coli*. *J. Bacteriol.* 190(2):718–26.

21. Cagliero C, Zhou YN, Jin DJ. 2014. Spatial organization of transcription machinery and its segregation from the replisome in fast-growing bacterial cells. *Nucleic Acids Res.* 42(22):13696–705.

22. Churchill JJ, Anderson DG, Kowalczykowski SC. 1999. The RecBC enzyme loads RecA protein onto ssDNA asymmetrically and independently of χ, resulting in constitutive recombination activation. *Genes Dev.* 13(7):901–11.

23. Cohen SS, Barner HD. 1954. Studies on unbalanced growth in Escherichia coli. *Proc. Natl. Acad. Sci. USA*. 40:885–93.

24. Corbin BD, Seeley EH, Raab A, Feldmann J, Miller MR, et al. 2008. Metal Chelation and Inhibition of Bacterial Growth in Tissue Abscesses. *Science.* 319(5865):962–65.

25. Cronan GE, Kouzminova EA, Kuzminov A. 2019. Near-continuously synthesized leading strands in *Escherichia coli* are broken by ribonucleotide excision. *Proc. Natl. Acad. Sci. USA*. 116(4):1251–60.

26. Cunningham RP, Saporito SM, Spitzer SG, Weiss B. 1986. Endonuclease IV (nfo) mutant of *Escherichia coli*. *J. Bacteriol.* 168(3):1120–27.

27. Danese PN, Oliver GR, Barr K, Bowman GD, Rick PD, Silhavy TJ. 1998. Accumulation of the enterobacterial common antigen lipid II biosynthetic intermediate stimulates *degP* transcription in *Escherichia coli*. *J. Bacteriol.* 180(22):5875–84.

28. Daws TD, Fuchs JA. 1984. Isolation and characterization of an *Escherichia coli* mutant deficient in dTMP kinase activity. *J. Bacteriol.* 157(2):440–44.

29. De Crécy-Lagard V, Boccaletto P, Mangleburg CG, Sharma P, Lowe TM, et al. 2019. Survey and summary: Matching tRNA modifications in humans to their known and predicted enzymes. *Nucleic Acids Res.* 47(5):2143–59.

30. Dornfeld K, Johnson M. 2005. AP endonuclease deficiency results in extreme sensitivity to thymidine deprivation. *Nucleic Acids Res.* 33(20):6644–53.

31. Eklund H, Uhlin U, Farnegardh M, Logan DT, Nordlund P. 2001. Structure and function of the radical enzyme ribonucleotide reductase. *Prog. Biophys. Mol. Biol.* 77(3):177–268.

32. El-Hajj HH, Wang L, Weiss B. 1992. Multiple mutant of *Escherichia coli* synthesizing virtually thymineless DNA during limited growth. *J. Bacteriol.* 174(13):4450–56.

33. Fernández DeHenestrosa AR, Ogi T, Aoyagi S, Chafin D, Hayes JJ, et al. 2000. Identification of additional genes belonging to the LexA regulon in *Escherichia Coli*. *Mol. Microbiol.* 35(6):1560–72.

34. Fontecave M, Mulliez E, Logan DT. 2002. Deoxyribonucleotide synthesis in anaerobic microorganisms: The class III ribonucleotide reductase. *Prog. Biophys. Mol. Biol.* 72:95–127.

35. Fonville NC, Bates D, Hastings PJ, Hanawalt PC, Rosenberg SM. 2010. Role of RecA and the SOS response in thymineless death in *Escherichia coli*. *PLoS Genet.* 6(3):e1000865.

36. Fonville NC, Vaksman Z, Denapoli J, Hastings PJ, Rosenberg SM. 2011. Pathways of resistance to thymineless death in *Escherichia coli* and the function of UvrD. *Genetics*. 189(1):23–36.

37. Gallant J, Suskind R. 1961. Relationship between thymineless death and ultraviolet inactivation in *Escherichia coli*. *J. Bacteriol.* 1961:187–94.

38. Gentry DR, Hernandez VJ, Nguyen LH, Jensen DB, Cashel M. 1993. Synthesis of the stationary-phase sigma factor sigma S is positively regulated by ppGpp. *J Bacteriol*. 175(24):7982–89.

39. Goulian M, Bleile B, Tseng BY. 1980. The effect of methotrexate on levels of dUTP in animal cells. *J. Biol. Chem.* 255(22):10630–37.

40. Goulian M, Bleile B, Tseng BY. 1980. Methotrexate-induced misincorporation of uracil into DNA. *Proc. Natl. Acad. Sci. USA*. 77(4 I):1956–60.

41. Grompone G, Seigneur M, Ehrlich SD, Michel B. 2002. Replication fork reversal in DNA polymerase III mutants of *Escherichia coli*: a role for the beta clamp. *Mol. Microbiol.* 44:1331–39.

42. Hammes GG, Benkovic SJ, Hammes-Schiffer S. 2011. Flexibility, diversity, and cooperativity: Pillars of enzyme catalysis. *Biochemistry*. 50(48):10422–30.

43. Hanawalt PC. 2015. A balanced perspective on unbalanced growth and thymineless death. *Front. Microbiol.* 6(JUN):1–7.

44. Harms A, Maisonneuve E, Gerdes K. 2016. Mechanisms of bacterial persistence during stress and antibiotic exposure. *Science.* 354(6318):aaf4268.

45. Haruki M, Tsunaka Y, Morikawa M, Kanaya S. 2002. Cleavage of a DNA–RNA–DNA/DNA chimeric substrate containing a single ribonucleotide at the DNA–RNA junction with prokaryotic RNases HII. *FEBS Lett.* 531:204–8.

46. Hengge-Aronis R. 2002. Signal transduction and regulatory mechanisms involved in control of the S (RpoS) subunit of RNA polymerase. *Microbiol. Mol. Biol. Rev.* 66(3):373–95.

47. Hicks DG, Janarthanan BR, Vardarajan R, Kulkarni SA, Khoury T, et al. 2010. The expression of TRMT2A, a novel cell cycle regulated protein, identifies a subset of breast cancer patients with HER2 over-expression that are at an increased risk of recurrence. *BMC Cancer*. 10(108).

48. Hirch M, Elliott T. 2002. Role of ppGpp in rpoS stationary-phase regulation in *Escherichia coli*. *J Bacteriol*. 184(18):5077–87.

49. Hoch JA. 2017. A life in *Bacillus subtilis* signal transduction. *Annu Rev Microbiol*. 21:1–19.

50. Hong Y, Li L, Luan G, Drlica K, Zhao X. 2017. Contribution of reactive oxygen species to thymineless death in *Escherichia coli*. *Nat. Microbiol.* 2(12):1667–75.

51. Hosono R, Hosono H, Kuno S. 1975. Effects of growth conditions on thymidine nucleotide pools in *Escherichia coli*. *J. Biochem.* 78(1):123–29.

52. Ingraham HA, Tseng BY, Goulian M. 1982. Nucleotide levels and incorporation of 5-fluorouracil and uracil into DNA of cells treated with 5-fluorodeoxyuridine. *Mol Pharmacol*. 21:211–16.

53. Itsko M, Schaaper RM. 2014. dGTP starvation in Escherichia coli provides new insights into the thymineless-death phenomenon. *PLoS Genet.* 10(5):e1004310.

54. Itsko M, Schaaper RM. 2017. Suppressors of dGTP starvation in Escherichia coli. *J. Bacteriol.* 199(12):e00142-17.

55. Jackson RC, Jackman AL, Calvert AH. 1983. Biochemical effects of a quinazoline inhibitor of thymidylate synthetase, N-(4-(N-((2-amino-4-hydroxy-6-quinazolinyl)methyl)prop-2-ynylamino)benzoyl)-l-glutamic acid (CB3717), on human lymphoblastoid cells. *Biochem. Pharmacol.* 32(24):3783–90.

56. Kelliher JL, Kehl-Fie TE. 2016. Competition for manganese at the host-pathogen interface. *Prog. Mol. Biol. Transl. Sci.* 142:1–25.

57. Khan SR, Kuzminov A. 2019. Thymineless death in *Escherichia coli* is unaffected by the chromosomal replication complexity. *J. Bacteriol.* 201(9):1–16.

58. Khodursky A, Guzmán EC, Hanawalt PC. 2015. Thymineless death lives on: New insights into a classic phenomenon. *Annu. Rev. Microbiol.* 69(1):247–63.

59. Kohanski MA, Dwyer DJ, Hayete B, Lawrence CA, Collins JJ. 2007. A common mechanism of cellular death induced by bactericidal antibiotics. *Cell*. 130(5):797–810.

60. Kornberg S, Lehman I, Bessman M, Simms E, Kornber A. 1958. Enzymatic cleavage of deoxyguanosine triphosphate to deoxyguanosine and tripolyphosphate. *J Biol Chem.* 233:159–62.

61. Kornfeld S, Glaser L. 1961. The enzymatic synthesis of thymidine-linked sugars. *J. Biol. Chem.* 236(6):1791–94.

62. Kouzminova E, Kuzminov A. 2006. Fragmentation of replicating chromosomes triggered by uracil in DNA. *J. Mol. Biol.* 355(1):20–33.

63. Kouzminova EA, Kadyrov FF, Kuzminov A. 2017. RNase HII saves *rnhA* mutant *Escherichia coli* from R-Loop-associated chromosomal fragmentation. *J. Mol. Biol.* 429(19):2873–94.

64. Kouzminova EA, Kuzminov A. 2004. Chromosomal fragmentation in dUTPase-deficient mutants of *Escherichia coli* and its recombinational repair. *Mol. Microbiol.* 51(5):1279–95.

65. Kuhn H, Meier-Deiter U, Mayer H. 1988. ECA , the enterobacterial common antigen. *FEMS Microbiol. Rev.* 54:195–222.

66. Kuong KJ, Kuzminov A. 2009. Cyanide, peroxide and nitric oxide formation in solutions of hydroxyurea causes cellular toxicity and may contribute to its therapeutic potency. *J. Mol. Biol.* 390(5):845–62.

67. Kuong KJ, Kuzminov A. 2010. Stalled replication fork repair and misrepair during thymineless death in *Escherichia coli*. *Genes to Cells.* 15(6):619–34.

68. Kuong KJ, Kuzminov A. 2012. Disintegration of nascent replication bubbles during thymine starvation triggers RecA- and RecBCD-dependent replication origin destruction. *J. Biol. Chem.* 287(28):23958–70.

69. Kuzminov A. 1999. Recombinational repair of DNA damage in *Escherichia coli* and bacteriophage lambda. *Microbiol. Mol. Biol. Rev.* 63(4):751–813.

70. Ladner R. 2001. The role of dUTPase and uracil-DNA repair in cancer chemotherapy. *Curr Protein Pept Sci.* 2(4):361–70.

71. Lam LKP, Lee AD, Kalantar TH, Kelland JG, Lane-Bell PM, et al. 1988. Analogs of diaminopimelic acid as inhibitors of meso-diaminopimelate dehydrogenase and LL-diaminopimelate epimerase. *J. Biol. Chem.* 263(24):11814–19.

72. Lindahl T, Ljungquist S, Siegert W, Nyberg B, Sperens B. 1977. DNA N-Glycosidases. *J. Biol. Chem.* 252(10):3286–94.

73. Liu Y, Imlay JA. 2013. Cell death from antibiotics without the involvement of reactive oxygen species. *Science.* 339(6124):1210–13.

74. Longley DB, Harkin DP, Johnston PG. 2003. 5-Fluorouracil: Mechanisms of action and clinical strategies. *Nat. Rev. Cancer*. 3(5):330–38.

75. Maaloe O, Hanawalt PC. 1961. Thymine deficiency and the normal DNA replication cycle. I. *J. Mol. Biol.* 3:144–55.

76. Madsen CT, Mengel-Jørgensen J, Kirpekar F, Douthwaite S. 2003. Identifying the methyltransferases for m5U747 and m5U1939 in 23S rRNA using MALDI mass spectrometry. *Nucleic Acids Res.* 31(16):4738–46.

77. Makino F, Munakata N. 1978. Deoxyuridine residues in DNA of thymine-requiring *Bacillus subtilis* strains with defective N-glycosidase activity for uracil-containing DNA. *J Bacteriol*. 134(1):24–29.

78. Marlière P, Patrouix J, Döring V, Herdewijn P, Tricot S, et al. 2011. Chemical evolution of a bacterium's genome. *Angew. Chemie*. 123(31):7247–52.

79. Marolda CL, Valvano MA. 1995. Genetic analysis of the dTDP-rhamnose biosynthesis region of the Escherichia coli VW187 (O7:K1) rfb gene cluster: Identification of functional homologs of rfbB and rfbA in the rff cluster and correct location of the *rffE* gene. *J. Bacteriol.* 177(19):5539–46.

80. Martin CM, Guzman EC. 2011. DNA replication initiation as a key element in thymineless death. *DNA Repair (Amst).* 10(1):94–101.

81. Martín CM, Viguera E, Guzmán EC. 2014. Rifampicin suppresses thymineless death by blocking the transcription-dependent step of chromosome initiation. *DNA Repair (Amst).* 18(1):10–17.

82. McCann MP, Kidwell JP, Matin A. 1991. The Putative sigma factor KatF has a central role in developmet of starvation-mediated general resistance in *Escherichia coli*. *J. Bacteriol.* 173(13):4188–94.

83. Meier-Dieter U, Starman R, Barr K, Mayer H, Rick PD. 1990. Biosynthesis of enterobacterial common antigen in *Escherichia coli*. Biochemical characterization of Tn10 insertion mutants defective in enterobacterial common antigen synthesis. *J. Biol. Chem.* 265(23):13490–97.

84. Messer W. 1972. Initiation of DNA replication in *E.coli* B/r: Chronology of events and transcriptional control of initiation. *J. Bacteriol.* 112(1):7–12.

85. Meyers J, Beauchamp B, Richardson C. 1987. Gene 1.2 protein of bacteriophage T7. Effect on deoxyribonucleotide pools. *J Biol Chem.* 262:5288–92.

86. Mishanina T V, Yu L, Karunaratne K, Mondal D, Corcoran JM, et al. 2016. An unpresedented nechanism of nucleotide methylation in organisms containing thyX. *Science.* 351(6272):507–10.

87. Mitchell AM, Srikumar T, Silhavy TJ. 2018. Cyclic Enterobacterial Common Antigen maintains the outer membrane permeability barrier of *Escherichia coli* in a manner controlled by YhdP. *MBio*. 9(4):1–16.

88. Morgonroth PA, Hanawalt PC. 2006. Role of DNA replication and repair in thymineless death in *Escherichia coli*. *J. Bacteriol.* 188(14):5286–88.

89. Myllykallio H, Lipowski G, Leduc D, Filee J, Forterre P, Liebl U. 2002. An alternative flavin-dependent mechanism for thymidylate synthesis. *Science.* 297(5578):105–7.

90. Nakayama H, Nakayama K, Nakayama R, Nakayama Y. 1982. Recombination-deficient mutations and thymineless death in *Escherichia coli* K12: reciprocal effects of *recBC* and *recF* and indifference of *recA* mutations. *Can. J. Microbiol.*, pp. 425–30.

91. Nakayama K, Kusano K, Irino N, Nakayama H. 1994. Thymine starvation-induced structural changes in *Escherichia coli* DNA. Detection by pulsed field gel electrophoresis and evidence for involvement of homologous recombination. *J Mol Biol*. 243(4):611–20.

92. Nakayama K, Shiota S, Nakayama H. 1988. Thymineless death in *Escherichia coli* mutants deficient in the RecF recombination pathway. *Can. J. Microbiol.* 34(7):905–7.

93. Neuhard J, Nygaard P. 1987. Purines and Pyrimidines. *Escherichia coli* and *Salmonella typhimurium.* Cellular and Molecular Biology. American Society for Microbiology, Washington D.C. 445–473 pp. F.C. Neidh ed.

94. Neuhard J, Nygaard P. 1987. *Escherichia coli* and *Salmonella typhimurium.* Cellular and molecular biology. ASM Press, Washington D.C. 445–473 pp. F.C. Neidh ed.

95. Ny T, Bjork G. 1980. Cloning and restriction mapping of the *trmA* gene coding for transfer ribonucleic acid (5-methyluridine)-methyltransferase in *Escherichia coli* K-12. *J Bacteriol*. 142:371–79.

96. O'Donovan GA, Edlin G, Fuchs JA, Neuhard J, Thomassen E. 1971. Deoxycytidine triphosphate deaminase: characterization of an *Escherichia coli* mutant deficient in the enzyme. *J. Bacteriol.* 105(2):666–72.

97. Ohkawa T. 1975. Studies of intracellular thymidine nucleotides. Thyminless death and the recovery after re-addition of thymine in *Escherichia coli* K 12. *Eur. J. Biochem*. 60:57–66.

98. Ohkawa T. 1976. Studies of intracellular thymidine nucleotides. Relationship between the synthesis of deoxyribonucleic acid and the thymidine triphosphate pool in *Escherichia coli* K12. *Eur. J. Biochem*. 61(1):81–91.

99. Okagaki H, Tsubota Y, Sibatani A. 1960. Unbalanced growth and bacterial death in thymine-deficient and ultraviolet irradiated *Escherichia coli*. *J. Bacteriol.* 80:762–71.

100. Okazaki R. 1959. Isolation of a new deoxyribosidic compound thymidine diphosphate rhamnose. *Biochem. Biophys. Res. Commun.* 1(1):34–38.

101. Okazaki R, Okazaki T. 1958. Studies of deoxyribonucleic acid synthesis and cell growth in the deoxyriboside-requiring bacteria Lactobacillus acidophilus. I. Biological and chemical nature of the intra-cellular acid-soluble deoxyribosidic compounds. *Biochim. Biophys. Acta.* 28(3):470–82.

102. Okazaki R, Okazaki T, Kuriki Y. 1959. Incorporation of [3H]thymidine in a deoxyriboside-requiring bacterium. *Biochim. Biophys. Acta.* 33:289–91.

103. Okazaki T, Strominger JL, Okazaki R. 1963. Thymidine diphosphate -L-rhamnose metabolism in smooth and rough strains of *Escherichia coli* and *Salmonella weslaco*. *J Bacteriol.* 86:118–24.

104. Paulander W, Wang Y, Folkesson A, Charbon G, Løbner-Olesen A, Ingmer H. 2014. Bactericidal antibiotics increase hydroxyphenyl fluorescein signal by altering cell morphology. *PLoS One*. 9(3):3–6.

105. Peterson CN, Mandel MJ, Silhavy TJ. 2005. *Escherichia coli* Starvation Diets : Essential nutrients weigh in distinctly. *J. Bacteriol.* 187(22):7549–53.

106. Phillips RJ, Hickleton DC, Boehmer PE, Emmerson PT. 1997. The RecB protein of *Escherichia coli* translocates along single-stranded DNA in the 3' to 5' direction: A proposed ratchet mechanism. *Mol. Gen. Genet.* 254(3):319–29.

107. Pisabarro A, Canada F, Vazquez D, Arriga P, Rodriguez-tebar A. 1986. Structural modification of Escherichia coli peptidoglycan induced by bicyclomycin. *J. Antibiot. (Tokyo)*. 39(7):914–21.

108. Potrykus K, Cashel M. 2008. (p)ppGpp: Still magical? *Annu. Rev. Microbiol.* 62:35–51.

109. Pubchem. *proguanil|C11H16CIN5- PubChem*. pubchem.ncbi.nlm.nih.gov.

110. Rao TVP, Kuzminov A. 2019. Sources of thymidine and analogs fueling futile damage-repair cycles and ss-gap accumulation during thymine starvation in *Escherichia coli*. *DNA Repair (Amst).* 75:1–17.

111. Renggli S, Keck W, Jenal U, Ritz D. 2013. Role of autofluorescence in flow cytometric analysis of *Escherichia coli* treated with bactericidal antibiotics. *J. Bacteriol.* 195(18):4067–73.

112. Reyes-Lamothe R, Possoz C, Danilova O, Sherratt DJ. 2008. Independent positioning and action of *Escherichia coli* replisomes in live cells. *Cell*. 133(1):90–102.

113. Reynes JP, Tiraby M, Baron M, Drocourt D, Tiraby G. 1996. *Escherichia coli* thymidylate kinase: Molecular cloning, nucleotide sequence, and genetic organization of the corresponding *tmk* locus. *J Bacteriol*. 178(10):2804–12.

114. Richardson CC, Schildkraut CL, Kornberg A. 1963. Studies on the replication of DNA by DNA polymerases. *Cold Spring Harb. Symp Quant Biol*. 28:9–19.

115. Rick PD, Wolski S, Barr K, Ward S, Ramsay-Sharer L. 1988. Accumulation of a lipid-linked intermediate involved in enterobacterial common antigen synthesis in *Salmonella typhimurium* mutants lacking dTDP-glucose pyrophosphorylase. *J. Bacteriol.* 170:4008–14.

116. Rochards RG, Browne OE, Gillison ML, Sedwick WD. 1986. Drug concentration-dependent DNA lesions are induced by the lipid-soluble antifolate, Piritrexim (BW301U). *Mol. Pharmacol.* 30:651–58.

117. Samuel G, Reeves P. 2003. Biosynthesis of O-antigens: Genes and pathways involved in nucleotide sugar precursor synthesis and O-antigen assembly. *Carbohydr. Res.* 338(23):2503–19.

118. Sandlie I, Kleppe K. 1980. Mechanism of inhibition of thymidine kinase from *Escherichia coli* by caffeine. *FEBS Lett.* 110(2):6–9.

119. Sangurdekar DP, Hamann BL, Smirnov D, Srienc F, Hanawalt PC, Khodursky AB. 2010. Thymineless death is associated with loss of essential genetic information from the replication origin. *Mol. Microbiol.* 75(6):1455–67.

120. Sat B, Reches M, Engelberg-kulka H. 2003. The *Escherichia coli mazEF* suicide module mediate thymineless death. *J. Bacteriol.* 185(6):1803–7.

121. Schwartz M. 1978. Thymidine phosphorylase from *Escherichia coli*. In *Methods in Enzymology*, pp. 442–45.

122. Schweder T, Lee KH, Lomovskaya O, Matin A. 1996. Regulation of *Escherichia coli* starvation sigma factor (Sigma S) by ClpXP protease. *J Bacteriol.* 178(2):470–76.

123. Scocchera E, Wright DL. 2018. The Antifolates. *Top. Med. Chem.* 26(3):123–49.

124. Sedwick CD, Kutler M, Brown OE. 1981. Anti-folate-induced misincorporation of deoxyuridine monophosphate into DNA: inhibition of high molecular weight DNA synthesis in human lymphoblastoid cells. *Proc Natl Acad Sci USA.* 78:917–21.

125. Setlow P. 2014. Spore resistance properties. *Microbiol. Spectr.* 2(5):1–14.

126. Sévin DC, Fuhrer T, Zamboni N, Sauer U. 2017. Nontargeted in vitro metabolomics for high-throughput identification of novel enzymes in *Escherichia coli*. *Nat. Methods*. 14(2):187–94.

127. Shlomai J, Kornberg A. 1978. Deoxyuridine Triphosphatase of *Escherichia coli*. Purification, properties, and use as a reagent to reduce uracil incorporation into DNA. *J. Biol. Chem.* 253(9):3305–12.

128. Smith GR, Stahl FW. 1985. Homologous recombination promoted chi sites and RecBC enzyme of *Escherichia coli*. *Bioessays*. 2(6):244–49.

129. Sonenshein AL, Hoch JA, Losick R. 2002. *Bacillus subtilis* and its closest relatives: from genes to cells. ASM Press, Washington D.C.

130. Stevenson G, Neal B, Liu D, Hobbs M, Packer NH, et al. 1994. Structure of the O antigen of *Escherichia coli* K-12 and the sequence of its rfb gene cluster. *J. Bacteriol.* 176(13):4144–56.

131. Tadokoro T, Kanaya S. 2009. Ribonuclease H: Molecular diversities, substrate binding domains, and catalytic mechanism of the prokaryotic enzymes. *FEBS J.* 279:1482–93.

132. Taylor AF, Weiss B. 1982. Role of exonuclease III in the base excision repair of uracil- containing DNA. *J Bacteriol*. 151(1):351–57.

133. Tinkelenberg BA, Hansbury MJ, Ladner RD. 2002. dUTPase and uracil-DNA glycosylase are central modulators of antifolate toxicity in *Saccharomyces cerevisiae*. *Cancer Res.* 62(17):4909–15.

134. Tomaz H, Franz W, Wilhelm G. 1979. Thymidylate Synthetase from *Escherichia coli* K12. Purification and dependence of kinetic properties on sugar conformation and size of the 2’ substituent. *Eur. J. Biochem*. 102:223–30.

135. Umezu K, Kolodner RD. 1994. Protein interactions in genetic recombination in *Escherichia coli*. Interactions involving RecO and RecR overcome the inhibition of RecA by single-stranded DNA-binding protein. *J. Biol. Chem.* 269(47):30005–13.

136. Vlamakis H, Chai YR, Beauregard P, Losick R, Kolter R. 2013. Sticking together: Building a biofilm the *Bacillus subtilis* way. *Nat Rev Microbiol*. 11:157–68.

137. Vollmer W, Blanot D, De Pedro MA. 2008. Peptidoglycan structure and architecture. *FEMS Microbiol. Rev.* 32(2):149–67.

138. Warner HR, Duncan BK, Garrett C, Neuhard J. 1981. Synthesis and metabolism of uracil-containing deoxyribonucleic acid in *Escherichia coli*. *J Bacteriol*. 145(2):687–95.

139. Yu M, Souaya J, Julin DA. 1998. The 30-kDa C-terminal domain of the RecB protein is critical for the nuclease activity, but not the helicase activity, of the RecBCD enzyme from *Escherichia coli*. *Proc. Natl. Acad. Sci. U. S. A.* 95(3):981–86.

140. Zaritsky A, Woldringh CL, Einav M, Alexeeva S. 2006. Use of thymine limitation and thymine starvation to study bacterial physiology and cytology. *J. Bacteriol.* 188(5):1667–79.

CHAPTER 2: SOURCES OF THYMIDINE AND ANALOGS FUELING FUTILE DAMAGE-REPAIR CYCLES AND SS-GAP ACCUMULATION DURING THYMINE STARVATION IN *ESCHERICHIA COLI*

2.1 Introduction

Death in the absence of dTTP synthesis in a *thyA* mutant of *E. coli* was first described in 1954 by Barner and Cohen and was called thymineless death (TLD)(4, 16). The *thyA* mutants can still be propagated in media containing either thymine or thymidine (collectively referred to as "T"), whereas changing cells to media lacking thymine/thymidine induces T-starvation, a condition that develops similarly in other *thy* mutant prokaryotes and eukaryotes that always ends with TLD (1). TLD is a unique phenomenon, as starvation in *E. coli* typically causes cessation of metabolism and stasis, rather than loss of viability, be it for an essential metabolite, like an amino acid or an RNA base(4, 9), or general starvation for carbon or nitrogen source (62). In contrast, T-starvation is characterized by a severe inhibition of DNA synthesis in combination with with normal rates of RNA and protein synthesis — in fact, such an "unbalanced growth" was the first general explanation for the viability loss during TLD (15, 16).

Synthesis of dTTP inside the cell requires additional steps compared to the other three DNA precursors. Ribonucleotide diphosphate reductase (the product of a generic *nrd* locus) converts ribonucleotide diphosphates (ADP, GDP, CDP and UDP) into deoxyribonucleotide diphosphates, an essential step in biosynthesis of DNA precursors (Fig. 2.1A) (69). The deoxyribonucleotide diphosphates (dADP, dGDP, dCDP, dUDP) are then phosphorylated by the nucleotide diphosphate kinase (*ndk*) to become

deoxyribonucleotide triphosphates, yielding three out of the four DNA precursors. Since DNA contains thymine instead of uracil, dUTP generated either by the action of Ndk on dUDP or by deamination of dCTP by deoxycytidine deaminase (*dcd*) is first hydrolyzed to dUMP by dUTPase (*dut*), while dUMP is then methylated to yield dTMP by thymidylate synthase (*thyA*) (Fig. 2.1A, the green pathway), the only pathway in *E. coli* for *de novo* production of dTTP (69).

In contrast to *thyA*, the *dut* mutants (point mutations with no detectable dUTPase activity) are still viable (35, 46), due to the dUMP production from dU via thymidine (deoxyuridine) kinase (*tdk*) (Fig. 2.1A) (69), while the *dut tdk* combination is lethal, apparently due to its inability to produce dUMP (86). Curiously, the *dut tdk* block cannot be circumvented by dT supplementation (86), as thymidine kinase is also required to phosphorylate dT into dTMP (69). In contrast to the *dut tdk* double mutants, *thyA* mutant grows normally on a medium supplemented with thymidine or thymine (Fig. 2.1A, the yellow pathway) (4, 16). Thymine is converted to thymidine by deoxyribosyl transferases (*deoA* or *udp*), while thymidine is phosphorylated to dTMP by thymidine kinase (*tdk*) (69). Then, dTMP is phosphorylated to dTDP by thymidine monophosphate kinase (*tmk*), while dTDP to dTTP phosphorylation is done by the non-specific nucleotide diphosphate kinase (*ndk*) (Fig. 2.1A) (69).

Since the absolute bulk of thymine in the cell is in DNA (69), T-starvation was always thought to kill via disbalancing DNA replication due to unavailability of dTTP (15). Starvation for all 4 DNA precursor by HU addition is only bacteriostatic (51), emphasizing that the key to lethality is the absence of only one of the DNA precursors, rather than slow replication per se. Interestingly, starvation for another DNA precursor,

dGTP, was recently characterized as a phenomenon that shares major features with TLD (39, 40), further strengthening the idea of replication disbalance as the cause of death during T-starvation. Indeed, while actively replicating cells are susceptible to T-starvation, cells that cannot initiate a new replication round become immune to it (57). Further linking T-starvation with replication fork problems were reports of branched chromosomal structures (stalled replication intermediates?), massive degradation of the overinitiated chromosomal macrodomain around *oriC* (24, 53, 77), induction of SOS response (38, 52) and correlation of severity of TLD with the number of chromosomal replication rounds before starvation (61).

T-starvation in *thyA* mutant of *E. coli* begins with a resistance phase, that lasts an equivalent of two generations in cultures grown in the presence of thymine, during which the number of colony forming units remains stable (52, 53). At 37°C, used throughout this work, the resistance phase lasts 1 hour, or about two divisions during uninhibited growth (Fig. 2.1B). Although the ongoing chromosomal replication in the *E. coli* cells exhausts the internal dTTP pools within several minutes into starvation (68, 72), the cells continue to maintain their titer during the resistance phase, cell body widening and elongating around the brighter and compact nucleoid mass (Fig. 2.1C).

If thymidine is not added at the end of the resistance phase, the culture titer plunges over the period of the next several hours by several orders of magnitude during the so-called rapid exponential death (RED) phase (Fig. 2.1B) (52, 53). During the RED phase, the cells elongate further, but nothing appears to happen with the centrally-located compact nucleoids (Fig. 2.1C). It is thus conceivable that the resistance phase of thymine starvation reflects cell's limited ability to recruit thymine from minor sources to maintain

a steady minimal rate of DNA synthesis producing normal nascent DNA, while the sudden onset of the RED phase may reflect a switch of T-starved cells to incorporation of thymine analogs, that will have to be excised from DNA, initiating a futile incorporation-excision cycle that eventually inactivates DNA (43).

In fact, the T-starvation pathology has been repeatedly explained by mis-incorporation of deoxy-uridine (dU) in place of thymidine (Fig. 2.1A, the magenta pathway) (1, 10, 30, 31, 43). Once incorporated, DNA-dU is rapidly removed by uracil-DNA-glycosylase (UDG), generating an abasic site, which is incised by exonuclease III (*xthA*) or endonuclease IV (*nfo*), generating a substrate for repair synthesis and ligation (Fig. 2.1A) (28). In the absence of dTTP, subsequent repair synthesis must again use dU in place of dT, initiating a futile DNA-dU insertion-excision cycle (Fig. 2.1A, the magenta cycle). Such futile insertion-excision cycle is proposed to kill either by itself (56), or via formation of double-strand gaps (49), or via improper recombinational repair (66).

The overall consideration of the DNA precursor biosynthesis, incorporation and excision pathways (Fig. 2.1A) naturally leads to an expectation that mutants affecting intracellular pools of thymidine or deoxyuridine should have significant effects on the TLD kinetics. The TLD kinetics curve under standard conditions is highly reproducible (note the tiny error bars in Fig. 2.1B), facilitating detection of either exacerbation or amelioration of TLD. Surprisingly, instead of defects in nucleotide metabolism, the only known defects strongly affecting TLD kinetics are those in recombinational repair(65). In particular, the *recBCD* mutants in double-strand break repair lack the resistance phase (Fig. 2.1D) (52, 65), suggesting formation of double-strand breaks in chromosomal DNA

early on during T-starvation, which was indeed confirmed (32, 52, 53). At the same time, the *recF, recO* and *recJ* mutants in blocked ss-gap repair slow down the RED phase (Fig. 2.1D), suggesting formation of single-strand gaps (ss-gaps) in chromosomal DNA later on during T-starvation (24, 52, 65). Since recombinational repair in bacteria is mostly used to address problems at replication forks (55), the strong TLD phenotypes of *rec* mutants support the view of thymineless death as "stalemate of starved replication forks". Indeed, even if an inhibited and broken replication fork is successfully repaired, this cellular effort remains non-productive during T-starvation, because the restored forks are still inhibited and will break again, in another futile cycle, this one of fork breakage-and-repair (Fig. 2.1E). Persistent replication fork problems during T-starvation induce massive SOS-response (52) (a transcription response of bacterial cells to replication problems (55)), which is proposed to be one of the killing mechanisms during TLD(24).

If cells employ strategies to avoid or delay the futile fork breakage-repair cycle at the beginning of T-starvation, for example by manipulating nucleotide pools, the resistance phase and transition to the RED phase hold keys to understanding these strategies. Therefore, we sought to identify mutants affecting the (deoxy)thymidine and (deoxy)uridine pools in *E. coli* that would either accelerate or slow down TLD, similar to the *recBCD* or *recF* mutants (compare Fig. 2.1D with Fig. 2.2). We anticipated that functions disabled in TLD-accelerating mutants normally provide a major (non-biosynthetic) source of endogenous thymine/thymidine, while functions disabled in TLD-slowing mutants normally suppress such a source, including base analogs, or excise misincorporated base analogs from DNA (Fig. 2.2). In our search for such mutants, we were guided by the four possible explanations of the resistance phase (Fig. 2.1F): I)

alternative internal sources of dT, maintaining slow fork progress; II) dU misincorporation; III) rU misincorporation; IV) discontinuous DNA synthesis, leading to accumulation of single-strand gaps (ss-gaps) in nascent DNA. Our findings reveal not only new survival strategies in response to T-starvation, but also a potential mechanistic cause of TLD pathology.

2.2 Results

2.2.1 The spike of chromosomal fragmentation could drive intrachromosomal DNA redistribution

If T-starvation is indeed the "stalemate of starved replication forks", the cell could resolve it by reducing the number of active replication forks. Two major physical processes were reported during the resistance phase of T-starvation (52, 53): 1) significant yet rapidly diminishing DNA synthesis; 2) chromosomal fragmentation, interpreted to reflect replication fork disintegration. However, the occurrence of chromosomal fragmentation during the resistance phase of TLD was dependent on conditions (32, 53, 66, 94), while its nature was unclear, so we decided to determine its kinetics.

The time course of chromosomal fragmentation in the repair proficient *thyA* mutants during thymine starvation showed an early peak with subsequent disappearance (Fig. 2.3AB), as reported before (52). In continued T-starvation, chromosomal fragmentation was reported to reappear at 28°C (52), but at 37°C we did not detect any significant increase at later times (Fig. 2.3AB). Thus, the peak of fragmentation at 37°C coincides with the resistance phase, while the disappearance occurs during the RED

phase, — suggesting that either irreparable chromosomal fragmentation is not involved in TLD pathology, or that subsequent breaks in the replicating chromosome fail to generate linear subchromosomal fragments (detectable by pulsed-filed gels).

Since previous measurements of the total chromosomal DNA during thymine starvation would uniformly report minimal changes (5, 10, 29, 53, 88), we reasoned that the coincidence of the residual DNA synthesis, double-strand breaks and the overall stability of DNA amount could reflect an intracellular zero-sum redistribution of the scarce thymidine. Specifically, the broken DNA, if degraded rather than repaired, could provide thymidine to support the still surviving replication forks during the resistance phase (Fig. 2.3C) (25). This strategy of intrachromosomal DNA redistribution ("intrachromosomal cannibalism") resolves the stalemate of starved replication forks by a combination of antagonistic methods to eliminate replication forks as the "problematic chromosomal points". Indeed, the failed forks could be denied repair, targeting the resulting linear chromosomal branches for degradation, so that the released thymidine would allow the surviving forks to terminate the current replication round, — eventually eliminating all replication forks in the chromosomes (Fig. 2.3C). Termination of chromosomal replication should trigger cell division — and indeed direct counting of cells revealed cell doubling in the T-starved cultures within the resistance phase (Fig. 2.3D).

2.2.2 Reducing linear DNA degradation has no effect on the resistance phase

If the resistance phase of TLD is due to such intrachromosomal DNA redistribution, then minimizing linear DNA degradation, while keeping recombinational

repair of disintegrated replication forks functional, should exacerbate the futile fork breakage-repair cycle (Fig. 2.1E). Indeed, even though the unstable replication forks are efficiently repaired, such repair becomes counterproductive without linear DNA degradation to generate any endogenous thymidine from extra chromosomal parts. If true, the "degradation-reduced" conditions should lead to the disappearance of the resistance phase during T-starvation and to deepening of the RED phase.

We tested this prediction in two ways. The *recBC sbcBC* mutant lacks the major linear duplex DNA degradase (RecBCD helicase/nuclease), as well as two major ssDNA degradases, Exo I and SbcCD nucleases (reviewed in (55)). The resulting mutant is grossly deficient in the linear DNA degradation (75, 95), as revealed by its inability to degrade chromosomal DNA after UV irradiation, if RecA is not available (Fig. 2.3E and S2A). At the same time, the mutant is fully proficient in recombinational repair, via the RecFOR pathway (55). Contrary to our expectations, TLD kinetics in the *recBC sbcBC thyA* mutant featured exactly the same 1-hour resistance phase as in the linear DNA degradation-proficient *thyA* mutant (Fig. 2.3F). At the same time, the *recBC sbcBC thyA* mutant does develop a faster RED phase and decreased survival, showing that cannibalizing the failed chromosomal branches indeed helps a small fraction (~1 out of 100) of starved cells to delay TLD.

To achieve a reduced linear DNA degradation with normal recombinational repair differently, we expressed (by arabinose induction off pKD46 plasmid (20)) phage lambda genes *alpha, beta* and *gamma* coding, correspondingly, for lambda exonuclease, ssDNA annealing protein and the inhibitor of the RecBCD enzyme (reviewed in (55)). This setup again shows no change in the resistance phase, yet a faster RED phase and decreased

survival, repeating the effects of the *recBC sbcBC* mutant (Fig. 2.4B). Since the resistance phase was independent of the linear DNA degradation capacity of *thyA* mutant, counter to the prediction of the intrachromosomal DNA redistribution idea, we tested the idea with physical assays.

2.2.3 Genomic DNA increase during the resistance phase

A strong prediction of the intrachromosomal cannibalism idea is that T-starvation should not change the total DNA amount, at least not during the resistance phase. As was mentioned above, previous multiple studies reported no significant chromosomal DNA change during T-starvation (5, 10, 29, 53, 88), consistent with this idea. At the same time, during the resistance phase the average rate of residual replication is still 10% of the normal (+dT) rate (53). Since the resistance phase was not due to linear DNA degradation, this significant DNA synthesis rate could translate into a measurable genomic DNA accumulation, apparently missed by the previous studies, perhaps because the standard DNA purification techniques become inadequate during T-starvation.

To resolve the issue, we used our plug-blotting technique for total cellular DNA content (47), to minimize sample handling and DNA loss due to extraction methods. In contrast to the previous studies, we found that in a *thyA* mutant during T-starvation, the amount of DNA increases by 1.5 times in the first hour, but then steadily decreases to the original amount by 5.5 hours (Fig. 2.3G). In other words, the resistance phase of T-starvation is associated with a significant chromosomal DNA accumulation, whereas the RED phase coincides with disappearance of a similar amount of DNA (perhaps mostly affecting the new DNA synthesized during T-starvation?). This later DNA disappearance

is not reduced (in fact appears stronger) in the *thyA recBCD* mutant (Fig. 2.4C), so its nature remains unclear at the moment. Important for our argument, though, the initial 1.5x increase is inconsistent with the zero-sum game of intrachromosomal DNA redistribution, suggesting instead non-chromosomal sources of dT.

2.2.4 Evolution of the copy number of origin versus terminus

Two parameters describe chromosomal replication: the rate of initiation from the replication origins and the rate of elongation of the resulting replication forks. In the bacterial chromosome, quantification of both parameters is facilitated by the unique replication origin and terminus. Indeed, initiation can be monitored by increase in the *origin* copy number, while elongation can be similarly monitored as completion of the chromosomal replication, by increase in the *terminus* copy number.

Perhaps the strongest prediction of the intrachromosomal DNA redistribution idea is the decrease of the cannibalized origin-containing parts of the chromosome, matched by a similar increase in the replicated terminus-containing parts of the chromosome (presented schematically in Fig. 2.3H). When we measured the evolution of the chromosomal origin copy number versus the terminus copy number during thymine starvation, in contrast to these predictions we found a sharp increase in the copy number of the origin during the resistance phase (Fig. 2.3I), suggesting adequate levels of dTTP for initiation of at least one round of chromosomal replication. At the same time, the subsequent gradual disappearance of the origin during the RED phase is consistent with the suspected instability of the DNA synthesized during the resistance phase. Thus, the observed evolution of the origin amounts (Fig. 2.3I) was at odds with predictions of the

DNA redistribution model (Fig. 2.3H), but generally consistent with prior measurements at 28°C (53).

The evolution of the terminus DNA copy number during thymine starvation was generally like the evolution of the overall DNA (Fig. 2.3G vs. I) (53). Specifically, terminus accumulates to 1.5X of the original value during the resistance phase, reflecting significant progress of replication forks and again suggesting adequate availability of dTTP. During the RED phase, terminus experiences a gradual drop to ~60% of the original value, which translates into almost three-fold loss from the peak value at 1 hour (Fig. 2.3I).

Overall, we found that the chromosomal replication during the resistance phase of T-starvation affects not only the terminus half of the chromosome, but also its origin half, apparently making the whole chromosome unstable during the subsequent RED phase (Fig. 2.4D). In summary, our studies of the chromosomal DNA dynamics during thymine starvation suggest: 1) limited but adequate supplies of dTTP or its analog during the resistance phase; 2) RED-phase instability of the DNA synthesized during the resistance phase, suggesting that the nascent DNA is defective; 3) unclear nature of this RED-phase chromosomal DNA instability. Most importantly for our model (Fig. 2.3C), the initial increase followed by a similar decrease in both origin and terminus during T-starvation argue against the intrachromosomal DNA redistribution idea, but imply the existence of an intracellular source of dT or its analog (incorporation of which would make DNA unstable).

2.2.5 Endogenous thymine from stable RNA

An apparent endogenous source of thymine is the ribo-thymine from tRNAs and rRNAs, if the two stable RNA species are somehow destabilized during T-starvation (Fig. 2.1A, the cyan pathway). Rapidly-growing *E. coli* cells have ~50,000 ribosomes and 500,000 tRNA molecules per cell (11). Every tRNA has a single thymine residue (T54), while every 23S rRNA has two thymines (Fig. 2.5A) (80). If all this thymine is somehow extracted from stable RNA, the 600,000 thymine residues could potentially support synthesis of four times as much DNA, ~$2.4x10^6$ nt, or about quarter of the genome equivalent, roughly half of the overall chromosomal DNA increase we detect during the resistance phase (Fig. 2.3G). As a quick check of the logic, we artificially destabilized tRNA and rRNA with a short sub-lethal heat-shock, — and found that such heat-shock does enhance survival during subsequent thymine starvation (Fig. 2.5B), — although other interpretations are possible with such a pleotropic treatment.

Then we checked stability of the two stable RNA species by growing *thyA* mutant cells in the medium +dT supplemented with ^{32}P-orthophosphoric acid, changing the medium to the one without both the label and dT, and measuring the amount of the remaining ^{32}P label in the rRNA and tRNA, separated on an agarose gel, at various time points during the ensuing T-starvation (Fig. 2.6A). We found that ~20% of both rRNA and tRNA are lost during the first hour of T-starvation, and ~40% is lost by 4 hours (Fig. 2.5C, Fig. 2.6BC). Thus, ribo-thymine does become available in T-starved cells, while any turnover of stable RNA, even though much slower than that of mRNA, should further contribute to this thymine source. Remarkably, this "mining" of ribo-thymine from stable RNA not only could support existing replication forks but should also block further

initiations from the origin by inhibiting proteins synthesis (Fig. 2.5D). In this respect, it could be an ingenious strategy to re-balance metabolism, thrown out of balance by T-starvation.

Specific RNA-uracil methylase TrmA methylates U54 in tRNA, while RumB and RumA methylases methylate, correspondingly, U747 and U1939 in 23S rRNA (58). We deleted the *trmA, rumB* and *rumA* genes in the *thyA* mutant background, expecting that, if ribo-thymine is indeed used for DNA synthesis during thymine starvation, the mutants would show a shorter resistance phase, but likely no increase in the depth of the RED phase. The results again turned out to be the opposite of our expectation, as the *thyA trmA* strain shows no changes in the resistance phase, but a faster and deeper RED phase than in the *thyA* strain (Fig. 2.5E). The *rumA* and *rumB* defects made the TLD curve only slightly deeper, suggesting a truly minor thymine contribution from 23S rRNA (Fig. 2.5F, Fig. 2.6D). Combining the *rum* and the *trmA* defects together resulted in a detectable additivity (Fig. 2.5G), showing overall that ribo-thymine from stable RNA is indeed a dTTP source in a small sub-population (~1 in 10^3) of *thyA* cells, that makes these cells immune to TLD.

The lack of the ribo-thymine influence on the bulk population is supported by the physical measurements, as the *trmA* defect changes neither the overall pattern of chromosomal DNA evolution during TLD (Fig. 2.5H), nor the origin and terminus copy number initial increase and subsequent decrease (Fig. 2.6EF). Altogether, we conclude that thymine derived from stable RNA does not explain the resistance phase, but the way removal of this source of thymine accelerates the RED phase and decreases survival (Fig.

2.5G) indicates a small sub-population of cells that does recruit enough thymine from stable RNA, mostly from tRNA, to survive thymineless death.

2.2.6 Abasic site nuclease deficiency exacerbates TLD

Having found no internal source of dT to support the resistance phase, we turned to dT analogs. Uracil in the form of dUTP is incorporated into DNA in place of thymine during normal replication (44). Much less frequently, cytosine in DNA spontaneously deaminates to uracil (26). Although uracil-DNA incorporation is 10^5 times more frequent than cytosine deamination, the former is not associated with any mutagenesis, in contrast to the latter scenario, where the next round of DNA replication yields transitions (G→A, C→T). To prevent this, the cell has a dedicated machinery to excise uracils from DNA (Fig. 2.1A, the magenta pathway) (28).

Inhibition of thymidylate synthase leads to a great expansion of dUTP pools in mammalian cells (30); in the Δ*thyA* mutants of *E. col* without dT supplementation, the intracellular dUTP pools must be also elevated, as judged by the increased DNA-dU incorporation (89). 75% of dUTP in the *E. coli* cells is generated by deoxycytidine deaminase (Dcd) acting on dCTP (Fig. 2.1A, the green pathway)(70). dUTP is converted to dTMP by the consecutive action of Dut and ThyA (Fig. 2.1A). When a sufficient pool of dTMP is generated, it inhibits the Dcd enzyme (6). In the absence of enough dTMP, Dcd remains active, elevating the pool size of dUTP,— which causes problems in the *dut* mutants, so that, for example, the *dut thyA* double mutants grow poorly even if supplemented with exogenous dT (Fig. 2.7A).

As mentioned in the introduction, the most popular explanation of TLD envisions that dUTP pool expansion in *thyA* mutants leads to repeated incorporation of dU into DNA in place of dT, followed by uracil excision that, via the futile repair cycle, somehow leads to TLD (Fig. 2.1A and 2.8A) (1, 10, 31, 30, 43). If during the resistance phase DNA-dU excision could be transiently suppressed (by unknown mechanisms), this would explain both the observed DNA synthesis and cell survival. Moreover, if suppression of this DNA-dU excision was then lifted during the RED phase, the resulting futile DNA-dU incorporation-excision cycle would provide an explanation for the RED phase.

The idea implies that, without dU incorporation into DNA of thymine-starved cells, there could be no thymineless death, only stasis. This reasoning predicts that *dcd* inactivation should ameliorate TLD (since 3/4 of all dUTP is generated via this route (70)), but we found the TLD kinetic unaffected by the *dcd* defect (Fig. 2.7B). We have also inactivated Exo III and Endo IV, the two abasic site endonucleases of *E. coli* that are critical for completion of uracil excision repair (28) (Fig. 2.1A, the magenta pathway), alone or together. The RED phase was somewhat accelerated in the single mutants and dramatically accelerated in the double *xthA nfo* mutant, ending with a reduced resistance phase and a lower survival (Fig. 2.8B), — which indicates significant base-excision repair efforts during the RED phase. It should be noted, though, that base excision repair removes all kinds of DNA modifications, so incorporation of modified nucleotides other than dU, or processing of other types of DNA lesions during T-starvation, cannot be excluded.

2.2.7 Supposed replacement of dT with stable DNA-dU does not prevent TLD

To test the validity and limitations of the futile DNA-dU incorporation-excision cycle for TLD, we employed mutants deficient in either uracil excision (*ung*) or dUTPase activity (*dut*), or both (*dut ung*), in the *thyA* background. TLD was supposed to be slightly relieved in the *ung thyA* mutant, deficient in uracil-DNA-glycosylase, because incorporated DNA-dU becomes stable in this mutant (Fig. 2.8A). In contrast, we expected a deeper death in the *dut thyA* mutant because of the further elevated dUTP pool stimulating an even more frequent uracil-DNA incorporation and thus exacerbating the futile cycle. The situation should again change in the *dut ung thyA* triple mutant, where, because of the increased DNA-dU incorporation without excision, replication forks should be stabilized, preventing TLD (Fig. 2.8A).

Since the *dut thyA* mutant grows extremely poorly even in the presence of thymidine (Fig. 2.7A), we alleviated its growth problems by blocking the major route of dUTP biosynthesis with the *dcd* mutation, which by itself has no influence on the TLD kinetics (Fig. 2.7B). We found almost no difference in the TLD kinetics between the *dut dcd thyA* and *ung dcd thyA* triple mutants and their *dcd thyA* double mutant parent (Fig. 2.7C), whereas the *dut ung dcd thyA* quadruple mutant showed a two-times longer resistance phase and the slightly slower RED phase with higher survival (Fig. 2.7C). Since the unexpectedly modest effects of the *dut* and *ung* mutations could be due to the nucleotide pool changes in the *dcd* background, we decided to return to the Dcd+ *thyA* mutant set, while better managing its growth and handling.

The major handling problem of the slow-growing *dut thyA* mutant was the attachment of cells to filters during changing the medium from +dT to –dT, so in this set

of strains we collected cells by centrifugation instead. The TLD curve of the *thyA* mutant was almost the same in the new protocol (Fig. 2.8C), but there was a noticeable aggravation of the RED phase by the *ung* defect (Fig. 2.8C) — as if uracil excision does not contribute to the pathology of thymine starvation, but does contribute a small alternative source of thymine. At the same time, as expected, we found that the *dut* defect shortens the resistance phase and lowers the survival, but without making the RED phase faster (Fig. 2.8C). Finally, the *dut ung thyA* mutant, that stably incorporates dU into its DNA in place of dT, after a "WT" resistance phase of one hour shows significant, though incomplete, relief of TLD, slowing the RED phase and elevating survival (Fig. 2.8C). The deeper TLD in the *dut thyA* and *ung thyA* mutants, and its 100-fold alleviation in the corresponding *dut ung thyA* combination, offer proof of principle for the toxicity of futile DNA-dU insertion-excision cycle. At the same time, even the *dut ung* defect does not eliminate TLD completely, — perhaps because at a high density DNA-dU incorporation becomes poisonous by itself (22, 23)?

2.2.8 Stable DNA-dU incorporation supports two rounds of chromosomal replication

The improved TLD survival of the *dut ung thyA* mutant implied that the disappearing thymidine was at least partially replaced in the nascent DNA with dU residues (not only numerous, but also stable in the chromosomal DNA in the *ung* background), — and therefore predicted more chromosomal DNA accumulation in the T-starved cells. Indeed, we found accumulation of up to 2.5-times of the original DNA in the *dut ung thyA* cells during 2 hours of thymine starvation (Fig. 2.8D). However, this

DNA became eventually unstable and started rapidly disappearing after 4 hours of T-starvation (Fig. 2.8D). The origin copy number kinetics in the *dut ung thyA* mutant showed one round of initiation by 1 hour into thymine starvation, with the origin copy number essentially plateauing for three hours before going down sharply (Fig. 2.8E). The terminus copy number in the *dut ung thyA* mutant climbs steadily for three hours to the value almost 4x of the initial one, confirming uninterrupted and steady progress of replication forks (Fig. 2.8F). Thus, the *dut ung thyA* mutant completes not only the replication round that was ongoing during the removal of dT, but also the new round initiated during starvation, — however, its chromosome succumbs to degradation anyway (Fig. 2.8DEF). In other words, DNA-dU incorporation without excision supports what looks like stable and complete chromosomal replication — but after the resistance phase the *dut ung thyA* mutant still suffers an unknown problem, resulting in a rapid loss of the chromosomal DNA later on (Fig. 2.7D).

2.2.9 TLD in the *dut ung* mutant is not affected by the *nfi* or *recF* mutations

One possible reason for the eventual degradation of DNA containing dUs in the *dut ung thyA* mutant is that the uracil DNA glycosylase-deficient cells still have endonuclease V, the alternative excision repair enzyme specific against DNA-inosines (91) , that has also a minor activity against DNA-dU in vitro (92). However, inactivation of this minor uracil excision activity in the *nfi* mutant (33) failed to further improve the already shallow TLD kinetics of the *dut ung thyA* mutant (Fig. 2.7E). Also, the quadruple *dut ung nfi thyA* mutant showed essentially the same DNA accumulation during T-starvation compared to its progenitor *dut ung thyA* triple mutant, which was followed by

a similarly dramatic loss of DNA (Fig. 2.7F). Thus, Endo V is neither the cause of the residual TLD in the *dut ung thyA* triple mutant, nor the reason for the eventual decline in the amount of genomic DNA in this mutant, — which is consistent with reports that Endo V does not attack DNA-dU in vivo (33).

The *dut ung thyA* mutants could still succumb to TLD due to the action of the RecFOR pathway for repair of persistent single-strand gaps. Because *recF*, *recO* and *recR* mutations alleviate TLD, persistent single-strand gaps were proposed to accumulate during T-starvation, triggering detrimental recombination (24, 52, 65). Curiously, the TLD curve of the *recF thyA* mutant looks very similar to the TLD curve of the *dut ung thyA* mutant (Fig. 2.8G). If the remaining TLD in the *dut ung thyA* mutant is due to the action of persistent ss-gap repair pathway, the *dut ung recF thyA* quadruple mutant should become virtually resistant to TLD. However, we found that the quadruple mutant has the same TLD kinetics as the *recF thyA* or *dut ung thyA* mutants (Fig. 2.8G), suggesting that stable DNA-dU incorporation is epistatic over the *recFOR* pathway inactivation, probably because formation of persistent single strand gaps in the chromosomal DNA is prevented by filling them in with dU.

We conclude that stable DNA-dU incorporation during T-starvation significantly relieves TLD, most likely by reducing formation of persistent single-strand gaps. Nevertheless, 99% of the T-starved *dut ung thyA* cells still die, perhaps from remaining single-strand gaps, but also possibly from another, unknown reason.

2.2.10 The density of DNA-dUs is increased during T-starvation

We quantified the density of DNA-dU residues by plasmid-relaxation in vitro (44) , treating supercoiled plasmid DNA, isolated from cultures under various conditions, with either Exo III alone (the background, no nicking expected) or UDG + Exo III (DNA backbone is nicked at the removed uracils, relaxing the plasmid) (Fig. 2.9A). The density of uracil is estimated by taking the supercoiled plasmid remaining after the UDG + Exo III treatment for the zero class of the Poisson distribution (44).

Using this sensitive procedure, we could not detect any uracil in the plasmid DNA isolated from growing cultures of the *thyA* or the *thyA dut* mutants (Fig. 2.9A), confirming previous results (44) and demonstrating the efficiency of uracil-DNA glycosylase in the DNA-dU removal. We did detect a modest density of DNA-dU in the plasmid DNA from *ung thyA* double mutant grown in the presence of thymidine (1 uracil in ~75,000 nucleotides in stationary cells, 1 uracil in ~25,000 nucleotides in growing cells) (Fig. 2.9AB), which is significantly increased to 1 uracil in ~6,000 nucleotides after five hours of T-starvation (Fig. 2.9B). However, this DNA-dU incorporation frequency in the Dut+ cells is clearly inadequate to sustain T-starved replication forks, explaining the lack of positive effect of the *ung* inactivation on TLD kinetics (Fig. 2.8C and 2.7C).

As expected, the high density of DNA-uracil in the *dut ung thyA* strain leads to the complete disappearance of the supercoiled species after the combined UDG and Exo III treatment (Fig. 2.9A), thus falling beyond the range of detection of the plasmid relaxation technique. We tried to release a much smaller supercoiled circle by employing Cre-*loxP* site-specific recombination (36), but the efficiency of this in vitro reaction turned out to be inadequate. Eventually, we determined the DNA-dU density in the 234

bp fragment of a plasmid DNA after its denaturation and separation in 3% alkaline agarose, taking for the zero class of the Poisson distribution the remaining full-length ssDNA (Fig. 2.9C). As expected, the frequency of DNA-dU in the *thyA dut ung* mutant was extremely high (Fig. 2.9D), ~1,000 times higher than in the *thyA ung* mutant (cf. Fig. 2.9B and D) and within the ranges reported for this mutant before (89). Unexpectedly, in the *dut ung thyA* mutant, T-starvation caused only ~25% further increase in DNA-dU density (from 1/95 to 1/72 dU/dN) (Fig. 2.9D), perhaps reflecting insufficient sensitivity of our detection system. We conclude that DNA-dUs are indeed stable in the *ung* mutants and massively incorporated in the *dut* mutants, but the unexpectedly small further increase in their density during T-starvation suggests that: 1) there is still some residual amount of dTTP around; 2) replicative polymerases discriminate against dUTP in favor of dTTP in vivo.

Overall, we conclude that significant dT replacement by dU is only possible in the *dut* mutants, which have elevated dUTP pools. From this perspective, the relief of TLD observed in the *dut ung thyA* mutant not only proves that dU can effectively substitute for dT in DNA synthesis during T-starvation, but also provides a strong evidence against contribution of DNA-dU misincorporation/excision to either the resistance or the RED phases in the Dut+ *thyA* mutant cells.

2.2.11 The role of translesion polymerases and rU incorporation

T-starvation strongly induces the SOS response (38, 52) — the increase in transcription of some 30 genes in *E. coli* in response to inhibition of DNA replication associated with accumulation of single-stranded DNA (55). Among other enzymes, the

SOS response elevates expression of three translesion DNA polymerases of *E. coli*, Pol II, Pol IV (gp *dinB*) and Pol V (gp *umuCD*) (67). Both Pol IV and Pol V have spacious active sites that allow them to accommodate template with bulky DNA lesions (41). In addition, Pol V incorporates ribonucleotides during translesion synthesis in vitro (87). It was therefore possible that during T-starvation, ribo-uridine (rU) could be misincorporated into DNA by Pol V across template adenine (Fig. 2.10A), which could exacerbate the RED phase of TLD via futile misincorporation/excision of DNA-rU (Fig. 2.1A, the orange pathway). However, we found no big difference in the TLD kinetics, whether the TLS polymerases are removed individually or together (with the possible exception of a slightly higher survival after 4 hours in the *dinB thyA* double mutant) (Fig. 2.10B).

If rU residues are indeed incorporated in place of dT during T-starvation, they should be subsequently excised by the RNase H enzymes (Fig. 2.10A). There are two RNases H in *E. coli*, I and II, encoded by the *rnhA* and *rnhB* genes, respectively (78). The two RNase H enzymes remove all kinds of rNs from DNA: RNA primers for Okazaki fragments, R-loops, misincorporated single RNA nucleotides. If DNA-rU incorporation starts another futile misincorporation-excision cycle during T-starvation, inactivation of RNase H enzymes should alleviate TLD (Fig. 2.1A, the orange pathway, and Fig. 2.10A). However, we found that the *rnhA thyA* and *rnhB thyA* mutants do not have a significantly different TLD kinetics compared with the *thyA* single mutant (Fig. 2.10C). If anything, and in contrast to our expectations, the *rnhB* defect confers a faster RED phase and lowers the final survival (Fig. 2.10C), as if rN excision from DNA is beneficial for T-starved cells.

To verify the *rnhB* inactivation, which leads to accumulation of single rNs in the DNA (DNA-rNs are undetectable in the RnhB+ cells)(45), we isolated plasmid DNA from *rnhB thyA* and *rnhAB thyA* mutants, grown in the presence or absence of thymidine, and treated it with RNase HII in vitro, to relax rN-containing supercoiled plasmid molecules (Fig. 2.10D) (45). We confirmed a high density of DNA-rNs characteristic of the *rnhB* and *rnhAB* mutants (18, 45) — 1 DNA-rN in 11,603 nt and in 10,644, correspondingly (Fig. 2.10E). We also found a modest increase in the density of DNA-rNs during T-starvation - 1 DNA-rN in 7,621 or in 8,106 nt, correspondingly (Fig. 2.10E). At the same time, this more frequent rU-DNA incorporation does not lead to more genomic DNA accumulation in the *rnhAB thyA* strain, where such DNA-rNs are stable, as compared to the *thyA* strain, but may lead to more DNA loss (Fig. 2.10F). Apparently, DNA-rU stability is mildly poisonous for the T-starved cells.

Since the effect of rU-incorporation by TLS polymerases could be masked by the subsequent efficient DNA-rU excision by RNase H enzymes, we also tested the effect of *dinB* or *umuCD* inactivation on TLD in the *rnhAB thyA* mutant background (Fig. 2.10G). None of the combinations has affected the resistance phase. We observed a slight detrimental effect of the UmuCD inactivation during the RED phase in the *rnhAB thyA* mutant, but this time *dinB* inactivation was also slightly detrimental (cf. Fig. 2.10B and G). Perhaps the most dramatic effect among all these mutants in TLS polymerases and RNase H enzymes is the two orders of magnitude lower survival of the *thyA dinB rnhAB* mutant compared to its *thyA dinB* progenitor (Fig. 2.11). We conclude that TLS polymerases might help tolerate T-starvation, but not by rU incorporation into DNA. In

fact, survival of T-starved cells (most clearly seen with *dinB thyA* mutants) strongly depends on the functional RNase H enzymes (Fig. 2.11).

2.2.12 Accumulation of ssDNA during dTTP starvation

Chromosomal replication during T-starvation was expected to generate persistent ss-gaps in DNA (1, 24, 52, 77). The RecFOR pathway initiates recombinational repair of persistent single strand gaps in DNA by licensing RecA polymerization onto them (55). A major paradox of thymine starvation was that inactivation of the RecFOR DNA repair pathway leads to amelioration of TLD (24, 52, 65), rather than to its aggravation (Fig. 2.1D), supporting the concept of "poisonous repair". Later epistatic analysis suggested that the major detrimental effect of the RecFOR pathway in TLD is via strong SOS induction (24). Here we show that the *recF* mutants accumulate significantly more chromosomal DNA during the resistance phase of thymine starvation, even though they display a similar degree of the chromosomal DNA instability during the subsequent RED phase (Fig. 2.12A). We interpreted this accumulation of more genomic DNA in the absence of the system to repair persistent ss-gaps to mean that the chromosomal DNA synthesis during thymine starvation is associated with formation of ss-gaps, while the RecFOR system curbs this DNA accumulation by trying to repair the ss-gaps. Formation of ss-gaps in the chromosomal DNA of thymine-starved cells was suggested from electron microscopy observations, but prior efforts to quantify this ssDNA accumulation have been unsuccessful (66).

To quantify ss-gaps in DNA during TLD, we have isolated DNA in duplicate agarose plugs and then transferred it, either without prior denaturation, or after standard

denaturation, to nylon membrane for hybridization with a whole genome probe (Fig. 2.12B). The probe can hybridize only to ssDNA, so in the non-denatured samples, hybridization is only possible with ss-gaps 20 nt or longer (due to our 65°C hybridization temperature, using *E. coli* chromosomal DNA, which is 50% GC-rich). The ratio of the signal in the non-denatured DNA plug to the signal in the corresponding denatured DNA plug reveals the fraction of ssDNA in this DNA preparation.

As a positive control for our detection and quantification of ss-gaps in genomic DNA, we treated growing cultures of WT cells with 100 ng/ml azidothymidine (AZT), a chain-terminator nucleotide causing ss-gaps in DNA (17). Without treatment, the cultures start with ~2% ssDNA, apparently reflecting active replication status of the cells, but several hours of normal growth steadily reduce ssDNA to the level just below 1% of the total (therefore, we took 1% as the background of the procedure), apparently due to the decline of DNA replication activity in stationary cells (Fig. 2.12C). In contrast, the AZT-treated cultures showed a steady increase in the amounts of single-stranded chromosomal DNA (Fig. 2.12C). Treatment with AZT leads to even more dramatic increase in ssDNA in the chromosomal DNA preparations of *xthA* and *recA* mutants (Fig. 2.13), as expected from their increased AZT sensitivity (17).

Using this new method of ssDNA detection, we found accumulation of ss-gaps in the chromosomal DNA of *thyA* mutant during T-starvation, but not in the same cells growing with dT (Fig. 2.12D). Some ssDNA already forms during the resistance phase, but the main increase happens once the RED phase begins. As expected, proportion of ss-gaps in DNA of the same *thyA* mutant cells growing with dT approaches background over time, apparently reflecting cessation of the chromosomal replication as the culture

saturates (Fig. 2.12D). The *thyA recF* mutant shows similar accumulation of ss-gaps during T-starvation (Fig. 2.12E). Interestingly, the *thyA dut ung* mutant accumulates less ss-gap DNA during T-starvation (Fig. 2.12F), suggesting that some of the ss-gaps are indeed prevented with the help of DNA-dU incorporation. We conclude that there is a significant ss-gap accumulation in the chromosomal DNA of thymine-starved cells.

If ss-gaps were linked to T-starvation toxicity, then AZT treatment of T-starved cells, by inducing even more ss-gaps in their DNA, should exacerbate TLD. We found it to be the case, as treatment with 100 ng/ml AZT, the dose that is mostly static for a Thy+ sibling in the same medium, reduces the resistance phase in half and deepens the RED phase for the *thyA* mutant (Fig. 2.14A). Remarkably, AZT treatment during T-starvation also rapidly kills the *thyA recF* mutant, that survives T-starvation without AZT much better than the *thyA* single mutant and is not extra-sensitive to AZT when Thy+ (Fig. 2.14B). We conclude that ss-gap accumulation contributes to T-starvation toxicity and may even be its major driver.

2.3 Discussion

To get insights into the mechanisms of TLD we sought mutants in the metabolism of nucleic acids and their precursors that would affect the resistance phase and transition to the RED phase the way the *recBCD* and *recF* mutants in recombinational repair do (Fig. 2.1D vs Fig. 2.2) . To understand the chromosomal aspects of the expected defects, we precisely quantified the total chromosomal DNA and determined its ssDNA fraction. We started by determining the kinetics of chromosomal fragmentation caused by T-starvation, finding to our surprise that after peaking during the resistance phase,

fragmentation disappears at the beginning of the RED phase, weakening the previously proposed link of double-strand breaks to TLD (52). We report a considerable accumulation of the chromosomal DNA during the resistance phase (coincident with fragmentation), followed by return to the original DNA amount during the RED phase (coincident with the disappearance of fragmentation) (cf. Fig. 2.3AB *vs* G). The nature of this chromosomal DNA disappearance is unclear, as the *recBCD* mutant deficient in the main linear DNA degradation activity of *E. coli* cells still shows it (Fig. 2.4C). In general, double-strand breaks, even though numerous early on during T-starvation, do not appear to directly contribute to thymineless death. However, we revealed that the chromosomal DNA in T-starved cells becomes increasingly single-stranded (Fig. 2.12), — providing a potential mechanistic insight into the pathology of thymineless death.

In our experiments with specific mutants, we were guided by two questions: 1) what is the nature of the resistance phase? 2) what is the nature of the abrupt transition from the resistance to the RED phase? — and by two models (Fig. 2.1F): 1) the slow progress during the resistance phase due to alternative sources of dT (I); 2) dT analog dU incorporation and excision during the RED phase (II). For the resistance phase, we explored two potential sources of dT: 1) dTMP generated by linear chromosomal DNA degradation; 2) reduction of ribo-thymine derived from stable RNA degradation. For the transition to the RED phase, we tested increased dU and rU incorporation into DNA with subsequent excision (Fig. 2.1F, II and III). We found that, even though changes in the levels of all four sources of thymine or its uracil replacements usually make the RED phase faster and deeper, none of them have impact on the resistance phase. Thus, the significant accumulation of chromosomal DNA during the resistance phase must be

supported by another source, whose identity is yet to be revealed, while the reason for the RED phase could be subsequent exhaustion of this mystery source marking the start of synthesis of defective DNA. In support of this idea, we have found that T-starved cells accumulate high levels of single-strand gaps in the chromosomal DNA (Fig. 2.7.1F, IV). We propose that accumulation of these ss-gaps, due to the suspected ss-gap instability outside the safety zone behind the replication fork (47), leads to destruction of one of the replication forks in a T-starved cell (Fig. 2.7.14C). The destruction becomes possible due to ~10-times stronger degradation of the origin-distal end, compared with the origin-proximal end, during double-strand break repair in *E. coli* (81). Remarkably, although the resulting formation of an irreparable double-strand gap in the template DNA ruins the chromosome (Fig. 2.7.14C), no chromosomal fragmentation is expected, as long as only one replication point was affected, and the chromosomal DNA stays one-piece and branched, — so it should not enter pulsed-field gels.

2.3.1 Instability of the chromosomal DNA during T-starvation

The peculiar chromosomal DNA stability during T-starvation was always one of the major mysteries of TLD. Traditionally, measurements of the total chromosomal DNA purified from the same volume of T-starved cells reported either no change or slightly increasing amounts during the time course of TLD ((5, 29, 53), also works cited in (10)). Moreover, pre-labeled chromosomal DNA shows surprising overall stability during T-starvation (53, 94). This DNA amount constancy (or slight increase), in combination with numerous reports of accumulation of single-strand DNA breaks in T-starved cells (1), and recent reports of complex patterns of double-strand DNA breaks (32, 52, 53)

naturally leads to the idea of the intrachromosomal DNA redistribution (cannibalism) (Fig. 2.3C). According to this idea, progress of replication forks during T-starvation is supported by thymidine from the degraded chromosomal parts that have extra copies, and whose degradation therefore will not inactivate the chromosome. In effect, the above-average-copy-number chromosomal parts are cannibalized to support replication of the below-average-copy-number chromosomal parts (Fig. 2.3H). In support of the chromosomal DNA instability during T-starvation, during a phage infection of T-starved cells, there is appreciable incorporation of the chromosomal DNA material in the phage genome, which is not observed in the non-starved cells (85). The potential for intrachromosomal cannibalism is further bolstered by the appearance in response to T-starvation of short-lived relatively small subchromosomal fragments (Fig. 2..3AB) (52).

In fact, intrachromosomal DNA redistribution seems like a winning solution for the problem of starved replication forks, resulting in replication fork elimination by "fork disproportionation" and leading to equal copy number of all chromosomal parts. However, a strong prediction of the intracellular chromosomal cannibalism idea, — that the origin copy number should decrease, while the terminus copy number should increase, — was not confirmed. Instead, we found that the origin and terminus behavior was similar during T-starvation, first increasing during the resistance phase, and then both decreasing during the RED phase (Fig. 2..3I) (53).

Moreover, employing the robust plug-blot procedure (47), we for the first time accurately measured evolution of the total chromosomal DNA amount during T-starvation. In contrast to previously reported stable amounts (see above), we now show that the chromosomal DNA amounts significantly expand during the resistance phase,

only to gradually shrink to the original level during the RED phase (Fig. 2.3G). A similar bi-modal DNA evolution curve was once reported before(10), when DNA-deoxyribose was followed. The initial significant accumulation of the total chromosomal DNA (1.5x the original amount) and its subsequent disappearance are both incompatible with the intrachromosomal cannibalism idea, which (being a zero-sum game) predicts constancy of the DNA amount. Thus, it was not surprising that our genetic inactivation of linear DNA degradation did not affect the resistance phase of TLD (Fig. 2.3F) (but it was surprising that it failed to stop the DNA disappearance either (Fig. 2.4C)).

The short-lived chromosomal fragmentation in response to T-starvation and the peculiar small size of the chromosomal fragments that we found in this work offer explanation for the previous conflicting results in this area. Whereas single-strand breaks in chromosomal DNA of T-starved cells are not disputed ((1)and also see below), there were reports of no double-strand breaks (66), significant early (32) or late (94) chromosomal fragmentation, as well as complex kinetics of chromosomal fragmentation in T-starved cells (the initial spike with subsequent slow increase (52) or redistribution from LMW to HMW (53)). Our current results (Fig. 2.3AB) explain how chromosomal fragmentation can be easily missed, or found to be significant, depending on the time points during T-starvation or on the size of the monitored DNA fragments.

2.3.2 Deoxy-uridine misincorporation

The most popular idea explaining both the resistance phase and its sudden change to the RED phase is dU misincorporation in place of dT (1, 10, 30, 31, 43), with subsequent excision initiated by UDG, which is followed by inevitable DNA synthesis

that has to use dU again (Fig. 2.8A). This so-called futile DNA-dU misincorporation/excision cycle (31) is proposed to degrade the chromosomal DNA beyond repair (several sub-scenarios reviewed in (52)). This concept remains popular in the TLD field not only because it elegantly explains the major features of TLD, but also because DNA-dU misincorporation is known to happen in thymine-requiring mutant of *Bacillus subtilis* (83), and because inactivation of various uracil-DNA-targeting glycosylases does alleviate toxicity of 5-fluorouracil (FU) in eukaryotic cells, offering proof of principle for the futile DNA-dU misincorporation/excision cycle (50, 74, 79).

However, the assumed mechanistic relationship between FU toxicity and TLD remains to be experimentally tested. One reason to suspect that TLD is different from FU toxicity is that TLD kinetics in *E. coli* is not improved by inactivation of uracil-DNA glycosylase ((52), Figs. 2.8C and 2.7C). The apparent reason for this, found here, is the lack of significant increase in DNA-dU misincorporation during T-starvation, even when dUTP concentrations are artificially elevated by the *dut* defect (Fig. 2.9). This suggests existence of mechanisms limiting DNA-dU misincorporation, at least in *E. coli*. In fact, TLD survival is barely improved by inactivation of UDG in *B. subtilis*, where DNA-dU misincorporation during T-starvation is considerable (59).

To test the idea that DNA-dU misincorporation influences TLD parameters, we inactivated *dcd* (the major route of dUTP production in *E. coli*) but found no effect on TLD (Fig. 2.7B). At the same time, during T-starvation, genetic inactivation of the abasic site incision stage of dU removal in the *xthA nfo* mutant accelerates the RED phase and decreases survival (Fig. 2.8B), indicating active BER in T-starved cells. In yeast, loss of AP-endonuclease activity makes the organism profoundly sensitive to aminopterin (21) –

a drug that induces thymine starvation. For TLD in *E. coli*, loss of abasic site repair pathway should have an even stronger effect in the *dut thyA* strain, due to the inability to complete excision of DNA-dU, but this could not be tested because of the co-lethality of the *dut xthA* combination (84).

As a proof-of-concept that the futile DNA-dU misincorporation/excision cycle could be set up in *E. coli*, we increased the dUTP concentration in T-starved cells by inactivating the *dut* dUTPase (35, 89), — and indeed observed disappearance of the resistance phase (Fig. 2.8C). In other words, DNA-dU incorporation, instead of supporting the initial fork progress in the absence of dTTP, was made predictably poisonous by active DNA-dU excision repair (Ung+). This means that one of the survival tactics during T-starvation could be further limitation of the DNA-dU misincorporation.

To test the idea that stabilization of DNA-dU misincorporation could save T-starved cells, we blocked DNA-dU excision in the *dut* mutants by *ung* mutation. The resulting *dut ung* mutants are known to accumulate significant amounts of dU in their DNA during normal growth, replacing up to 15% of DNA-dT with DNA-dU (89). The expected effect during T-starvation was a complete suppression of TLD. Compared with the TLD kinetics of the *thyA dut* mutant, the TLD kinetics of the *thyA dut ung* mutant does have a prolonged resistance phase, a slower RED phase and 100-times higher survival (Fig. 2.8C). In fact, the "unlimited" DNA-dU incorporation without subsequent excision allows T-starved cells not only to finish the ongoing replication round, but also to initiate and finish one more replication round (Fig. 2.8DEF). Thus, stabilized DNA-dU misincorporation is indeed capable of ameliorating chromosomal problems of T-starved cells. Remarkably, even fully-replicated chromosomes cannot save 99% of the *thyA dut*

ung mutant cells from TLD, suggesting an unrelated (non-chromosomal?) nature of its pathology, at least in this case.

It should be kept in mind that the surprising TLD of *thyA dut ung* mutant may still have chromosomal nature. For example, subsequent initiations of chromosomal replication appear blocked in the T-starved *thyA dut ung* cells, — is it because, in the presence of dU in DNA, *oriC* cannot initiate? Uncharacterized metabolic or regulatory problems were reported in cells with chromosomal DNA that contains a lot of dU (89). The peculiar inviability of mutants in which dT in chromosomal DNA was mostly replaced with dU was systematically explored before, in conjunction with inability to obtain deletions of the *dut* gene (22, 23).

2.3.3 Ribo-uridine incorporation?

Until fairly recently, ribo-uridine (rU) was not considered to incorporate into DNA even in T-starved cells because of the generally efficient discrimination of DNA polymerases against rNTPs. Characterization of RNase H mutants, deficient in excision of single rNs from DNA (13, 73) suggested that this discrimination power of DNA polymerases is overrated. Indeed, studies with the three eukaryotic replicative polymerases in vitro showed incorporation from two to 16 rNs every 10,000 nt synthesized (71); the replicative polymerase of *E. coli* in vitro incorporates ~4 rNs per 10,000 nt (93). We recently determined the in vivo density of rNs in the DNA of the *E. coli rnhB* mutant, unable to remove single DNA-rNs, as 1 rN per 14,000 nt (45) or 1 rN per ~9,000 nt (18). Giving all this information, it was not impossible that, during T-

starvation, rU incorporation in place of missing dT would be significantly elevated, supporting chromosomal DNA replication.

However, we found only modest (~25%) increase in DNA-rN density in T-starved cells (Fig. 2.10E). Since this increase is, presumably, all specific to rU, which, assuming otherwise equal incorporation of the four rNs, represents 1/4 of the total, the specific rU density increase becomes ~2-fold, which is still modest. Moreover, the *rnhAB* mutant deficient in removal of any DNA-rN has a slightly lower TLD survival, meaning that DNA-rNs exacerbate, rather than alleviate TLD. Interestingly, inactivation of TLS polymerases tend to aggravate TLD in the *rnhAB* mutants further, suggesting that TLS polymerases help to synthesize across DNA-rNs. In summary, the modest increase in incorporation of rN into DNA of T-starved cells (Fig. 2.14, III) aggravates TLD, especially in the absence of TLS polymerases, which means that increasing the discrimination power of replicative DNA polymerases against DNA-rN incorporation could be another tactic to survive T-starvation.

2.3.4 Accumulation of ssDNA during T-starvation

Long single-strand gaps in chromosomal DNA were postulated to form during T-starvation (12, 24, 52, 53), due to the fact that, with little dTTP around, any A-run of three or longer in the template DNA becomes in essence a non-coding lesion (53), to which the replisomes are known to react by reinitiating downstream and thus forming a "daughter-strand gap" (76) (Fig. 2.1F, IV). Indeed, T-starved cells have problems maturating their Okazaki fragments (27), even though their DNA ligase is functional,

indicating formation of ss-gaps. However, quantification of long ss-gaps in chromosomal DNA of T-starved cells received surprisingly little experimental attention.

While numerous studies report accumulation of single-strand *breaks* in the chromosomal DNA during T-starvation, only three studies explicitly addressed the possibility of formation of long single-strand *gaps*. First, Nakayama and colleagues mentioned a significant single-stranded character of their non-migrating DNA without presenting experimental data (66). Second, Khodursky and colleagues presented S1 nuclease treatment of the chromosomal DNA from T-starved cells (77), which is more consistent with ss-breaks, rather than gaps, as S1 treatment massively fragments this DNA only after ExoIII action (which converts nicks into ss-gaps). Finally, a recent report describes accumulation of SSB-YFP foci in T-starved cells (37); unfortunately, no quantification was attempted, and normalization controls were missing. It looks like we are the first to quantify accumulation of significant single-strandedness in the chromosomal DNA of T-starved cells; we also propose how some of these ss-gaps could turn into irreparable double-strand gaps in the template DNA of T-starved cells (Fig. 2.14C).

Persistent single-strand gaps in the chromosomal DNA of *E. coli* initiate the RecFOR pathway of recombinational repair (55), that licenses RecA polymerization on such gaps, to catalyze their filling-in using the corresponding strand of the intact sister duplex. Since the *recF* defect alleviates TLD ((24, 52, 65), this work), the persistent ss-gap repair by recombination is apparently detrimental, rather than helpful, somehow leading to formation of dysfunctional chromosomes. However, modern schemes of such poisonous recombination (25, 52, 66) still lack specific details to become experimentally

testable. Alternatively, the main RecFOR contribution to TLD could well be via the induction of massive and persistent SOS response (Fig. 2.14D) (24, 52).

2.3.5 Survival strategies and tactics in response to T-starvation

Our original focus was on finding mutants with a reduced resistance phase or with a slower RED phase (Fig. 2.2). We found two mutants without the resistance phase, *dut* (enhancing the futile cycle of DNA-dU misincorporation/excision) and the *xthA nfo* (blocked base-excision repair), as well as one mutant with a slower RED phase, *dut ung* (stabilized DNA-dU misincorporation). At the same time, several mutants we tested exhibited an unexpected third phenotype, — a decreased survival (a deeper RED phase). Before this finding, we assumed that the level of survival is a characteristic of particular growth conditions, being mostly determined by the level of persisters, — dormant cells with a minimal metabolic activity resistant to TLD because they do not replicate their chromosome (34). Our finding of mutants with significantly reduced survival in the same growth conditions revealed existence of an active response to T-starvation, with defects leading to reduced survival identifying various strategies and tactics of this response.

By trying to find a source of dT for the resistance phase, we instead identified two possible strategies to increase survival during T-starvation: 1) degradation of linear DNA with a possible intra-chromosomal DNA redistribution of the degraded material (Fig. 2.3C), allowing cells to liquidate extra replication forks and at the same time to derive dTMP for termination of the remaining forks — thus getting rid of *all* replication forks, which are the points of chromosomal vulnerability during T-starvation; 2) degradation of stable RNA, allowing cells to both inhibit translation and at the same time to mine a

significant amount of ribo-thymine to convert to dT in support of DNA replication (Fig. 2.5D) — thus, ameliorating the metabolic disbalance of T-starved cells. Both tactics represent an attempt of the cell to derive thymine from dispensable molecules (whether DNA or RNA), so as to redistribute it to the critical molecules in dire need of it (surviving replication forks), while inhibiting the processes that contribute to the disbalance, whether in the chromosome or in the general metabolism. The benefit for the T-starved cells of the degradation of extra chromosomal parts to generate dT to support the surviving replication forks was considered before (25).

We have also noticed certain DNA damage avoidance and repair tactics that affect the survival of T-starved cells: 1) ABS-endonuclease activities reduce accumulation of abasic sites in the chromosomal DNA; 2) dUTP hydrolase Dut controls the dUTP pool to minimize DNA-dU misincorporation and to avoid the futile misincorporation/excision cycle, while uracil-DNA-glycosylase Ung ensures timely removal of uracils from DNA; 3) the RNase H enzymes control accumulation of rNs in DNA. These tactics all work to decrease chances of replication fork encounters with non-coding DNA lesions that would otherwise lead to even more ss-gaps in chromosomal DNA. However, a possible alternative explanation for the decreased survival of all these excision repair mutants (*xthA nfo, ung, rnhB*) is that DNA repair causes dT release from DNA, which is then used for some other, still unknown, critical cellular process. From this perspective, all these strategies and tactics become ways of releasing thymine, either from DNA or from stable RNA.

2.4 Conclusion

The overall picture of TLD pathology keeps evolving as a result of the latest round of investigations (24, 25, 53, 52, 61, 77) and now begins with accumulation of persistent ss-gaps that are either converted into double-strand breaks, to be repaired by the RecBCD pathway, or are recognized by the RecFOR + RecQJ pathway as substrates for RecA polymerization (Fig. 2.14D). Both pathways become potentially lethal as T-starvation progresses. The RecBCD-promoted degradation of the origin-distal end of the double-strand break may lead to the destruction of the intact template for repair of a similar double-strand break in the other sister chromatid, ruining the replication point (Fig. 2.14C). At the same time, robust RecA filament formation at ss-gaps, in conditions continuously generating new ss-gaps, makes it a positive-feedback loop that could kill the cell via runaway SOS-induction. Finally, death of 99% of cells of the *thyA dut ung* mutants, that successfully complete two chromosomal replication rounds and accumulate two times less DNA in ss-gaps, suggest an additional, still unknown, TLD mechanism, perhaps independent of DNA replication altogether (Fig. 2.14D).

Our finding of a significant accumulation of ss-gaps in the chromosomal DNA of T-starved cells raises immediate questions about the nature of this accumulation. Our original assumption all along this project was that it is important for the cell to maintain certain minimal rates of the replication fork progress for the fork stability. In other words, we automatically assumed that, when there was nothing to incorporate opposite "A" in template DNA, ss-gaps would accumulate behind slowly-progressing replication forks. In addition, RecQ and RecJ, due to their enzymatic activities, could lengthen these gaps (24, 77). In the future, we will be testing the assumed replication-dependence of this ss-gap

accumulation, its chromosomal position relative to the replication forks, as well as its genetics. Also, the origin and terminus instability during TLD (24, 53, 77) should be related to this ssDNA accumulation. The apparent insensitivity of the replication forks to incompletely-replicated nascent DNA, reflected in the accumulation of ssDNA in T-starved cells, is another paradox that requires experimental attention. Finally, the source of thymidine that supports significant chromosomal replication during the resistance phase awaits identification.

2.5 Acknowledgements

We would like to thank Susan Rosenberg (Baylor) for critical reading of the manuscript and many helpful suggestions. This work was supported by grant # GM 073115 from the National Institutes of Health. The authors have no conflict of interest to declare.

2.6 Materials and Methods

2.6.1 Bacterial strains

E. coli strains (all K-12) and plasmids used in this study are described in Table S1. Strains were created by P1 transduction (63), followed by transformation with pCP20 to remove antibiotic resistance when needed (20). Precise deletion-replacement mutations were obtained from *E. coli* genetic stock center and confirmed by PCR. The Δ*thyA* defect was additionally confirmed by inability to form colonies in the absence of thymidine. The *recA*, *recB* and *recF* mutant strains were verified by characteristic UV-sensitivities. The *dut-1* mutation was confirmed by sensitivity to 10 mM uracil on plates (46).

2.6.2 Growth conditions

Overnight cultures were grown in M9 minimal medium supplemented with 0.2% casamino acids, 0.2% glucose (M9CAA) and 10 µg/ml thymidine (dT). The growth temperature was 37°C unless indicated. While screening for mutations linked to antibiotic resistance genes or cells carrying plasmids, the growth medium was supplemented with the following concentrations of antibiotics: 100 µg/ml ampicillin, 50 µg/ml kanamycin, 10 µg/ml tetracycline or 10 µg/ml chloramphenicol.

2.6.3 Viability assays

Overnight cultures were diluted 100-fold in M9CAA + dT and grown to OD_{600} 0.1- 0.15. Cells were collected on 0.2 µm nitrocellulose membrane by filtration and washed thrice with 5 ml of 1% NaCl to completely remove dT. Washed cells were suspended back into the same volume of M9CAA, but without dT. In some protocols, dT was removed by harvesting the cultures by centrifugation and resuspending the cell pellet and re-pelleting thrice with 1 ml of 1% NaCl in Eppendorf tubes before suspension in M9CAA. The resuspended cultures were vigorously shaken at 37°C. Culture aliquots taken at the indicated times were serially diluted in 1% NaCl and spotted on LB plates. Colony forming units were counted under a stereomicroscope after overnight growth at room temperature.

Direct cell counts in liquid cultures were obtained using Petroff-Hauser counting chamber and light microscope with phase contrast at magnification x400.

2.6.4 Fluorescent microscopy of DAPI-stained cells

This was performed exactly as described in (45).

2.6.5 Genomic DNA accumulation assay

Cultures were grown to OD ~ 0.15 in M9CAA +dT from saturated overnight cultures, before filtration to start T-starvation. At indicated times, 1.5 ml of culture growing in the absence of dT was harvested to isolate DNA in plugs. The cells were suspended in 60 µl of TE and mixed with 2.5 µg of Proteinase K and 65 µl of lysis agarose (1.2% agarose in 20% lysis buffer) and poured into molds to set. Plugs were incubated overnight in at 65°C in lysis buffer (1% laurylsarcosine, 25 mM EDTA, 50 mM Tris-HCl), washed with 1 ml of TE thrice for 20 minutes, treated with 0.25 N HCl for 20 minutes, 0.5 N NaOH for 20 minutes and 1 M Tris-HCl pH = 8.0 for 20 minutes. The DNA from the plugs was vacuum transferred to nylon membrane, crosslinked and incubated in the hybridization buffer (5% SDS, 0.5 M sodium phosphate pH = 7.4) for an hour and probed with the whole genome probe in the same buffer overnight at 65°C. The probe was based on genomic DNA of stationary (aligned) cells of AB1157. The membranes were washed with 0.01x hybridization buffer thrice for 20 minutes each and exposed to phosphorimaging screen. The screens were developed in PhosphorImager FujiFilm FLA-3000.

2.6.6 Measurement of origin and terminus

3 ml of culture were used to isolate DNA in duplicate agarose plugs as described above. After overnight lysis of cells in plugs and transfer of DNA to a nylon membrane,

one set of plugs was hybridized to the *ori* probe, while the duplicate set of plugs was hybridized to the *dif* probe. This was followed by washing of the unhybridized probe, exposing to a phosphorimaging screen and analysis with a phosphorimager as above.

2.6.7 Single strand gap assay

For cultures treated with AZT, the indicated concentrations of the drug were added once the strains reached OD_{600} ~ 0.15. For both AZT-treated and T-starved cultures, 1.5 ml aliquots were removed at the indicated times to isolate DNA in agarose plugs as described for genomic DNA isolation. After overnight lysis of plugs, they were washed with TE six times 10 minutes each, incubated with 100 µl of 2x NEB buffer 2.1 at 4°C for 1 hour, followed by restriction with 20 units of HaeIII and 4-32 µg of RnaseA in 1x NEB buffer 2.1 in 130 µl reaction overnight at 37°C. The next day the plugs were cut in half, and one set of them was denatured by treating with 0.25 N HCl for 20 minutes, 0.5 N NaOH for 20 minutes and 1 M Tris-HCl pH = 8.0 for 20 minutes. After this the DNA from both the native set and the denatured set of plugs was transferred onto nylon membrane by electric transfer at 80V for 1.5-3.0 hours, crosslinked and probed with the whole genomic probe. The membrane was exposed to an imaging screen and analyzed by a phosphorimager.

2.6.8 Measuring stability of RNA

The strain KKW58 was subcultured in MOPS-minimal phosphate medium supplemented (7) with casamino acids (CAA), 10 µg/ml dT and 2 µCi/ml ^{32}P-orthophosphoric acid and grown to OD_{600} = 0.07 at 37°C. The label was removed by

centrifugation, and the strain was grown in the same medium for another 30 minutes, until the ^{32}P-redistribution in the cell mostly subsided. dT was removed from half of the culture by centrifugation, cells were washed by resuspension in 1 ml of 1% NaCl thrice, and the final pellet was suspended back into MOPS-CAA. 1 ml of thymidine-starved culture and gradually decreasing volumes of cultures growing in the presence of thymidine were harvested to isolate total RNA. RNA was isolated by RNA*snap* protocol (82). One-fifth of the isolated RNA was run on 1.2% agarose gel in 0.5x TBE buffer at 40 V for 80 minutes. The gel was placed on a nylon membrane, dried at 50°C and exposed to an imaging screen to be analyzed by a phosphorimager.

2.6.9 Chromosomal fragmentation assay

Saturated overnight culture of KKW58 was diluted 100-fold in the presence of dT, 2 µCi/ml ^{32}P-orthophosphoric acid in MOPS-CAA, and grown to OD_{600} ~ 0.15 at 37°C, when the culture was harvested by centrifugation to remove dT and the radioactive label. The cells were washed by resuspension in 1% NaCl thrice and suspended back in MOPS-CAA. At indicated times, 1.5 ml of culture aliquots were taken, and cells were collected and lysed as described for genomic DNA isolation. The conditions for running pulsed-field gel electrophoresis and quantification of chromosomal fragmentation were exactly as before (48).

2.6.10 Measurement of density of deoxyuridine and ribonucleotides in DNA

Deoxyuridine (DNA-dU) densities were measured in pMTL20 plasmid, isolated from *thyA*, *thyA dut* and *thyA ung* strains. The strains were grown in 30 ml M9CAA +dT

supplemented with 100 µg/ml ampicillin till early exponential phase (OD_{600} ~ 0.1 – 0.15), after which dT was removed from 20 ml of the culture by filtration and three washes with 5 ml of 1% NaCl each. The cells from the filter were suspended in 20 ml M9CAA (no dT), and after 5.5 hours plasmid was isolated by the standard alkaline lysis protocol. 10 ml of strains growing in the presence of dT were grown to OD_{600} ~ 0.6 or for 5.5 hours before plasmid isolation. For DNA-dU density determination, 250 ng of the isolated pMTL20 was treated either with 1 unit of ExoIII alone, or with 1 unit each of UDG and ExoIII together, at 37°C for 30 minutes. The plasmid intermediates were separated in 1.2 % agarose gel in TAE buffer (60). The gels were gently rocked with 0.25 M HCl for 40 minutes, 0.5 M NaOH for 40 minutes and 1 M Tris-Cl for 40 minutes before capillary transfer of DNA onto nylon membrane (Hybond-N+) for hybridization with a pMTL20-specific ^{32}P random-primer-labeling probe. The calculations to determine DNA-dU density, taking the signal of the supercoiled plasmid as the zero class of the Poisson distribution, were as before (44).

DNA-dU density in the *thyA dut ung* mutant was measured using a small fragment released from pBR322 plasmid. The plasmid was isolated from this strain after growth in the absence of dT for 5.5 hours. 250 ng of plasmid was treated with either 1 unit of ExoIII, or 1 unit each of UDG and ExoIII together at 37°C for 30 minutes. This was followed by digestion of the plasmid with BglI and denaturation of the restricted DNA with 200 mM NaOH and 20 mM EDTA for 20 minutes on ice. The reaction products were run on 3% agarose gel, and DNA was transferred onto nylon membrane and probed against the 234 bp BglI fragment. The intact single stranded 234 bp fragment was used as the zero class of the Poisson distribution.

Ribonucleotide (DNA-rN) densities were measured using pEAK86-transformed strains. Strains were grown either in the presence of dT till OD_{600}=0.6, or in the absence of dT for 5.5 hours before plasmid extraction by alkaline lysis protocol, which was done on ice after addition of S2 to inhibit DNA-rN hydrolysis (18, 45). 250 ng of pEAK86 was treated with 1 unit of NEB RNase HII in 1X NEB thermopol buffer for 30 minutes at 37°C, loaded on 1.2% agarose gel, run in TAE buffer and transferred to nylon membrane to be probed with pEAK86-specific ^{32}P-labeled probe. DNA-rN densities were determined using the Poisson distribution as described above and before (45).

2.6.11 Chromosomal DNA degradation

The protocol was adapted from (95) with some changes. Briefly, 10 ml of culture was chronically labelled with tritiated thymidine, grown to OD_{600} ~0.35 (if *recA*+) or OD_{600} ~ 0.6 (if *recA*-) and harvested by centrifugation. Cell pellets were washed with 10 ml of 67 mM phosphate buffer (pH=7.4) and suspended in 5 ml of the same phosphate buffer containing 0.01% Triton X-100. 2.5 ml of this suspension was mixed with 2.5 of 2x LB (unirradiated control). The other half was exposed to 50 J/m^2 of UV radiation after spreading (in two portions of 1.25 ml each) as a thin layer in a sterile 100 mm x 150 mm Petri plate, and was mixed with 2.5 ml of 2x LB after UV and shaken at 37°C (42). At the indicated times, 500 µl aliquots were taken and mixed with 5 ml of ice-cold 10% trichloroacetic acid (TCA) and incubated on ice for 1 hour. The samples were filtered through Fisherbrand G6 glass fiber filters, washed with 5 ml of 10% TCA and 5 ml of EtOH. The filters were neutralized by spotting 100 µl of 1 M KOH, dried, submerged in

scintillation fluid (Bio-Safe II, RPI) and counted for tritium on Beckman-Coulter LS 6500.

2.7 Figures

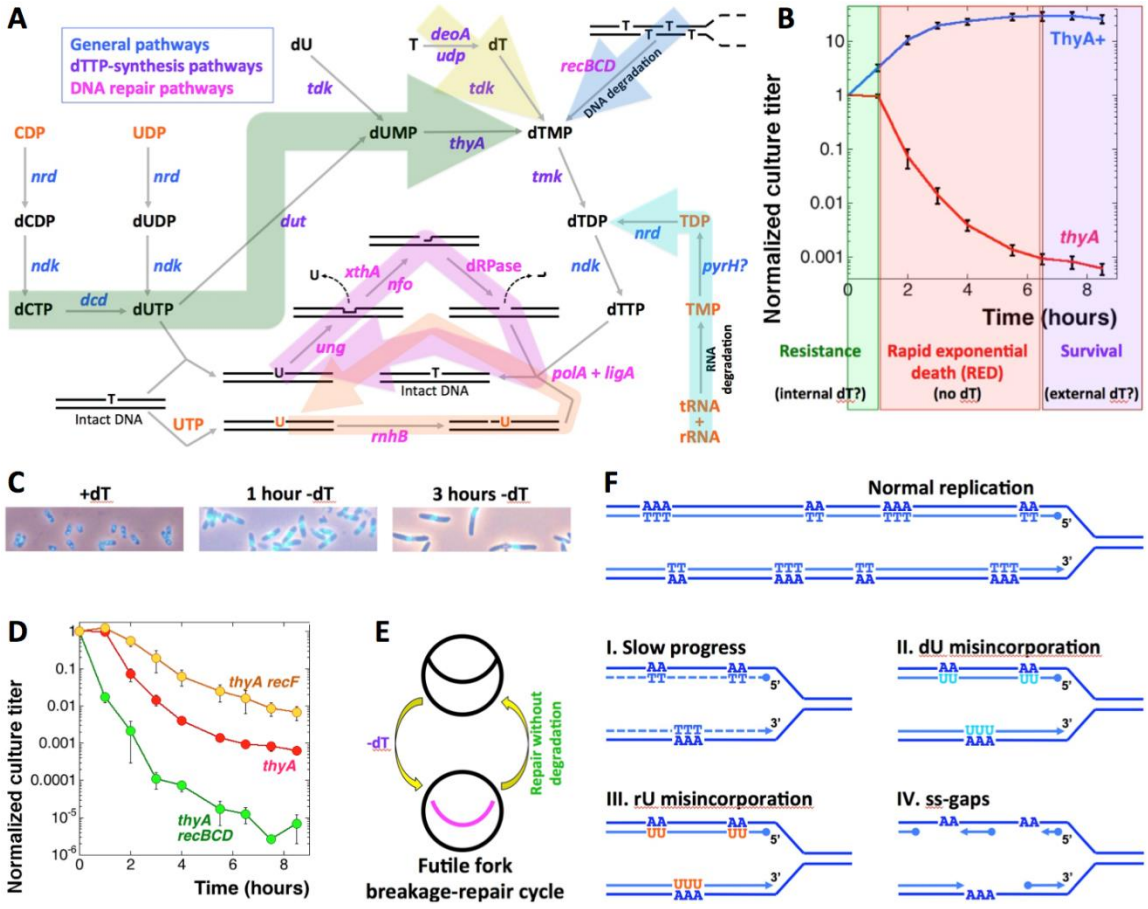

Figure 2.1. The metabolism of dTTP production, the phenomenon of TLD, the futile cycles, and the expected changes in nucleotide metabolism mutants and kinetics of chromosomal fragmentation. A. The metabolic pathways. Compounds of DNA metabolism are in black, compounds of RNA metabolism are in orange. Genes are colored according to functions: general (blue), dTTP-synthesis (purple) or DNA repair (magenta). The big arrow shades are: green, general biosynthesis; yellow, salvage; blue, DNA degradation; cyan, RNA degradation; magenta, futile DNA-dU misincorporation/excision cycle; orange, futile DNA-rU misincorporation/excision cycle. **B.** Extended time course of the culture titer during thymine starvation in our standard conditions, to highlight the survival phase. The strains are: ThyA+, KKW59; *thyA*, KKW58. The three phases of TLD are shown in color: green for the resistance phase, red for the RED phase, purple for the survival phase. The values in this and subsequent figures are means of 4-40 independent measurements ± SEM. **C.** DAPI-staining of cells grown in the presence of dT, as well as the same cells T-starved for 1 hour or for 3 hours. **D.** The *thyA recBCD* mutants lack the resistance phase, while the *thyA recF* mutants die slowly. The strains are: *thyA*, KKW58; *thyA recBCD*, KJK63; *thyA recF*, RA31. Here

Figure 2.1. (cont.)
and henceforth: if error bars are not visible, they are masked by the symbols. **E.** A scheme of the futile fork-break-and-repair cycle. **F.** Various models of replisomes traversing A-runs in the template DNA during T-starvation that we tested in this work.

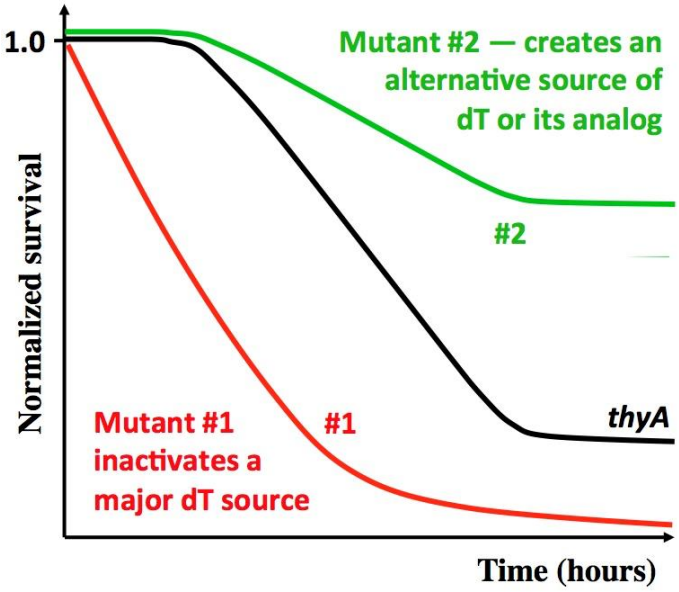

Figure 2.2. The two major expected types of TLD-affected mutants in nucleotide metabolism and their interpretations. A stylized TLD kinetics of a *thyA* mutant is shown in black.

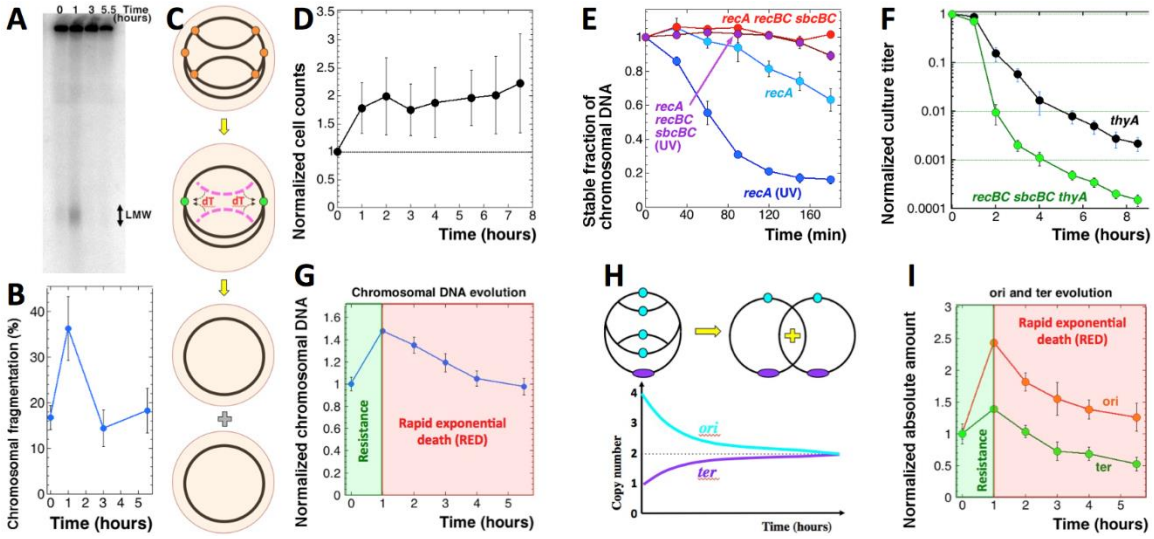

Figure 2.3. Testing the intrachromosomal DNA redistribution idea. A. A pulsed-field gel showing kinetics of chromosome fragmentation induced by thymine starvation. LMW, low molecular weight species, ~50-200 kbp in size. The strain is KKW58. **B.** Quantitative kinetics of chromosomal fragmentation, from several gels like in "A". The data are means (n = 4 or 5) ± SEM. **C.** The scheme of how cannibalizing linear DNA (magenta arcs) generated by disintegration of some of the stalled forks (orange circles) could allow cells to keep the remaining forks active (green circles), explaining the resistance phase. **D.** Cell counts in T-starved cultures of the *thyA* mutant (KKW58) normalized to time of dT removal. **E.** Stabilization of prelabeled chromosomal DNA (TCA-precipitable counts) in UV-irradiated *recA* mutant cells by *recBC sbcBC* defect. The strains are: *recA*, RA46; *recA recBCD sbcBC*, RA47. The UV-dose was 50 J/m^2. **F.** Time course of TLD in the *recBCD sbcBC thyA* mutant. The strains are: *thyA*, KKW58; *recBCD sbcBC thyA*, RA45. **G.** Change in the total amount of chromosomal DNA over time ("chromosomal DNA evolution") in the *thyA* mutant (KKW58) during T-starvation. The first two phases of T-starvation are shown in the same colors as in Fig. 2.7.1A. **H.** Expectations about the origin and terminus copy number evolution during T-starvation according to the intrachromosomal DNA redistribution idea. **I.** Evolution of the amount of origin and terminus under the same conditions as in "G".

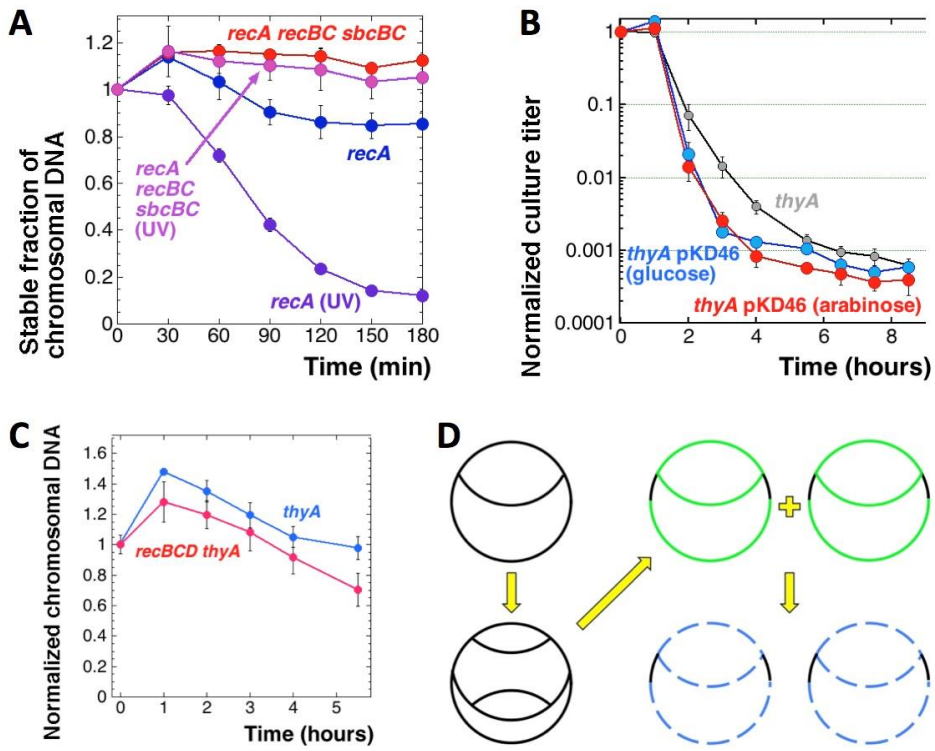

Figure 2.4. The role of linear DNA degradation in thymine starvation phenomena and suggested patterns of chromosomal DNA instability. A. Stabilization of prelabeled chromosomal DNA (TCA-precipitable counts) in UV-irradiated *recA* mutant cells by *recBC sbcBC* defect. The strains are (all ThyA+): *recA*, RA50; *recA recBC sbcBC*, RA49. The UV-dose was 50J/m^2. **B.** Time course of TLD in the *thyA* pKD46 strain (KKW58). Glucose suppresses expression of the lambda Red proteins (inhibit RecBCD), arabinose induces them. **C.** Evolution of the total amount of chromosomal DNA in the *thyA recBCD* mutant (KJK63) during T-starvation. The *thyA* mutant curve from Fig. 2.7.3E is shown for comparison. **D.** A possible explanation for the observed pattern of the chromosomal DNA evolution. The accumulation during the resistance phase at first reflects the completion of the ongoing replication rounds with no new initiations, whereas the subsequent DNA instability, mostly during the RED phase reflects unknown defects in the nascent DNA (solid green), which eventually make this DNA unstable (dashed blue).

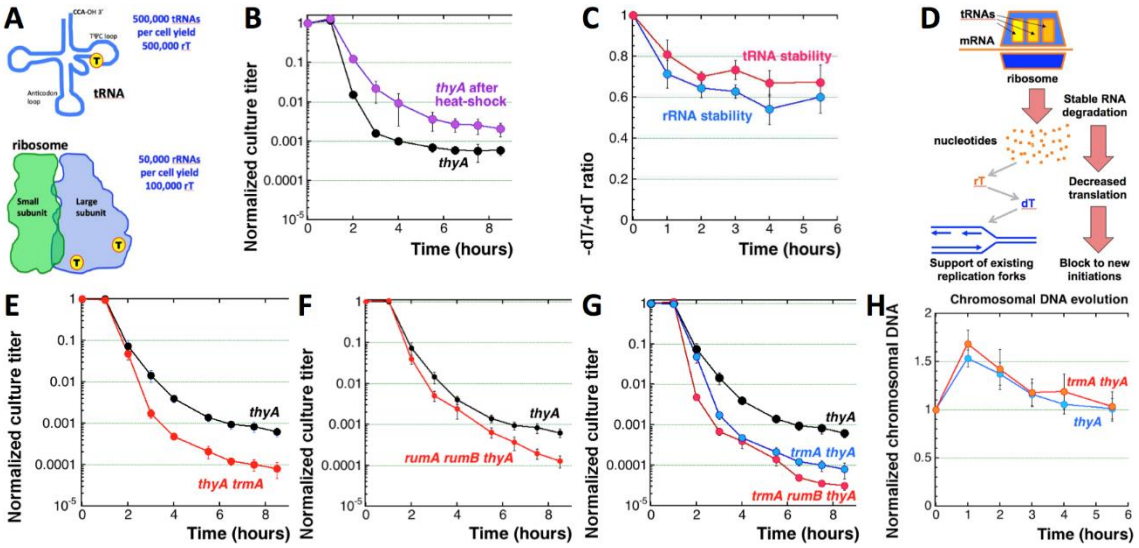

Figure 2.5. Testing the contribution of ribo-thymine from stable RNA. A. A scheme of stable RNAs (tRNA has one rT, 23S rRNA has two) and how many thymine residues they can yield per average rapidly-growing cell. **B.** Time course of TLD after 15' @ 54°C heat shock. The strain is KKW58. In this case, the experiment-specific *thyA* TLD curve was used. **C.** Stability of tRNA and rRNA during thymine starvation. The strain is KKW58. Stability is expressed as the ratio of the corresponding RNA species in the cells incubated without dT to cells from the same culture incubated in the presence of dT. The actual measurements, normalized to time 0, are shown in Figures S3B and S3C. **D.** Recruitment of rT by degrading stable RNA kills two birds with one stone: it yields dT to support stalling replication forks and at the same time it inhibits translation, blocking new initiations and slowing down general metabolism. Both changes contribute to metabolism rebalancing. **E.** Time course of TLD in the *thyA trmA* mutant (RA9). **F.** Time course of TLD in the *thyA rumA rumB* mutant (RA13). **G.** Time course of TLD in the *trmA thyA* and *trmA rumB thyA* mutants. The strains are: *thyA*, KKW58; *trmA thyA*, RA9 (from "E"); *trmA rumB thyA*, RA14. **H.** Evolution of the chromosomal DNA absolute amount in the *thyA* and *trmA thyA* mutants (strains like in "E") during T-starvation.

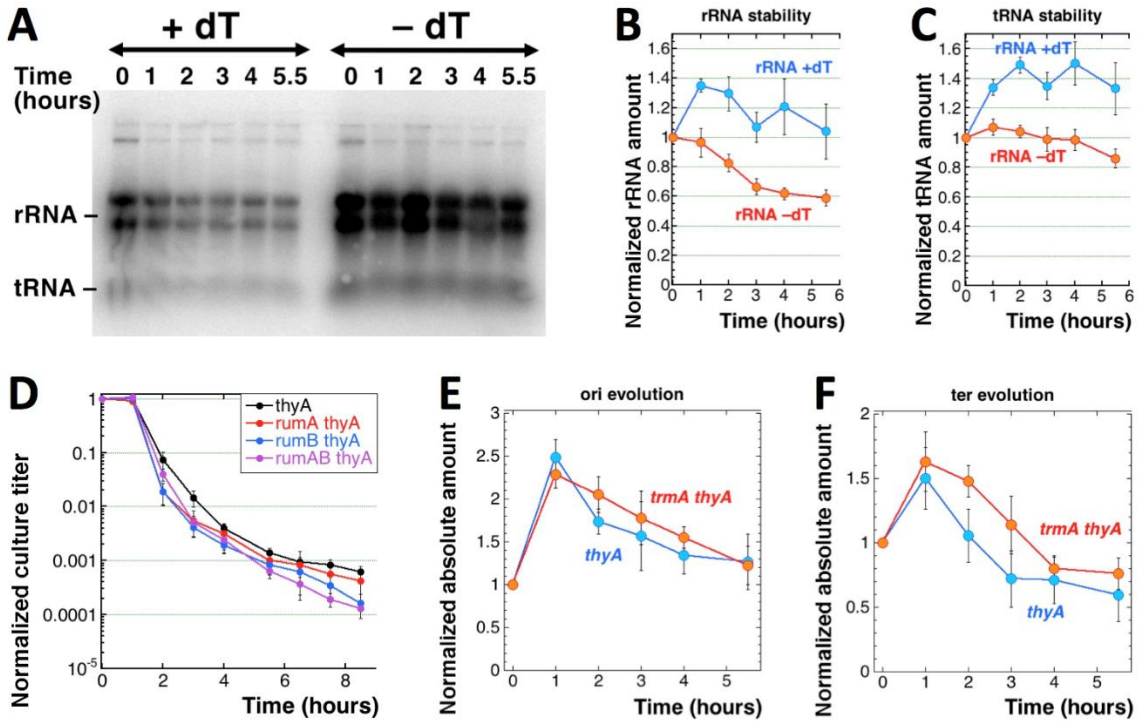

Figure 2.6. (A lack of) stable RNA contribution to resistance phase of TLD. A. The gel to determine stability rRNA and tRNA during growth. The *thyA* mutant (strain #) was labeled with 32P-orthophosphate during growth in the presence of dT, and then the medium was changed to one with or without dT, but having no label, and shaking of the culture continued at the same temperature. The culture grown in the presence of dT was gradually diluted several fold during growth, unlike the dT-less culture, — this is why the "+ dT" signal decreases substantially. **B.** Stability of rRNA during thymine starvation, determined from several gels like in "B". The exogenous ^{32}P-orthophosphoric acid keeps incorporating for at least one hour under these conditions (53). At the indicated time points, the label in the rRNA bands was normalized to the label at the = 0. The strain is KKW58. **C.** The same as in "C", but done for tRNA. **D.** Time course of TLD in the *rumA* and *rumB* mutants. The strains are: *thyA*, KKW58; *rumA thyA*, RA10; *rumB thyA*, RA11; *rumAB thyA*, RA13. **E.** Evolution of the replication origin absolute amount in the *thyA* and *trmA thyA* mutants (strains like in Fig. 2.7.5D) during T-starvation. **F.** Same as in "F", but for the terminus.

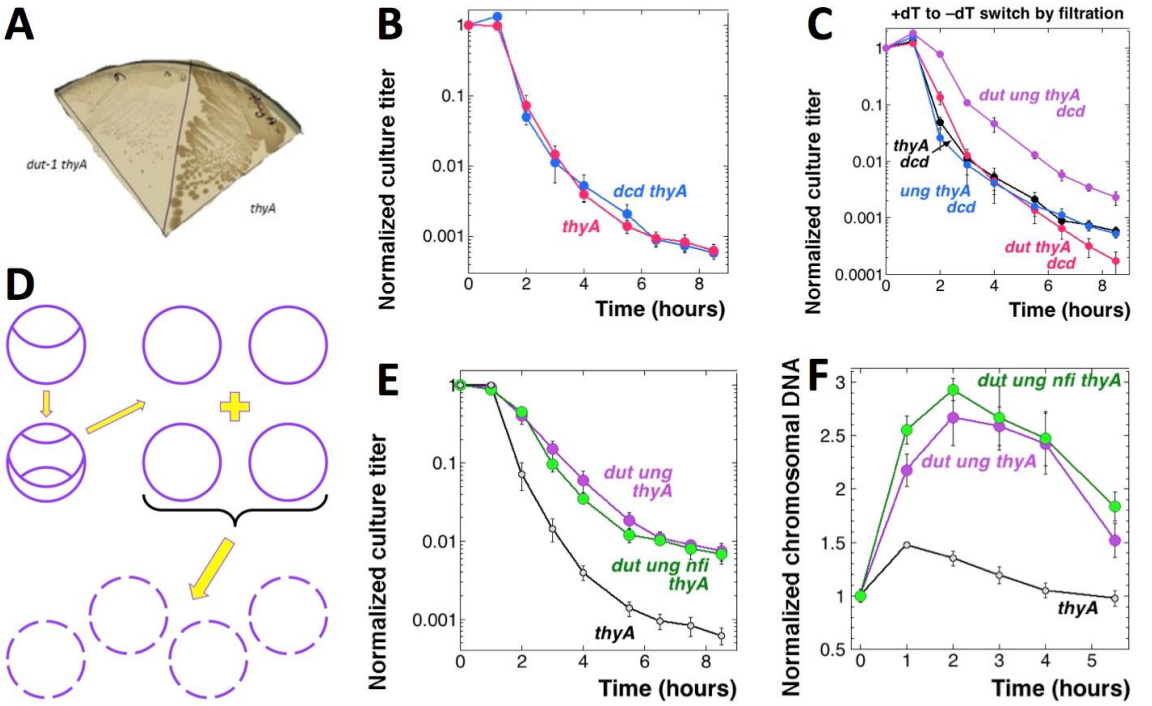

Figure 2.7. Testing uracil incorporation-excision as the cause of TLD and analysis of TLD in the *dut ung thyA* mutants. A. The extremely slow growth of the *dut thyA* mutant, even on rich medium supplemented with 3 μg/ml dT (optimal concentration). The strains are: *thyA*, KKW58; *thyA dut-1*, RA16. **B.** Time course of TLD in the *dcd thyA* mutant. The strains are: *thyA*, KKW58; *dcd thyA*, RA25. **C.** Time course of TLD in the *dcd dut thyA* and *dcd ung thyA* mutants. The +dT/-dT medium switch is by filtration (standard procedure). Strains are: *dcd thyA*, RA25; *dcd dut thyA*, RA27; *dcd ung thyA*, RA26; *dcd dut ung thyA*, RA28. **D.** A scheme of the chromosome behavior during T-starvation of the *thyA dut ung* mutant. The elevated pool of dUTP, in combination with DNA-dU stability, facilitates chromosomal replication to the extent that both the existing and the newly-initiated rounds are finished, yielding four complete chromosomes. However, most cells still die while their chromosomes are degraded, by unclear mechanisms. **E.** TLD kinetics of the *dut ung thyA* versus *dut ung nfi thyA* mutants. The *thyA* mutant is shown as a control. Strains are: *thyA*, KKW58; *dut ung thyA*, RA18; *dut ung nfi thyA*, RA30. **F.** Evolution of the chromosomal DNA amount during thymine starvation. The strains are like in "E".

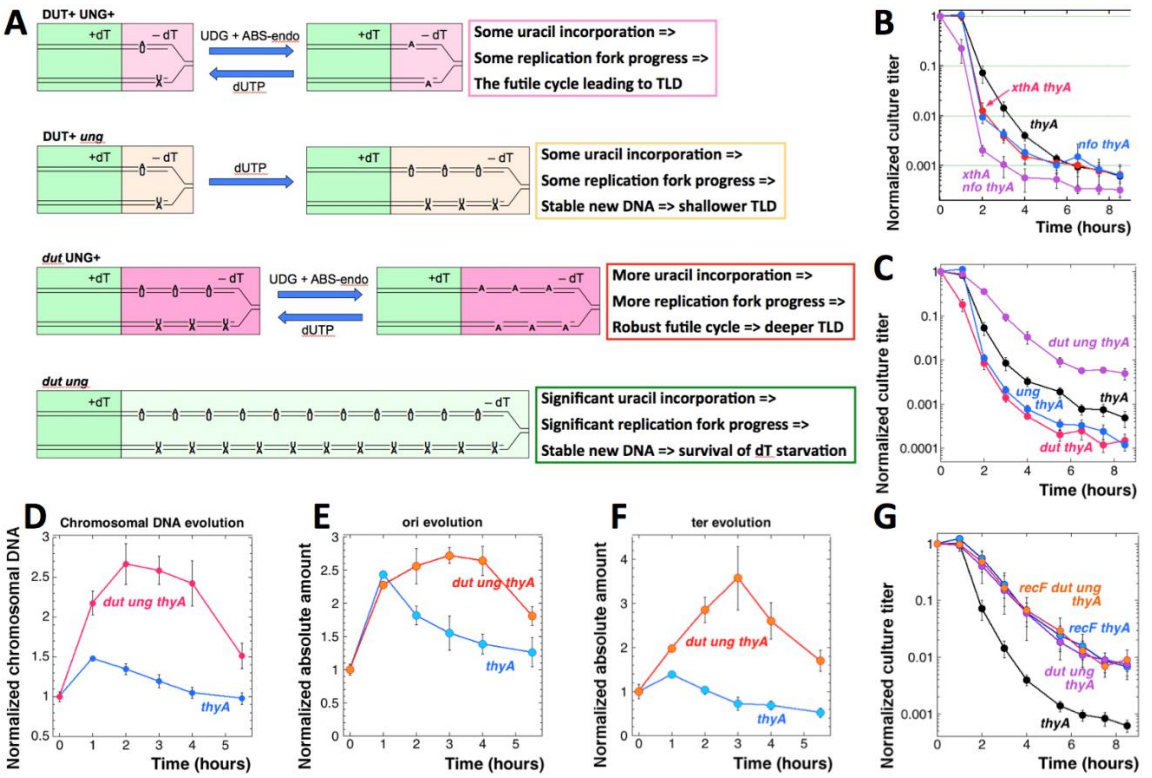

Figure 2.8. The role of deoxy-uridine in TLD. A. A scheme of DNA-dU misincorporation and its consequence in *thyA*, *ung thyA*, *dut thyA* and *dut ung thyA* mutants undergoing thymine starvation. Green fill, growth with dT. Light pink fill, attempted replication without dT using little dU (Dut+) with active DNA-uracil removal (Ung+). Yellow fill, replication without dT using little dU (Dut+), with no DNA-uracil removal (*ung*). Pink fill, attempted replication without dT but with plenty of dU (*dut*) with active DNA-uracil removal (Ung+). Light green fill, normal replication without dT but with plenty of dU (*dut*) and without DNA-uracil excision (*ung*). **B.** Time course of TLD in ABS-endo mutants. Strains are: *thyA*, KKW58; *xthA thyA*, RA22; *nfo thyA*, RA23; *xthA nfo thyA*, RA24. **C.** Time course of TLD in the *dut thyA* and *ung thyA* mutants. The +dT/-dT medium switch in this case was by centrifugation. Strains are: *thyA*, KKW58; *dut thyA*, RA16; *ung thyA*, KJK78; *dut ung thyA*, RA18. **D.** Evolution of the chromosomal DNA amount in the *thyA* (KKW58) and *dut ung thyA* (RA18) mutants during thymine starvation. **E.** Evolution of the replication origin copy number in the *thyA* and *dut ung thyA* mutants (strains like in "D") during thymine starvation. **F.** Evolution of the chromosomal terminus copy number in the *thyA* and *dut ung thyA* mutants (strains like in "D") during thymine starvation. **G.** TLD kinetics of the *recF dut ung thyA* mutant. The strains are *thyA*,KKW58; *thyA recF*, RA31; *thyA dut ung*, RA18; *thyA dut ung recF*, RA32.

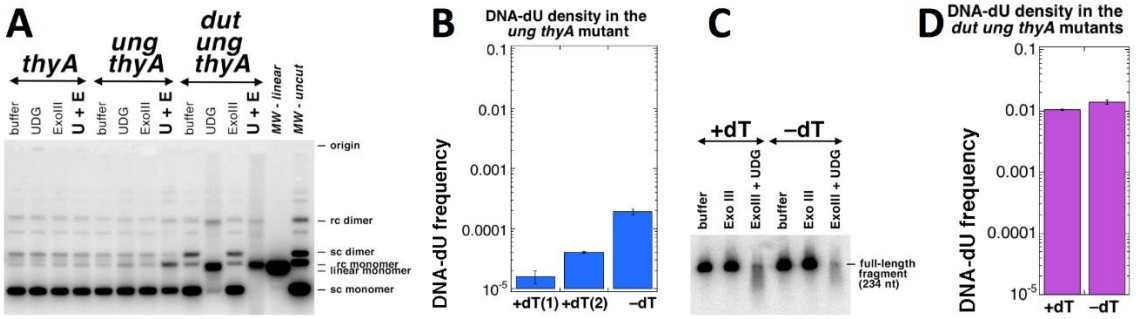

Figure 2.9. Density of DNA-dU in the *ung thyA* and *dut ung thyA* mutants, either starved or not for dTTP. +dT, growth in the presence of thymidine; –dT, starvation without thymidine. Strains are: *thyA*, KKW58; *ung thyA*, KJK78; *dut ung thyA*, RA18. **A.** A representative gel (1.1% agarose) of DNA-dU density determination in plasmid DNA (pMTL20). UDG, treatment with uracil-DNA glycosylase; Exo III, treatment with exonuclease III; U + E, treatment with both UDG and Exo III. **B.** Quantification of the DNA-dU density (presented as frequency = 1/density) in the *ung thyA* mutant grown in the presence or absence of dT, from several gels like in "A". The "–dT" culture is processed 5 hours after dT removal by filtration. There are two different conditions of growth in the presence of dT, though: "+dT #1" is also processed 5 hours after the filtration (but dT was re-added in this case), so the culture becomes stationary. In contrast, "+dT #2" is processed when the culture reaches OD=0.6. **C.** A representative gel (3% alkaline agarose) of DNA-dU density determination in a 234 nt long fragment of pBR322. **D.** Quantification of the DNA-dU density (presented as frequency, = 1/density, and in the same scale as in "B", for direct comparison) in the *dut ung thyA* mutant grown in the presence or absence of dT for 5 hours, from several gels like in "C".

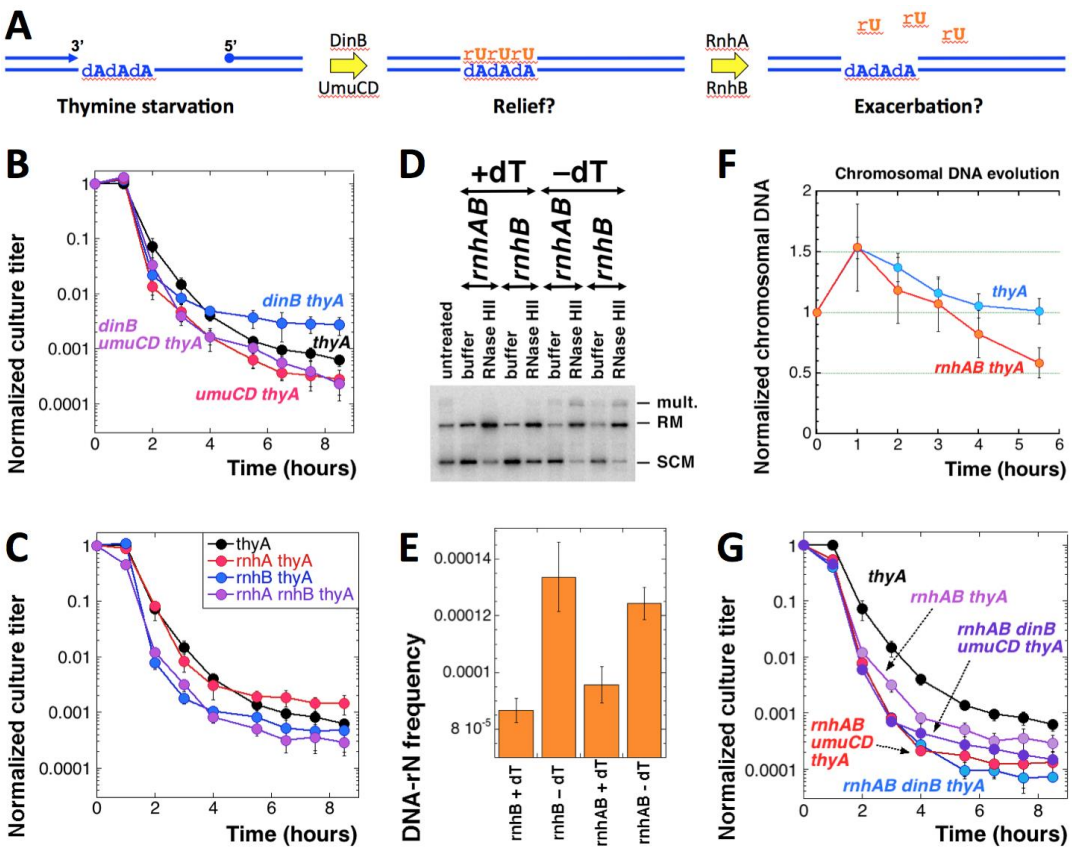

Figure 2.10. The effect of rN incorporation and excision on TLD. A. A scheme of the possible futile DNA-rU misincorporation/excision cycle. **B.** TLD kinetics of the *dinB thyA* and *umuCD thyA* mutants. The strains are: *thyA*, KKW58; *dinB thyA*, KJK90; *umuCD thyA*, KJK87; *dinB umuCD thyA*, RA36. **C.** TLD kinetics of the *rnhA thyA* and *rnhB thyA* mutants. The strains are: *thyA*, KKW58; *rnhA thyA*, RA33; *rnhB thyA*, RA34; *rnhAB thyA*, RA35. **D.** A representative gel (1.1% agarose) of DNA-rN density determination in plasmid DNA (plasmid is pEAK86) isolated from *rnhB* mutant cells. +dT, growth in the presence of thymidine; –dT, starvation without thymidine. Rnase HII, in vitro treatment with Rnase HII. Strains are: *rnhB*, RA34; *rnhAB*, RA35. **E.** DNA-rN density (presented as frequency = 1/density) in the *rnhB* and *rnhAB* mutants grown in the presence or absence of dT for 5 hours, from several gels like in "E". **F.** Evolution of the chromosomal DNA amount in the *thyA* (KKW58) versus *rnhAB thyA* (RA35) mutants during dTTP starvation. **G.** TLD kinetics of the *dinB rnhAB thyA* and *umuCD rnhAB thyA* mutants. The strains are: *rnhAB thyA*, RA35; *umuCD rnhAB thyA*, RA40; *dinB rnhAB thyA*, RA39; *dinB umuCD rnhAB thyA*, RA41.

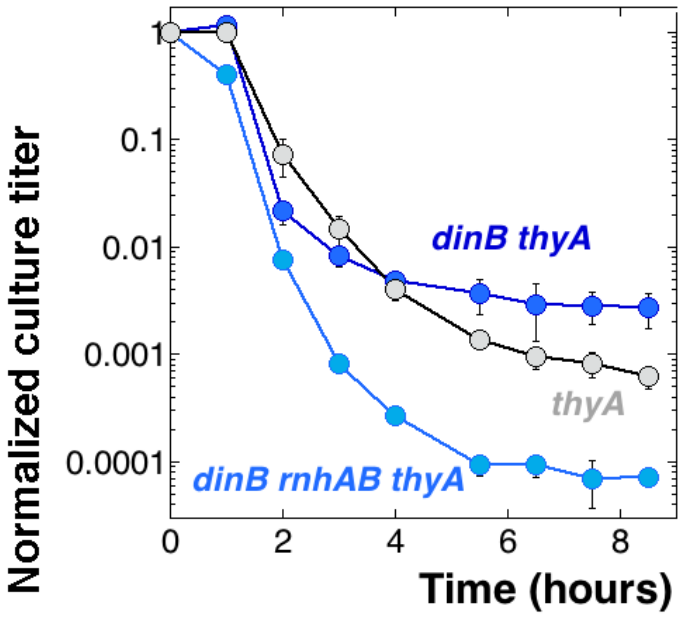

Figure 2.11. TLD kinetics of the *dinB thyA* mutant and its *dinB rnhAB thyA* variant. Strains are: *dinB thyA*, KJK90; *dinB rnhAB thyA*, RA39.

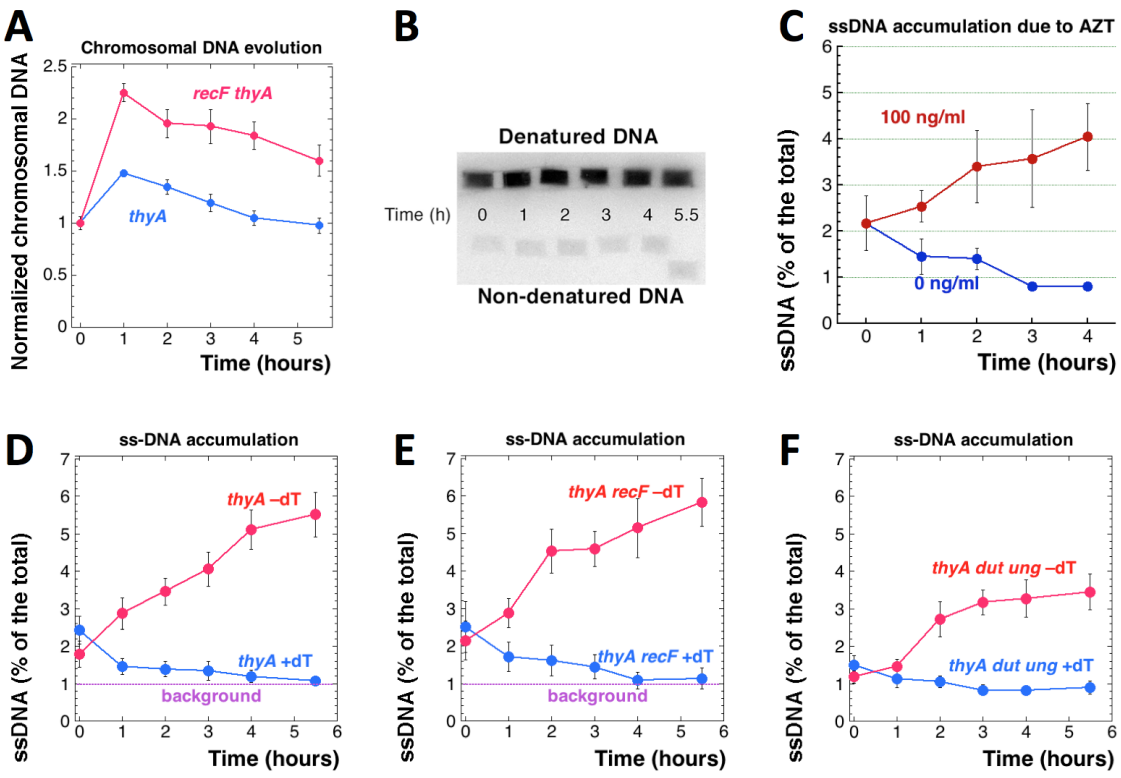

Figure 2.12. Accumulation of ss-gaps during T-starvation. A. Evolution of the chromosomal DNA amount in the *thyA* (KKW58) versus *recF thyA* (RA31) mutants during T-starvation. **B.** An example of plug-blot procedure to quantify ssDNA accumulation during T-starvation. After electric transfer to positively-charged nylon membrane, the genomic DNA was hybridized to the total genomic probe. **C.** Accumulation of ssDNA as percentage of the total DNA signal in the WT cell (AB1157) cultures grown in the presence of the indicated concentrations of AZT. **D.** The level of ssDNA in *thyA* mutant (KKW58) cultures grown in the presence (+dT) or absence (–dT) of thymidine. **E.** The level of ssDNA in the *thyA recF* (RA31) mutant. **F.** The level of ssDNA in the *thyA dut ung* (RA18) mutant.

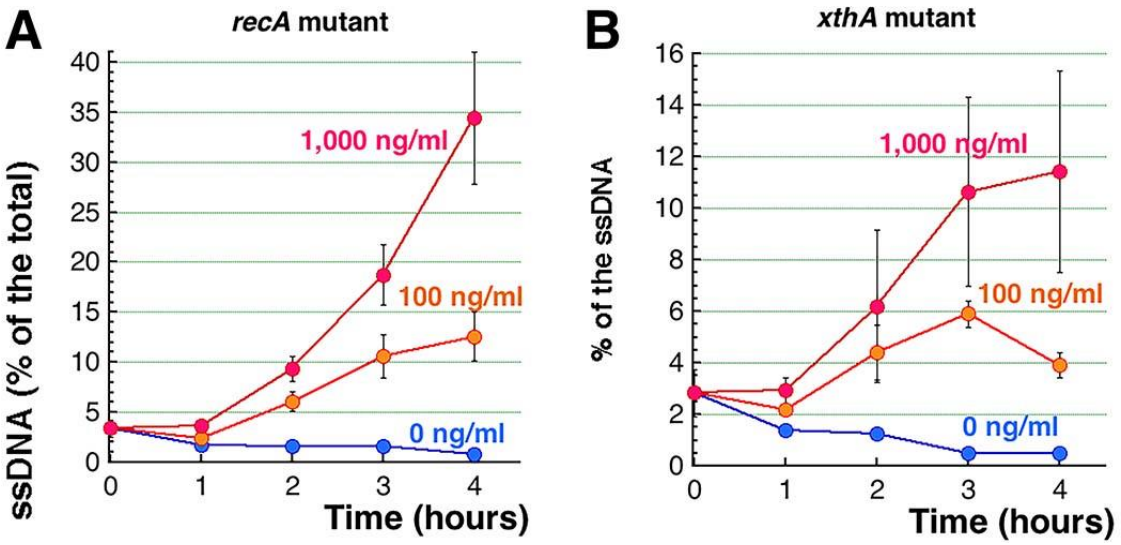

Figure 2.13. Single-stranded DNA accumulation in genomic DNA of growing cultures treated with 0, 100 or 1,000 ng/ml AZT. A. The *recA* mutant (RA50). **B.** The *xthA* mutant (HT50).

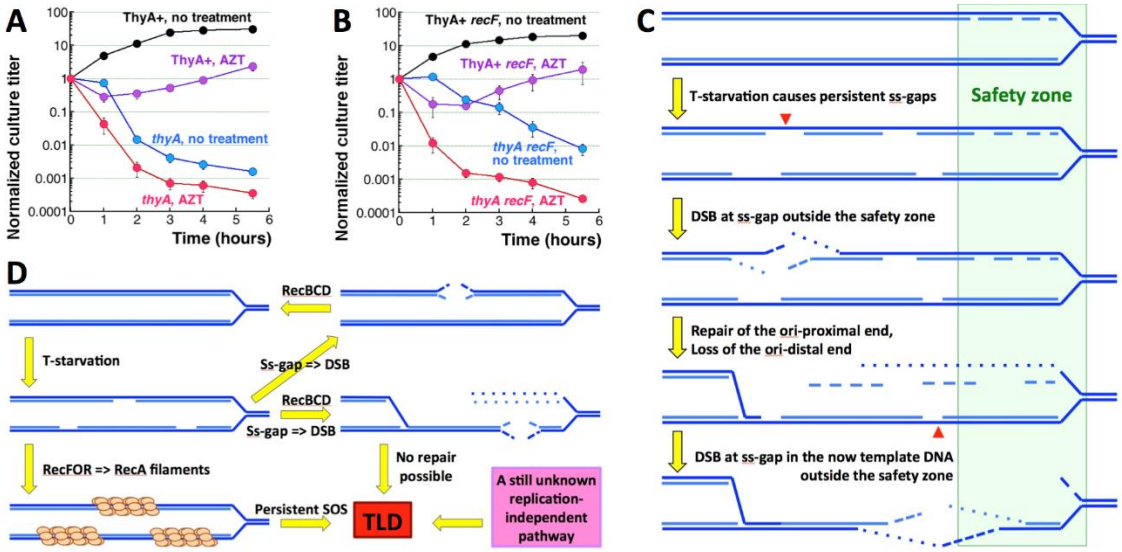

Figure. 2.14. Persistent single-strand gaps kill. A. TLD kinetics of the *thyA* mutant (KKW58) in the presence of AZT. After growth in the medium +dT, cells were washed and resuspended in the same volume of the same medium, but without dT, supplemented or not with 100 ng/ml AZT. The ThyA+ strain (KKW59) is also shown, to demonstrate the toxicity of this AZT dose in this medium (without dT). **B.** TLD kinetics of the *thyA recF* mutant (RA31) in the presence of 100 ng/ml AZT (done like in "A"). The ThyA+ *recF* strain (RA48) is also shown, to illustrate AZT toxicity. **C.** A model to explain loss of the replication forks due to ss-gaps accumulating outside the "safety zone" (green rectangle) around the replication points, within which DNA with ss-interruptions is safe (note the Okazaki fragments on the lagging strand). Red arrowheads mark the position of double-strand breaks. **D.** The known and the suspected unknown aspects of TLD. The two known aspects, instability of ss-gaps and SOS-induction, are linked with replication forks. However, TLD in the *thyA dut ung* mutant suggests an unknown, replication-independent pathway.

2.8 Tables

Table 2.1. Strains used in this study.

Strain Name	Genotype[a]	Reference / Source
AAM1	Δ*thyA71::cat*	(52)
AM3	*recF20::cat*	(64)
BW1161	*nfi::cat*	(33)
ER131	Δ*rnhA::cat*	(45)
GY9701*	*recA938::cam* miniF-kan *recA+*	R. Devoret via Benedicte Michel
HT50	*xthA::cat*	(85)
JB1 pSA122	Δ*recBCD3*::*kan* pRecBC+	Lab Collection
JC7623	*recB21 recC22 sbcB15 sbcC201*	(54)
JW0178-1*	Δ*rnhB782::kan*	(3)
JW0221-1*	Δ*dinB749::kan*	(3)
JW0843-1*	Δ*rumB760::kan*	(3)
JW2756-1*	Δ*rumA783::kan*	(3)
JW3937-1*	Δ*trmA753::kan*	(3)
KJK63	Δ*thyA72* Δ*deoCABD2* Δ*recBCD3::kan*	(52)
KJK78	Δ*thyA72* Δ*deoCABD2* Δ*ung::cat*	(52)
KJK87	Δ*thyA72* Δ*deoCABD2* Δ*umuCD595::cat*	Lab Collection
KJK90	Δ*thyA72* Δ*deoCABD2* Δ*dinB749::kan*	Lab Collection
KJK183	Δ*deoCABD2 dut1 zic 4901::*Tn*10*	Lab Collection
KKW47	Δ*deoCABD1::cat*	(52)
KKW58	Δ*thyA72* Δ*deoCABD2*	(52)
KKW59	Δ*deoCABD2*	(52)
L76	AB1157 *dcd329::kan*	Lab Collection
L418	Δ*rnhA::cat* Δ*rnhB782::kan*	(45)
RPC501	AB1157 *nfo-1::kan*	(19)
RW82	*uvrA6 umuCD595::cat*	(90)
RA9	Δ*thyA72* Δ*deoCABD2* Δ*trmA753::kan*	KKW58 x P1 JW3937-1
RA10	Δ*thyA72* Δ*deoCABD2* Δ*rumA783::kan*	KKW58 x P1 JW11916
RA11	Δ*thyA72* Δ*deoCABD2* Δ*rumB760::kan*	KKW58 x P1 JW8879
RA12	Δ*thyA72* Δ*deoCABD2* Δ*rumA*	RA10 treated with pCP20
RA13	Δ*thyA72* Δ*deoCABD2* Δ*rumA rumB760::kan*	RA12 x P1 JW8879
RA14	Δ*thyA72* Δ*deoCABD2* Δ*trmA753::kan* Δ*rumB*	RA11 treated with pCP20 and transduced with P1 JW3937-1
RA15	Δ*thyA72* Δ*deoCABD2* Δ*rumA* Δ*rumB* Δ*trmA753::kan*	RA13 treated with pCP20 and transduced with P1 JW3937-1
RA16	Δ*thyA71::cat* Δ*deoCABD2 dut-1 zic 4901::*Tn*10*	KJK183 x P1 AAM1

Table 2.1. (cont.)

RA17	Δ*thyA72* Δ*deoCABD2 dut-1 zic 4901::*Tn*10*	RA16 treated with pCP20
RA18	Δ*thyA72* Δ*deoCABD2 dut-1 zic 4901::*Tn*10* Δ*ung::cat*	RA17 x P1 KJK78
RA22	Δ*thyA72* Δ*deoCABD2* Δ*xthA::cat*	KKW58 x P1 HT50
RA23	Δ*thyA72* Δ*deoCABD2* Δ*nfo-1::kan*	KKW58 x P1 RPC501
RA24	Δ*thyA72* Δ*deoCABD2* Δ*xthA::cat* Δ*nfo-::kan*	RA22 x P1 HT50
RA25	Δ*thyA72* Δ*deoCABD2 dcd329::kan*	KKW58 x P1 L76
RA26	Δ*thyA72* Δ*deoCABD2* Δ*ung::cat dcd329::kan*	KJK78 x P1 L76
RA27	Δ*thyA72* Δ*deoCABD2 dut-1 zic 4901::*Tn*10 dcd329::kan*	RA16 x P1 L76
RA28	Δ*thyA72* Δ*deoCABD2 dut-1 zic 4901::*Tn*10* Δ*ung::cat dcd329::kan*	RA17 x P1 L76
RA29	Δ*thyA72* Δ*deoCABD2 dut-1 zic 4901::*Tn*10* Δ*ung*	RA18 treated with pCP20
RA30	Δ*thyA72* Δ*deoCABD2 dut-1 zic 4901::*Tn*10* Δ*ung Δnfi::cat*	RA29 x P1 BW1161
RA31	Δ*thyA72* Δ*deoCABD2* Δ*recF20::cat*	KJK78 x P1 AM3
RA32	Δ*thyA72* Δ*deoCABD2 dut-1 zic 4901::*Tn*10* Δ*ung* Δ*recF20::cat*	RA29 x P1 AM3
RA33	Δ*thyA72* Δ*deoCABD2* Δ*rnhA::cat*	KKW58 x P1 ER131
RA34	Δ*thyA72* Δ*deoCABD2* Δ*rnhB782::kan*	KKW58 x P1 JW0178-1
RA35	Δ*thyA72* Δ*deoCABD2* Δ*rnhA::cat* Δ*rnhB782::kan*	KKW58 x P1 L418
RA36	Δ*thyA72* Δ*deoCABD2* Δ*dinB749::kan umuCD595::cat*	KJK87 x P1JW0221-1
RA37	Δ*thyA72* Δ*deoCABD2* Δ*rnhA::cat* Δ*rnhB782::kan* pEAK86	
RA38	Δ*thyA72* Δ*deoCABD2* Δ*rnhA2* Δ*rnhB2*	RA35 treated with pCP20
RA39	Δ*thyA72* Δ*deoCABD2* Δ*rnhA2* Δ*rnhB2* Δ*dinB749::kan*	RA38 x P1 JW0221-1
RA40	Δ*thyA72* Δ*deoCABD2* Δ*rnhA2* Δ*rnhB2 umuCD595::cat*	RA38 x P1 RW82
RA41	Δ*thyA72* Δ*deoCABD2* Δ*rnhA2* Δ*rnhB2 ΔdinB749::kan umuCD595::cat*	RA39 x P1 RW82
RA42	Δ*deoCABD::cat recB21 recC22 sbcB15 sbcC201*	JC7623 x P1 KKW47
RA43	Δ*deoCABD2 recB21 recC22 sbcB15 sbcC201*	RA42 treated with pCP20
RA44	Δ*thyA71::cat* Δ*deoCABD2 sbcB15 sbcC201*	RA43 x AAM1
RA45	Δ*thyA71::cat* Δ*deoCABD2 sbcB15 sbcC201* Δ*recBCD::kan*	RA44 x P1 JB1 pSA122
RA46	*recA938::cat* Δ*thyA72* Δ*deoCABD2*	KKW58 x P1 GY9701

Table 2.1. (cont.)

RA47	Δ*recBCD sbcB15 sbcC201 recA938::cat* Δ*thyA72* Δ*deoCABD2*	RA45 treated with pCP20 and transduced with P1 GY9701
RA48	Δ*deoCABD2 recF20::cat*	KKW59 x P1 AM3
RA49	*recA938::cat recB21 recC22 sbcB15 sbcC201*	JC7623 x P1 GY9701
RA50	*recA938::cat*	AB1157 x P1 GY9701

a — Background for all strains, except those marked with * is AB1157, which also includes: F– λ– *rac– thi-1 hisG4* Δ*(gpt-proA)62 argE3 thr-1 leuB6 kdgK51 rfbD1 araC14 lacY1 galK2 xylA5 mtl-1 tsx-33 supE44*(glnV44) *rpsL31*(strR).

Table 2.2. Plasmids used in this study.

Plasmid	Replicon/Drug Resistance/Other Genes	Reference
pBR322	cloning vector / *bla tet*	(8)
pMTL20	pBR322 / *bla* / *lacZ alpha*	(14)
pEAK86	pSC101* / *bla* / *csdA*	(45)
pCP20	Rep^{ts} / *bla cat* / *FLP+*	(20)
pKD46	Rep^{ts}/ *bla* / *exo gam bet araC*	(20)
pSA122	p15A / *cat* / *recB+ recC+*	(2)

Table 2.3. Primers used in this study.

Purpose	Sequence
trmA deletion verification	PR01 CCGTCATTATGGTGTTCTGG
	PR02 CAAGTGGATGCTACAGGTTG
rumA deletion verification	PR06 CCAGGATCAGAATCATCATGCGTG
	PR07 GTGCACTTCTTACCGCAACC
rumB deletion verification	PR08 CCAGTCGGCGGTTCTTCCAG
	PR09 CAATCTGAAGCCGCACATGC
Dcd329 verification	PR10 GTGATAACCTAGTATGCCCTTGACG
	PR11 CAGGAGTATCATCAGCGTCG
Nfi deletion verification	PR14 TTGCAGGTTTCGGTCACGGC
	PR15 CGGTAAATTTGCCCATCACC
Nfo deletion verification	PR23 AAAGCTGGGGCGAAACCTCTG
	PR24 GAGCAATGAATTGTACCGGG
deoCABD deletion verification	PR42 TTGATCCTGATGCGTTTGCC
	PR43 ATCCAGAGGAATTTCCGCAG
recB21 insertion verification	PR44 AAGAATGAGTGATGTCGCCG
	PR45 GCATCATGACTTAACAGTGCCG
rnhA deletion verification	#167 GCACCAATCTGGTTCATACC
	#168 CAATGTCGTAAACCACAGGC
rnhB deletion verification	#269 GAACTGCATCAGCAGATCCG
	#270 CAGACATCTTCAGATTCCGG
dinB deletion verification	dinB(Exp)F CGCGAATTCCGCAGCGAACGCGTTAAATG
	dinB(PCR)B AACGCTTCGAATGCGCTGGC

Table 2.3. (cont.)

umuDC deletion verification	umuCD(Exp)F CGCGAATTCCAGTCATAATCATTCGCCTC
	umuCD (PCR)B GATCTGTTCGGTCGCTAATC
xthA deletion verification	xthA(F) CGGTAAGCAACGCGAAATTC
	xthA(B) GTATAACAAAGGACGGCAGG

2.9 References

1. Ahmad SI, Kirk SH, Eisenstark A. 1998. Thymine metabolism and thymineless death in prokaryotes and eukaryotes. *Annu. Rev. Microbiol.* 52:591–625.

2. Amundsen SK, Taylor AF, Smith GR. 2000. The RecD subunit of the *Escherichia coli* RecBCD enzyme inhibits RecA loading, homologous recombination, and DNA repair. *Proc. Natl. Acad. Sci. USA*. 97(13):7399–7404.

3. Baba T, Ara T, Hasegawa M, Takai Y, Okumura Y, et al. 2006. Construction of Escherichia coli K-12 in-frame, single-gene knockout mutants: The Keio collection. *Mol. Syst. Biol.* 2:2006.0008.

4. Barner HD, Cohen SS. 1954. The induction of thymine synthesis by T2 infection of a thymine requiring mutant of *Escherichia coli*. *J. Bacteriol.* 68(1):80–88.

5. Barner HD, Cohen SS. 1958. Protein synthesis and RNA turnover in a pyrimidine deficient bacterium. *Biochim. Biophys. Acta*. 30:12–20.

6. Beck CF, Eisenhardt AR, Neuhard J. 1975. Deoxycytidine triphosphate deaminase of *Salmonella typhimurium*. *J. Biol. Chem.* 250(2):609–16.

7. Bochner BR, Ames BN. 1982. Complete analysis of cellular nucleotides by two-dimensional thin layer chromatography. *J. Biol. Chem.* 257(16):9759–69.

8. Bolivar F, Boyer HW, Betlach MC. 1977. Construction and characterization of new cloning vehicles 1. Ampicillin- resistant derivatives of the plasmid pMB9. *Gene*. 2:75–93.

9. Breitman TR, Finkleman A, Rabinovitz M. 1971. Methionineless death in *Escherichia coli*. *J. Bacteriol.* 108(3):1168–73.

10. Breitman TR, Maury PB, Toal JN. 1972. Loss of deoxyribonucleic acid-thymine during thymine starvation of *Escherichia coli*. *J. Bacteriol.* 112(1):646–48.

11. Bremer H, Dennis PP, Neidhardt FC. 1996. Modulation of Chemical Composition and Other Parametrs of the Cell by Growth Rate. *Escherichia coli* and *Salmonella typhimurium.* ASM Press, Washington D.C. 1553–1569 pp.

12. Buick RW, Harris WJ. 1975. Thymineless death in *Bascillus subtilis*. *J. Gen. Microbiol.* 88(1):115–22.

13. Cerritelli SM, Crouch RJ. 2009. Ribonuclease H: the enzymes in eukaryotes. *FEBS J.* 276(6):1494–1505.

14. Chambers SP, Prior SE, Barstow DA, Minton NP. 1988. The pMTL nic- cloning vectors. I. Improved pUC polylinker regions to facilitate the use of sonicated DNA for nucleotide sequencing. *Gene*. 68(1):139–49.

15. Cohen SS. 1971. On the nature of thymineless death. *Ann. N. Y. Acad. Sci.* 186:292–301.

16. Cohen SS, Barner HD. 1954. Studies on unbalanced growth in Escherichia coli. *Proc. Natl. Acad. Sci. USA*. 40:885–93.

17. Cooper DL, Lovett ST. 2011. Toxicity and tolerance mechanisms for azidothymidine, a replication gap-promoting agent, in *Escherichia coli*. *DNA Repair (Amst).* 10(3):260–70.

18. Cronan GE, Kouzminova EA, Kuzminov A. 2019. Near-continuously synthesized leading strands in *Escherichia coli* are broken by ribonucleotide excision. *Proc. Natl. Acad. Sci. USA*. 116(4):1251–60.

19. Cunningham RP, Saporito SM, Spitzer SG, Weiss B. 1986. Endonuclease IV (nfo) mutant of *Escherichia coli*. *J. Bacteriol.* 168(3):1120–27.

20. Datsenko KA, Wanner BL. 2000. One-step inactivation of chromosomal genes in *Escherichia coli* K-12 using PCR products. *Proc. Natl. Acad. Sci. U. S. A.* 97(12):6640–45.

21. Dornfeld K, Johnson M. 2005. AP endonuclease deficiency results in extreme sensitivity to thymidine deprivation. *Nucleic Acids Res.* 33(20):6644–53.

22. El-Hajj HH, Wang L, Weiss B. 1992. Multiple mutant of *Escherichia coli* synthesizing virtually thymineless DNA during limited growth. *J. Bacteriol.* 174(13):4450–56.

23. El-Hajj HH, Zhang H, Weiss B. 1988. Lethality of a dut (deoxyuridine triphosphatase) mutation in Escherichia coli. *J. Bacteriol.* 170(3):1069–75.

24. Fonville NC, Bates D, Hastings PJ, Hanawalt PC, Rosenberg SM. 2010. Role of RecA and the SOS response in thymineless death in *Escherichia coli*. *PLoS Genet.* 6(3):e1000865.

25. Fonville NC, Vaksman Z, Denapoli J, Hastings PJ, Rosenberg SM. 2011. Pathways of resistance to thymineless death in *Escherichia coli* and the function of UvrD. *Genetics*. 189(1):23–36.

26. Frederico LA, Kunkel TA, Shaw BR. 1990. A sensitive genetic assay for the detection of cytosine deamination: determination of rate constants and the activation energy. *Biochemistry*. 29:2532–37.

27. Freifelder D, Katz G. 1971. Persistence of small fragments of newly synthesized DNA in bacteria following thymidine starvation. *J. Mol. Biol.* 57(2):351–54.

28. Friedberg EC, Walker GC, Siede W, Wood RD, Schultz RA, Ellenberger T. 2006. *DNA Repair and Mutagenesis.* ASM Press, Washington D.C.

29. Gallant J, Suskind R. 1961. Relationship between thymineless death and ultraviolet inactivation in *Escherichia coli*. *J. Bacteriol.* 1961:187–94.

30. Goulian M, Bleile B, Tseng BY. 1980. The effect of methotrexate on levels of dUTP in animal cells. *J. Biol. Chem.* 255(22):10630–37.

31. Goulian M, Bleile B, Tseng BY. 1980. Methotrexate-induced misincorporation of uracil into DNA. *Proc. Natl. Acad. Sci. USA.* 77(4):1956–60.

32. Guarino E, Salguero I, Jiménez-Sánchez A, Guzmán EC. 2007. Double-strand break generation under deoxyribonucleotide starvation in *Escherichia coli*. *J. Bacteriol.* 189(15):5782–86.

33. Guo G, Weiss B. 1998. Endonuclease V (nfi) mutant of *Escherichia coli* K-12. *J. Bacteriol.* 180(1):46–51.

34. Helaine S, Kugelberg E. 2014. Bacterial persisters: formation, eradication, and experimental systems. *Trends Microbiol.* 22(7):417–24.

35. Hochhausert SJ, Weiss B. 1978. Escherichia coli mutants deficient in deoxyuridine triphosphatase. *J. Bacteriol.* 134(1):157–66.

36. Hoess R, Wierzbicki A, Abremski K. 1985. Formation of small circular DNA molecules via an in vitro site-specific recombination system. *Gene.* 40(2–3):325–29.

37. Hong Y, Li L, Luan G, Drlica K, Zhao X. 2017. Contribution of reactive oxygen species to thymineless death in *Escherichia coli*. *Nat. Microbiol.* 2(12):1667–75.

38. Huisman O, D'Ari R. 1981. An inducible DNA replication-cell division coupling mechanism in *E. coli*. *Nature*. 290(5809):797–99.

39. Itsko M, Schaaper RM. 2014. dGTP starvation in Escherichia coli provides new insights into the thymineless-death phenomenon. *PLoS Genet.* 10(5):e1004310.

40. Itsko M, Schaaper RM. 2017. Suppressors of dGTP starvation in *Escherichia coli*. *J. Bacteriol.* 199(12):e00142-17.

41. Jarosz DF, Beunning PJ, Cohen SE, Walker GC. 2007. Y-family DNA polymerases in Escherichia coli. *Trends in Microbiol.* 15(2):70–77.

42. Khan SR, Kuzminov A. 2012. Replication forks stalled at ultraviolet lesions are rescued via RecA and RuvABC protein-catalyzed disintegration in *Escherichia coli*. *J. Biol. Chem.* 287(9):6250–65.

43. Khodursky A, Guzmán EC, Hanawalt PC. 2015. Thymineless death lives on: New insights into a classic phenomenon. *Annu. Rev. Microbiol.* 69(1):247–63.

44. Kouzminova E, Kuzminov A. 2006. Fragmentation of replicating chromosomes triggered by uracil in DNA. *J. Mol. Biol.* 355(1):20–33.

45. Kouzminova EA, Kadyrov FF, Kuzminov A. 2017. RNase HII saves *rnhA* mutant *Escherichia coli* from R-Loop-associated chromosomal fragmentation. *J. Mol. Biol.* 429(19):2873–94.

46. Kouzminova EA, Kuzminov A. 2004. Chromosomal fragmentation in dUTPase-deficient mutants of *Escherichia coli* and its recombinational repair. *Mol. Microbiol.* 51(5):1279–95.

47. Kouzminova EA, Kuzminov A. 2012. Chromosome demise in the wake of ligase-deficient replication. *Mol. Microbiol.* 84(6):1079–96.

48. Kouzminova EA, Rotman E, Macomber L, Zhang J, Kuzminov A. 2004. RecA-dependent mutants in *Escherichia coli* reveal strategies to avoid chromosomal fragmentation. *Proc. Natl. Acad. Sci. USA.* 101(46):16262–67.

49. Kunz BA, Little JG, Eckardt F, Haynes RH. 1982. Thymineless recombination in Saccharomyces cerevisiae is independent of the ability to undergo meiosis. *Curr. Genet.* 5(1):29–31.

50. Kunz C, Focke F, Saito Y, Schuermann D, Lettieri T, et al. 2009. Base excision by thymine DNA glycoylase mediates DNA-directed cytotoxicity of 5-fluorouracil. *Plos Biol.* 7(4):e91.

51. Kuong KJ, Kuzminov A. 2009. Cyanide, peroxide and nitric oxide formation in solutions of hydroxyurea causes cellular toxicity and may contribute to its therapeutic potency. *J. Mol. Biol.* 390(5):845–62.

52. Kuong KJ, Kuzminov A. 2010. Stalled replication fork repair and misrepair during thymineless death in *Escherichia coli*. *Genes to Cells.* 15(6):619–34.

53. Kuong KJ, Kuzminov A. 2012. Disintegration of nascent replication bubbles during thymine starvation triggers RecA- and RecBCD-dependent replication origin destruction. *J. Biol. Chem.* 287(28):23958–70.

54. Kushner SR, Nagaishi H, Templin A, Clark a J. 1971. Genetic recombination in *Escherichia coli*: the role of exonuclease I. *Proc. Natl. Acad. Sci. U. S. A.* 68(4):824–27.

55. Kuzminov A. 1999. Recombinational repair of DNA damage in *Escherichia coli* and bacteriophage lambda. *Microbiol. Mol. Biol. Rev.* 63(4):751–813.

56. Ladner R. 2001. The role of dUTPase and uracil-DNA repair in cancer chemotherapy. *Curr Protein Pept Sci.* 2(4):361–70.

57. Maaloe O, Hanawalt PC. 1961. Thymine deficiency and the normal DNA replication cycle. I. *J. Mol. Biol.* 3:144–55.

58. Madsen CT, Mengel-Jørgensen J, Kirpekar F, Douthwaite S. 2003. Identifying the methyltransferases for m5U747 and m5U1939 in 23S rRNA using MALDI mass spectrometry. *Nucleic Acids Res.* 31(16):4738–46.

59. Makino F, Munakata N. 1978. Deoxyuridine residues in DNA of thymine requiring Bacillus subtilis strains with defective N- glycosidase activity for uracil containing DNA. *J. Bacteriol.* 134(1):24–29.

60. Maniatis T, Fritsch EF, Sambrook J. 1982. *Molecular cloning. A laboratory manual.* Cold Spring Harbor, NY: Cold Spring Harbor Laboratory Press.

61. Martín CM, Guzmán EC. 2011. DNA replication initiation as a key element in thymineless death. *DNA Repair (Amst).* 10(1):94–101.

62. McCann MP, Kidwell JP, Matin A. 1991. The Putative sigma factor KatF has a central role in developmet of starvation-mediated general resistance in *Escherichia coli*. *J. Bacteriol.* 173(13):4188–94.

63. Miller JH. 1972. Experiments in Molecular Genetics. , p. 466. Cold Spring Harbor, NY: Cold Spring Harbor Laboratory Press.

64. Miranda A, Kuzminov A. 2003. Chromosomal lesion suppression and removal in Escherichia coli via linear DNA degradation. *Genetics*. 163(4):1255–71.

65. Nakayama H, Nakayama K, Nakayama R, Nakayama Y. 1982. Recombination-deficient mutations and thymineless death in *Escherichia coli* K12: reciprocal effects of *recBC* and *recF* and indifference of *recA* mutations. *Can. J. Microbiol.*, pp. 425–30.

66. Nakayama K, Kusano K, Irino N, Nakayama H. 1994. Thymine starvation-induced structural changes in *Escherichia coli* DNA. Detection by pulsed field gel electrophoresis and evidence for involvement of homologous recombination. *J Mol Biol*. 243(4):611–20.

67. Napolitano R, Janel-Bintz R, Wagner J, Fuchs RP. 2000. All three SOS-inducible DNA polymerases (Pol II, Pol IV and Pol V) are involved in induced mutagenesis. *EMBO J.* 19(22):6259–65.

68. Neuhard J, Munch-Petersen A. 1966. Studies on the acid-soluble nucleotide pool in thymine-requiring mutants of *Escherichia coli* during thymine starvation. II. Changes in the amounts of deoxycytidine triphosphate and deoxyadenosine triphosphate in *Escherichia coli* 15 T-A-U." B. *Biochim. Biophys. Acta.* 114(1):61–71.

69. Neuhard J, Nygaard P. 1987. Purines and Pyrimidines. *Escherichia coli* and *Salmonella typhimurium.* Cellular and Molecular Biology. American Society for Microbiology, Washington D.C. 445–473 pp. F.C. Neidh ed.

70. Neuhard J, Thomassen E. 1971. Deoxycytidine triphosphate deaminase: identification and function in *Salmonella typhimurium*. *J. Bacteriol.* 105(2):657–65.

71. Nick McElhinny SA, Watts BE, Kumar D, Watts DL, Lundstrom E-B, et al. 2010. Abundant ribonucleotide incorporation into DNA by yeast replicative polymerases. *Proc. Natl. Acad. Sci. USA*. 107(11):4949–54.

72. Ohkawa T. 1975. Studies of intracellular thymidine nucleotides. Thyminless death and the recovery after re-addition of thymine in *Escherichia coli* K 12. *Eur. J. Biochem.* 60:57–66.

73. Ohtani N, Haruki M, Morikawa M, Kanaya S. 1999. Molecular diversities of RNases H. *J. Biosci. Bioeng.* 88(1):12–19.

74. Qian A, Robins P, Lindahl T, Barnes DE. 2007. 5-Fluorouracil incorporated into DNA is excised by the Smug1 DNA glycosylase to reduce drug cytotoxicity. *Cancer Res.* 67(3):940–45.

75. Rinken R, Thoms B, Wackernagel W. 1992. Evidence that *recBC*-dependent degradation of duplex DNA in *Escherichia coli recD* mutants involves DNA unwinding. *J. Bacteriol.* 174(16):5424–29.

76. Rupp WD, Howard-Flanders P. 1968. Discontinuities in the DNA synthesized in an excision-defective strain of Escherichia coli following ultraviolet irradiation. *J. Mol. Biol.* 31(2):291–304.

77. Sangurdekar DP, Hamann BL, Smirnov D, Srienc F, Hanawalt PC, Khodursky AB. 2010. Thymineless death is associated with loss of essential genetic information from the replication origin. *Mol. Microbiol.* 75(6):1455–67.

78. Schroeder JW, Randall JR, Matthews LA, Simmons LA. 2015. Ribonucleotides in bacterial DNA. *Crit. Rev. Biochem. Mol. Biol.* 50(3):181–93.

79. Seiple L, Jaruga P, Dizdaroglu M, Stivers JT. 2006. Linking uracil base excision repair and 5-fluorouracil toxicity in Yeast. *Nucleic Acids Res.* 34(1):140–51.

80. Sergeeva OV, Bogdanov AA, Sergiev PV. 2015. What do we know about ribosomal RNA methylation in *Escherichia coli*? *Biochimie.* 117:110–18.

81. Sivaramakrishnan P, Sepúlveda LA, Halliday JA, Liu J, Núñez MAB, et al. 2017. The transcription fidelity factor GreA impedes DNA break repair. *Nature*. 550(7675):214–18.

82. Stead MB, Agrawal A, Bowden KE, Nasir R, Mohanty BK, et al. 2012. RNAsnapTM: A rapid, quantitative and inexpensive, method for isolating total RNA from bacteria. *Nucleic Acids Res.* 40(20):1–9.

83. Tamanoi F, Okazaki T. 1978. Uracil incorporation into nascent DNA of thymine-requiring mutant of *Bacillus subtilis* 168. *Proc. Natl. Acad. Sci. USA*. 75(5):2195–99.

84. Taylor AF, Weiss B. 1982. Role of exonuclease III in the base excision repair of uracil- containing DNA. *J Bacteriol*. 151(1):351–57.

85. Thakur AR, Poddar RK. 1977. Growth and reactivation of single stranded DNA phage phiX174 in *E. coli* dndergoing "Thymineless Death". *Mol. Gen. Genet.* 151(3):313–18.

86. Ting H, Kouzminova EA, Kuzminov A. 2008. Synthetic lethality with the *dut* defect in Escherichia coli reveals layers of DNA damage of increasing complexity due to uracil incorporation. *J. Bacteriol.* 190(17):5841–54.

87. Vaisman A, Kuban W, McDonald JP, Karata K, Yang W, et al. 2012. Critical amino acids in *Escherichia coli* UmuC responsible for sugar discrimination and base-substitution fidelity. *Nucleic Acids Res.* 40(13):6144–57.

88. Wachsman JT, Kemp S, Kogg L. 1964. Thymineless death in *Bacillus megaterium*. *J. Bacteriol.* 87(5):1079–86.

89. Warner HR, Duncan BK, Garrett C, Neuhard J. 1981. Synthesis and metabolism of uracil-containing deoxyribonucleic acid in *Escherichia coli*. *J Bacteriol*. 145(2):687–95.

90. Woodgate R. 1992. Construction of a *umuDC* operon substitution mutation in *Escherichia coli*. *Mutat. Res. Lett.* 281(3):221–25.

91. Yao M, Hatahet Z, Melamede RJ, Kow YW. 1994. Purification and characterization of a novel deoxyinosine-specific eznyme, deoxyinosine 3' endonuclease from *Escherichia coli*. *J Biol Chem.* 269(23):16260–68.

92. Yao M, Kow YW. 1997. Further characterization of *Escherichia coli* endonuclease V. Mechanism of recognition for deoxyinosine, deoxyuridine, and base mismatches in DNA. *J. Biol. Chem.* 272(49):30774–79.

93. Yao NY, Schroeder JW, Yurieva O, Simmons LA, O'Donnell ME. 2013. Cost of rNTP/dNTP pool imbalance at the replication fork. *Proc. Natl. Acad. Sci. USA.* 110(32):12942–47.

94. Yoshinaga K. 1973. Double-strand scission of DNA involved in thymineless death of *Escherichia coli* 15 TAU. *Biochim. Biophys. Acta.* 294(2):204–13.

95. Zahradka K, Buljubašić M, Petranović M, Zahradka D. 2009. Roles of Exol and SbcCD nucleases in "Reckless" DNA degradation in recA mutants of *Escherichia coli*. *J.Bacteriol.* 191(5):1677–87.

CHAPTER 3: EXOPOLYSACCHARIDE DEFECTS CAUSE HYPER THYMINELESS DEATH IN *ESCHERICHIA COLI* VIA MASSIVE LOSS OF CHROMOSOMAL DNA AND CELL LYSIS

3.1 Introduction

Acute starvation for thymidine triphosphate (dTTP), one of the four precursors for DNA synthesis, is lethal in both bacterial and eukaryotic cells(1). Following a short resistance phase, the rapid death of *thyA* auxotrophs in media lacking thymine or thymidine ("T-starvation") known as thymineless death (TLD) was first described in *E. coli* (4, 12) and since then was extensively studied to identify the cause of lethality (1, 11, 30). Because the bulk of thymidine (dT) in any cell is used for chromosomal DNA synthesis, lack of dT was always assumed to cause some form of chromosomal damage, and hence the role of DNA repair pathways during T-starvation was the focus of intense investigation(19, 20, 36, 45). These studies revealed that certain pathways, like double strand break repair initiated by the RecBCD helicase/nuclease, Holliday junction resolution by RuvABC and anti-recombination activity of the UvrD helicase, keep cells alive during the resistance phase of T-starvation (20, 36). Other events, like attempted single-strand-gap repair initiated by the RecFOR complex, the function of the RecQ helicase and RecJ exonuclease, and SOS-induction of the cell division inhibitor SulA, — are detrimental for T-starved *E. coli* cells (19, 46–48). However, the *thyA* mutants of *E. coli* inactivated for all the latter "toxic DNA repair pathways" still die by two orders of magnitude during T-starvation (19), indicating some other yet-to-be identified major lethality factors.

Since actively-growing cells continuously require a lot of dT to replicate chromosomal DNA, existing replication forks were inferred to be the points of TLD pathology (19, 24, 36, 37, 44). Indeed, T-starvation severely inhibits chromosomal DNA replication (37) and is associated with accumulation of single-stranded DNA, suggesting generation of single-strand gaps by attempted replication in the absence of dT (36, 60). These ss-gaps induce the SOS response (19, 36, 65), which contributes to the pathology of TLD by induction of the SulA cell division inhibitor(19). Also, replication initiation spike in the T-starved cells triggers the destruction of the origin-centered chromosomal subdomain during TLD, suggesting that it is the demise of the nascent replication bubbles, rather than the existing replication forks, that eventually kills the chromosome (37, 65).

Although the *thyA* mutants cannot synthesize dT, they grow normally if supplemented with exogenous dT/T. Upon removal of dT from the growth medium, the *E. coli thyA* strain has a two-generation-long resistance phase (also called the lag phase (1)), when the CFU titer of the culture stays constant (Fig. 3.1A, top). This is followed by the rapid exponential death (RED) phase, when CFU titer falls by ~3 orders of magnitude within several hours (Fig. 3.1A, top).

An obvious explanation for the resistance phase is existence of an intracellular source of dT to support slow replication, — however, chromosomal DNA amount was consistently reported to remain flat during TLD (5, 9, 21, 37); besides, the recent systematic test of potential candidates for a source of dT or its analogs returned empty-handed(60). Thus, the mechanisms behind the initial resistance to T-starvation, followed by the sudden shift to the RED phase remain unclear, leading to a reasonable assumption

that the resistance phase is an integral part of the TLD phenomenon, during which chromosomal damage accumulates until it becomes irreparable, ushering the RED phase (1, 30). Specific early events during the resistance phase of TLD that would later turn poisonous during the RED phase were proposed to be futile incorporation-excision cycles(1, 22), ss-gap accumulation causing the SOS-induction (1, 19, 60), futile fork breakage-repair cycles (29, 60) and overinitiation from the origin (30, 37).

Two recent observations, in combination with an old popular TLD explanation, further support the idea of the resistance phase as the TLD period during which chromosomal damage accumulates without affecting viability for the time being. First, the resistance phase coincides with accumulation of double strand breaks in the chromosome, which then paradoxically disappear during the RED phase (36, 60). Second (and in contrast to the mentioned above reports of constant chromosomal DNA amount during T-starvation (5, 9, 21, 37)), we have recently found that during the resistance phase the amount of the chromosomal DNA actually increases ~1.5 times over the pre-starvation level, but then the chromosomal DNA is apparently destabilized during the RED phase, since it is slowly reduced to the original level (60) (Fig. 3.1A, bottom). Therefore, both the apparent chromosomal replication and the significant chromosome fragmentation during the resistance phase could lead to accumulation of chromosomal damage (SOS-induction is an indicator of this accumulation(36)).

On the other hand, the early DNA synthesis and the resistance phase in T-starved cells could reflect the existence of a source of dT, available early on during T-starvation, that fuels the initial DNA accumulation and delays viability loss until this pool is exhausted. In other words, the resistance phase could simply postpone TLD, rather than

being an integral part of it. Previously, we have tested the two obvious high-molecular-weight (HMW) dT sources – namely the stable RNAs and the chromosomal DNA, — but found that incapacitation of neither one reduced the resistance phase or precluded the early DNA synthesis during T-starvation(60). Thus, the question of whether the resistance phase is a part of the TLD phenomenon remains unresolved.

In the current study, we investigated a seemingly remote possibility of a substantial *low-molecular-weight* (LMW)-dT pool supporting the resistance phase of T-starvation in *E. coli*. While the bulk of dTTP in *E. coli* immediately incorporates into the chromosomal DNA, a fraction of dTTP is recruited into the dTDP-hexose pool (58), to participate in the synthesis of the exopolysaccharide (EPS) capsule, made of core lipopolysaccharide (LPS) (67), O-antigen (OA) (64) and enterobacterial common antigen (ECA) (35) in *E. coli*. The first step of this recruitment is to conjugate dTTP with glucose; the hexose moiety of the resulting dTDP-glucose then undergoes several modifications, before eventually incorporating into oligosaccharide precursors of the outer antigens, while the activating dTDP-handle is released back into the DNA precursor pools (35). We ignored LMW-dT before because, if the total dT content of the chromosomal DNA is taken for 100%, the pool of dTTP constitutes ~0.7% of it, while dTDP-glucose (unresolved from other dTDP-hexoses?) adds only another 2.4% (50). No more LMW-dT species are known in the cell, so the total expected LMW-dT pool came to ~3% of the total dT content of the chromosomal DNA, — not nearly enough to support the resistance phase with its ~50% increase in the chromosomal DNA mass (Fig. 3.1A).

To investigate the role of LMW-dT pool in TLD, we started by developing a simple protocol to extract LMW-dT pool from growing cells and to compare it to the

(HMW) chromosomal dT content. Here we show that early on during T-starvation the pool of dTDP-sugars becomes the major source of dTTP for the chromosomal DNA replication. This unexpected rebalancing of the dTTP pool with the help of cell envelope metabolism delays TLD and prevents its aggravation into hyper-TLD, a phenomenon that leads to complete chromosome destruction and cell lysis.

3.2 Results

3.2.1 *E. coli* possesses a substantial LMW-dT pool

As explained in the introduction, we expected the overall LMW-dT pools in *E. coli* to be ~3% of the total dT content of the chromosomal DNA. To facilitate comparison of the overall LMW-dT pool to the chromosomal DNA dT content, we used a standard "^{3}H-dT incorporation into the chromosomal DNA" technique, but in addition to collecting labeled cells on the filter (HMW-dT), we also collected and quantified the LMW flow-through and then related its ^{3}H-label to the ^{3}H-DNA label retained on the filter.

To chronically label *thyA* mutants with ^{3}H-dT, we grew these cells in LB, as LB contains enough dT to support limited growth of *thyA* mutant, but not enough to prevent ^{3}H-dT labeling (27). The LMW ^{3}H-dT is separated from HMW ^{3}H-dT by permeabilizing cells with cold 50% methanol to facilitate efficient metabolite extraction (a standard metabolome isolation protocol (40)), while trapping HMW species (proteins, nucleic acids) inside the cell envelope (Fig. 3.1B). Upon subsequent filtration, the HMW-dT of the chromosomal DNA is retained on the filter within cells, while the LMW-dT pool is collected as the flow-through (subsequently also dried on the filter, to equalize the

counting conditions). Agarose gel electrophoresis and DNase/RNase digestion reveals chromosomal DNA and long (mostly ribosomal) RNA in the HMW (filter) fraction, while no DNA, but some short RNA in the LMW (flow-through) fractions, most of this short RNA material coming from the growth medium itself (Fig. 3.1C).

Taking the chromosomal dT content (HMW-dT) for 100%, we found that in the exponentially growing *thyA* mutant cultures just before T-starvation the size of the LMW-dT pool equals to ~60% of the chromosomal DNA dT content, instead of the expected ~3% (Fig. 3.1D and 3.2A). The ThyA+ parental strain has the same size of LMW-dT pool and starts shrinking it as the cultures grow slower at higher densities (Fig. 3.2BC).

In order to see whether this 20-fold higher-than-expected pool of endogenous LMW-dT is accessible to support chromosomal replication during T-starvation, we measured it in the T-starved cells. At the end of the resistance phase of thymine starvation, the LMW-dT fraction falls to ~20% of the chromosomal dT content (Fig. 3.1D), suggesting that two thirds of this LMW-dT is presumably utilized for chromosomal replication during this period, which may explain the DNA accumulation and constant viability during the resistance phase of T-starvation. This fraction of LMW-dT remains at similar levels thereafter (Fig. 3.1D). In the ThyA+ parent, the LMW-^{3}H-dT is similarly incompletely chased with unlabeled endogenous dT (Fig. 3.2C), showing that at least ~70% (and may be up to 95%, see below) of dT can be exchanged out of the LMW-dT pool in *E. coli*.

3.2.2 The *thyA* mutants lacking dTDP-glucose develop envelope stress in the absence of dT

Our finding of the considerable LMW-dT pool in *E. coli* and its two-third reduction during the resistance phase of T-starvation raised the question about its nature. It could not be mostly dTTP, as the DNA precursor pools are reported to be around 1% of the nucleotide contents of the chromosomal DNA (50). What remained was the pool of dTDP-hexoses and the unknown pool of derived oligosaccharide precursors of the outer antigens (58).

E. coli uses dTDP-hexoses in the synthesis of O-antigen (OA) and enterobacterial common antigen (ECA) — the two constituents of the EPS capsule of Gram-negative cells (35, 64). Two supposedly redundant dTDP-glucose pyrophosphorylase enzymes (see for example,(18)), encoded by paralogous *rfbA* and *rffH* genes in *E. coli* (41), synthesize dTDP-glucose, which is the first intermediate for dTDP-conjugated hexoses to be integrated in both OA and ECA (Fig. 3.3A) (61, 68). *E. coli* K12 background that we use lacks OA and synthesizes only ECA (39); after several modifications the hexose part of the conjugate is deposited on the growing ECA sugar chain in the inner membrane, while dTDP is phosphorylated to dTTP and returns to the DNA precursor pools (Fig. 3.3A) (59). The EPS capsule synthesis is a significant endeavor in growing cells (the dry weight of the combined lipopolysaccharide exceeds the one of the chromosome (49)) and apparently demands an adequate pool of dTDP-hexoses, potentially explaining the substantial size of the LMW-dT pool we detect.

Our *rfbA* and *rffH* mutations that we P1-transduced into our *thyA* mutant were precise deletions from the Keio collection(2). We later discovered that our *rffH* deletion

allele had an inadvertent second mutation, — therefore, until we describe the nature of it in the next section, we will refer to this allele as *rffH**.

The complete defect in dTDP-glucose production should destabilize the EPS capsule, as even (ThyA+) *rfbA* and *rffH* single mutants already exhibit sensitivity to surfactants, like SDS and bile salts (14, 61). However, on LB +SDS +dT, all four combinations in the Δ*thyA* background grew almost equally well (Fig. 3.3B), indicating no obvious envelope problems (while the *seqA* mutant, our positive control for SDS-sensitivity, was characteristically inhibited (62)). In contrast, on LB +SDS –dT, the *thyA* and especially *thyA rfbA* mutants were visibly inhibited, as if the limited dT affected their envelope stability, while both *thyA rffH** and *thyA rfbA rffH** could not form colonies (Fig. 3.3B), indicating that exogenous dT was critical for their envelope stability. We conclude that, in the absence of dT, all *thyA* mutants become sensitive to SDS, suggesting cell envelope vulnerability, while the defect in dTDP-glucose pyrophosphorylases further increases this sensitivity.

We want to stress that both the *thyA rfbA* and *thyA rffH** mutants, as well as the *thyA rfbA rffH** mutant grew without problem and obvious phenotypes on LB +dT (Fig. 3.3B). On LB –dT, *thyA* and *thyA rfbA* mutants also grew normally (LB has enough of its own dT), and *thyA rfbA rffH** mutant formed smaller colonies, as expected from its supposedly defective envelope. However, the (RfbA+) *thyA rffH** mutant surprisingly struggled (Fig. 3.3B), as if RffH was more than just a redundant paralog of RfbA, or the mutant had an additional defect causing hypersensitivity to T-starvation.

3.2.3 The *thyA rffC* mutant is hypersensitive to T-starvation

The extreme sensitivity of the *thyA rffH** and *thyA rfbA rffH** mutants to detergents, further confirmed by their poor plating on MacConkey agar ±dT (Fig. 3.4) (MacConkey, instead of SDS, contains bile salts), and the hypersensitivity of the *thyA rffH** mutant to T-starvation made us look for possible downstream effects of our precise *rffH* deletion. It turned out that the downstream *rffC* gene overlaps the upstream *rffH* by 22 bp, so a complete *rffH* deletion also removes the beginning of the *rffC* gene, making it effectively *rffHC* two-gene inactivation (Fig. 3.3C). In fact, deletion of *rffC* makes the *thyA* mutant grow poorly on LB –dT, just like the original Δ*rffHC* (=*rffH**) allele does (Fig. 3.5, the "vector" variants). Moreover, complementation of the *rffHC* and *rffC* mutants with plasmids carrying either *rffH+* or *rffC+* genes confirms that it is the *rffC+* plasmid, rather than *rffH+* plasmid, that complements the T-hyperstarvation of both mutants (Fig. 3.5). Finally, in contrast to T-hyperstarvation of the original *thyA rffHC* or the new *thyA rffC* mutations, the shorter *rffH* deletion that does not disrupt the *rffC* gene (Fig. 3.3C) makes *thyA* mutant grow without problem on LB –dT (Fig. 3.3D), establishing the *rffC* defect as the one responsible for the hyper-sensitivity to T-starvation of the *rffHC* mutants.

The product of the *rffC* gene is dTDP-fucosamine acetyltransferase that catalyzes the penultimate step in the dTDP-hexose modification (Fig. 3.3A) before the modified hexose joins the trisaccharide repeats (ECA lipid III), from which ECA itself is assembled, and so the *rffC* mutant accumulates its precursor, ECA lipid II (59) (also see Fig. 3.14A below). Our further analysis has revealed that the *rffH* mutation has no T-starvation phenotypes, unless combined with the *rfbA* defect, — for example, the *thyA*

rfbA rffH combination grows slowly on LB –dT and is additionally inhibited by SDS (Fig. 3.6). At the same time, the complete inability of the double *rfbA rffH* mutant to make dTDP-glucose blocks the pathway in which RffC later acts (Fig. 3.3A), — making the double *rfbA rffH* defect epistatic to (masking) the *thyA rffC* mutant hypersensitivity to T-starvation (compare Fig. 3.3B and 3.6). Since by the time we have established it is the *rffC* defect that causes hypersensitivity to T-starvation of the original *thyA rffH** mutant, the bulk of our data was already collected with the *thyA rffHC* and *thyA rfbA rffHC* strains, — we continue to present these results, verifying the key findings in the *thyA rffC* (RffH+) and *thyA rfbA rffH* (RffC+) mutants. In interpreting these results, it helps to remember that whenever RfbA is functional, the *thyA rffHC* mutant displays TLD phenotypes of *thyA rffC*, whereas whenever RfbA is inactivated, the resulting *thyA rfbA rffHC* mutant displays TLD phenotypes of the *thyA rfbA rffH* double.

3.2.4 The *thyA rffHC* and *thyA rfbA rffHC* mutants lyse during T-starvation

The *thyA* mutants undergo one cell division during T-starvation, revealed by direct cell count under the light microscope (60). In contrast, the *thyA rfbA*, *thyA rffHC* and *thyA rfbA rffHC* mutants failed to divide even once, when incubated in liquid cultures without dT (Fig. 3.7). Also, we noticed that the *thyA rffHC* and *thyA rfbA rffHC* mutant cells appeared "lighter" in phase contrast at later time points, and some of the cells exhibited what looked like segmental cytoplasm voids (see below).

To test for cell lysis in T-starved cultures of the four mutants, we measured the extracellular presence of the cytoplasmic enzyme beta-galactosidase (15, 72). We detected no or little cell lysis in the *thyA* and *thyA rfbA* mutants (at least during the first 6

hours of T-starvation), but a significant cell lysis within two hours of T-starvation in the *thyA rffHC* mutant (Fig. 3.3E) (at the peak amounting to ~50% of the total cellular beta-galactosidase content — see below). As expected from the pathway configuration (Fig. 3.3A), this lysis was partially suppressed in the *thyA rfbA rffHC* mutant (Fig. 3.3E); the incomplete nature of the suppression apparently reflected the sensitivity to T-starvation of the double *rfbA rffH* defect (Fig. 3.6). As we detected no phage in the supernatants of the T-starved *thyA rffHC* mutant cultures, this cell lysis was not due to prophage induction. We conclude that the loss of RffC enzyme makes *thyA* mutant cell envelope hypersensitive to T-starvation; in contrast, the loss of both RfbA and RffH enzymes sensitizes cells to T-starvation to a lesser extent, while at the same time suppressing the *rffC* defect by shutting down the ECA-biosynthesis pathway (Fig. 3.3A). In general, these gross cellular phenotypes during T-starvation of the mutants in dTDP-sugar metabolism indicate involvement of the latter in the TLD phenomenon.

3.2.5 DAPI staining confirms the second dimension of TLD and reveals TLD severity levels

The dramatic cytoplasm and cell envelope instability phenotypes of the *thyA rfbA rffHC* and *thyA rffHC* mutants during T-starvation made us wonder whether the *thyA* single mutant undergoes similar changes, perhaps on a lesser scale. Still, the test for the periplasm instability using alkaline phosphatase (15, 72) showed no periplasm leaking in the T-starved *thyA* mutants; as a positive control, a massive release of this periplasmic enzyme was evident in the T-starved *thyA rffHC* mutant cells (Fig. 3.3F).

Fluorescent microscopy of DAPI-stained cells detects gross cytoplasm, envelope and chromosome stability issues. When grown in the presence of dT, *thyA* mutant cells were expectedly small and dividing normally (Fig. 3.8, top row). After 1 hour of T-starvation, the cells became ~1.5x wider and 2-3x elongated, with centrally-positioned bright nucleoids. After 3 hours of T-starvation, the *thyA* mutant cells mostly kept their new width, but became 4-6x times longer than non-starved cells, with centrally-positioned single nucleoid and somewhat mottled cytoplasm (developing lighter segments), but still no signs of cell lysis (Fig. 3.8), similar to the report before (73). Interestingly, after 20 hours of T-starvation, the *thyA* mutant cells developed sickly appearance: they were further elongated, with segmental cytoplasm loss in at least half of the cells, with no DNA in the majority of cells and with little DNA remaining in a few still centrally-located surviving nucleoids (Fig. 3.8). However, T-starved cultures would be long-stabilized at that time in the "survival" phase (36, 60), so these dramatic changes were likely reflecting metabolic decomposition of long-dead cells. We conclude that, during the RED phase (2-5 hours under our conditions), T-starved *thyA* mutant cells develop some cytoplasm irregularities, but no cell lysis or even periplasm leakage. However, this was not true for the *rfbA rffHC* and *rffHC* mutants.

When grown in the presence of dT, cells of all four strains (*thyA*, *thyA rfbA*, *thyA rffHC* and *thyA rfbA rffHC*) were similarly small and dividing normally (Fig. 3.8, the leftmost column). The *thyA rfbA* mutant progressed through T-starvation similar to the *thyA* single mutant, although cells appeared more mottled at 3 hours of T-starvation, and half of the cells turned to "ghosts" completely lacking cytoplasm after 20 hours of T-starvation (Fig. 3.8, the second row). As expected, the *thyA rfbA rffHC* mutant cells were

more affected by T-starvation, compared to the *thyA rfbA* mutant, showing some lysis at 3 hours of T-starvation and almost complete cytoplasm loss after 20 hours of T-starvation (Fig. 3.8, the third row). Finally, the T-starved *thyA rffHC* mutant cells, looking somewhat wider even in the presence of dT (in agreement with the reported measurements of ECA lipid II-accumulating mutants (26)), became extra wide after 1 hour of T-starvation and developed huge central nucleoids (Fig. 3.8, the bottom row). Corroborating the cell lysis measurements (Fig. 3.3E), by 3 hours of T-starvation most of the *thyA rffHC* mutant cells lost cytoplasm, and the resulting ghosts had little DNA (Fig. 3.8, the bottom row).

Our investigations in the ECA-defective mutants so far revealed a previously unknown dimension of T-starvation affecting the cytoplasm dynamics and envelope stability within the standard time frame of TLD (the first six hours of T-starvation). Specifically, the cytoplasm and envelope effects of T-starvation distinguish at least three severity levels of TLD: 1) the mildest one in the *thyA* and *thyA rfbA* mutants; 2) the severe T-starvation associated with significant lysis in the *thyA rfbA rffHC* mutant, likely due to lack of dTDP-glucose synthesis; 3) the T-hyperstarvation in the *thyA rffHC* mutant displaying massive lysis, likely due to accumulation of ECA lipid II. Next we compared the size and dynamics of the LMW-dT pools, as well as the TLD parameters in the *thyA rfbA rffHC* versus *thyA rffHC* mutants.

3.2.6 RfbA and RffH recruit dTTP into the LMW-dT pool

Since both RfbA and RffH were supposed to contribute to the dTDP-glucose pool (41, 68), we expected the size of the LMW-dT pool to be smaller when both enzymes are

inactivated. Indeed, we found that, in contrast to 60% of the chromosomal dT content in *thyA* mutant, the LMW-dT pool is less than 1.5% of the chromosomal dT content in the *thyA rfbA rffH* (RffC+) mutant, increasing slightly during T-starvation (Fig. 3.9A). Interestingly, we found insignificantly higher numbers (~3%) and similar evolution of the pool in the *thyA rfbA* mutant (Fig. 3.9A), suggesting that RfbA is the major contributor to dTDP-glucose synthesis. In contrast, the pool was still about half of the WT in the *thyA rffH* mutant and it did not go much lower during T-starvation (Fig. 3.9A), suggesting that the still functional RfbA was actively re-building it even without exogenous dT. We conclude that: 1) dTDP-glucose and its derivatives make >95% of the overall LMW-dT pool in the *thyA* mutant; 2) this pool is accessible to the cell and is used during T-starvation.

3.2.7 LMW-dT pool supports DNA synthesis during the resistance phase, delaying and alleviating TLD

Not only the LMW-dT pool is all but eliminated in the *thyA rfbA* and *thyA rfbA rffH* mutants (Fig. 3.9A), but the *thyA rfbA rffHC* and *thyA rfbA rffH* (RffC+) mutants have shorter resistance phases and die deeper during the RED phase, while the *thyA rfbA* mutant only has a deeper RED phase (Fig. 3.9B). At the same time, the *thyA rffH* mutant is no more sensitive to T-starvation than the *thyA* mutant (Fig. 3.9C). In other words, LMW-dT pool supports at least part of the resistance phase of TLD and prevents an even deeper RED phase. Previously, an uncharacterized mutant lacking dTDP-glucose pyrophosphorylase was reported to have a shorter resistance phase and a deeper RED phase during T-starvation (53).

Confirming the recently published results (29, 60) (Fig. 3.1A), DNA amount initially increased to ~1.5 times during the resistance phase in the *thyA* mutant before slowly declining during the RED phase (Fig. 3.9D). In contrast, both *thyA rfbA rffHC* and *thyA rfbA* mutants fail to accumulate chromosomal DNA early on upon T-starvation, even though the later chromosomal DNA disappearance parallels the one in *thyA* mutant cells (Fig. 3.9D). Thus, LMW-dT pool indeed supports the initial chromosomal DNA accumulation in T-starved cells.

By monitoring the copy number of the origin and the terminus of the chromosome, we characterize the dynamics of chromosomal DNA replication and loss during T-starvation(60). Indeed, increase in the amount of origin DNA registers initiations of the chromosomal replication, while increase in the amount of the terminus indicates completion of the chromosomal replication, reflecting the general progress of replication forks. As reported before, the *thyA* mutants show robust replication initiation during the resistance phase, followed by origin-containing chromosomal domain destruction during the RED phase (Fig. 3.9E) (19, 37, 65). The initial terminus 1.5x increase in the *thyA* mutants indicates successful termination of the pre-starvation replication forks during the resistance phase, before the RED phase ushers gradual chromosomal DNA loss (Fig. 3.9F) (29, 37, 60). We found that both the origin and the terminus copy number show only a limited initial increase in the *thyA rfbA rffHC* and *thyA rfbA* mutants (Fig. 3.9EF), indicating both decreased initiation from the replication origin and decreased overall progress of replication forks. At this point, we conclude that the two paralogous dTDP-glucose pyrophosphorylases, RfbA with the help of RffH, are responsible for the bulk of LMW-dT pool in *E. coli*, which is employed in EPS synthesis.

In the *thyA* mutants, this LMW-dT pool maintains cell viability through the resistance phase of TLD by supporting the shrinking dTTP pool and, via this, the initial chromosome replication (Fig. 3.9G) — in effect, postponing the onset of acute T-starvation.

3.2.8 RffC helps to extract dTTP out of the LMW-dT pool during T-starvation

The severe growth defect of the *thyA rffC* and *thyA rffHC* mutants on LB without dT (Fig. 3.3B and D) and lysis of the latter during T-starvation (Fig. 3.3E and Fig. 3.8) suggested an important RffC function in the dTTP <—> dTDP-hexose equilibrium, so critical during the resistance phase of TLD. The (partial) suppression of both phenotypes in the *thyA rfbA rffHC* mutant (Fig. 3.3B, 3.3E and 3.8) meant that the *rffC* mutants are poisoned by functional RfbA and RffH, consistent with RffC action facilitating the release of dTDP from dTDP-hexose conjugates (Fig. 3.3A).

We found that the LMW-dT pool in the *thyA rffHC* mutant is similar to the one in WT cells during exponential growth; however, in contrast to its shrinking in WT, it significantly expands during T-starvation (Fig. 3.10A), — perhaps reflecting dT redistribution from the degraded chromosomal DNA? The *thyA rffC* (RffH+) mutant showed higher LMW-dT pools and even more dramatic expansion during T-starvation (Fig. 3.11A). Thus, RffC action has no adverse LMW-dT effect during growth in the presence of dT, while during T-starvation it helps extract dTTP from the RfbA+RffH-made LMW-dT pool, returning it back to the DNA precursor pools (Fig. 3.3A and 4G). However, before securing this conclusion, we had to address an obvious caveat about the *rfbA*, *rffH* and *rffC* defects.

Since on the one hand these mutations affect the cell envelope integrity, while on the other hand they also impact the LMW-dT pools, they could potentially do the latter by modifying either the nucleoside transport into the cell, or the release of LMW species from the cell. To detect these possible nonspecific effects of *rfbA*, *rffH* and *rffC* mutations, we applied our HMW/LMW separation protocol (Fig. 3.1B) to measure the distribution of ^{3}H-uracil between HMW-rU content (cellular RNA) and LMW-rU pool (made of the RNA precursor UTP and EPS-capsule precursors UDP-sugars) in these mutants (Fig. 3.10B). We found that all four strains of the set have about the same ratio of LMW-rU to the total HMW-rU (~8%), whether exponentially-growing or after 3 hours of T-starvation (Fig. 3.10C). In other words, the *rfbA* and *rffHC* mutations do not affect the HMW/LMW balance of uracil pools, making it unlikely that the dramatic effects of these mutations on the HMW/LMW balance of dT pools is due to non-specific changes in permeability of the cell envelope. Thus, our overall conclusion is that, while RfbA and RffH recruit dTTP into the LMW-dT pools, RffC helps "extract" dTTP out of these pools, which becomes critical during T-starvation (Fig. 3.9G).

3.2.9 Inability to release dTTP from the LMW-dT pool results in hyper-TLD

If RffC helps extracting dTTP from LMW-dT pools during T-starvation, its inactivation should exacerbate the TLD phenotypes. Indeed, we found that the *thyA rffC* and *thyA rffHC* mutants completely lack the resistance phase, and develop the dramatically-deeper RED phase (Fig. 3.10D and 3.12) reminiscent of the *thyA recBCD* mutants ((36, 60) and see below). The better viability of the *thyA rfbA rffHC* mutant compared to the (RfbA+) *thyA rffHC* mutant (Fig. 3.10D) confirms RfbA+RffH toxicity

in the *thyA rffHC* mutant, likely resulting from the continuous sequestration of dTTP into the LMW-dT pool by dTDP-glucose synthases even during T-starvation (Fig. 3.10A and 3.11AB).

Change in the chromosomal DNA amounts during T-starvation (Fig. 3.1A) is also dramatically different in the *thyA rffHC* mutant. In contrast to the significant initial chromosomal DNA replication of the *thyA* mutant or even the initially flat profile of the *thyA rfbA* and *thyA rfbA rffHC* mutants (Fig. 3.9D), the chromosomal DNA of the *thyA rffC* and *thyA rffHC* mutants becomes immediately unstable upon thymidine removal, with more than one-third of it already gone after one hour of T-starvation and only 10% of the original DNA remaining by four hours of T-starvation (Fig. 3.10E and 3.13). Moreover, this chromosomal DNA disappearance in *thyA rffHC* mutant affects equally and dramatically both the origin and the terminus (Fig. 3.10FG), — suggesting a catastrophic loss of the entire chromosome. The instability of the chromosomal DNA in the *thyA rffHC* mutant is again partially suppressed by RfbA inactivation (although the terminus is mostly degraded even in the *thyA rfbA rffHC* mutant) (Fig. 3.10E-G).

We conclude that the RfbA+RffH action promotes chromosomal DNA loss in T-starved cells and is counteracted by the RffC action. Overall, during T-starvation there is a tug-of-war between RfbA+RffH on the one hand and RffC on the other, the former continuously sequestering dTTP into LMW-dT pool and aggravating TLD, while the latter releasing dTTP from this pool, alleviating TLD.

3.2.10 Does cell lysis drive the hyper-TLD phenomenon?

The lysis of the *thyA rffHC* mutant cells in response to T-starvation seems like an obvious reason for the catastrophic chromosomal DNA loss and for the absence of the resistance phase in this mutant, — yet a closer look shows that these events are separated in time and therefore independent. First, at 1 hour of T-starvation, the *thyA rffHC* cultures suffer little or no lysis (Fig. 3.3EF and 5H) and no cytoplasm/envelope irregularities (Fig. 3.8), even though only 3% of them remain viable at this point (Fig. 3.10D, I, and Fig. 3.12), and at the population level they have already lost 36% of their genomic DNA (Fig. 3.10E) and 55% of the replication origin DNA (Fig. 3.10F). Second, from quantification of beta-galactosidase release, lysis affects about half of the T-starved *thyA rffHC* cells (Fig. 3.10H), whereas their general survival is below 10e-4 (Fig. 3.10D, I). Finally, lysis of the *thyA rffHC* mutants is strongly suppressed during T-starvation at 28°C (Fig. 3.10H), whereas TLD, although also reduced, still reaches 10e-3 at this temperature (Fig. 3.10I). Thus, lysis of the *thyA rffHC* mutants without dT, even though significant at 37°C at 2 hours of T-starvation, must be a later event separate from their immediate lethality and chromosomal DNA loss.

3.2.11 Hyper-TLD is observed in other mutants that cannot finish ECA synthesis

ECA synthesis up to Lipid III is a multi-step three-branch process (Fig. 3.14A). As we have shown, blocking initiation of its dTDP-branch with the *rfbA rffH* double defect exacerbates TLD via reducing the LMW-dT pool (Fig. 3.9). We have also found that the *rffC* defect, that blocks completion of this branch, makes *thyA* mutants hypersensitive to T-starvation via inability to release dTDP from LMW-dT pool (Fig.

3.10). If the lack of dTDP release from ECA synthesis pathway was indeed the reason for hyper-TLD of the *thyA rffC* mutants, then any other mutation in ECA synthesis that blocks dTDP release should also make *thyA* mutants hypersensitive to T-starvation. Indeed, spotting on an "enhanced" LB reveals that, like the *rffC* defect, addition of the *rfe*, *rffM* or *rffT* defects makes the *thyA* mutants grow poorly without dT, with the *thyA rffT* mutant essentially copying the behavior of the *thyA rffC* mutant (Fig. 3.14B), which makes sense from the ECA biosynthesis scheme (Fig. 3.14A). In the standard TLD assay, blocking the other branch of ECA synthesis that converges with the dTDP-branch with either *rfe*, *rffM* or *rffT* defects makes the *thyA* mutants hypersensitive to T-starvation (Fig. 3.14C). Thus, dTTP release from the LMW-dT pool could be the common denominator of the various degrees of the hyper-TLD phenotype of all these mutants that synthesize dTDP-glucose but cannot finish the ECA synthesis.

3.2.12 Hyper-TLD of the *thyA rffHC* mutant is independent of replication and Endo I

Finding mutants that cannot finish their ECA synthesis and thus undergo faster death upon T-starvation, — while establishing that the resistance phase is not an integral part of TLD, — posed the question about the nature of the accompanying catastrophic chromosomal DNA loss, which we observed in the *thyA rff(H)C* mutants (Fig. 3.10EFG and 3.13). TLD was always considered a chromosomal replication-centered phenomenon (1, 30), but we have recently demonstrated a surprising TLD *in*dependence of the chromosomal replication (29). For this, we used the "awakening protocol" to eliminate all the replication activity in the chromosome by bringing dT-supplemented cultures of the

thyA dnaA(Ts) mutants to saturation at the permissive temperature and then outgrowing ("awakening") them without dT at the non-permissive temperature of 42°C (Fig. 3.14D) (29). Because of the non-permissive temperature, the *thyA dnaA*(Ts) mutant cannot initiate replication of its chromosome even in the presence of dT and remains static (Fig. 3.14E). At the same time, in confirmation of our previous conclusion about replication-independence of TLD, in the absence of dT this *thyA dnaA* mutant undergoes exactly the same death as its DnaA+ progenitor (Fig. 3.14E).

Since SOS-induction significantly contributes to TLD (19, 36), if the inability to initiate replication from the origin also induces SOS, the observed TLD in the *thyA dnaA*(Ts) mutant at 42°C could be due to this SOS induction even in the absence of chromosomal DNA replication. However, we found that the *thyA dnaA*(Ts) mutants do not induce the SOS response at 42°C, as long as they are supplemented with dT, — while undergoing strong SOS induction in both the standard (Fig. 3.15) and the awakening protocols of T-starvation (Fig. 3.14F). The latter result indicates replication-independence of the SOS-inducing chromosomal lesions during T-starvation. We also report that in the same awakening protocol to block chromosomal replication, the *thyA rffHC dnaA*(Ts) mutants die with somewhat deeper kinetics compared to the *thyA rffHC* mutant (Fig. 3.14G). Thus, the hyper-TLD in the *thyA rffHC* mutants is also independent of DNA replication.

As already reported (29), in contrast to the standard T-starvation protocol (Fig. 3.14D), in the awakening protocol at 42°C the *thyA* mutant suffers significant chromosomal DNA loss, independently of its *dnaA* status (compare Fig. 3.9D *versus* Fig. 3.14H). Although for the *thyA rffHC* mutant in the awakening protocol at 42°C the

massive chromosomal DNA loss is slightly delayed, its overall kinetics is hardly affected (if a bit accelerated) by the *dnaA*(Ts) defects (Fig. 3.14H), indicating that the catastrophic chromosomal DNA loss due to the *rffC* defect is also completely replication-independent.

Following the recent report of Endo I-catalyzed massive chromosomal DNA fragmentation during slow lysis of cells in agarose plugs(28), we tested whether the fast chromosomal DNA disappearance in the *thyA rffHC* mutants is due to Endo I gaining access to the chromosomal DNA during lysis, but the DNA loss turned out to be Endo I-independent (Fig. 3.16A). Also, the *endA* inactivation failed to affect TLD kinetics of both the *thyA* and *thyA rffHC* mutant (Fig. 3.16B).

3.2.13 Chromosome is the primary target of TLD in the *thyA rffHC* mutant

The most likely candidate for an enzyme capable of such a rapid chromosomal DNA degradation is the RecBCD helicase/nuclease (17), yet the catastrophic chromosomal DNA loss in the *thyA rffHC recBCD* mutant is only slightly slower than in its RecBCD+ parent (Fig. 3.17A), suggesting that only a minor fraction of the chromosomal DNA of the T-starved *thyA rffHC* mutant is lost to the linear DNA degradation by RecBCD. As already mentioned, the hyper-TLD in the *thyA rffHC* mutant is reminiscent of the hyper-TLD observed in the *thyA recBCD* mutant (Fig. 3.17B), as if RecBCD and RffC work in the same pathway of hyper-TLD prevention. Interestingly, the TLD curve of the combined *thyA rffHC recBCD* mutant suggests an even deeper defect (Fig. 3.17B); unfortunately, TLD in the *thyA recBCD* and *thyA rffHC* mutants is already too fast in the standard conditions (M9CAA medium) to detect further significant acceleration. To reveal the type of genetic interactions between the two defects, we

employed a milder T-starvation in LB, as we did before for the *thyA recBCD uvrD* combination (36). Under these conditions, the *thyA* mutant grows ~10x before plateauing and then essentially fails to die, the *thyA recBCD* mutant dies by 2.5 orders of magnitude, while the *thyA rffHC* mutant dies by 1.5 orders of magnitude (Fig. 3.17C). Remarkably, the deep TLD of the *thyA recBCD rffHC* mutant in LB is clearly the product of the individual TLD effects of the *recBCD* and *rffHC* mutations (Fig. 3.17C), indicating independent action of the two strongest TLD-accelerating defects.

Since the *recBCD* defect makes cells unable to repair double-strand DNA breaks (reviewed in (38)), and assuming that the substrate of the "*rffC*-pathway" is also chromosomal DNA, the independence of the *recBCD* and *rffC* pathways (Fig. 3.17C) predicts a higher chromosomal fragmentation during T-starvation in the *thyA rffHC* mutants. In the *thyA* mutants, chromosome fragmentation is induced during the resistance phase of T-starvation but then, counterintuitively, goes away during the RED phase (Fig. 3.17DE) (60). We found that not only *thyA rffHC* mutants suffer much higher chromosome fragmentation in response to T-starvation, but also this fragmentation keeps increasing and stays high (Fig. 3.17DE), even though these cells start lysing around 2 hours of T-starvation (Fig. 3.3E and 5H). In other words, the *rffC* defect induces more double-strand breaks during T-starvation (it could have also blocked their subsequent repair, but the independence of the *rffC* and the *recBCD* mutant effects argues against this formal possibility). Confusingly, when we do block repair of double-strand breaks genetically with the *recBCD* mutation, chromosomal fragmentation in the *thyA recBCD rffHC* mutant is suppressed and resembles the smoother fragmentation kinetics of the *thyA recBCD* mutants (Fig. 3.17DF), as if the RecBCD-promoted linear DNA

degradation or repair of double-strand breaks in the *thyA rffHC* mutant stimulates even more breaks (compare Fig. 3.17E vs F).

On the basis of our analysis of T-starvation phenotypes in the *thyA rffHC* mutants, we conclude that this hyper-TLD does not require replication forks, but it does massively break chromosomal DNA (independently of Endo I), which explains its synergy with the double-strand DNA break repair defect (*recBCD*) and is the likely reason for the catastrophic loss of chromosomal DNA.

3.3 Discussion

In contrast to typically static responses to starvation for amino acids or RNA bases in *E. coli* (4), T-starvation leads to cell death, but not right away. The nature of the two-generations-long resistance phase, followed by the sudden shift to the RED phase (Fig. 3.1A), has remained a long-standing puzzle of TLD. This static period at the beginning of T-starvation, with its significant initiation of DNA replication (37, 60), SOS-induction (19, 36, 65), accumulation of ss-gaps and high levels of chromosomal fragmentation (60), was considered an integral period of TLD when chromosomal damage accumulates to eventually become irreparable, ushering the RED phase (1, 30). Here we show that the resistance phase is not a part of TLD, but rather is a delay in acute T-starvation, during which the cells are supported by recruiting dTTP from the unexpectedly large internal LMW-dT pool. This pool in rapidly-growing cells comprises ~60% of the dT content of the chromosomal DNA; once it is exhausted as a result of T-starvation, the RED phase begins.

While two paralogous thymidine glucose pyrophosphorylases of *E. coli*, RfbA and RffH, recruit dTTP into the LMW-dT pool, we found that RffC (and likely RffT), by facilitating ECA synthesis completion, helps to release dTTP from LMW-dT pool, which becomes critical in the absence of exogenous dT (Fig. 3.9G). As a result of the reduced accessible LMW-dT pool, the *thyA rfbA rffH* mutant experiences a shorter resistance phase with no chromosomal DNA accumulation, followed by a deeper RED phase. In contrast, TLD in the *thyA rffC* mutant lacks the resistance phase altogether, is accompanied by a precipitous loss of the chromosomal DNA and ends in massive cell lysis. Moreover, the dramatic phenotypes of the *thyA rffC* mutant during T-starvation, including cell lysis, were (partially) suppressed by *rfbA*+*rffH* inactivation, confirming that functional dTDP-glucose synthases poison T-starved cells lacking RffC activity, by continuous recruiting the remaining dTTP into the LMW-dT pool.

T-hyperstarvation in the *thyA rffC* mutants is distinct from regular TLD by causing a complete demise of the chromosomal DNA, as well as eventual lysis of about half of the cells, suggesting a still unknown role of either dT or the chromosomal DNA itself, in maintaining the cell envelope.

3.3.1 The dTDP-sugar-utilizing pathways and the EPS-capsule

We are not sure why such a significant pool of dTDP-sugars avoided detection, — maybe because nobody directly compared its size with that of the chromosomal DNA? Its significant size is indirectly confirmed by the similar size of LMW-rU pools (Fig. 3.10BC), which likely are mostly represented by UDP-sugars — even though they are only 8% of the rU content of the total stable RNA, the total mass of cellular RNA is 6-7x

larger than that of chromosomal DNA (50), making the absolute sizes of the two pools similar. Indeed, EPS capsule synthesis utilizes both dTDP-sugars and UDP-sugars. There is still a possibility, though, that the bigger than expected LMW-dT pool is K12-specific, because this *E. coli* background does not synthesize OA (39)— and therefore might be upregulated for EPS-capsule production.

Okazaki was the first in the late 1950s to report that thymidine internalized by bacteria enters into a LMW pool in the form, the bulk of which is chemically distinct from the DNA precursor dTTP (57), and represents a dTDP-rhamnose conjugate(55). By analogy with the already well-known at that time UDP- and GDP-sugar conjugates, Okazaki suggested that dTDP-rhamnose participates in EPS-capsule synthesis (56), but since he also found that the dTDP portion of this conjugate can be chased into DNA (58), he speculated that dTDP-sugars could represent common intermediates for both polysaccharide and DNA synthesis (56).

An enzyme synthesizing dTDP-glucose was soon reported (31), while the pools of dTDP-sugars under various conditions were found to be consistently several-fold higher than dTTP pool (8, 25, 54). Moreover, an *E. coli* mutant deficient in dTDP-glucose synthesis was shown to have a faster and deeper TLD (53). Nevertheless, the original idea of Okazaki about dTDP-sugars as common intermediates for both EPS-capsule and DNA replication came full circle only some 60 years later, with our current report that the pool of dTDP-sugars becomes the major source of dT for the chromosomal replication during T-starvation.

3.3.2 Is ECA lipid II accumulation poisonous during T-starvation?

Unexpectedly, the *thyA rfbA rffH* (RffC+) mutant, which should be deficient for ECA synthesis (essentially leaving our O-minus K12 background (39) without EPS-capsule), does not have the most severe sensitivity to T-starvation. Instead, the *thyA rffC* mutant has the worst T-starvation phenotypes. This severity is partially suppressed by the *rfbA rffH* inactivation, suggesting that it is not the inability to synthesize ECA, but something else, which makes the *thyA rffC* mutant extremely vulnerable to T-starvation.

The loss of *wecE*, the gene responsible for the step preceding the *rffC* step in the ECA biosynthesis (Fig. 3.14A), has been previously shown to lead to the accumulation of ECA lipid II intermediates, which can cause membrane instability by diverting the undecaprenol moiety away from use in PG synthesis (26). On the basis of our results, we suspect that the *rffC* mutants have similar problems. The ECA-synthesis activity that acts after RffC making ECA lipid III and releasing dTDP from dTDP-sugar conjugates is RffT (Fig. 3.14A), mutation in which also makes the *thyA* mutant hyper-sensitive to T-starvation (Fig. 3.14BC). The various defects due to inability to finish ECA lipid III synthesis would be suppressed by the inactivation of the *rfe* gene that blocks the accumulation of all ECA lipid intermediates (Fig. 3.14A), — we will be testing this possibility in the future. Remarkably, our findings indicate that accumulation of ECA lipid II becomes toxic only in the absence of dT, suggesting a novel role of dT in maintaining cell envelope.

3.3.3 The nature of chromosomal damage during T-starvation

Since TLD is only observed in growing cultures (29), and since the only critical role of thymidine in the cell was thought to generate the DNA precursor dTTP, faulty chromosomal replication during T-starvation has been always considered the primary cause of TLD, this thinking being supported by the significant effects of recombinational repair mutants on the TLD kinetics (19, 20, 36, 45). Paradoxically, even though high levels of chromosome fragmentation develop during the resistance phase of TLD, this fragmentation does not directly contribute to lethality in the repair-proficient cells(36, 37, 60). Instead, genetic studies strongly suggested that the main contributor to the chromosome poisoning during T-starvation was the repair of persistent single-strand gaps (19, 36, 45), and we have indeed previously reported ss-gap accumulation in the chromosomal DNA during the RED phase (60). Still, the mechanism of T-starvation-induced chromosomal lesions remained unclear.

To explain how faulty replication could lead to irreparable chromosomal lesions, futile cycles of DNA-uracil incorporation-excision were repeatedly proposed as the source of irreparable DNA damage during T-starvation (1, 23, 30). However, while testing this idea, we found that dUTP concentrations are too low in the Dut+ cells to support such futile incorporation/excision cycles (60). Moreover, even preventing DNA-uracil excision after massive uracil incorporation (in the *thyA dut ung* mutants) only makes the RED phase shallower, but does not eliminate it altogether (60). Instead, we proposed a similar concept of futile fork breakage-repair cycles as a source of irreparable chromosomal lesions (60).

To address the fork breakage-repair idea, we tested the necessity of chromosomal replication for TLD and were perplexed to find normal TLD in the complete absence of replication(29); here we have confirmed this game-changing observation and extended it to the *thyA rffHC* mutants. The lack of replication requirement, while eliminating the biggest group of TLD models, further highlights the mystery of the massive chromosomal DNA loss during T-starvation, that becomes catastrophic in the *thyA rffC* mutants (Fig. 3.10EFG) or in *thyA* mutants undergoing T-starvation at 42°C (Fig. 3.14H) (29). Since our testing of the most obvious ideas about this DNA loss in this work failed to produce insights, we can only speculate on its nature.

One possibility is based on the known association of random pieces of the chromosomal DNA with cell envelope (6), specifically with the outer membrane (13, 51), reflected in the chromosomal DNA capture by the outer membrane vesicles (7, 70)). Though random and transient for any particular DNA segment (with the exception of the hemimethylated *oriC* (52)), this association may be in fact secure in terms of DNA anchoring to the cell envelope, if mediated by special spool-like proteins. If such spooling is jammed in the absence of dTTP, while the cell volume dramatically expands due to the same T-starvation (Fig. 3.8), a DNA segment trapped between adjacent envelope-association points may become overextended and snaps, causing a double-strand break (Fig. 3.18). While most of these breaks are repaired, a few of them could be irreparable (for whatever reason), causing the observed chromosomal DNA loss and TLD. The same scenario is magnified and accelerated during T-hyperstarvation (Fig. 3.18), leading to a complete loss of DNA and eventually to cell lysis (due to the cell envelope overextension, combined with the lack of ECA and with poisoning by

accumulation of ECA lipid II). The nature of this chromosomal DNA disappearance, and its relation to T-starvation-triggered chromosome fragmentation, should become one of the main directions of the future TLD studies.

3.4 Conclusion

In conclusion, our current investigation of the nature of the bacteriostatic beginning of T-starvation reveals that this resistance phase is not a part of the TLD phenomenon, but rather a delay of acute T-starvation, as the cells switch to recruiting dTTP from a substantial LMW-dT pool that we found. This LMW-dT pool all but disappears in the mutant deficient in synthesis of dTDP-glucose, suggesting that it mostly comprises dTDP-sugar conjugates (precursors of EPS-capsule). Finally, the inability to release dTTP from this LMW-dT pool leads to hyper-TLD, — instant death, catastrophic chromosome loss and, eventually, to cell lysis, — opening up future research venues. Learning the nature of the catastrophic chromosomal DNA loss should provide critical insights into the phenomenon of TLD. Apart from this, interconversion of dTTP and dTDP-sugars is the first non-DNA-repair function, defects in which were found to exacerbate TLD. Our imaging studies in the *thyA* single mutants revealed the overall stability of the cell envelope during the RED phase of TLD, but they did detect some unusual cytoplasm dynamics, like segmental voids and retractions. Others report that live cell imaging of *E. coli* strains defective in their envelope maintenance present the retraction of cytoplasm as a highly-dynamic event, accompanied by vesicle release (43, 69). The discovered role of thymidine in the cell envelope maintenance in the *thyA* mutants unable to finish ECA synthesis is a new lead into the mysterious TLD

mechanisms. Overall, the multiple layers of damage in different cell components may explain the irreversibility of TLD despite the apparent preservation of at least one copy of the genome and the origin after four hours of T-starvation in the *thyA* single mutants (37, 65). Finally, the role of such a substantial pool of LMW-dT in *E. coli* cells needs to be explored.

3.5 Acknowledgements

We wish to thank Sanna Koskiniemi (Uppsala Universitet, Sweden) for reminding us about dTDP-hexoses and William W. Metcalf (Microbiology, UIUC) for challenging us to measure LMW-dT pools and for the hospitality in his light microscopy facility. We are grateful to all members of this laboratory for constructive criticism and support and, in addition, to Lenna Kouzminova for critically reading the manuscript. This work was supported by grant # GM 073115 from the National Institutes of Health. The authors have no conflict of interest to declare.

3.6 Materials and Methods

3.6.1 Bacterial strains

The list of strains used in this study is in Table S1. Deletion-insertion alleles of the Keio collection (2) were obtained from the *E. coli* Genetic Stock Center and transduced into KKW58 or its derivatives by P1 transduction (42). Gene-tailored deletion-replacement alleles were created by the method of Datsenko and Wanner (16).

When required, the antibiotic resistance was removed by transforming in pCP20 (16). All the deletion and replacement alleles were confirmed by PCR.

3.6.2 Growth conditions

All growth was done at 37°C with shaking at 200 RPM, unless mentioned otherwise, and monitored by measuring A_{600} (= OD). Overnight cultures were agitated in M9 minimal medium (42) supplemented with 0.2% glucose, 0.2% casamino acids and 10 µg/ml dT (M9CAA+dT), diluted at least 100-fold into fresh M9CAA+dT and shaken at 37°C until the early exponential phase (OD ~0.15), before beginning T-starvation. The T-starvation was carried out as described before (60). The only exception was the assay of Fig. 3.14H, where M9CAA was replaced with LB (10 g of tryptone, 5 g of yeast extract, 5g of NaCl, 250 µl of 4 M NaOH per liter (42)). LB2xYE used in Fig. 3.14B has 10 g of yeast extract per liter instead of 5. When required, the growth medium was supplemented with 100 µg/ml Ampicillin, 50 µg/ml kanamycin, 10 µg/ml tetracycline, 10 µg/ml chloroamphenicol or 1 mM IPTG.

3.6.3 Genomic DNA, origin and terminus amounts

The assay was carried out essentially as described before (60).

3.6.4 Detection of LMW dT/U species

The overnight LB cultures were diluted 100-fold into fresh LB supplemented with either ^{3}H-dT or ^{3}H-uridine (both from Moravek) grown till OD ~ 0.25, at which time the cultures were harvested, washed with 1% NaCl to remove the label (+ cold dT of LB) and

suspended in M9CAA without thymidine. At the indicated times, 1 ml of the culture was harvested, suspended in 0.5 ml M9CAA and incubated with 0.5 ml of MeOH on ice for at least 1 hour before filtration through Fisherbrand G6 glass fiber filter to trap the cells with all their HMW content on it and to separate the LMW flow-through. The filter was washed twice with 0.5 ml of ice-cold MeOH and once with 0.5 ml of ice-cold EtOH. All the LMW filtrates were collected and counted separately. For this, a 100 µl fraction of the LMW filtrate was spotted on the G6 glass fiber filters, the HMW and LMW filters were submerged in the 5 ml of scintillation fluid (Bio Safe II, Research Products International) in 7 ml scintillation vials, and the tritium counts were detected using the Beckman Coulter LS 6500 counter.

3.6.5 Beta-galactosidase assay

The strains were pregrown in the presence of IPTG and 10 µg/ml dT in M9CAA to OD ~ 0.15. The strains were harvested, washed with 1% NaCl and suspended in equal volume of M9CAA. At appropriate times 2ml samples were taken to measure OD, and 400 µl of the culture was either used as is or was lysed (with 25 µl of chloroform and 0.00125% SDS) before mixing with 1,600 µl Z-buffer (100 mM Sodium Phosphate pH = 7.0, 10 mM KCl, 1 mM $MgSO_4$, 50 mM β-mercaptoethanol) containing 240 µg of ONPG substrate. The reaction was incubated at 30°C for 10 minutes before stopping with 1 ml of 1 M Na_2CO_3. Absorbance was measured at 420 nm and 550 nm. Miller units were calculated (42), and percentage of culture lysis was calculated by taking the value of the lysed half of the same culture for 100%.

3.6.6 Alkaline phosphatase assay

The cultures were grown in MOPS-CAA medium (8) + 10 µg/ml dT to induce the expression of alkaline phosphatase gene *phoA*. dT was removed by filtration, cells were washed and suspended in MOPS-CAA without dT. Alkaline phosphatase activity was measured as described (10). At intervals, 1 ml aliquots were taken and harvested, 0.5 ml of the supernatant was mixed with 0.5 ml of post-lysis buffer (1 M Tris-HCl pH 8.0, 10 mM $MgCl_2$, 10 mM $ZnCl_2$) for 10 minutes. 200 µl of the mix was then added to 1,600 µl of 1 M Tris-HCl buffer pH = 8.0 containing 200 µl of 0.4% para-nitrophenylphosphate. The reaction was incubated at 37°C for 30 minutes, and absorbance was measured at 405 nm. The pellet from the 1 ml culture was also osmotically shocked and then similarly treated with post-lysis buffer before determining the absorbance at 405nm.

The protocol for preparing osmotically shocked cells was adapted from (34). Briefly, osmotically-shocked cells were prepared by washing cells with 400 µl of ice cold 50 mM potassium phosphate buffer, incubating in 400 µl plasmolysis buffer (50 mM Tris HCl pH 8.0, 25 mM EDTA, 20% w/v sucrose) at room temperature for 10 minutes, pelleting by centrifugation and resuspending the cells in 200 µl of ice cold DI water for 20 minutes and pelleting again to separate the periplasmic fraction. 200 µl of the periplasmic fraction was mixed with an equal volume of post-lysis buffer and left at room temperature for 10 minutes. 200 µl of this mix was then processed as above to measure absorbance at 405 nm. The values are reported as the ratio of absorbance in culture supernatant fraction to the absorbance from osmotically-shocked cells.

3.6.7 The awakening protocol for TLD

The protocol was used as described (29). Briefly, the strains were grown to saturation in M9CAA with 10 µg/ml dT for 48 hours at 28°C. The cultures were then washed thrice with equal volume of 1% NaCl, diluted 20-fold in M9CAA without dT and moved to 42°C in to prevent initiation in the *dnaA*(Ts) mutants during T-starvation. Viability and genomic DNA accumulation was determined as described above.

3.6.8 Fluorescent microscopy

DAPI staining and fluorescence microscopy was done exactly as described (32).

3.6.9 Pulsed-field gel electrophoresis to detect chromosome fragmentation

The previously described protocol was used (60) with minor changes. During the assay cultures of strains RA49 and RA52 were harvested at slower centrifugation speeds of 3000-5000g and pellets from all strains were suspended in MOPS CAA instead of TE buffer for plug preparation. The conditions for running pulse field gel electrophoresis and its quantification was done as has been described before (33).

3.6.10 SOS-induction

Strains *thyA* (SOS) and *thyA dnaA*(Ts) (SOS) containing a P_{sulA}-lacZ fusion were grown either according to the normal protocol - sub-culture overnights at 28°C and grow in M9CAA + dT medium to OD ~ 0.15 when dT is removed by filtration and the cultures are shifted to 42°C for the rest of the assay or according to the awakening protocol – 48 hr stationary phase cultures diluted 20X in M9CAA without dT and moved to 42°C

immediately. At indicated times, 2ml aliquots were taken to measure OD and 400 µl of culture was lysed with SDS and chloroform mixture before performing the Beta-galactosidase assay as described above.

3.7 Figures

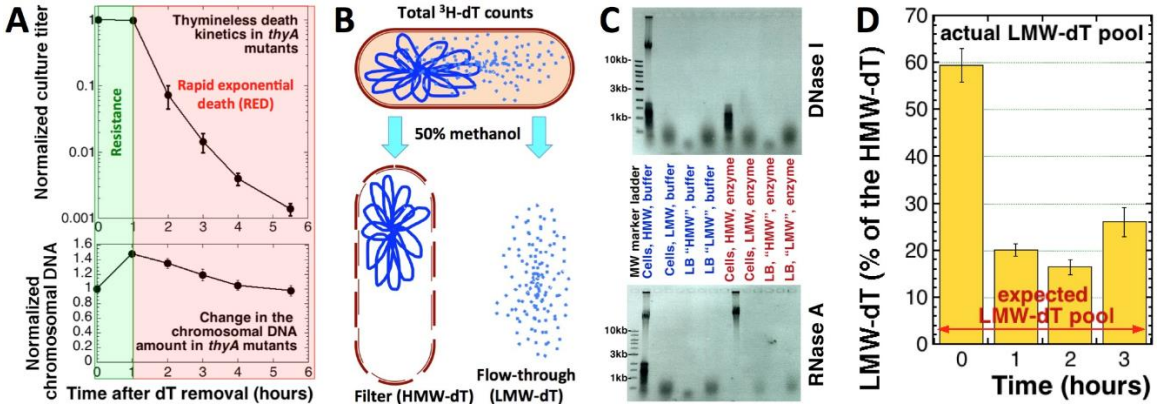

Figure 3.1. A significant endogenous pool of LMW-dT decreases during T-starvation. A. The phenomenon of TLD in *E. coli* suggests accumulation of chromosomal damage during the resistance phase (green) that would later kill cells during the RED phase (red). The data are adapted from (60). Henceforth, the data are means (n≥3) ± SEM. Cultures were grown at 37°C in the presence of dT, which was removed at time =0, while incubation in the growth medium continued. Top, cell death begins after 1 hour-long resistance phase, during which the culture titer is stable. Bottom, during the same first hour without dT, cells manage to synthesize the amount of DNA equal to half of what they already had before dT removal. However, during the RED phase genomic DNA is gradually lost. **B.** A scheme of 50% methanol fractionation of the intracellular thymidine into HMW-dT (the dT content of the chromosomal DNA) and LMW-dT. **C.** 0.7% agarose gel analysis of the HMW and LMW fractions of the 50% methanol-treated cells, as well as pure LB treated the same way, for DNA and RNA content (staining with EtBr). Inverse images of EtBr-stained gels are shown, in which the indicated samples were either incubated in the buffer or with the indicated enzyme (DNase I for the top gel, RNase A for the bottom gel). **D.** The size of LMW-dT pool, normalized to the HMW-dT content of the chromosome, either during normal growth in dT-supplemented medium or during T-starvation. Thymidine was removed at time =0. The strain is KKW58.

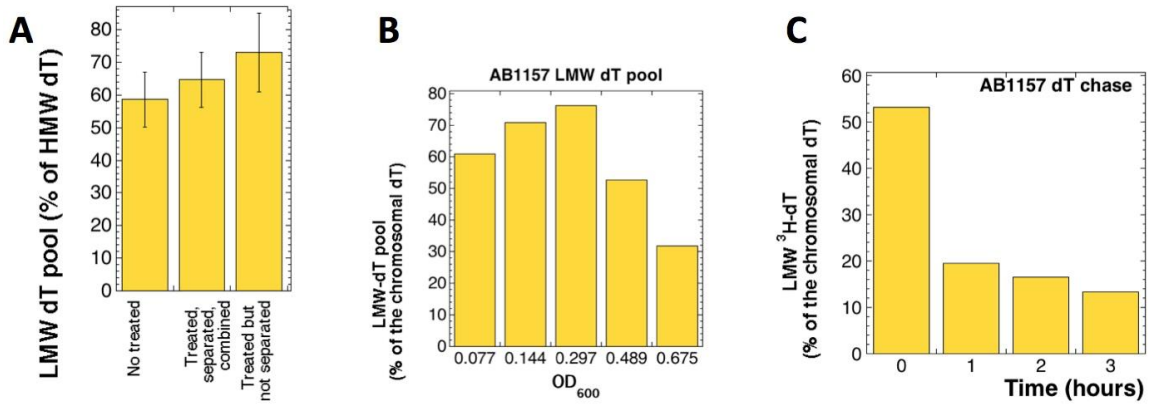

Figure 3.2. Some controls about the LMW-dT pool. A. Control for the efficiency of HMW-dT counts (= the chromosomal dT content). Since the LMW-dT was released from cells (even though still counted on filters), there was a possibility that the unexpectedly high ratio of LMW-dT relative to the chromosomal dT content reflected the inefficient counting of HMW-dT, since it was still trapped inside the cell remnants. To investigate this, we treated both filters (HMW and LMW) with strong acid followed by strong base (1 M HCl at 100°C x 10 minutes, 0°C x 5 minutes, 2 M NaOH at 100°C x 10 minutes, 0°C x 5 minutes, 1 M Tris-HCl pH 8.0). We then either removed the elutable counts from filters and then combined the eluted counts with counts remaining on the filter, or simply counted the treated filters directly. Then we recalculated the LMW/HMW ratios. Comparison with the untreated filters shows no statistically-significant change in the ratio, indicating the efficiency of HMW-dT counting. **B.** The size of the LMW-dT pool in the parental Thy+ strain (AB1157) is 1) the same as in our *thyA* mutant (KKW58); 2) decreases as the cells slow down their exponential growth (that is, depends on the growth phase of the culture). **C.** The LMW-dT pool in AB1157 is slowly chased with endogenous (cold) dT, apparently into the chromosome, but free dT cannot be recruited from ~1/4 of it. AB1157 culture was grown to OD = 0.3 with ^{3}H-dT and at time =0 washed of the label, resuspended in M9CAA without dT and continued shaking.

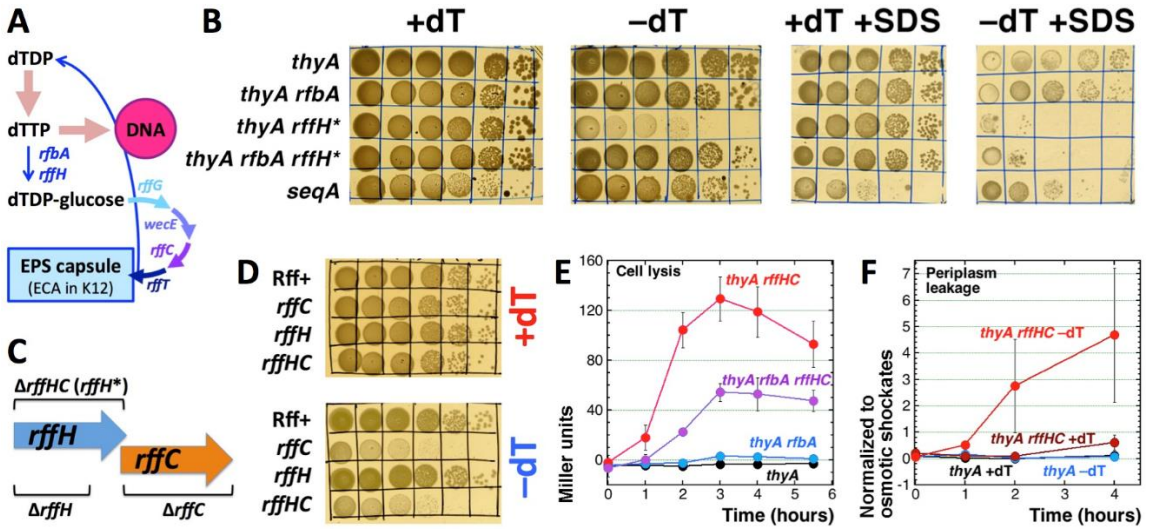

Figure 3.3. The T-hyperstarvation in the *thyA rfbA rffH* and *thyA rffC* mutants leads to cell lysis. A. A scheme of dTTP pool partitioning into the chromosomal DNA (by DNA polymerases) *vs* the pool of dTDP-glucose (by RfbA and RffH dTDP-glucose pyrophosphporylases). dTDP-glucose is converted into precursors for EPS capsule synthesis, while dTDP is returned to the DNA precursors pool by RffT). The *rffG*, *wecE*, *rffC* and *rffT* genes are specific to the ECA synthesis pathway. **B.** Spotting of serial dilutions of *thyA* (KKW58), *thyA rfbA* (RA48), *thyA rffH** (RA49) and *thyA rfbA rffH** (RA51) mutants on LB ±dT ±1.5% SDS. The *seqA* mutant (ER15) spotting is shown as a control for SDS sensitivity. **C.** A scheme of the *rffH* and *rffC* genes overlap, with the deletions we use. **D.** The T-starvation hypersensitivity phenotype of the *thyA rffHC* mutant is due to the *rffC* defect, rather than *rffH* defect. The *thyA* mutant strains are: Rff+, KKW58; *rffC*, RA57; *rffH*, RA60; *rffHC*, RA50. **E.** Cell lysis, measured as leakage of the cytoplasmic enzyme beta-galactosidase out of the cell, in liquid M9CAA cultures in the absence of dT. Thymidine was removed at time =0. Strains are as in "B". **F.** Periplasm leakage during T-starvation, measured as the presence of periplasmic enzyme alkaline phosphatase in the medium. The values were normalized to those obtained by osmotic shock from the same culture. Thymidine was removed at time =0.

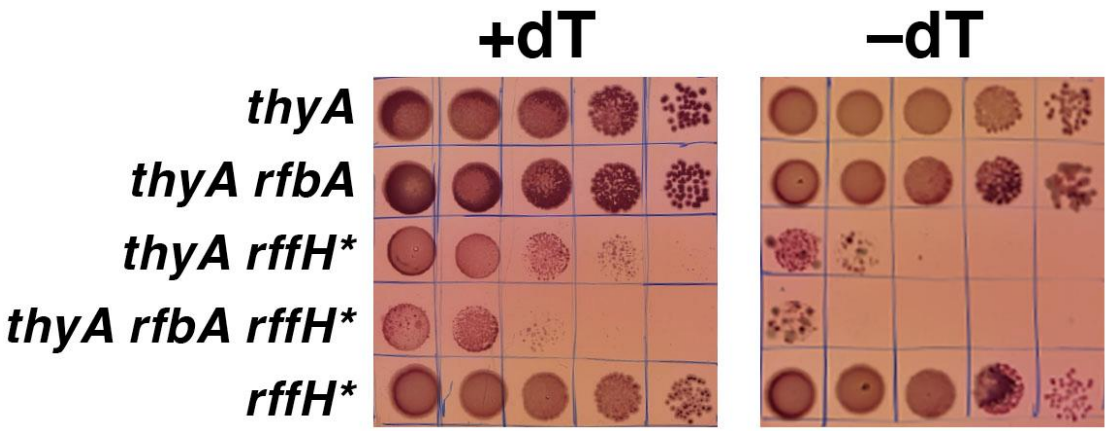

Figure 3.4. Spotting of serial dilutions of the same four strains on MacKonkey + lactose agar. The control strain in this case is a single *rffH* (RA64) mutant. The other strains are *thyA* (KKW58), *rfbA thyA* (RA48), *rffH thyA* (RA49), *rfbA rffH thyA* (RA51).

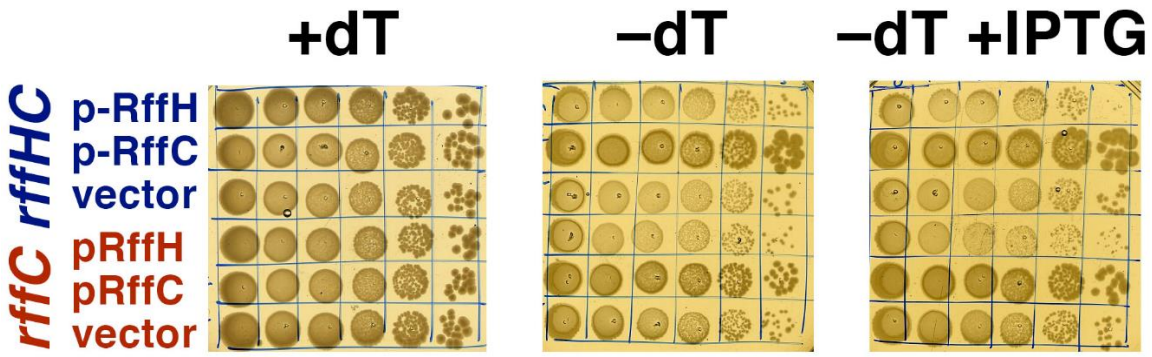

Figure 3.5. Spotting of serial dilutions of *thyA rffHC* (RA50) and *thyA rffC* (RA55) mutants, harboring the indicated plasmids, on LB ±dT ±IPTG. Plasmids are: vector, pLac22; pRffH, pPR3; pRffC, pPR5

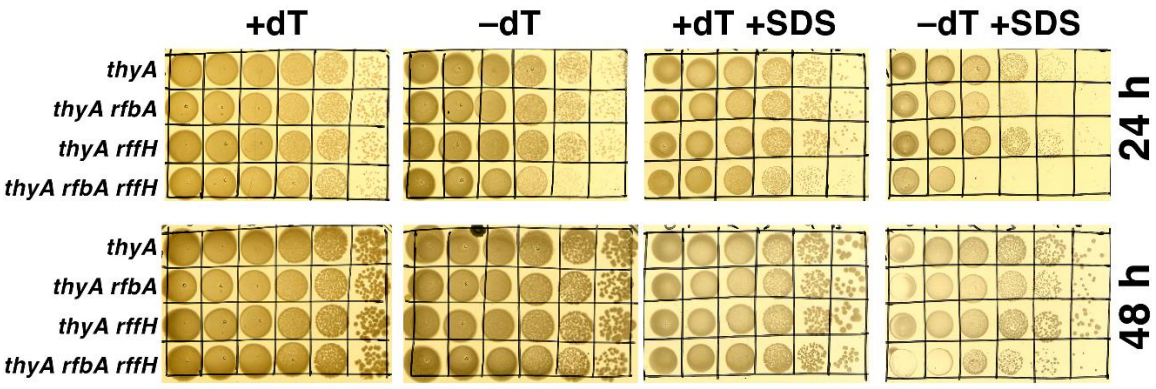

Figure 3.6. Spotting ±dT ±SDS reveals the enhanced T-starvation and SDS sensitivity of the *thyA rfbA rffH* (RffC+) mutant. Strains are: *thyA* (KKW58), *thyA rfbA* (RA48), *thyA rffH* (RA60), *thyA rfbA rffH* (RA65).

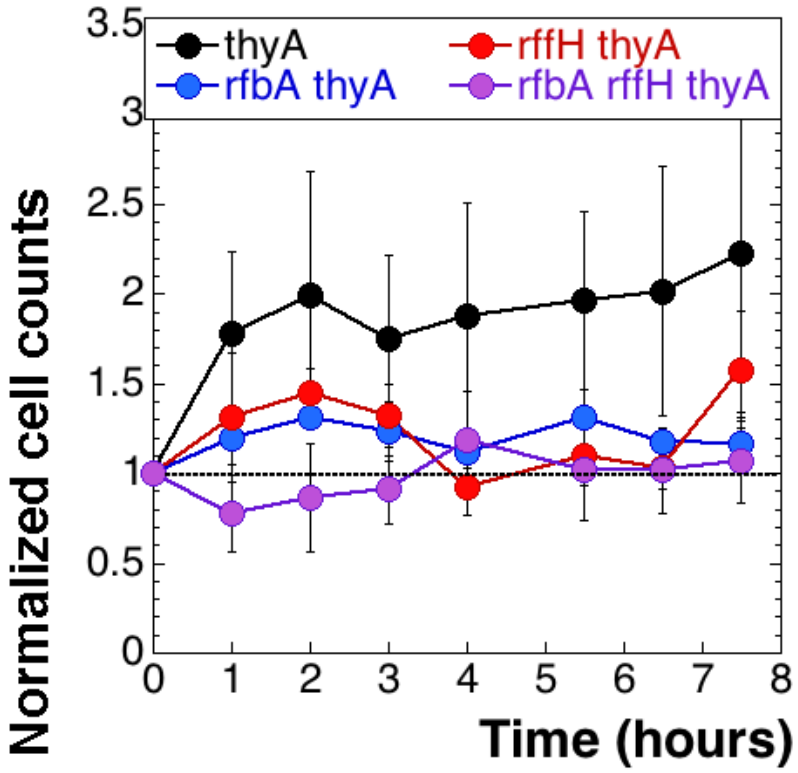

Figure 3.7. Direct cell counts in liquid M9CAA cultures in the absence of dT. Thymidine was removed at time =0. The strains are *thyA* (KKW58), *thyA rfbA* (RA48), *thyA rffHC* (RA49), *thyA rfbA rffHC* (RA51).

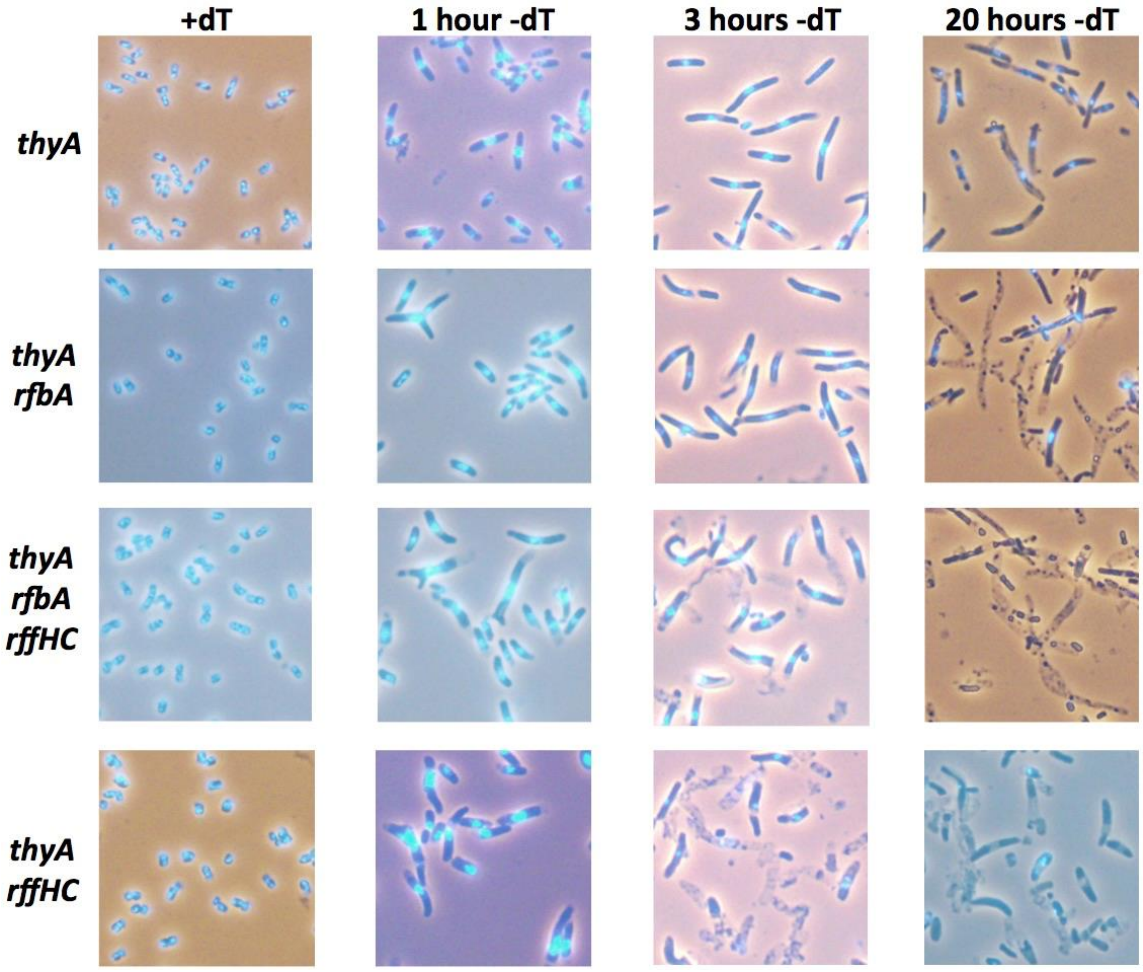

Figure 3.8. DAPI staining of the *thyA*, *thyA rfbA*, *thyA rfbA rffHC* and *thyA rffHC* mutants, undergoing T-starvation for 0, 1, 3 or 20 hours.The strains are: *thyA* (KKW58), *thyA rfbA* (RA48), *thyA rffHC* (RA49) and *thyA rfbA rffHC* (RA51).

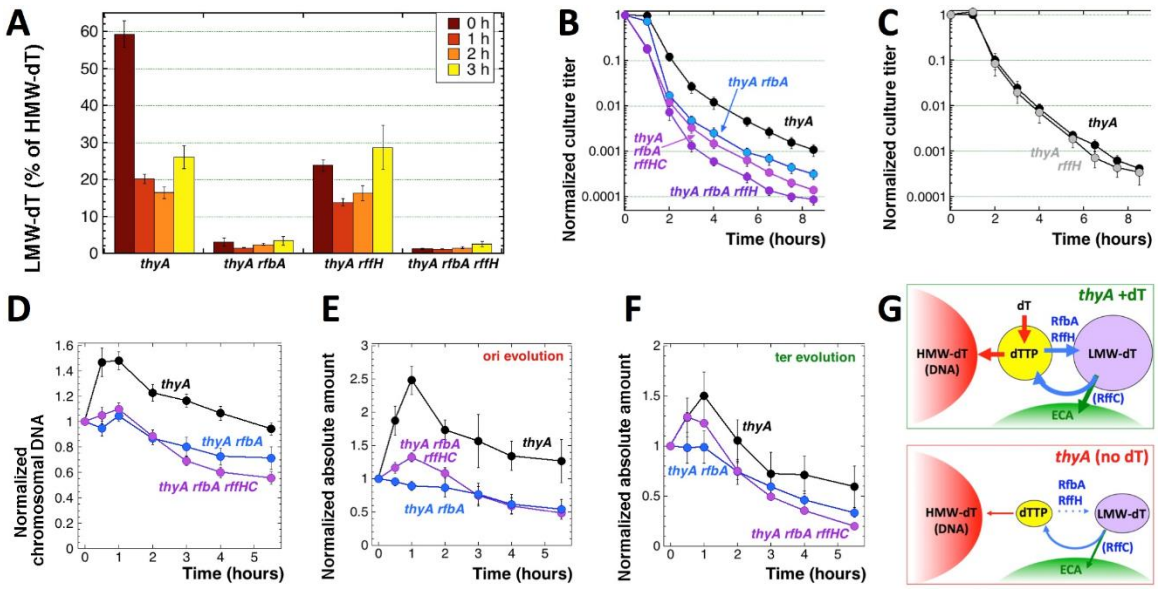

Figure 3.9. RfbA builds LMW-dT pool that supports DNA synthesis during the resistance phase of TLD. The strains are *thyA* (KKW58), *thyA rfbA* (RA48), *thyA rffH* (RA60), *thyA rfbA rffHC* (RA51) and *thyA rfbA rffH* (RA65) mutants. **A.** The evolution of LMW-dT pools in the *thyA rfbA*, *thyA rffH* and *thyA rfbA rffH* mutants during T-starvation. Thymidine was removed at time =0, after which aliquots were taken for the "0 h" cultures. Values for *thyA* mutant from Fig. 3.1D are for comparison. **B.** Time course of TLD in the *thyA*, *thyA rfbA*, *thyA rfbA rffHC* and *thyA rfbA rffH* (RffC+) mutants. **C.** Time course of TLD in the *thyA* and *thyA rffH* mutants. **D.** Loss of chromosomal DNA in the *thyA*, *thyA rfbA* and *thyA rfbA rffHC* mutants during T-starvation. **E.** Change over time of the absolute amounts of replication origin DNA in the *thyA*, *thyA rfbA* and *thyA rfbA rffHC* mutants during T-starvation. **F.** Same as in "D", but for the terminus. **G.** The current model of RfbA + RffH vs ECA synthesis action in *thyA* mutants in two growth conditions: with dT supplementation (top) or during the resistance phase of T-starvation (bottom).

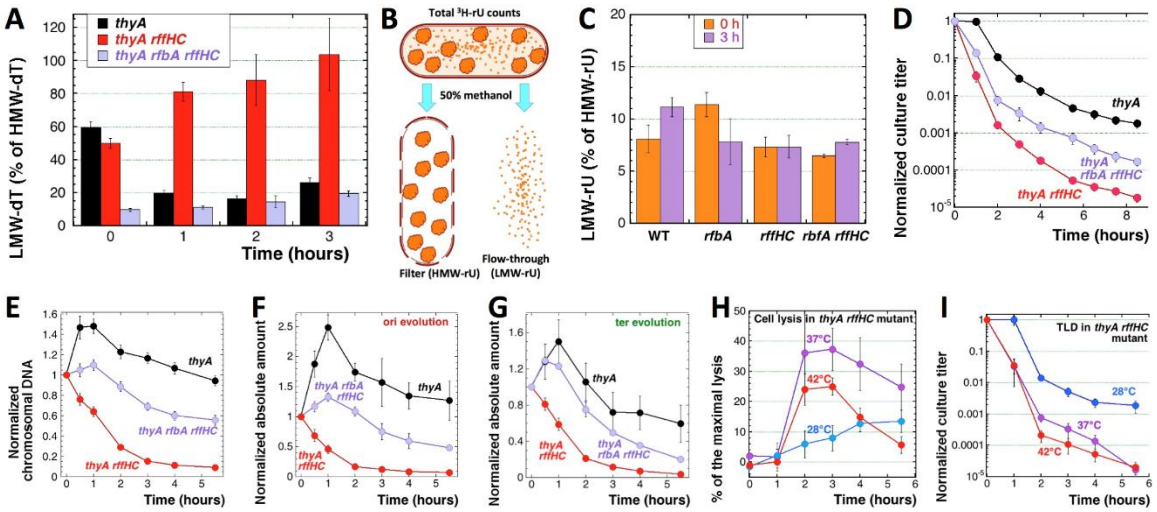

Figure 3.10. RffC helps to extract dTTP out of the LMW-dT pool during T-starvation. The strains are *thyA* (KKW58), *thyA rfbA* (RA48), *thyA rffHC* (RA49) and *thyA rfbA rffHC* (RA51). **A.** The evolution of LMW-dT pools in the *thyA rffHC* mutant during T-starvation (the red bars). Thymidine was removed at time =0, after taking aliquots for the "0 h" cultures. Values for *thyA* mutant (black bars) are shown for comparison from Fig. 3.1D are shown for comparison. **B.** A scheme of separation of the intracellular uridine into HMW-rU (the rU content of the cellular RNA, mostly ribosomes) and LMW-rU (nucleotides and sugar conjugates). **C.** The size of LMW-rU pool, normalized to the HMW-rU content of the cellular RNA, either during normal growth in dT-supplemented medium or after 3 hours of T-starvation. **D.** Time course of TLD in the *thyA rffHC* mutant. In panels D-G, the *thyA rfbA rffHC* mutant curve is shown to illustrate partial suppression. **E.** Loss of the chromosomal DNA absolute amounts in the *thyA rffHC* mutants during T-starvation. **F.** Loss of the replication origin DNA in the *thyA rffHC* mutant during T-starvation. **G.** Same as in "F", but for the terminus. **H.** Cell lysis upon T-starvation in the *thyA rffHC* mutant cultures at various temperatures. In contrast to Fig. 3.3E, where lysis was expressed in Miller units, here lysis is expressed as % of the total cellular content of beta-galactosidase, which undergoes its own peculiar kinetics during T-starvation. **I.** Time course of TLD in the *thyA rffHC* mutant cultures at the same temperatures as in "H".

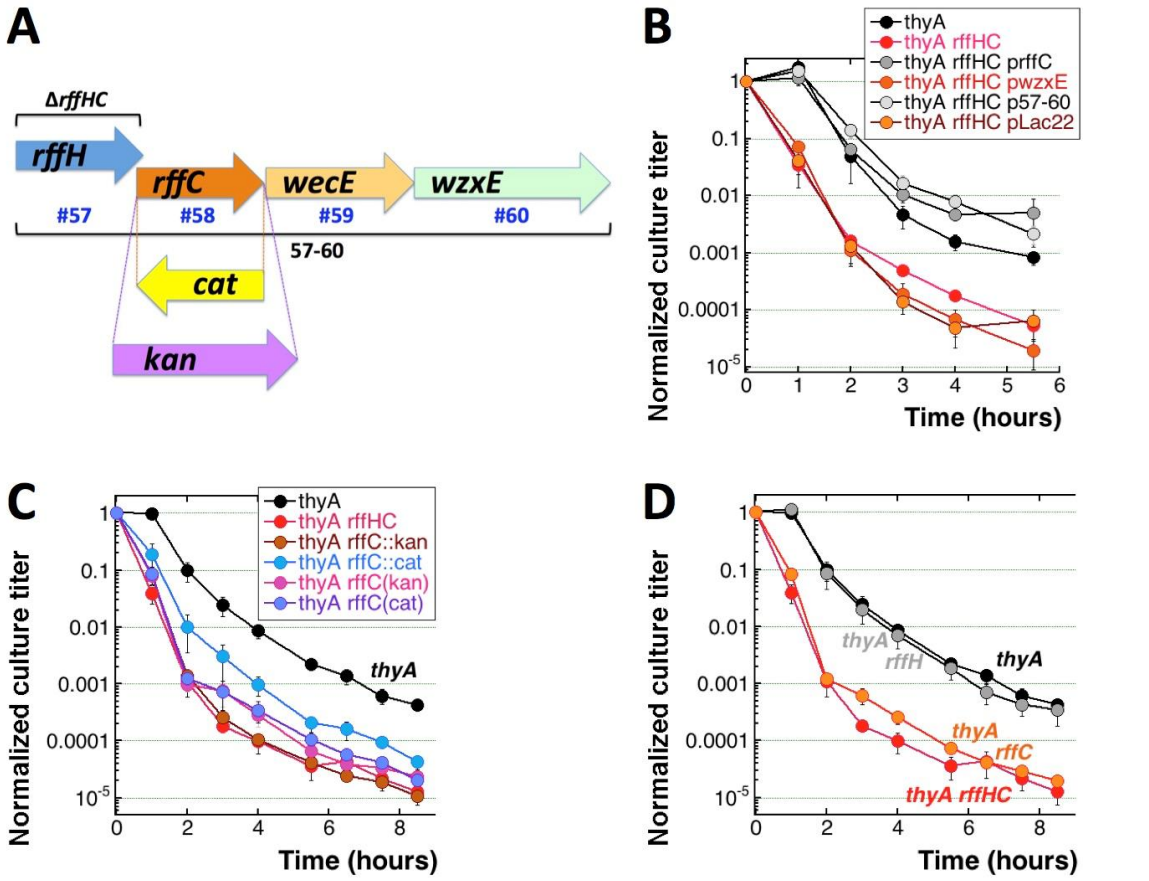

Figure 3.11. Kinetics of TLD of the *thyA rffHC* and *thyA rffC* mutants coincide. In all experimental panels, the *thyA* strain is KKW58, while the *thyA rffHC* mutant is RA49. **A.** A scheme of the *rffH-wzxE* region. The four genes are assigned the following numbers: *rffH*, #57; *rffC*, #58; *wecE*, #59; *wzxE*, #60. The orientation of the drug-resistant genes in the two deletion-replacement alleles of *rffC*, the *cat* and the *kan*, is also shown. **B.** Complementation of the hyper-TLD of the *thyA rffHC* mutant with plasmids carrying either all four genes (p57-60) or the *rffC*+-carrying plasmid. pLac22 is the vector; p*rffC* is pPR5; p*wzxE* is pPR6; p57-60 is pPR4. **C.** Similar hyper-TLD phenotypes of all Δ*rffC* alleles with the exception of Δ*rffC*::*cat*. Note that upon removal of the marker ((kan) or (cat)) hyper-TLD is still observed. The strains are: *thyA rffC*::*kan* (RA55); *thyA rffC*::*cat*,(RA56); *thyA rffC(kan)* (RA57); *thyA rffC(cat)* (RA58). **D.** TLD kinetics of the *thyA rffH* mutant coincides with the one of *thyA*, while the TLD kinetics of the *thyA rffC* mutant coincides with the one of *thyA rffHC*. The strains are *thyA* (KKW58), *thyA rffHC* (RA49), *thyA rffH* (RA60), *thyA rffC* (RA57).

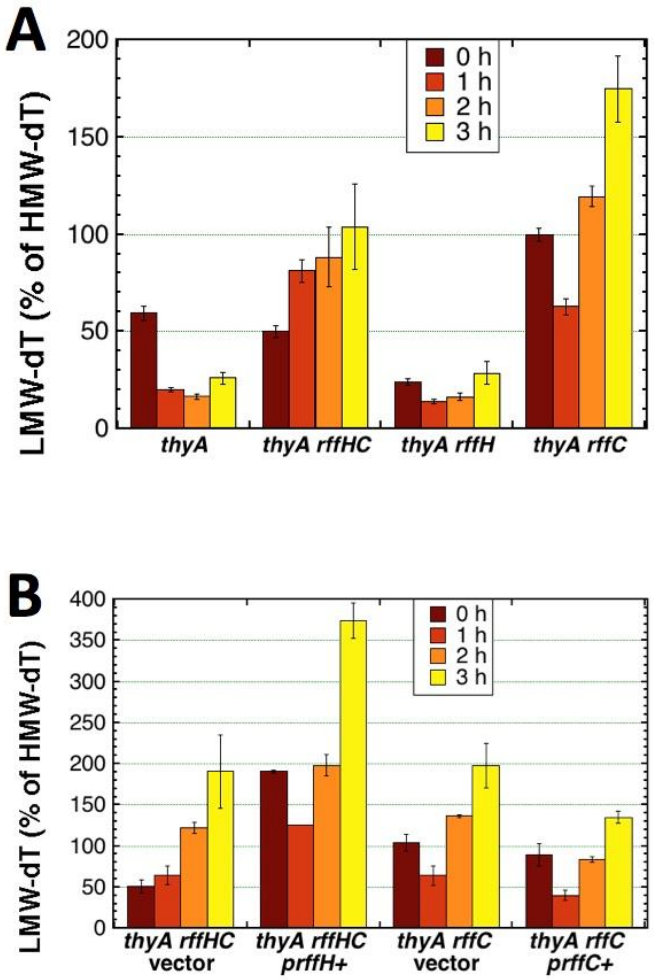

Figure 3.12. Comparison of the LMW-dT pools in the *thyA rffHC*, *thyA rffH* and *thyA rffC* mutants and complemented mutants. The pools were measured in the growing cells (t=0), as well as 1, 2 and 3 hours after switching to M9CAA without dT. The strains are *thyA* (KKW58), *thyA rffHC* (RA49), *thyA rffH* (RA60), *thyA rffC* (RA57). **A.** The uncomplemented mutants compared to the *thyA* single mutant. Note that the *thyA rffC* mutant behaves similar to the original *thyA rffHC* mutant. **B.** Complementation of the *thyA rffHC* mutant with the plasmid carrying *rffH*+ gene, and the *thyA rffC* mutant with a plasmid carrying the *rffC*+ gene. Note that increased copy number of *rffH*+ significantly elevates the LMW-dT pools at t=0. Plasmids are: vector, pLac22; p*rffH*+, pPR3; p*rffC*+, pPR5.

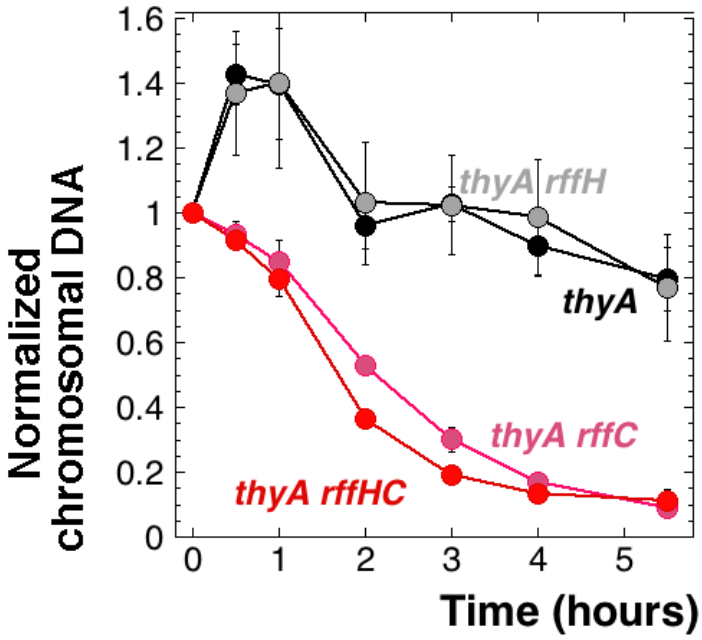

Figure 3.13. Changes in the relative amounts of the chromosomal DNA in the *thyA rffHC* and *thyA rffC* mutants coincide. The same is true for the very different patterns in the *thyA* and *thyA rffH* mutants. The strains are *thyA* (KKW58), *thyA rffHC* (RA49), *thyA rffH* (RA60), *thyA rffC* (RA57).

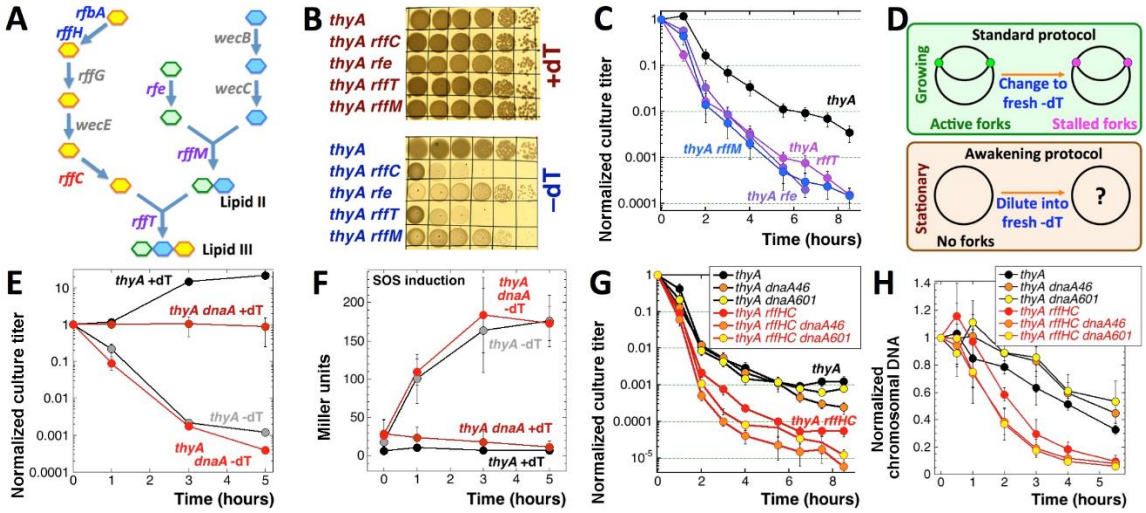

Figure 3.14. Hyper-TLD is observed in other ECA-defective mutants and is independent of DNA replication. The strains are *thyA* (KKW58), *thyA rffHC* (RA49), *thyA dnaA46*(Ts) (KJK170), *thyA dnaA601*(Ts) (SRK291), *thyA*(SOS) (RA66), *thyA dnaA46*(Ts) (SOS) (RA67), *thyA dnaA46*(Ts) *rffHC* (RA53), *thyA dnaA601*(Ts) *rffHC* (RA54), *thyA rfe* (RA61), *thyA rffM* (RA63) and *thyA rffT* (RA62). **A.** A scheme of ECA biosynthesis up to Lipid III. The relevant genes are in color: *rfbA* and *rffH* are blue, *rffC* is red, while *rfe*, *rffM* and *rffT* are purple. **B.** Spotting of serial dilutions of the indicated mutants on LB2xYE ±dT. **C.** Time course of TLD in the *thyA rfe*, *thyA rffM* and *thyA rffT* mutants. Note that the control *thyA* strain was dying shallower in this set. **D.** The standard T-starvation protocol compared to the "awakening protocol", used in panels "E" through "H". **E.** Time course of TLD at 42°C of the *thyA* and *thyA dnaA46*(Ts) mutants in the awakening protocol. The same culture are also diluted into the fresh medium +dT, to show the *dnaA*(Ts) defect. The strains are like in Fig. 3.15. **F.** No SOS induction in the *thyA dnaA*(Ts) (SOS) mutants supplemented with dT at 42°C. Strains were grown at 28°C and switched to 42°C ±dT at time =0. The *thyA* (SOS) mutant +dT provides a negative control, while the robust SOS induction in the –dT conditions in the two strains provides a positive control. **G.** Time course of TLD at 42°C in the *dnaA46*(Ts) and *dnaA601*(Ts) variants of either the *thyA* mutant (black lines) or *thyA rffHC* mutant (red lines).**H.** Loss of the chromosomal DNA during T-starvation at 42°C in the *dnaA46*(Ts) and *dnaA601*(Ts) variants of either the *thyA* mutant (black lines) or *thyA rffHC* mutant (red lines).

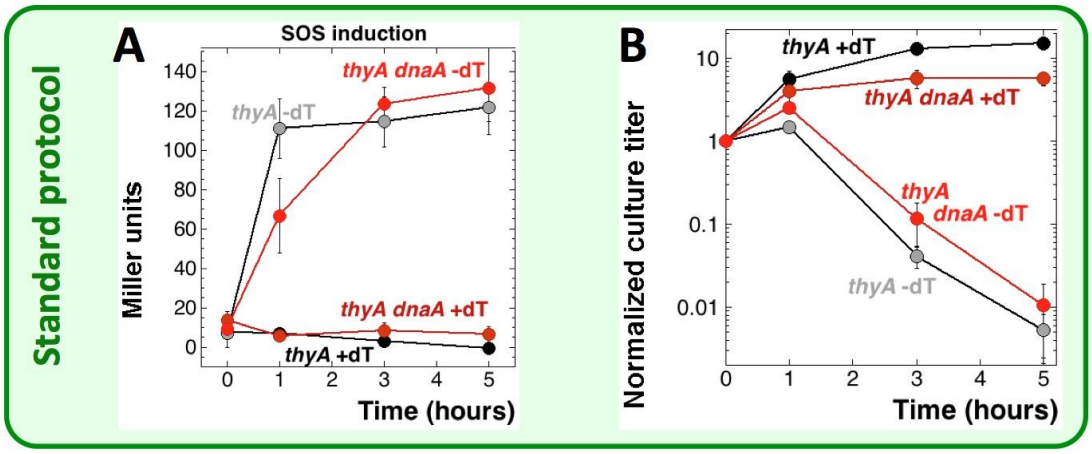

Figure 3.15. No SOS induction in the *thyA dnaA*(Ts) mutants supplemented with dT at 42°C. The *thyA* and *thyA dnaA*(Ts) mutants (with the SOS-induction indicator) were grown at 28°C in the presence of dT, according to the standard protocol (to OD~0.15), and then their medium was changed to a fresh one ±dT, and the cultures were shifted to 42°C. At time points 0, 1, 3 and 5 hours, the measurements of the SOS induction and the culture titer were taken. The data are averages of two independent measurements ±SEM. The strains are: *thyA* (SOS), (RA66); *thyA dnaA46*(Ts) (SOS), (RA67).

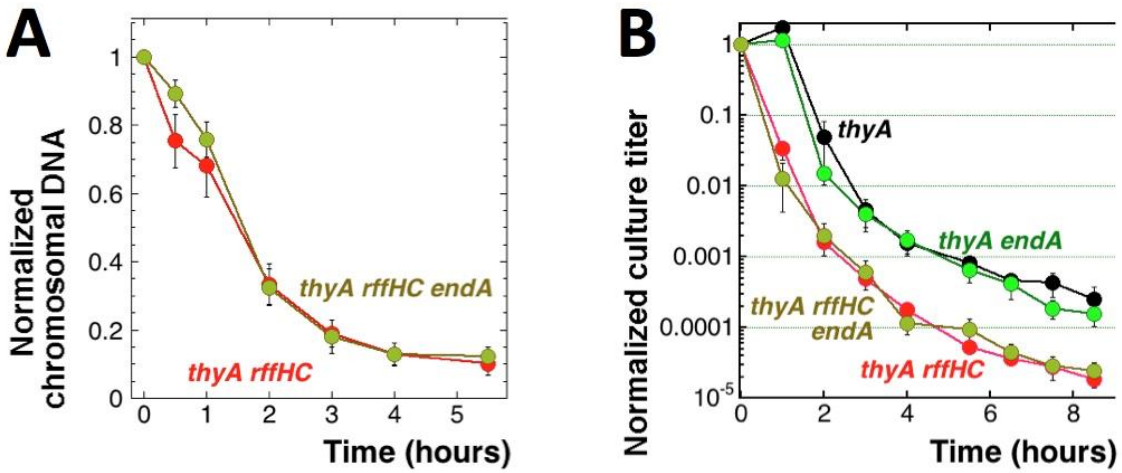

Figure 3.16. Hyper-TLD does not require Endo I. The strains are *thyA* (KKW58), *thyA rffHC* (RA49), *thyA endA* (SRK294), *thyA endA rffHC* (RA68). **G.** Stability of the chromosomal DNA in the *thyA rffHC endA* mutant during T-starvation (standard conditions). **H.** Time course of TLD in the *thyA endA* and *thyA rffHC endA* mutants. The *thyA* and *thyA rffHC* mutants are shown as controls.

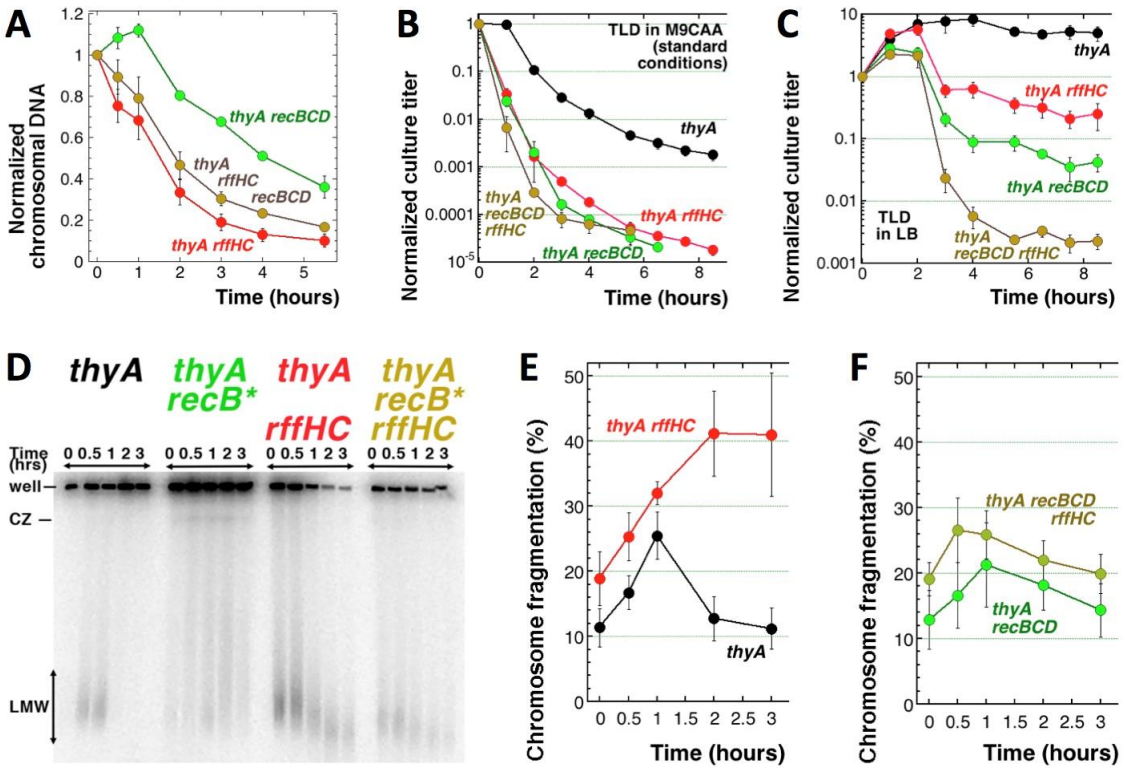

Figure 3.17. Chromosome fragmentation in the T-starved *thyA rffHC* mutant. The strains are *thyA* (KKW58), *thyA rffHC* (RA49), *thyA recBCD* (KJK63), *thyA recBCD rffHC* (RA52). **A.** Loss of the chromosomal DNA in the *thyA recBCD rffHC* mutant during T-starvation. **B.** Time course of TLD in the *thyA*, *thyA recBCD*, *thyA rffHC* and *thyA recBCD rffHC* mutants in the standard conditions (M9+CAA medium). **C.** Time course of TLD in the same four mutants as in "B', but in LB. **D.** A pulsed-field gel showing kinetics of chromosome fragmentation during T-starvation. A shorter time frame is used because no action happens in *thyA* and *thyA recBCD* mutants past 3 hours without dT, while the *thyA rffHC* mutants start lysing after 2 hours without dT. CZ, compression zone; LMW, "low molecular weight" fragments, ~50-200 kbp in size, *recB* = recBCD*. **E.** and **F.** Quantitative kinetics of the chromosomal fragmentation, from several gels like in "D". The higher background (time = 0) chromosome fragmentation in the *thyA rffHC* mutants reflects a peculiar sensitivity of this mutant to centrifugation (used to collect cells before encasing them in agarose plugs). Minimizing the speed of centrifugation minimizes this fragmentation even for *thyA rffHC* cells still supplemented with dT (as well as for the T-starved cells).

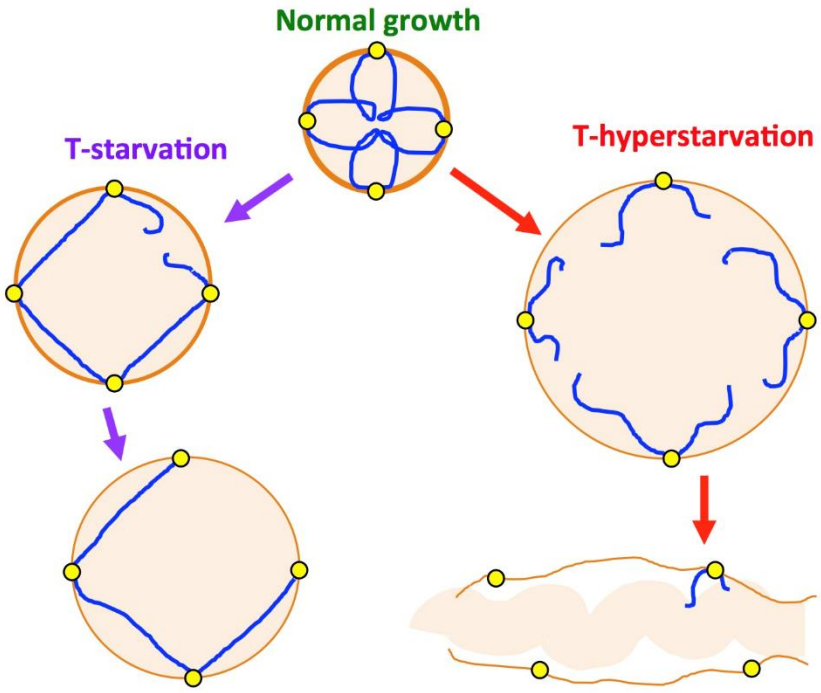

Figure 3.18. The model of chromosome and cell behavior during T-starvation versus T-hyperstarvation. The shaded circle depicts cross-section of the cell, while the chromosomal DNA is shown by the blue line, attached to the cell envelope at certain points (small yellow circles). In the absence of dT, DNA attachment to the envelope is proposed to "freeze". As a result, during T-starvation, increase in cell volume causes chromosomal breakage and limited loss. In contrast, during T-hyperstarvation, a larger increase in cell volume breaks DNA in many places, leading to a complete loss, while the cell envelope also eventually bursts.

3.8 Tables

Table 3.1. Strains used in this study.

Strain Name	Genotype	Reference
AB1157*	Wild type	(3)
ER15	Δ*seqA20::kan*	(63)
JB1 pSA122	Δ*recBCD3::kan* pRecBC+	Lab Collection
JW2042-1**	Δ*rfbA737::kan*	(2)
JW2912-1**	Δ*endA720::kan*	(2)
JW3763-2**	Δ*rffH740::kan*	(2)
KJK63	Δ*thyA*Δ *deoCABD2 recBCD3::kan*	(36)
KJK170	Δ*thyA* Δ*deoCABD2 dnaA46(Ts)*	(29)
KKW58	Δ*thyA72* Δ*deoCABD2*	(36)
KKW59	Δ*deoCABD2*	(36)
NS373**	*dnaA46(Ts) tna::Tn10*	(66)
SRK270	*dnaA601(Ts) yidX+ cat yidA+*	(29)
SRK291	Δ*thyA* Δ*deoCABD2 dnaA601(Ts)*	(29)
JW10741	Δ*rfe735::kan*	(2)
JW10745	Δ*rffT744::kan*	(2)
JW11482	Δ*rffM745::kan*	(2)
AK43	*sulA::lacZ* (MuΔX *cat*)	(33)
RA48	Δ*thyA72* Δ*deoCABD2* Δ*rfbA737::kan*	KKW58 x P1 JW2042-1
RA49	Δ*thyA72* Δ*deoCABD2* Δ*rffH740::kan*	KKW58 x P1 JW3763-2
RA50	Δ*thyA72* Δ*deoCABD2* Δ*rffH740*	RA49, *kan* removed by pCP20
RA51	Δ*thyA72* Δ*deoCABD2* Δ*rffH* *Δrfb*A737::kan	RA50 x P1 JW2042-1
RA52	Δ*thyA72* Δ*deoCABD2* Δ*recBCD3::kan* Δ*rffH*	RA50 x P1 JB1 pSA122
RA53	Δ*thyA72* Δ*deoCABD2 dnaA46*(Ts) Δ*rffH740::kan*	KJK170 x P1 JW3763-2
RA54	Δ*thyA72* Δ*deoCABD2* *dnaA601*(Ts) Δ*rffH740::kan*	SRK291 x P1 JW3763-2
RA55	Δ*thyA72* Δ*deoCABD2* Δ*rffC::kan*	Precise *rffC* deletion using Datsenko Wanner procedure
RA56	Δ*thyA72* Δ*deoCABD2* Δ*rffC::cat*	Precise rffC deletion using Datsenko Wanner procedure
RA57	Δ*thyA72* Δ*deoCABD2* Δ*rffC(kan)*	RA55, *kan* removed by pCP20
RA58	Δ*thyA72* Δ*deoCABD2* Δ*rffC(cat)*	RA56, *cat* removed by pCP20

Table 3.1. (cont.)

RA59	Δ*thyA72* Δ*deoCABD2* Δ*rffH::kan*	Precise *rffH* deletion using Datsenko Wanner procedure
RA60	Δ*thyA72* Δ*deoCABD2* Δ*rffH*	RA59, *kan* removed by pCP20
RA61	Δ*thyA72 Δ deoCABD2* Δ*rfe735::kan*	KKW58 x P1 JW10741
RA62	Δ*thyA72 Δ deoCABD2* Δ*rffT744::kan*	KKW58 x P1 JW10745
RA63	Δ*thyA72 Δ deoCABD2* Δ*rffM745::kan*	KKW58 x P1 JW11482
RA64	Δ*deoCABD2* Δ*rffH740*	KKW59 x P1 JW3763-2
RA65	Δ*thyA72* Δ*deoCABD2* Δ*rfbA737::kan* Δ*rffH*	RA60 x P1 JW2042-1
RA66	Δ*thyA72* Δ*deoCABD2 sulA::lacZ* (MuΔX *cat*)	KKW58 x P1 AK43
RA67	Δ*thyA72* Δ*deoCABD2 dnaA46*(Ts) *sulA::lacZ* (MuΔX *cat*)	KJK170 x P1 AK43
RA68	Δ*thyA72* Δ*deoCABD2* Δ*endA720::kan* Δ*rffH*	RA50 x P1 JW2912-1
SRK294	Δ*thyA72* Δ*deoCABD2* Δ*endA720*::*kan*	KKW58 x P1 JW2912-1

* other mutations include: F– λ– *rac– thi-1 hisG4* Δ*(gpt-proA)62 argE3 thr-1 leuB6 kdgK51 rfbD1 araC14 lacY1 galK2 xylA5 mtl-1 tsx-33 supE44*(glnV44) *rpsL31*(strR).

** a non-AB1157 strain.

Table 3.2. Plasmids used in this study.

Plamid Name	Replicon/Drug Resistance/Other Genes	Reference
pKD46	pSC101 ori^{TS}/*bla*/ λ *beta gam exo*	(16)
pKD3	oriR6K/*cat, bla*	(16)
pKD4	oriR6K/*kan, bla*	(16)
pCP20	pSC101 ori^{TS} /bla, *cat /flp*	(16)
pLAC22	ColE1/ *bla, tet* / lacI^{q} *rpo*	(71)
pPR3	ColE1/ *bla, tet* / lacI^{q} *rpo rffH*1061	This study
pPR4	ColE1/ *bla, tet* / lacI^{q} *rpo rffH rffC wecE wzxE*	This study
pPR5	ColE1/ *bla, tet* / lacI^{q} *rpo rffC*	This study
pPR6	ColE1/ *bla, tet* / lacI^{q} *rpo wzxE*	This study

Table 3.3. Primers used in this study.

Purpose	Name/Sequence
rfbA deletion verification	PR36 TGCACTCAACAAGCTCAACG
	PR37 AAAGCTGACCGGATAGCCTAG
rffH deletion verification	PR38 TCGGTAAAACGGTTCAGTGG
	PR39 TGGCATTGTTCACGGGTAGC
rfe deletion verification	PR50 TTTGGAACGGACTTTCCC
	PR51 CAGCCCCATGCCAATAATCC
rffT deletion verification	PR52 GCGGTTTTATATTCTGGCGG
	PR53 AAAGCGAAATACCAGCACGC
rffM deletion verification	PR54 CGCAAAACTGTTGTACTGGC
	PR55 GCTCTGGTTTGTTATCTGCC
rffC deletion verification	PR76 ATATCTGCTGGAGTTACTTC
	PR77 TGCGTTAAATGGAATCATGTG
endA deletion verification	endA (scr)F GCTTTCGCTACGTTGCTG
	endA (scr)B CGTCGTCTCCCCACGCGG
rffH precise deletion by Datsenko-Wanner method	PR71 TTTAGGTCTGAAAGGCTAATTTTCAGCGGAGGCAAACG TGTAGGCTGGAGCTGCTTC
	PR73 AGGCAAATCCGCGCCCGAGCAGTTCAACGGTCAGGTT CATATGAATATCCTCCTTAG
rffC precise deletion by Datsenko-Wanner method	PR74 AAAACTGGCTACGGCCAATATCTGCTGGAGTTACTTCG TGTAGGCTGGAGCTGCTTC
	PR75 TCCCACCACCGGCGGTGCGTTAAATGGAATCATGTGAC ATATGAATATCCTCCTTAG

Table 3.3. (cont.)

pPR3 cloning	PR64 CAGGAAAGATCTTTGATGCTTCGAAAATTGCC
	PR55’ TCGACGGAATTCTCAATACTGGCGCGGACGGG
pPR4 cloning	PR57 CAATTTCACACAGGAAAGATCTTTGATGCTTCGAAAATTGCC
	PR60 TAAGCTGTCAAACATGAGAATTCTCATGCCCGCCTACGCCAGAG
pPR5 cloning	PR65 ATATATAGATCTGTGCCCGTCCGCGCCAGTATTG
	PR66 CGATCGGAATTCTCACCTGTATAACCAGTACGC
pPR6 cloning	PR69 GCATGCAGATCTATGTCGTTGGCAAAAGCGTCC
	PR70 TTGCATGAATTCTCATGCCCGCCTACGCCAGA

3.9 References

1. Ahmad SI, Kirk SH, Eisenstark A. 1998. Thymine metabolism and thymineless death in prokaryotes and eukaryotes. *Annu. Rev. Microbiol.* 52:591–625.

2. Baba T, Ara T, Hasegawa M, Takai Y, Okumura Y, et al. 2006. Construction of Escherichia coli K-12 in-frame, single-gene knockout mutants: The Keio collection. *Mol. Syst. Biol.* 2:2006.0008.

3. Bachmann BJ. 1996. Derivations and genotypes of some mutant derivatives of *Escherichia coli* K-12. *Escherichia coli Salmonella typhimurium Cell. Mol. Biol.*, pp. 2460–2488.

4. Barner HD, Cohen SS. 1954. The induction of thymine synthesis by T2 infection of a thymine requiring mutant of *Escherichia coli*. *J. Bacteriol.* 68(1):80–88.

5. Barner HD, Cohen SS. 1958. Protein synthesis and RNA turnover in a pyrimidine deficient bacterium. *Biochim. Biophys. Acta*. 30:12–20.

6. Bayer ME. 1979. The fusion sites between outer membrane and cytoplasmic membrane of bacteria: their role in membrane assembly and virus infection. In Bacterial Outer Membranes, ed M Inouye, pp. 167–202. John Wiley & Sons, New York.

7. Bitto NJ, Chapman R, Pidot S, Costin A, Lo C, et al. 2017. Bacterial membrane vesicles transport their DNA cargo into host cells. *Sci. Rep.* 7(1):1–11.

8. Bochner BR, Ames BN. 1982. Complete analysis of cellular nucleotides by two-dimensional thin layer chromatography. *J. Biol. Chem.* 257(16):9759–69.

9. Breitman TR, Maury PB, Toal JN. 1972. Loss of deoxyribonucleic acid-thymine during thymine starvation of *Escherichia coli*. *J. Bacteriol.* 112(1):646–48.

10. Brickman E, Beckwith J. 1975. Analysis of the regulation of *Escherichia coli* alkaline phosphatase synthesis using deletions and phi80 transducing phages. *J. Mol. Biol.* 96(2):307–16.

11. Cohen SS. 1971. On the nature of thymineless death. *Ann. N. Y. Acad. Sci.* 186:292–301.

12. Cohen SS, Barner HD. 1954. Studies on unbalanced growth in *Escherichia coli*. *Proc. Natl. Acad. Sci. USA*. 40:885–93.

13. D'Alençon E, Taghbalout A, Kern R, Kohiyama M. 1999. Replication cycle dependent association of SeqA to the outer membrane fraction of *E. coli*. *Biochimie.* 81(8–9):841–46.

14. Danese PN, Oliver GR, Barr K, Bowman GD, Rick PD, Silhavy TJ. 1998. Accumulation of the enterobacterial common antigen lipid II biosynthetic intermediate stimulates *degP* transcription in *Escherichia coli*. *J. Bacteriol.* 180(22):5875–84.

15. Dassa E, Boquet PL. 1981. ExpA: A conditional mutation affecting the expression of a group of exported proteins in *Escherichia coli* K-12. *Mol. Gen. Genet.* 181(2):192–200.

16. Datsenko KA, Wanner BL. 2000. One-step inactivation of chromosomal genes in *Escherichia coli* K-12 using PCR products. *Proc. Natl. Acad. Sci. U. S. A.* 97(12):6640–45.

17. Dillingham MS, Kowalczykowski SC. 2008. RecBCD enzyme and the repair of double-stranded DNA breaks. *Microbiol. Mol. Biol. Rev.* 72(4):642–71.

18. El-Kazzaz W, Morita T, Tagami H, Inada T, Aiba H. 2004. Metabolic block at early stages of the glycolytic pathway activates the Rcs phosphorelay system via increased synthesis of dTDP-glucose in *Escherichia coli*. *Mol. Microbiol.* 51(4):1117–28.

19. Fonville NC, Bates D, Hastings PJ, Hanawalt PC, Rosenberg SM. 2010. Role of RecA and the SOS response in thymineless death in *Escherichia coli*. *PLoS Genet.* 6(3):e1000865.

20. Fonville NC, Vaksman Z, Denapoli J, Hastings PJ, Rosenberg SM. 2011. Pathways of resistance to thymineless death in *Escherichia coli* and the function of UvrD. *Genetics*. 189(1):23–36.

21. Gallant J, Suskind R. 1961. Relationship between thymineless death and ultraviolet inactivation in *Escherichia coli*. *J. Bacteriol.* 1961:187–94.

22. Goulian M, Bleile B, Tseng BY. 1980. Methotrexate-induced misincorporation of uracil into DNA. *Proc. Natl. Acad. Sci. USA.* 77(4):1956–60.

23. Goulian M, Bleile B, Tseng BY. 1980. The effect of methotrexate on levels of dUTP in animal cells. *J. Biol. Chem.* 255(22):10630–37.

24. Guarino E, Salguero I, Jiménez-Sánchez A, Guzmán EC. 2007. Double-strand break generation under deoxyribonucleotide starvation in *Escherichia coli*. *J. Bacteriol.* 189(15):5782–86.

25. Hosono R, Hosono H, Kuno S. 1975. Effects of growth conditions on thymidine nucleotide pools in *Escherichia coli*. *J. Biochem.* 78(1):123–29.

26. Jorgenson MA, Kannan S, Laubacher ME, Young KD. 2016. Dead-end intermediates in the enterobacterial common antigen pathway induce morphological defects in *Escherichia coli* by competing for undecaprenyl phosphate. *Mol. Microbiol.* 100(1):1–14.

27. Khan SR, Kuzminov A. 2012. Replication forks stalled at ultraviolet lesions are rescued via RecA and RuvABC protein-catalyzed disintegration in *Escherichia coli*. *J. Biol. Chem.* 287(9):6250–65.

28. Khan SR, Kuzminov A. 2017. Degradation of RNA during lysis of *Escherichia coli* cells in agarose plugs breaks the chromosome. *PLoS One.* 12(12):1–24.

29. Khan SR, Kuzminov A. 2019. Thymineless death in *Escherichia coli* is unaffected by the chromosomal replication complexity. *J. Bacteriol.* 201(9):1–16.

30. Khodursky A, Guzmán EC, Hanawalt PC. 2015. Thymineless death lives on: New insights into a classic phenomenon. *Annu. Rev. Microbiol.* 69(1):247–63.

31. Kornfeld S, Glaser L. 1961. The enzymatic synthesis of thymidine-linked sugars. *J. Biol. Chem.* 236(6):1791–94.

32. Kouzminova EA, Kadyrov FF, Kuzminov A. 2017. RNase HII saves *rnhA* mutant *Escherichia coli* from R-Loop-associated chromosomal fragmentation. *J. Mol. Biol.* 429(19):2873–94.

33. Kouzminova EA, Rotman E, Macomber L, Zhang J, Kuzminov A. 2004. RecA-dependent mutants in *Escherichia coli* reveal strategies to avoid chromosomal fragmentation. *Proc. Natl. Acad. Sci. USA.* 101(46):16262–67.

34. Krishnakumar R, Craig M, Imlay JA, Slauch JM. 2004. Differences in enzymatic properties allow SodCI but not SodCII to contribute to virulence in *Salmonella enterica* serovar typhimurium strain 14028. *J. Bacteriol.* 186(16):5230–38.

35. Kuhn H, Meier-Deiter U, Mayer H. 1988. ECA , the enterobacterial common antigen. *FEMS Microbiol. Rev.* 54:195–222.

36. Kuong KJ, Kuzminov A. 2010. Stalled replication fork repair and misrepair during thymineless death in *Escherichia coli*. *Genes to Cells.* 15(6):619–34.

37. Kuong KJ, Kuzminov A. 2012. Disintegration of nascent replication bubbles during thymine starvation triggers RecA- and RecBCD-dependent replication origin destruction. *J. Biol. Chem.* 287(28):23958–70.

38. Kuzminov A. 1999. Recombinational repair of DNA damage in *Escherichia coli* and bacteriophage lambda. *Microbiol. Mol. Biol. Rev.* 63(4):751–813.

39. Liu D, Reeves PR. 1994. *Escherichia coli* K12 regains its O antigen. *Microbiology.* 140(3):49–57.

40. Maharjan RP, Ferenci T. 2003. Global metabolite analysis: The influence of extraction methodology on metabolome profiles of *Escherichia coli*. *Anal Biochem.* 313(1):145–54.

41. Marolda CL, Valvano MA. 1995. Genetic analysis of the dTDP-rhamnose biosynthesis region of the Escherichia coli VW187 (O7:K1) *rfb* gene cluster: Identification of functional homologs of *rfbB* and *rfbA* in the *rff* cluster and correct location of the *rffE* gene. *J. Bacteriol.* 177(19):5539–46.

42. Miller JH. 1972. Experiments in Molecular Genetics. , p. 466. Cold Spring Harbor, NY: Cold Spring Harbor Laboratory Press.

43. Mychack A, Amrutha RN, Chung C, Cardenas Arevalo K, Reddy M, Janakiraman A. 2019. A synergistic role for two predicted inner membrane proteins of *Escherichia coli* in cell envelope integrity. *Mol. Microbiol.* 111(2):317–37.

44. Nakayama H. 2005. *Escherichia coli* RecQ helicase: A player in thymineless death. *Mutat Res.* 577(1–2):228–36.

45. Nakayama H, Nakayama K, Nakayama R, Nakayama Y. 1982. Recombination-deficient mutations and thymineless death in *Escherichia coli* K12: reciprocal effects of *recBC* and *recF* and indifference of *recA* mutations. *Can. J. Microbiol.*, pp. 425–30.

46. Nakayama K, Irino N, Nakayama H. 1985. The *recQ* gene of *Escherichia coli* K12: Molecular cloning and isolation of insertion mutants. *Mol Gen Genet.* 200(2):266–71.

47. Nakayama K, Kusano K, Irino N, Nakayama H. 1994. Thymine starvation-induced structural changes in *Escherichia coli* DNA. Detection by pulsed field gel electrophoresis and evidence for involvement of homologous recombination. *J Mol Biol.* 243(4):611–20.

48. Nakayama K, Shiota S, Nakayama H. 1988. Thymineless death in *Escherichia coli* mutants deficient in the RecF recombination pathway. *Can. J. Microbiol.* 34(7):905–7.

49. Neidhardt FC. 1987. *Escherichia coli* and *Salmonella typhimurium. Cellular and molecular biology.* American Society for Microbiology, Washington D.C. 3–6 pp. F.C. Neidh ed.

50. Neuhard J, Nygaard P. 1987. *Escherichia coli* and *Salmonella typhimurium.* Cellular and molecular biology. ASM Press, Washington D.C. 445–473 pp. F.C. Neidh ed.

51. Nicolaidis AA, Holland IB. 1978. Evidence for the specific association of the chromosomal Origin with outer membrane fractions isolated from *Escherichia coli*. *J. Bacteriol.* 135(1):178–89.

52. Ogden GB, Pratt MJ, Schaechter M. 1988. The replicative origin of the *E. coli* chromosome binds to cell membranes only when hemimethylated. *Cell*. 54(1):127–35.

53. Ohkawa T. 1975. Studies of intracellular thymidine nucleotides. Thyminless death and the recovery after re-addition of thymine in *Escherichia coli* K 12. *Eur. J. Biochem.* 60:57–66.

54. Ohkawa T. 1976. Studies of intracellular thymidine nucleotides. Relationship between the synthesis of deoxyribonucleic acid and the thymidine triphosphate pool in *Escherichia coli* K12. *Eur. J. Biochem.* 61(1):81–91.

55. Okazaki R. 1959. Isolation of a new deoxyribosidic compound thymidine diphosphate rhamnose. *Biochem. Biophys. Res. Commun.* 1(1):34–38.

56. Okazaki R. 1960. Studies of deoxyribonucleic acid synthesis and cell growth in the deoxyriboside-requiring bacteria, *Lactobacillus acidophilus*. III. Identification of thymidine diphosphate rhamnose. *Biochim. Biophys. Acta.* 44:478–190.

57. Okazaki R, Okazaki T. 1958. Studies of deoxyribonucleic acid synthesis and cell growth in the deoxyriboside-requiring bacteria Lactobacillus acidophilus. I. Biological and chemical nature of the intra-cellular acid-soluble deoxyribosidic compounds. *Biochim. Biophys. Acta.* 28(3):470–82.

58. Okazaki R, Okazaki T, Kuriki Y. 1959. Incorporation of [3H]thymidine in a deoxyriboside-requiring bacterium. *Biochim. Biophys. Acta.* 33:289–91.

59. Rahman A, Barr K, Rick PD. 2001. Identification of the structural gene for the TDP-Fuc4NAc: Lipid II Fuc4NAc transferase involved in synthesis of enterobacterial common antigen in *Escherichia coli* K-12. *J Bacteriol.* 183(22):6509–16.

60. Rao TVP, Kuzminov A. 2019. Sources of thymidine and analogs fueling futile damage-repair cycles and ss-gap accumulation during thymine starvation in *Escherichia coli*. *DNA Repair (Amst).* 75:1–17.

61. Rick PD, Wolski S, Barr K, Ward S, Ramsay-Sharer L. 1988. Accumulation of a lipid-linked intermediate involved in enterobacterial common antigen synthesis in *Salmonella typhimurium* mutants lacking dTDP-glucose pyrophosphorylase. *J. Bacteriol.* 170:4008–14.

62. Rotman E, Bratcher P, Kuzminov A. 2009. Reduced lipopolysaccharaide phosphorylation in *Escherichia coli* lowers the elevated ori/ter ratio in *seqA* mutants. *Mol. Microbiol.* 72(5):1273–92.

63. Rotman E, Kuzminov A. 2007. The *mutT* defect does not elevate chromosomal fragmentation in *Escherichia coli* because of the surprisingly low levels of MutM/MutY-recognized DNA modifications. *J. Bacteriol.* 189(19):6976–88.

64. Samuel G, Reeves P. 2003. Biosynthesis of O-antigens: Genes and pathways involved in nucleotide sugar precursor synthesis and O-antigen assembly. *Carbohydr. Res.* 338(23):2503–19.

65. Sangurdekar DP, Hamann BL, Smirnov D, Srienc F, Hanawalt PC, Khodursky AB. 2010. Thymineless death is associated with loss of essential genetic information from the replication origin. *Mol. Microbiol.* 75(6):1455–67.

66. Schaus N, O'Day K, Peters W, Wright A. 1981. Isolation and characterization of amber mutations in gene *dnaA* of *Escherichia coli* K-12. *J. Bacteriol.* 145(2):904–13.

67. Schnaitman CA, Klena JD. 1993. Genetics of Lipopolysaccharide biosynthesis in enteric bacteria. *Microbiol. Rev.* 57(3):655–82.

68. Sivaraman J, Sauvé V, Matte A, Cygler M. 2002. Crystal structure of *Escherichia coli* glucose-1-phosphate thymidylyltransferase (RffH) complexed with dTTP and Mg2+. *J. Biol. Chem.* 277(46):44214–19.

69. Sutterlin HA, Shi H, May KL, Miguel A, Khare S, et al. 2016. Disruption of lipid homeostasis in the Gram-negative cell envelope activates a novel cell death pathway. *Proc. Natl. Acad. Sci. USA.* 113(11):E1565–74.

70. Toyofuku M, Nomura N, Eberl L. 2019. Types and origins of bacterial membrane vesicles. *Nat. Rev. Microbiol.* 17(1):13–24.

71. Warren JW, Walker JR, Roth JR, Altman E. 2000. Construction and characterization of a highly regulable expression vector, pLAC11, and its multipurpose derivatives, pLAC22 and pLAC33. *Plasmid*. 44(2):138–51.

72. Witte A, Lubitz W. 1989. Biochemical characterization of Phi X174 - protein -E-mediated lysis of *Escherichia coli*. *Eur. J. Biochem*. 180(2):393–98.

73. Zaritsky A, Woldringh CL, Einav M, Alexeeva S. 2006. Use of thymine limitation and thymine starvation to study bacterial physiology and cytology. *J. Bacteriol.* 188(5):1667–79.

CHAPTER 4: A COMPARITIVE TRANSMISSION ELECTRON MICROSCOPIC STUDY OF THYMINE-STARVED AND NALIDIXIC ACID-TREATED *E. COLI* CELLS

4.1 Introduction and Results

We observed cytoplasm irregularities in DAPI stained *thyA* mutant cells after 3 hours of T-starvation and widespread cytoplasmic problems after overnight starvation (Chapter 3, Fig. 3.8). To look at these irregularities more closely and to reveal (subtle yet critical) cytoplasm or envelope changes during T-starvation we decided to examine the T-starved *thyA* strain by transmission electron microscopy (TEM) (Fig. 4.1 - 4.6). As a general control for cytoplasm behavior during "genetic death", we used nalidixic acid-treated WT cultures (Fig. 4.7 – 4.12) (nalidixic acid inhibits DNA gyrase and therefore kills cells by targeting their chromosome), that died with kinetics similar to our TLD. A previous TEM study in the *Salmonella thyA* mutant after 4 hours of T-starvation showed local cytoplasm recession from the cell envelope, yet no cell envelope problems which seem to corroborate our images after DAPI staining (1).

TEM showed that the *thyA* mutant cells grown in the presence of dT have a regular shape and the WT dimensions of 2 μm x 1 μm, with nucleoids clearly visible as irregular lighter areas in the otherwise homogeneous cytoplasm (Fig. 4.1). One hour into T-starvation, the cells became elongated and thicker, with some cell poles appearing damaged, suggesting defective cell division (Fig. 4.2). In contrast to the bright and compact nucleoids in the DAPI-stained T-starved cells (Fig. 4.1), TEM barely discerned nucleoids in the center of the elongated T-starved cells (Fig. 4.2). Interestingly, by 3

hours into T-starvation, the nucleoid-free cytoplasm of the further elongated cells accumulated numerous small round clearings (Fig. 4.3). By 5 hours of T-starvation, some cells started losing their EPS-capsule (the outer-most layers of the cell envelope); in fact, we also observed accumulation of what looked like cell-separated EPS-capsule material (Fig. 4.4). Yet, in most cells the cytoplasm remains within the cell envelope, with only occasional segmental voids developing within the envelope (Fig. 4.4). In fact, the test for the periplasm stability using alkaline phosphatase showed no periplasm leaking in the T-starved *thyA* mutants; as a positive control, a massive release of the periplasmic material was evident in the T-starved *thyA rffH* mutant cells (Chapter 3, Fig. 3.3F).

After 20 hours of T-starvation, we saw ~10x elongated cells with a lighter and sometimes segmented cytoplasm and cell ghosts (Fig. 4.5), but even more dramatic cytoplasm irregularities, similar to those reported in *Salmonella* TLD TEM, were observed in the nalidixic acid-treated control (Fig. 4.11), so these likely reflect metabolism degradation in genetically-dead cells. One distinction we encounter between T-starved and nalidixic acid treated cells was the appearance of the small cytoplasmic clearings at 1 hour and 3-hour points during T-starvation. We conclude that, by the end of the exponential death phase, T-starved *thyA* mutant cells develop both cytoplasm and EPS-capsule irregularities, but this does not lead to cell lysis (or even periplasm leakage) and thus provides little insight into the lethality of TLD in *thyA* mutants.

4.2 Acknowledgements

We would like to thank Lou Ann Miller at the MRL facility UIUC, for preparation and imaging of the TEM samples.

4.3 Materials and Methods

4.3.1 TEM sample preparation

The strain KKW58 (*thyA*) was grown to early exponential phase in M9CAA with 10µg/ml thymidine at 37°C and then subjected to T-starvation in M9CAA medium. Strain AB1157 was grown to early exponential phase in LB and treated with 20 µg/ml nalidixic acid. At indicated times, 1 ml aliquots were taken and harvested, the pellet was then dispersed into 1ml of TEM-grade fixation buffer and stored at 4°C until all samples were collected. The samples were then submitted to the MRL facility at UIUC for further preparation and TEM imaging. The protocol used for TEM sample preparation can be found in Chapter 8 of (2).

4.4 Figures

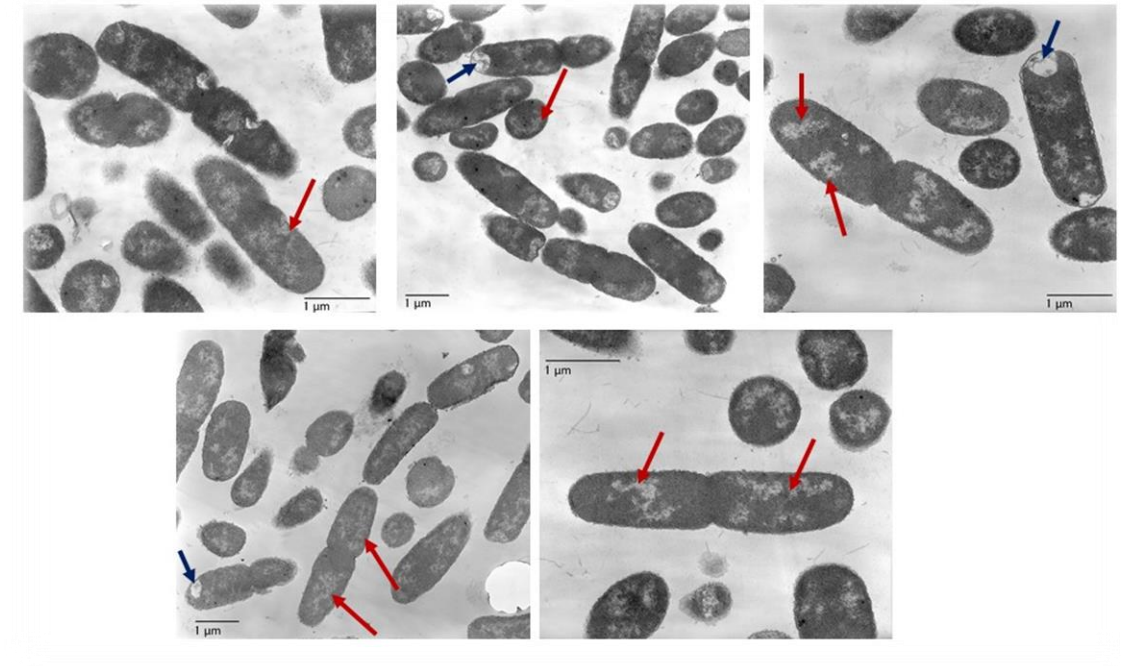

Figure 4.1. Representative images of exponentially growing cultures of *thyA* mutant in M9CAA + dT medium. The nucleoid (red arrows) is clearly visible in all cells. Occasionally we observe retraction of the cytoplasm (blue arrows). Cells that are in plane have an approximate length of 2 µm and a diameter of 1 µm. Several cells with their individual nucleoids in the process of division can be seen.

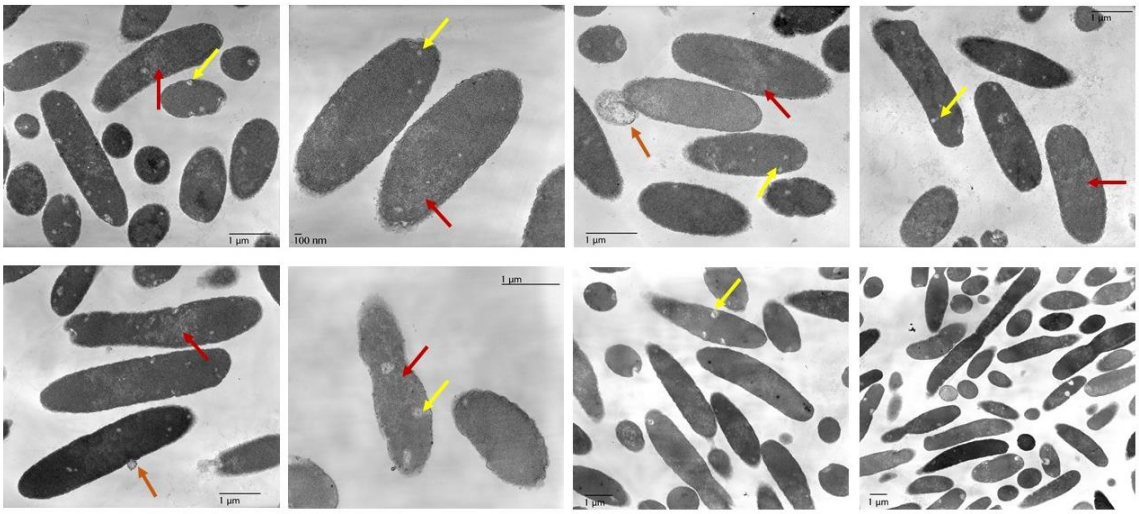

Figure 4.2. Representative images of *thyA* mutants 1 hour into thymine starvation in M9CAA medium. As expected, the cells are filamenting bad have variable lengths ranging from approximately 2µm to 4µm. The nucleoid (red arrows) are less clearly visible at this stage. We also see appearance of small cytoplasmic voids (yellow arrow) in the cells at this stage. A few protrusions which resemble vesicles (brown arrows) are also be seen Both the reduced visibility of nucleoid and appearance of small cytoplasmic voids in the cell are new phenotypes associated with TLD.

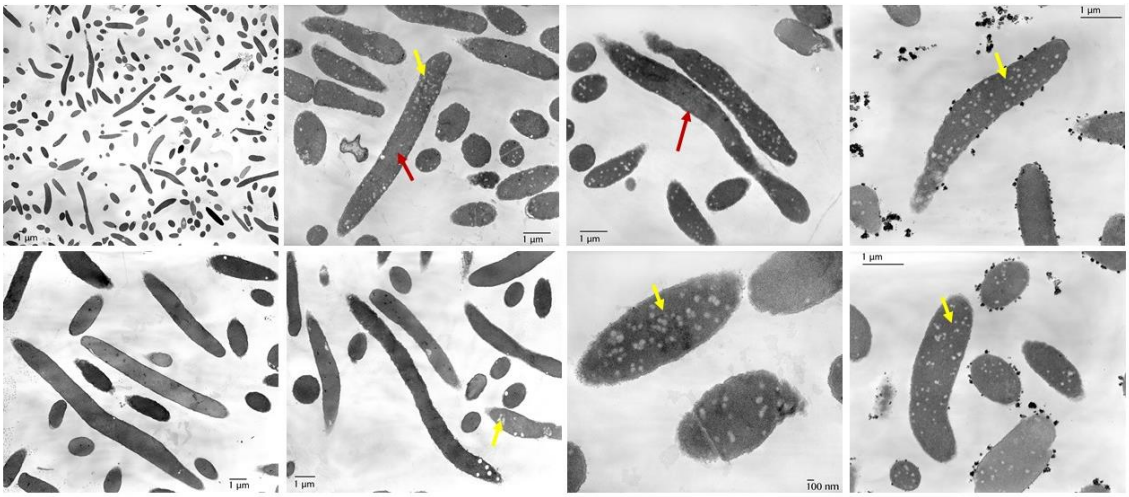

Figure 4.3. Representative images of *thyA* mutant thymine starved for 3 hours in M9CAA. The cells are visibly longer with some being as long as 10µm with the diameter still at 1µm. The position of nucleoid can be estimated in a few cells (red arrows), but not in other cells. The cytoplasmic voids (yellow arrow) are numerous and clearly visible. Their biological significance is currently unknown.

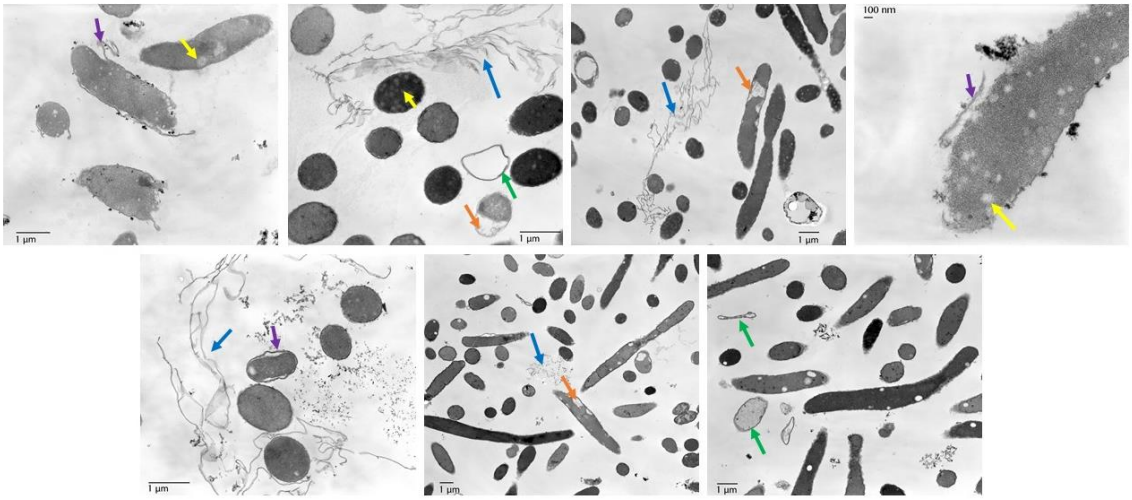

Figure 4.4. Representative images of *thyA* mutant thymine starved for 5 hours in M9CAA. The nucleoid isn't visible- suggesting that the nucleoid isn't compact anymore. Numerous cell shape defects are apparent. A layer of cell envelope can be seen separating from the cell (purple arrows). Since the cell shape is intact, this may be the antigen layer peeling away. We see accumulation of thread like structures (blue arrows) – possible derivates of the separated antigen layer. The small cytoplasmic voids (yellow arrows) are still visible in some cells. Cells completely devoid of cytoplasmic content (green arrows) and with larger clearings in the cytoplasm (orange arrows) are also visible. The frequency of these events have not been quantified but they seem widespread.

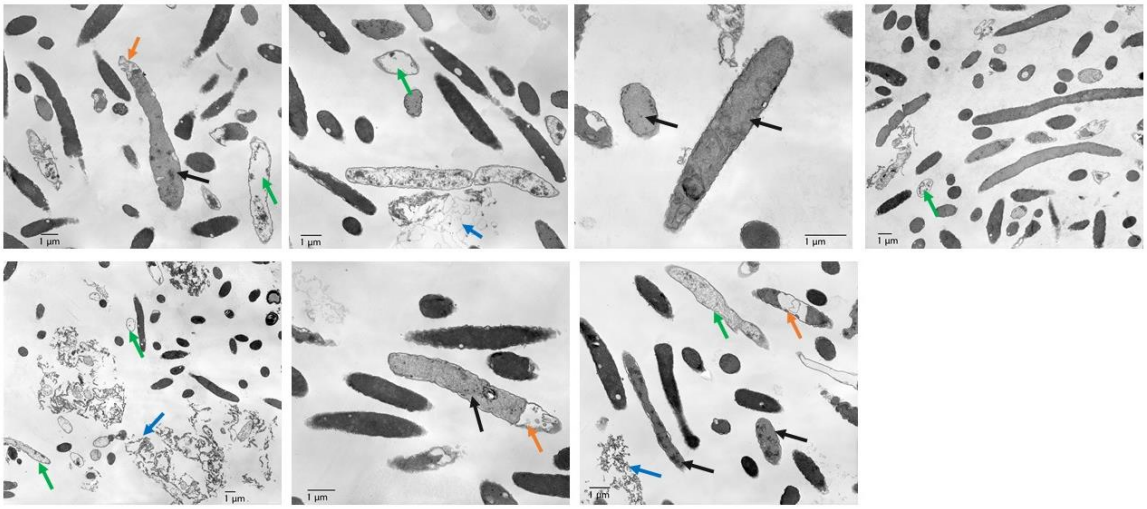

Figure 4.5. *thyA* mutant after overnight (16-20 hours) starvation for thymine in M9CAA. Several empty cell bodies (green arrows) and lighter or less dense cells (black arrows) are visible. Bigger regions of cytoplasmic retraction (orange arrows) can be seen.

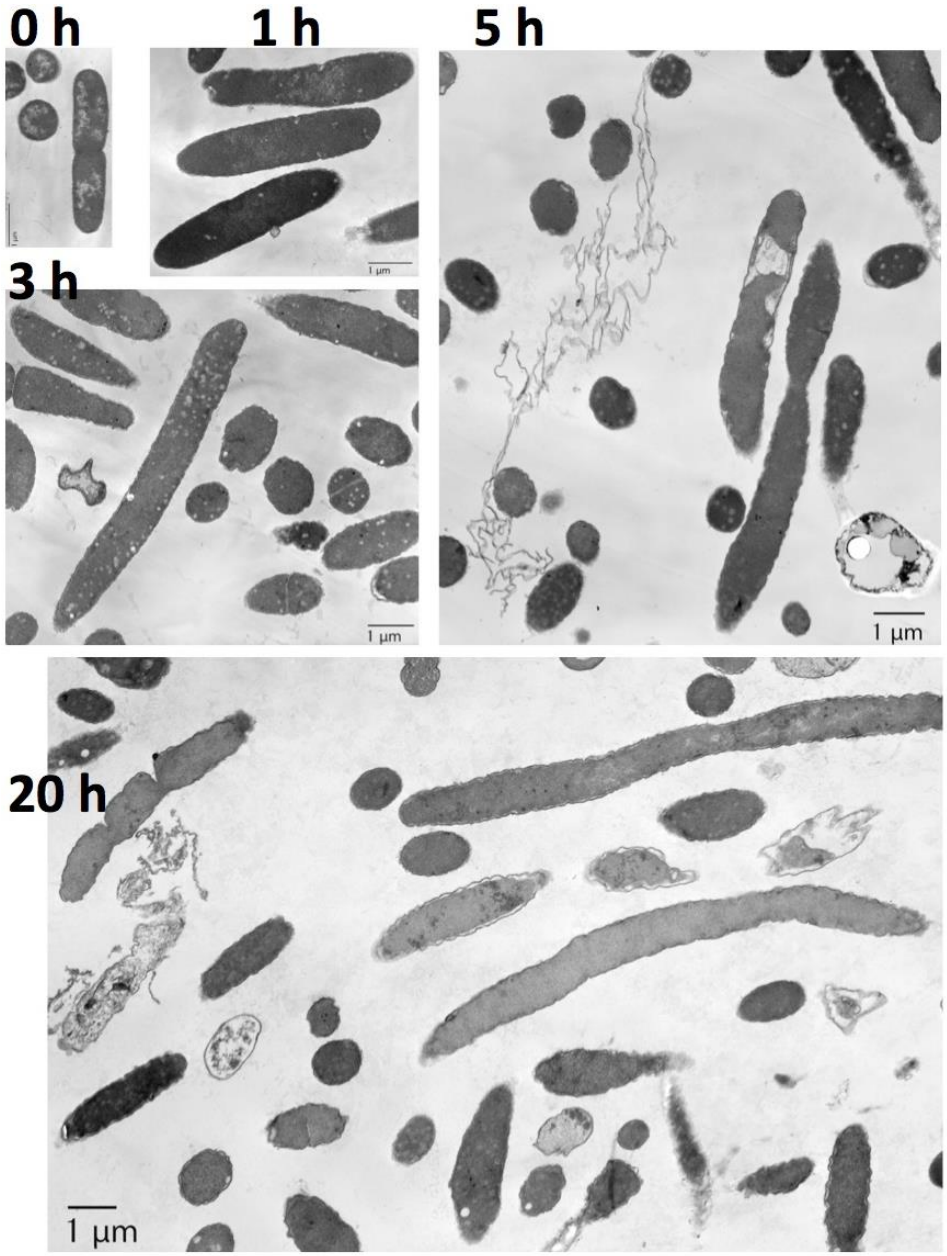

Figure 4.6. Progression of *thyA* mutants through T-starvation. The hours into T-starvation are indicated on the left of each image. The scale bars have the same dimension in all panels to compare difference in size.

Figure 4.7. Representative images of exponentially growing AB1157 WT *E. coli*) in LB. The nucleoid cloud (red arrow) is visible with each cell. The cells have an average size of 2 - 3 µm in length and ~ 0.7 µm in diameter.

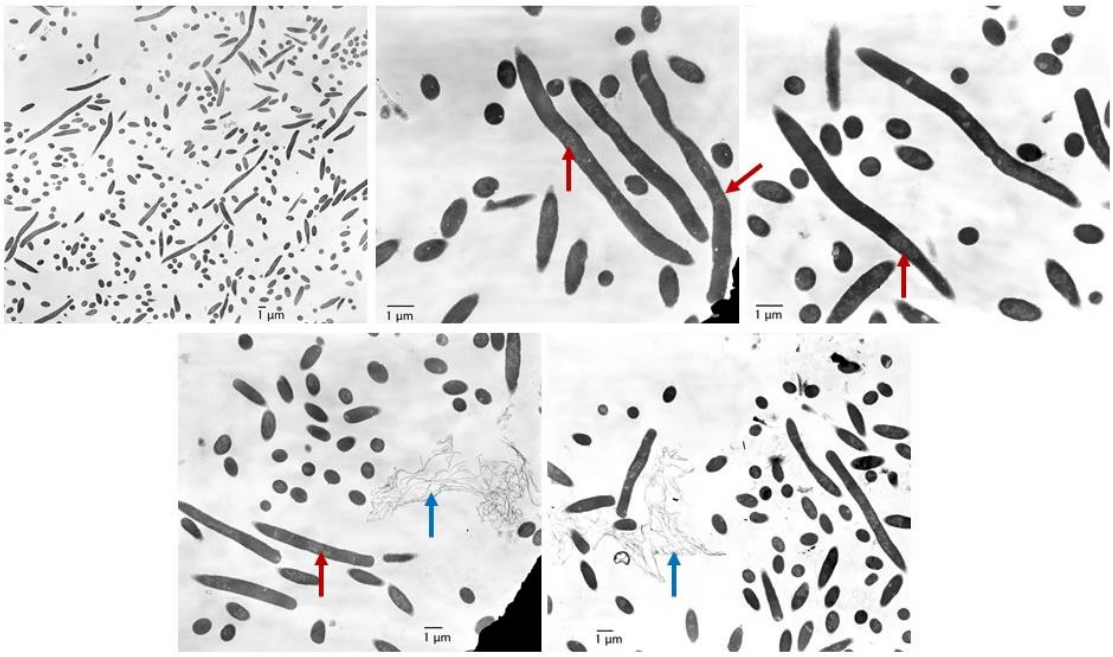

Figure 4.8. Representative images of AB1157 (WT *E. coli*) treated with 20 µg/ml nalidixic acid – a DNA damaging agent in LB for 1 hour. Cells have filamented to variable lengths ranging from ~2 – 10 µm. Nucleoid mass (red arrow) can be made out some filamenting cells but is less distinct than in untreated cultures. Like thymine starved strains we see accumulation of thread like structures (blue arrows) that might indicate the loss of antigen layer since the cell shapes are maintained.

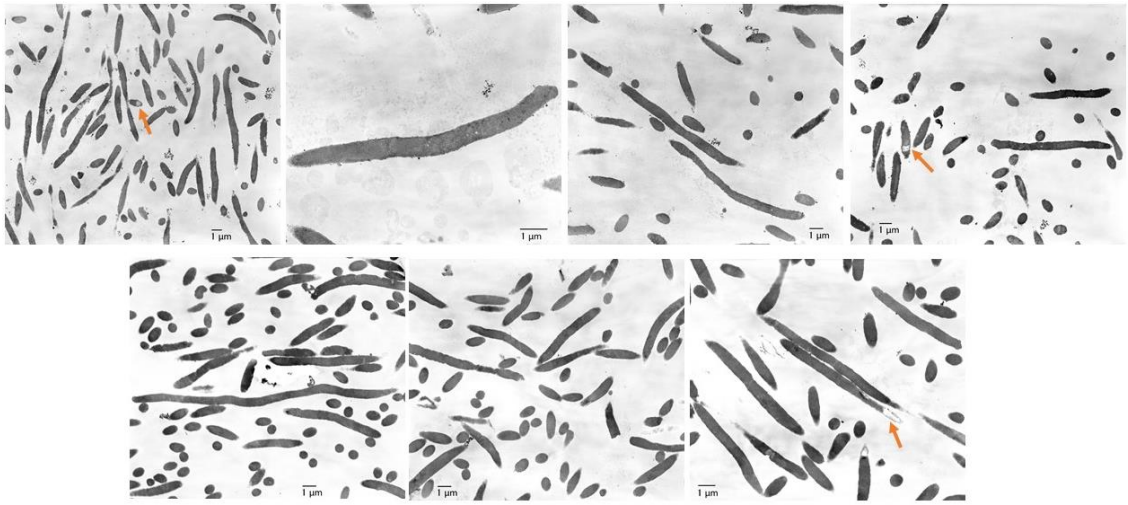

Figure 4.9. Representative images of AB1157 treated with 20 µg/ml nalidixic acid for 3 hours. Cell length ranges from 5 - 20 µm. Occasionally cells with retracted cytoplasm (orange arrows) are visible.

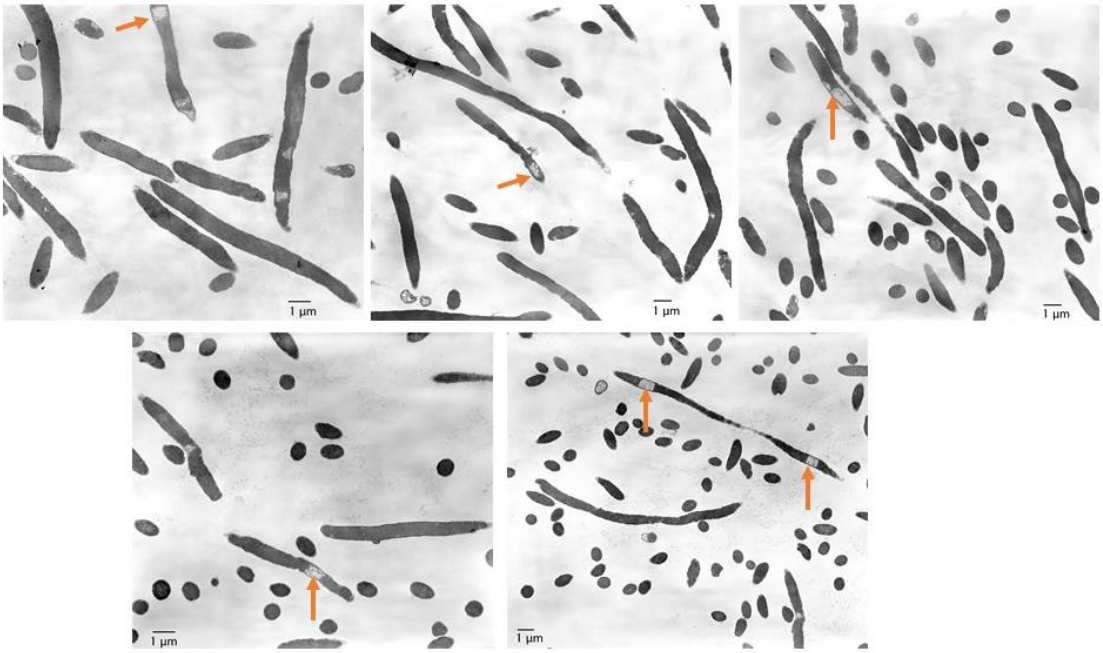

Figure 4.10. Representative images of AB1157 treated with 20 µg/ml nalidixic acid for 5 hours. Cell length ranges from 5 - 20 µm. Occasionally cells with retracted cytoplasm (orange arrows) are visible.

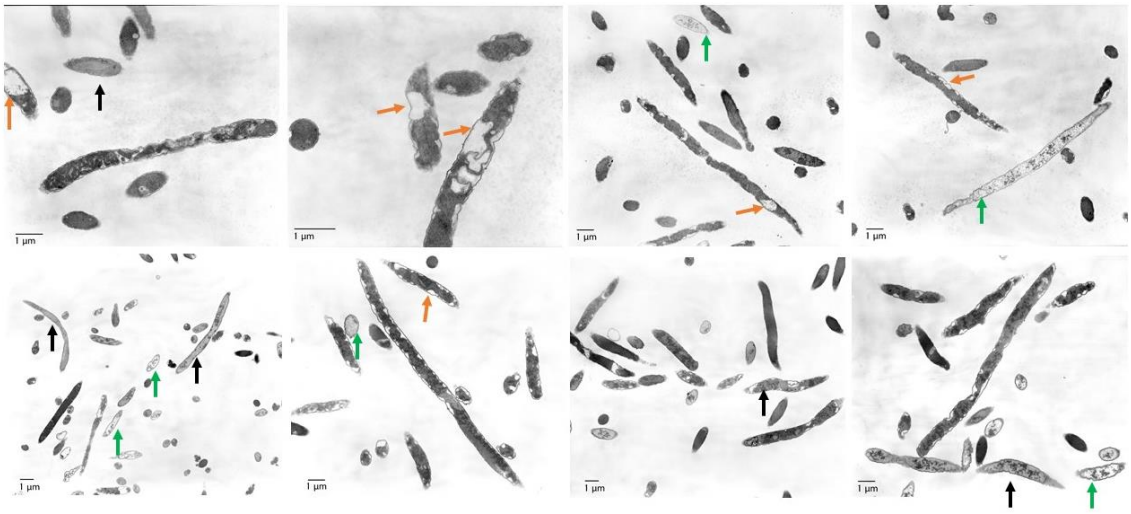

Figure 4.11. Representative images of AB1157 treated with 20 µg/ml nalidixic acid for 20 hours. Cell length ranges from 5 - 20 µm. Cytoplasm retraction (orange arrows) is more widespread and several cells appear lighter/less dense (black arrows) or empty (green arrows) in the sample.

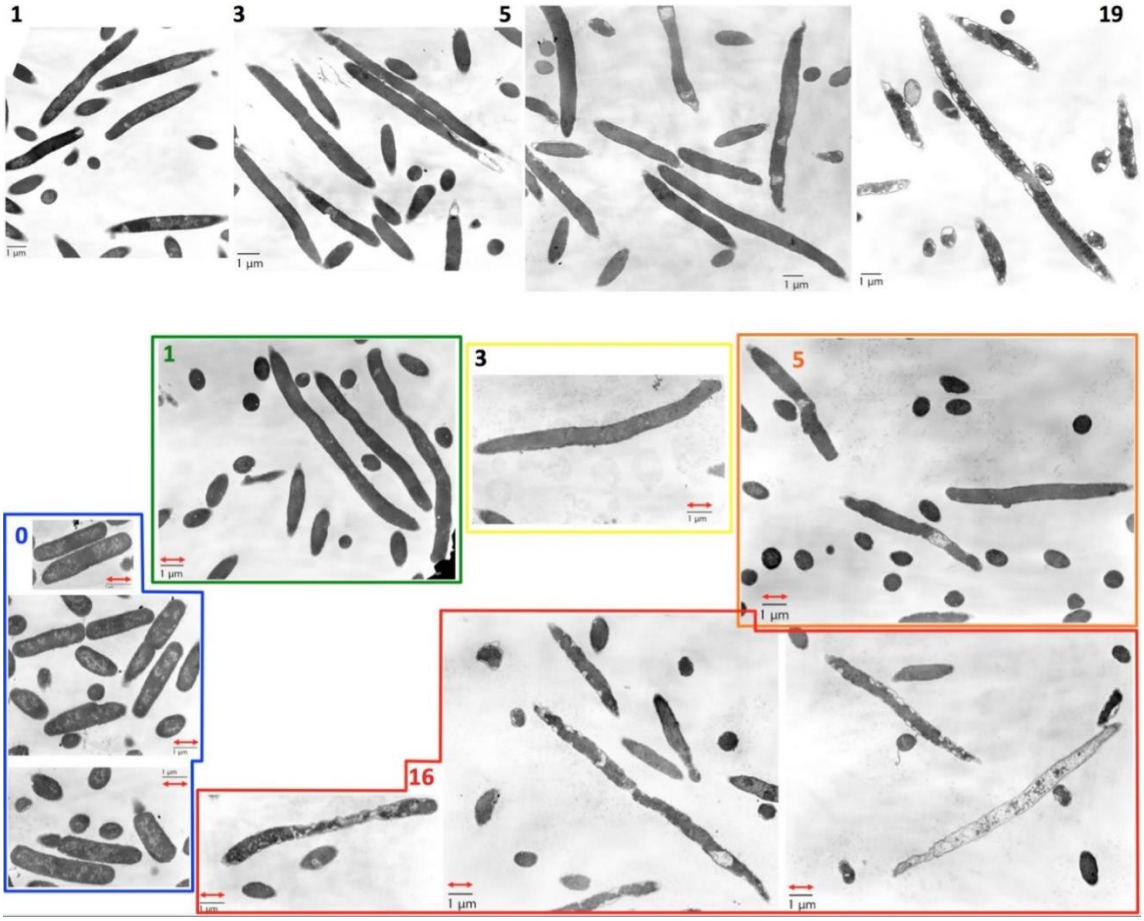

Figure. 4.12. Compilation of TEM images of AB1157 treated with 20 µg/ml nalidixic acid. The two panels are images derived from biological replicates. The number on the corners of the images refers to the length of the treatment with the DNA damaging drug. The scale bars have the same dimension in all the images to compare the lengths of the cell.

4.5 References

1. Loessner H, Endmann A, Rohde M, Curtiss R, Weiss S. 2006. Differential effect of auxotrophies on the release of macromolecules by *Salmonella enterica* vaccine strains. *FEMS Microbiol. Lett.* 265(1):81–88.

2. Miller LA. 2001. *Microwave Techniques and Protocols*. Humana Press. 89–100 pp.

CHAPTER 5: *ESCHERICHIA COLI* MUTANTS DEFECTIVE IN REPLICATION INITIATION DEPEND ON RECBCD-PROMOTED LINEAR DNA DEGRADATION

5.1 Introduction

Replication in *E. coli* begins at *oriC* and proceeds bidirectionally around the circular chromosome until the replication forks meet at the terminus. The DnaA protein in the ATP bound form binds to specific short sequences in the origin DNA called DnaA boxes to initiate replication (23, 24, 82). *oriC* has several high and low affinity DnaA boxes where DnaA-ATP binds (23, 53, 59, 96). At the time of initiation the DnaA-ATP complex bound at the high affinity sites (13, 79) promotes subsequent DnaA-ATP binding to neighboring low affinity sites by cooperative interaction (44, 64), leading to formation of the DnaA-ATP spiral multisubunit filament (12, 83). This allows localized unwinding of the AT rich DNA unwinding element (DUE) in the *oriC* forming a single-strand bubble (Fig. 5.1A)(82). In the next step, two DnaB helicase hexamers are loaded at the opposite corners of the single-strand bubble (12, 60), followed by primase (57) and, eventually, the replicative polymerase itself, that begins DNA synthesis (100) (Fig. 5.1A). Apart from *oriC*, high affinity DnaA boxes are also found at the *datA* locus that titrates the bulk of DnaA-ATP and regulates initiation by controlling the levels of unbound DnaA-ATP (41, 42). DnaA is also known to regulate transcription of several genes, including itself (3, 7).

The process of replication is extremely fast and accurate, but since only two replication forks traverse the entire chromosome per cell cycle, it takes *E. coli* a

minimum of 40 minutes to finish its replication (29, 30). For an efficient and rapid replication, the template must be free of lesions and impediments. But often the template could have modified bases incorporated or proteins bound ahead of the fork, which can cause replication fork stalling and if left unrepaired may lead to fork disintegration causing double strand DNA breaks (40, 61, 75). The disintegrated fork is reassembled by recombinational repair proteins RecA and RecBCD, and the replication is resumed after replisome reloading (4, 63, 89). The RecBCD enzyme is a helicase-nuclease that targets double strand DNA ends for degradation and recombinational repair (17, 35, 94, 99). The complex generates a DNA substrate with a 3' overhang, which is used by RecA for homology-guided strand invasion into an intact duplex DNA (2, 20, 52, 87). This invasion creates a Holliday junction intermediate, which is removed by either the RuvABC resolvasome or the RecG helicase (34, 97).

recBCD mutants of *E. coli* have ~30% viability suggesting an active role of RecBCD in repairing the endogenous DNA damage (10). In addition to its role in presenting 3' SS DNA to RecA for strand invasion during homologous recombination repair, the DNA degradation function of RecBCD can act independently of RecA to degrade the broken arm in a sigma replicating chromosome instead of restoring fork structure (66). Recent whole genome sequencing studies in *E. coli recBCD* mutants also show that their terminus is under-represented (49, 77, 84), suggesting a critical role for RecBCD in preserving the terminus region.

The function of RecBCD as a recombinase or DNA degradation enzyme during replication has been studied extensively in the *E. coli* mutants defective in their ongoing replication process. For example it has been found that the slow moving replication forks

in *rep* mutants in *E. coli* (19) are susceptible to stalling and disintegration, so the *rep* mutants require the RecBCD complex for survival (89). It has been proposed that in the absence of RecBCD the stalled forks in *rep* mutants undergo RuvAB-dependent replication fork reversal forming a Holliday Junction (HJ), which is cleaved by RuvC. A similar stalling, reversal and cleavage of the fork in the other replichore causes release of linear DNA and lethality in the *rep recBC* mutant (89). In a *rep* mutant RecBCD function either restores the disintegrated replication fork structure via homologous recombination or degrades the linear DNA (4).

Apart from *rep*, *E. coli* mutants with defects either in the replicative helicase DnaB or subunits of the replicative polymerase (β-clamp, ψ and ϵ subunits) show defect in the replication elongation stage (62). These mutants also experience RuvABC-dependent double strand breaks from reversed forks and require RecBCD activity for viability (22, 25). At the same time, mutants in the replication initiation functions were assumed to not require recombinational repair, because the complete elimination of replication forks should eliminate the need in their repair.

Remarkably, we have found that a combination of defects in the DnaA and RecBCD proteins is also co-lethal in *E. coli*. We have investigated this *dnaA recBC* synthetic lethality with genetic and physical approaches. Our conclusion is that, since the DnaA protein binds to various locations on the chromosome, a mutant DnaA protein that binds tighter, blocks the replication fork progress. The linear DNA degradation by RecBCD removes this block, dissociating the mutant DnaA from the chromosome and making it available for initiation at the origin.

5.2 Results

5.2.1 Synthetic lethality of *dnaA recBC*

Many instances of co-lethality due to combinations of defects in recombinational repair and replication elongation functions have been reported previously (62, 63, 75). Unexpectedly, we stumbled upon a co-lethality between defects in replication initiation and recombinational repair. The *dnaA46*(Ts) allele is progressively defective in binding ATP at higher temperatures, so it no longer supports cell growth at 42°C due to a block in replication initiation (11, 32). The *recBC*(Ts) allele we used, is disabled for both DNA degradation and repair at 37°C and above. The colethality between the *dnaA46* and *recBC*(Ts) mutations was demonstrated by growing the strains AB1157, *recBC*(Ts), *dnaA46*(Ts) and *recBC dnaA46* at 28°C till OD= 0.1, making dilutions at this time, spotting them on LB plates and incubating one plate at 28°C, while the other at 39°C. At the lower temperature all strains grow equally well, but at the higher temperature the double mutant shows no growth, while the single mutants grow as well as the WT (Fig. 5.1B). Another allele, *dnaA601*, which is defective in its ATP binding site (28), also shows co-lethality with *recBC*(Ts). We have used the *dnaA46* allele for the rest of our study, unless otherwise mentioned; henceforth, we will refer to our temperature sensitive alleles simply as *dnaA* or *recBC*.

We next tried to replicate the lethality in liquid cultures, as the subsequent tests to determine the nature of defect at higher temperature would all be done in liquid cultures. The lethality in liquid cultures of the exponentially growing *recBC dnaA* (OD = 0.1 at the start of assay) at 39°C was only 10-fold (Fig. 5.2A), in contrast to the 10,000-fold loss of titer seen on plates. However, we found that diluting the culture 30 times or deeper before

shifting them to 39°C approximates death on plates (Fig. 5.2B). Interestingly, these conditions also severely inhibit growth of the single *dnaA* mutant. The low-cell-density-dependent lethality of the *dnaA recBC* double mutant in liquid cultures explains why we always observed residual growth in the highest density spot of the strain (Fig. 5.1B). The density-dependent survival of the double mutant may be related to various systems of quorum sensing in *E. coli* (1).

Traditionally genes that show synthetic lethal relationship are thought to encode proteins that perform essential redundant function. For example *degP surA* double mutant of *E. coli* is inviable, and the lethality of the double mutant is explained by loss of an essential periplasmic protein chaperone activity that can be performed by redundant DegP or SurA chaperones (74). The *dnaA recBC* colethality does not fit the loss of an essential redundant function paradigm, though, as the *dnaA* and *recBCD* gene products have very different functions and cannot be redundant. DnaA is responsible for initiation of chromosomal replication from *oriC* in *E. coli*, while RecBCD complex degrades linear DNA and initiates recombinational repair of double strand breaks. Therefore, either the *dnaA*(Ts) mutant suffers from double strand breaks, which require the activity of RecBCD protein for survival, or the *recBC*(Ts) mutant is compromised for initiation, and this is further exacerbated by the *dnaA46*(Ts) defect. Our genetic and physical assays were designed to distinguish between the two scenarios.

5.2.2 Other synthetic lethal combinations

The *dnaN* defect in combination with the *recBCD* defect is also synthetic lethal (Fig. 5.3A), as first described by Michel and colleagues (25). The *dnaN* gene, which

encodes the DNA clamp that makes the DNA Pol III processive (39), is positioned immediately downstream of *dnaA* in the same operon (71). Since DnaA autoregulates itself transcriptionally by binding to the DnaA box at the *dnaA* promoter (3, 7), the *dnaA recBCD* colethality could have been due to problems with the *dnaN* expression instead. We tested this possibility by introducing plasmids that carried wild type *dnaA* or *dnaN* genes into the *dnaA recBCD* strain (Fig. 5.3 C, D). We found that, while *dnaA*-only expressing plasmid could rescue *dnaA recBCD* lethality, the *dnaN*-only expressing plasmid failed to do so (Fig. 5.3C). At the same time, the *dnaN recBC* lethality was due to the defect in the *dnaN* gene, as it was complemented by the *dnaN*-expressing plasmid, but not by the *dnaA*-expressing plasmid (Fig. 5.3D). Thus, the *dnaA recBCD* colethality is due to the *dnaA* defect, rather than a cryptic *dnaN* defect.

Besides its main DNA clamp function, DnaN also plays a role in initiation, by helping Hda protein to stimulate DnaA-ATP disassembly from the origin via ATP hydrolysis (36, 38). Thus, potentially, it could have been the initiation defect that made *recBC*(Ts) *dnaN* strain colethal. DnaC is the DnaB inhibitor and the second *E. coli* function specific for replication initiation (92, 98). To test against the possibility that inactivation of any initiation function makes *recBCD* mutants inviable, we tested the viability of the *dnaC recBC* mutant. Unexpectedly, we found that the *dnaC*(Ts) defect is also synthetic lethal with the *recBC*(Ts) defect at the semipermissive temperatures (Fig. 5.3B), suggesting that general problems with initiation lead to RecBCD-dependence.

5.2.3 Suppressor analysis

To understand the mechanism of co-lethality in the *dnaA recBC, dnaN recBC* and *dnaC recBC* double mutants, we isolated suppressors for each of these combinations by transposon mutagenesis (Fig. 4.4, 4.5, 4.6) using the plasmid pRL27 (54). If the three co-lethalities had a common nature, they would have been suppressed by the same or similar sets of mutations.

The *dnaA recBC* colethality was suppressed by insertions at only two loci. We found 18 different insertions in the *hslUV* operon (Fig. 5.4A, B) encoding one of the five major ATP-dependent proteases of *E. coli* involved in protein quality control. HslUV protease is likely involved in the degradation of misfolded DnaA46 protein at higher temperatures (37). An *hslUV* over-expressing plasmid exaggerates lethality in the *dnaA recBC* strain (Fig. 5.4C), confirming suppression by *hslUV* inactivation. To prevent isolation of more inserts into *hslUV*, in future we will isolate suppressors in the *dnaA recBC* harboring a multicopy plasmid with the *hslUV*+ operon.

We also isolated four insertions in and upstream of *seqA* gene as suppressors of the *dnaA recBC* colethality (Fig. 5.4A, B). SeqA is a negative regulator of the replication initiation (56, 68) (as well as the proposed organizer of the sister-chromatid cohesion zone behind the replication fork (93)) and likely inhibits initiation by the partially inactivated DnaA46 protein at higher temperatures .We are also inactivating the Hda protein, another negative regulator of initiation (38) to see if over-initiation generally suppresses the *dnaA recBC* colethality. We have also found that both the *hslUV* and *seqA* inactivation suppress the synthetic lethal combination of *recBC* with *dnaA601*, which is another DnaA allele defective in binding to ATP (Fig. 5.4D).

Since the insertion in the *dnaK* gene was upstream of the promoter, we have tried both overexpression of DnaK and DnaJ proteins, as well as deletion of *dnaK* gene, to reveal the nature of a possible *dnaK* suppression (Fig. 5.4E, F). The *dnaK dnaA recBC* suppressor we isolated was very weak and our subsequent efforts of overexpression of the DnaK, or both DnaK and DnaJ, from the plasmids pNRK416 and pMob-*dnaKJ* provided by Benedicte Michel, did not rescue the *dnaA recBC* strain at 39°C, while being inhibitory for the single *dnaA* mutant at 39°C (Fig. 5.4E) (8). We have not been able to create a Δ*dnaK recBC dnaA* as the *dnaA recBC* strain could not be transduced with the Δ*dnaK* (Fig. 5.4F). In the light of these observations we haven't pursued the *dnaK* suppressor in our future physical analysis. Overall, we confirmed that *dnaA recBC* lethality was suppressed *seqA* and *hslUV* inactivation while *dnaK* inactivation couldn't be tested nor its over-expression restore its viability (Fig. 5.4B).

The *dnaN recBC* colethality was suppressed by seven independent insertions in the *iscRSUA* operon (Fig. 5.5A, B). The *iscRSUA* operon and the *hscBA* operon downstream are responsible for synthesis and repair of iron-sulfur clusters that are used by key enzymes of the central metabolism (90). We have also obtained insertions in the *hscA* gene, which is a chaperone interacting with the IscU protein, as well as in *pta*, *icd* and *ubiC* genes (Fig. 5.5A). All the insertions mentioned above are in genes related to the central metabolism.

We have also isolated 4 insertions in the *lon* gene, which codes for another ATP-dependent protease degrading misfolded proteins, and 2 insertions in the *diaA* gene (Fig. 5.5A, C) which assists DnaA in forming a filament at *oriC* for replication initiation (33, 81). We have confirmed that a Δ*diaA* allele indeed rescues the *dnaN recBC* double

mutant (Fig. 5.5C), strongly suggesting that the *dnaN recBC* co-lethality is due to over-initiation. Michel and colleagues have shown that the *dnaN recBC* double mutant undergoes RuvABC-dependent chromosome fragmentation (25), proposing this as an explanation for its colethality.. We inactivated the *ruvA* gene to test if blocking chromosome fragmentation suppresses the lethality. The strain *ruvA dnaN recBC* is still lethal (Fig. 5.5D), demonstrating that prevention of RuvABC-dependent double strand breaks in the DNA does not rescue the strain.

The *dnaC recBC* co-lethality was suppressed by three inserts into and upstream of *diaA* (Fig. 5.6A). We have confirmed that Δ*diaA* rescues the *dnaC recBC* co-lethality (Fig. 5.6B, C). Thus, the *diaA* inactivation, that reduces the DnaA polymerization potential, suppresses both the *dnaC recBC* and *dnaN recBC* co-lethalities (Fig. 5.5C, 5.6C), suggesting that chromosome problems in both cases stems from too much DnaA binding to (*oriC*) DNA.

We also found that insertions in both *recR* and *recA* genes suppress the *dnaC recBC* co-lethality (Fig. 5.6A, B). We are testing inactivation of the *recF* gene as a probable suppressor for *dnaC recBC*, as the RecR and RecF proteins work together in a RecA-mediated pathway to repair blocked single strand gaps in the DNA (51). The isolation of *recA* and *recR* inactivation as suppressors for *dnaC recBC*, suggests formation of blocked single strand gaps with subsequent recombinational repair as poisonous when DnaC malfunctions.

Insertions inactivating the *bssS* gene and between the *yjjP* and *yjjQ* genes also suppressed the *dnaC recBC* co-lethality (Fig. 5.6A, B). The *diaA* and *recR* suppressors of the *dnaC recBC* colethality failed to suppress the *dnaA recBC* colethality (Fig. 5.6D), and

we are currently testing whether the suppressors of the *dnaA recBC* co-lethality suppress the *dnaC recBC* double mutant. However, our analysis so far suggests that though both DnaA and DnaC are initiation functions *dnaA recBC* and *dnaC recBC* are lethal due to independent mechanisms.

5.2.4 Recombinational repair is not required in the *dnaA* mutant

As mentioned in the introduction, the RecBCD enzyme has two important roles in the cell: linear DNA degradation and preparing the substrate for recombinational repair via RecA polymerization (51). To test the role of recombinational repair in the *dnaA* mutant we combined it with the *recA938* defect. We observed that the *recA* defect shows only a weak interaction with the *dnaA*(Ts) defect, further inhibiting, but not blocking, the growth of the double mutant (Fig. 5.7A). Likewise, introducing the *recA938* defect in the *recBC dnaA* strain does not further exacerbate the synthetic lethality of the *dnaA recBC* double mutant (Fig. 5.7A). Altogether, this demonstrates that the recombinational repair function of RecBCD is not essential for the *dnaA* strain. We have tested this further by introducing the plasmid pKD46 (18) – which restores the recombinational repair of double-strand breaks without restoring the capacity for linear DNA degradation, into the Δ*recBCD dnaA* strain (Fig. 5.7B, C) (18). We found that, though the strain *recBCD dnaA* pKD46 is recombinational repair-proficient (judging by its enhanced UV survival (Fig. 5.7B)), it still cannot grow at 39°C (Fig. 5.7C).

5.2.5 DNA degradation activity is essential for *dnaA* mutant

In order to determine which of the two general functions of RecBCD is essential for survival of the *dnaA* mutants at the semi-permissive temperature, we introduced plasmids which would restore either of the two functions of the RecBCD complex – recombination repair or DNA degradation, in the *dnaA recBC* background (Fig. 5.8A). Since the chromosomally-expressed RecBC(Ts) proteins may interfere with the the RecBCD proteins produced from the plasmids, we did our complementation in the Δ*recBCD dnaA* background (Fig. 5.8A). The low copy number plasmid introduced ~6 times more RecBCD protein than in the WT cells. With such a mild overexpression, introduction of either recombination function plus partial DNA degradation, or full DNA degradation capacity without recombination, was sufficient to restore the viability in the Δ*recBCD dnaA* strain (Fig. 5.8A). At the same time, synthetic lethality of the *dnaA recD1011* double mutant (the *recD1011* mutant is defective in the linear DNA degradation activity, but is fully recombination-proficient and has a normal copy number) (Fig. 5.8B) shows that linear DNA degradation is more important for the *dnaA* mutant than recombinational repair (73). Interestingly, inactivation of *ruvA* in the *dnaA recBC*(Ts) strain did not rescue the strain, while at the same time the *ruv* defect showed synthetic inhibition in combination with the *dnaA* defect (Fig. 5.9A). The latter result indicates chromosomal problems in the *dnaA* mutant that require resolution of Holliday junctions. Remarkably, *recG* defect suppresses this synthetic inhibition of the *dnaA ruv* mutants (Fig. 5.9B), suggesting that the Holliday Junctions accumulating in the *dnaA* mutant are improperly processed by RecG in the absence of the RuvABC resolvasome. At the same time, comparable viability of *dnaA recBC ruvA* and *dnaA recBC* shows that

chromosomal problems in the *dnaA recBC* double mutant are not the result of Holliday junction resolution by RuvABC resolvasome.

5.2.6 Possible role of RecBCD in DnaA(Ts) mutants

In order to explain the importance of DNA degradation in a *dnaA* mutant we have proposed a model (Fig. 5.10). The DnaA protein binds to sequences called DnaA boxes that are present in many locations around the chromosome. When a replication fork approaches a tightly-bound DnaA46 protein and the replicative helicase DnaB cannot disperse DnaA46 filament from DNA, the fork stalls and regresses, but the replisome still controls the regressed fork (explaining the lack of effect of *ruvA* inactivation). RecBCD then degrades the open dsDNA end, restoring the replication fork framework and resetting the replisome. After resetting the replication fork structure, an auxiliary helicase Rep is recruited at the restarted fork and helps DnaB to remove the Dna46 protein block. In the absence of RecBCD the expelled DNA duplex is not degraded, but since the replisome still protects the regressed fork, this leads to a permanently blocked replication fork. This model generates several testable predictions:

— Chromosomal fragmentation should be minimal in the *dnaA recBC* mutant;

— the *dnaA46* allele should be dominant over the WT *dnaA* allele.

— The auxiliary helicase Rep involved in removal of DNA-bound proteins ahead of the replication fork should be required for survival in the *dnaA* mutants.

5.2.7 The *dnaA* defect does not lead to chromosome fragmentation

A co-lethality of a particular mutation with the *recBC* defect usually indicates formation of double-strand breaks as a result of this mutation (45, 52, 63). The two major reasons for such endogenous double-strand breaks are (i) DNA damage and intermediates of excision repair; (ii) malfunctioning of the replication enzymes. The second reason could potentially result in chromosomal fragmentation in the *dnaA* mutants. A useful characteristic of the *recBC* mutants is quantitative "preservation" of their levels of chromosomal fragmentation, because these mutants can neither repair double-strand breaks, nor degrade linear DNA. We compared the three synthetic lethal strains: *recBC*(Ts) *dnaA, recBC*(Ts) *dnaN* and *recBC*(Ts) *dnaC* for their levels of chromosomal fragmentation (Fig. 5.11). We found that *recBC dnaN* strain shows 15% chromosomal fragmentation above the background at 37°C (Fig. 5.11A), but little fragmentation at 39°C (Fig. 5.11B). In contrast, the *recBC dnaC* strain shows a mild ~5% chromosome fragmentation over the background, but independently of the temperature (Fig. 5.11A, B). At the same time, we could not detect any statistically-significant fragmentation in the *dnaA recBC* strain, indicating that the *dnaA*(Ts) defect does not result in double-strand DNA breaks. This lack of double strand breaks is a deviation from the typical behavior of RecBCD-dependent mutants observed so far (4, 22, 25). The absence of chromosomal fragmentation in the *dnaA recBC* mutants does not mean the absence of DNA damage, — only that the damage is such that linear chromosomal pieces are not produced or released. The linear DNA could still be trapped in conformations like a σ-replicating structure, that is not conducive for growth and survival, but would not yield linear chromosomal pieces in pulse-field gels (43).

5.2.8 Dominance of DnaA46 allele

Our model predicts that the DnaA46 protein will be dominant over the DnaA protein. In order to test this prediction, we cloned the WT *dnaA* and *dnaA46* genes in the pMTL20 vector and introduced these constructs in AB1157, *recBC*, *dnaA46* and *dnaA46 recBC* strains (Fig.5.12A, B). We observed that overexpressing the DnaA46 protein is toxic for all strains at lower temperatures, while overexpressing WT DnaA is not (Fig. 5.12A, B). The toxicity upon overexpression of DnaA46 at lower temperatures in WT strain was shown once before, while in the same study there was no effect of DnaA46 overexpression in the *dnaA46* mutant strain at lower temperatures (28). This DnaA46 overexpression toxicity is also relieved at higher temperatures as shown before (28). The DnaA46, like WT DnaA protein, is able to rescue the *dnaA46 recBC* strain at 39°C and *dnaA46* strain at 42°C (Fig. 5.12A, B), which demonstrates that increasing the concentration of defective DnaA46 can compensate for the defect in its function and is consistent with our isolation of HslUV protease-deficient suppressors of the *dnaA recBC* colethality. It is possible that the DnaA46 protein at lower temperatures may bind the chromosome tighter, compared to the WT DnaA protein. At higher temperatures due to mis-folding of DnaA46 it likely interacts with the chromosome less, which allows for some relief of inhibition in AB1157, *dnaA* and *recBC* strains, and for increased survival in the *dnaA recBC* double mutant.

5.2.9 Rep helicase is required at low temperatures in *dnaA recBC* strain

It has been shown *in vitro* that the Rep helicase removes obstacles ahead of the fork (26). Consequently, the *rep* mutants have slow moving forks due to frequent pauses

(19, 26). If the DnaA46 protein is indeed a hindrance for replication forks, the activity of the Rep helicase should be essential in the *dnaA recBC* mutant at lower temperatures. We have found that at lower temperatures, the *rep recBC dnaA* triple mutant is severely inhibited compared to the *rep dnaA* or *rep recBC* double mutants, suggesting increased impediments ahead of the fork (Fig. 5.13B). The *rep recBC* double mutant is a known synthetic lethal at non-permissive temperatures (89) and we find that it is inhibited for growth even at lower temperatures (Fig. 5.13B), verifying that incomplete activity of RecBCD compromises the survival of the *rep* mutant. This is also substantiated by the observation that *rep* mutant is more inhibited by the overexpression of DnaA46, compared to WT DnaA at lower temperature (Fig. 5.13A). The DnaA46 overexpressing plasmid is tolerated better by this strain at higher temperatures reflecting the inability of DnaA46 protein to bind at higher temperatures.

5.2.10 Exploring the role of *datA* sites in *dnaA recBC* lethality

Since our evidence so far suggested that DnaA46 presents an obstacle to the replication fork, we tested whether DnaA46 bound at the *datA* site on the chromosome is the obstacle. The *datA* site which is ~ 1kbp in length has 6 DnaA boxes and is known to titrate excess DnaA so that pre-mature replication initiation is avoided, consequently in Δ*datA* mutants, replication initiation is asynchronous (42). The affinity of DnaA for the *datA* site is 8-fold higher than that for *oriC* and it is thought that about 60% of the cellular DnaA protein is bound at the data site (41). We deleted the *datA* locus from the *recBC dnaA* strain and find that the strain still dies at 39°C (Fig. 5.15A). Introducing extra copies of *datA* on a medium copy number plasmid pACYC177 is lethal for *E.coli* (69),

and we observed the same in the *dnaA recBC* (Fig. 5.15B). Our results suggest that binding of DnaA46 at the *datA* locus is not the cause for lethality in the *dnaA recBC* strain.

5.2.11 Possible accumulation of branched DNA structures

Our model also proposes the existence of branched DNA structures in the *dnaA recBC* strain close to DnaA binding sites when RecBCD is not functional. We probed for the existence of such structures (Fig. 5.14A) around the origin where high affinity DnaA binding sites are present. We isolated DNA from *dnaA, recBC* and *recBC dnaA* mutant cells after 4 hours at 39°C and digested it with XmnI or StuI + NdeI, releasing, respectively, either 4 kbp or 15 kbp fragments centered around the origin (Fig. 5.14B). The branched DNA structures generated as a result of fork stalling would migrate above the origin band on an agarose gel, while a broken branch will migrate below it. We were able to detect smearing above and below the origin bands (Fig. 5.14B), suggesting existence of long-lived branched DNA structures (stalled forks) in both the *dnaA* and *recBC dnaA* strains. The smearing above was absent in the DNA isolated from the *recBC* strain. We also saw significant smearing below the origin centered bands in the *recBC dnaA* strain suggesting release of branches from broken forks. In fact, about 50% of the total signal in the *dnaA* and *dnaA recBC* mutant is in the smear below the band, while in the *recBC* mutant only 35% of the signal is in the smear. This demonstrates that there are a lot of broken replication forks present around the origin in the *dnaA* and *dnaA recBC* strains. In the future we will be probing for the branched DNA structures using 2D DNA gels.

5.2.12 Both replication initiation and existing fork elongation are blocked in the *dnaA recBC*(Ts) double mutant

Our genetic studies show that the DNA degradation activity of the RecBCD complex is essential for the *dnaA* mutant growing at the semi-permissive temperature. We were curious to know whether compromising the DNA degradation in a *dnaA* mutant affects the replication elongation as well. To this end we investigated the kinetics of accumulation of origin and terminus signal over time in the double mutant (Fig. 5.16), compared to the corresponding single mutants and the WT strain. This analysis monitors both replication initiation (by tracking the amount of *oriC*) and replication elongation (by tracking the amount of the *ter* region). We found that, in contrast to the single *recBC* mutant that continues initiation at 39°C, *dnaA* and *recBC dnaA* cells show a single initiation event and then stop further initiations (Fig. 5.16A). The existing replication forks in the *dnaA* single mutant operate normally, as the increase in the terminus quantity indicates. In contrast, the *dnaA recBC* double mutant fails to replicate the terminus to the same extent, suggesting replication fork stalling (Fig. 5.16B). The suppressed strains *seqA dnaA recBC* and *hslUV dnaA recBC* both show higher initiation than either *dnaA* or *dnaA recBC* strains while their efficiency of finishing the ongoing rounds of replication is comparable to *dnaA* mutant suggesting under-initiation as a cause of lethality (Fig. 5.16).

The *dnaN* mutant which has a defective DNA clamp protein affecting the processivity of DNA pol III at 37°C, shows slow rate of finishing replication with no effect on initiation comparable to the *dnaN*+ strains for some time (Fig 5.17). The slow-moving replication forks in may eventually be affecting the initiation as well in the *dnaN* strains.

5.2.13 RecBCD restarts frozen replication forks in the up-shifted *dna* mutants

Since DnaA in involved in initiation of replication, we reasoned that comparing the rate of replication between *dnaA* and *dnaA recBC* strains at 39°C could give us insights into the lethality of the double mutant (Fig. 5.18A, B). As controls for no replication we have chloroamphenicol treated strains, which prevents initiation of new rounds of replication after the ongoing rounds finish (58). We find that upon shift to 39°C, *dnaA* mutants stop DNA synthesis (Fig. 5.18A). If functional RecBCD is present DNA synthesis resumes after a period of adjustment, while if RecBCD is inactive the DNA synthesis never resumes and remains at the level of background provided by chloroamphenicol treated cultures. We find that both initiation as well as ongoing rounds of replication are impeded upon shift to 39°C.

We repeated similar experiments under conditions of no viability loss for *recBC dnaA* (100x dilution of the overnight cultures) (Fig 5.18B). We grew strains at 28°C till they reached OD = 0.1, at which time they were continued at 28°C for another 60 minutes, shifted to 39°C for 90 minutes and brought back to 28°C for another 90 minutes. Under these conditions as well we found the double mutant grossly inhibited for replication upon shifting to higher temperature. The *dnaA* single mutant also after experiencing an initial difficulty upon 28°C to 39°C shift, eventually recovered, revealing the positive effect of the functional RecBCD enzyme. The wild type and the *recBC* mutant behaved comparably in showing no trouble replicating their DNA at either lower or higher temperatures. Thus: 1) the *dnaA*(Ts) mutants, independently of their RecBCD status, initially stall the existing replication forks upon 28°C—>39°C shift; 2) the

RecBCD enzyme helps to restart the stalled forks. The double mutant also experiences a significant lag before it could resume its replication upon shift to 28°C.

A similar role for RecBCD in resuming DNA synthesis is also observed in *dnaN* mutants (Fig 5.19). We find that at 37°C the *dnaN* mutants show a reduced rate of DNA synthesis compared to *dnaN*+ strains as expected due to lower processivity. There is an initial period of inhibition in both *dnaN* and *dnaN reCBC* mutant at 37°C. However, this inhibition is overcome in the presence of RecBCD suggesting that an active RecBCD complex is required to deal with pauses during replication. Although the *dnaN recBC* strain can replicate at very low rates distinct from the measured background, it is not sufficient to maintain its viability. It will be informative to measure the total DNA accumulation in this mutant.

5.3 Discussion

Recombinational repair proteins RecA and RecBCD are not essential for viability in *E.coli*, but the low viability of the *recA* , *recBCD* and especially *recA recBCD* double mutants indicates a vital function that these proteins play in actively growing cells (10). In fact, RecA and RecBCD functions are required to repair collapsed or stalled/regressed replication forks in replication mutants (52, 62, 63). One such example was the *dnaN*(Ts) mutant, which was found to depend on RecBCD for survival (25). The lethality in the *dnaA recBCD* we described in this paper was originally suspected to be due to mis-regulation of the *dnaN* gene, as DnaA is an autoregulator for the *dnaA-dnaN-recF* operon (3, 7). By plasmid complementation analysis we were able to show that the *dnaA recBC* and *dnaN recBC* lethalities were due to separate *dnaA* and *dnaN* defects. We then

confirmed that the inactivation of DnaC, another replication initiation function (92), is also lethal in combination with the *recBC* defect.

5.3.1 Distinct suppressors of lethality suggest independent mechanisms of lethality

To get insights into the nature of the co-lethalities we carried out suppressor analysis and have obtained a unique set of suppressors that relieve the *dnaA recBC* co-lethality, as compared to the *dnaN recBC* and *dnaC recBC* co-lethalities, suggesting distinct mechanism of toxicity in the former strain. Though both DnaA and DnaC are initiation functions, suppressors of the *dnaC recBC* lethality do not rescue the *dnaA recBC* lethality. The *diaA* inactivation suppresses both the *dnaN recBC* and *dnaC recBC* strains, suggesting that these co-lethalities are relieved by either less frequent initiations or by less efficient DnaA binding to its DNA sites. Interestingly, *dnaC recBC* is also rescued by loss of RecF-dependent recombination activity.

The activity of the HslUV protease/chaperone (67) and the SeqA organizer of nascent DNA (93) is a source of toxicity for the *dnaA recBC* mutant. The *hslU* inactivation has been previously reported as a suppressor for the *dnaA46* defect (37). Since HslUV is expressed under heat shock (16, 67) it is proposed that it degrades DnaA46 at higher temperatures when it is more likely to misfold (37). SeqA prevents premature initiation from *oriC* by binding to the hemi-methylated *oriC* and protecting it from the Dam methylase (9, 91, 93). The suppressed strains *dnaA recBC hslUV*::pRL27 and *dnaA recBC seqA*::pRL27 both initiate more than the *dnaA* and *dnaA recBC* strain at the non-permissive temperature, showing that an increase in the initiation potential helps in the survival of *dnaA recBC* double mutant. The stability of the DnaA204 allele

increases in *hslV* protease mutant, and DnaA46 mutant protein could be similarly increased, thus leading to increased initiation potential (86). The overexpression of DnaA46(Ts) suppresses the growth defect of *dnaA46*(Ts) strains, suggesting that the *dnaA46*(Ts) strain has a lower effective concentration of DnaA protein. We propose that the effective DnaA concentration in *dnaA recBC* could be increased by inactivating either the HlsUV protease which targets misfolded DnaA proteins or inactivating the SeqA protein which antagonizes DnaA initiation function. The colethality of the *recBC* defect has been observed with both the *dnaA46*(Ts) and *dna601*(Ts) alleles, which share one of the point mutation in the ATP binding domain of DnaA (28). At the same time, the *dnaA46* Δ*recBCD* mutant is also co-lethal at 39°C.

5.3.2 DnaA and RecBCD do not form an avoidance-repair couple

Synthetic lethal pairs often comprise genes coding for proteins redundantly contributing to the same essential function. But, this definition cannot explain the synthetic lethality observed in the *dnaA recBC, dnaN recBC* and *dnaC recBC* mutants as DnaA, DnaC and DnaN are involved with replication initiation and/or elongation while the RecBCD complex degrades linear DNA and licenses RecA loading onto double strand DNA ends (51). Thus, alternative explanations that can be used to describe these synthetic lethalities are: 1) avoidance-repair couple; 2) hypomorph compensation (88). In the avoidance-repair couples, one of the proteins is involved in avoiding, while the other one is engaged in repairing a toxic event for the cell. In the single mutants, one of the pathways, either the avoidance or the repair route, is still active, supporting viability. In the double mutant, however, both pathways are inactivated leading to an accumulation of

the irreparable damage, which kills the cell. Mutants that are dependent on RecBCD for viability often require RecBCD for repair of double strand breaks (4, 25, 45, 46, 76) — and the corresponding proteins form an avoidance-repair couple with RecBCD. Thus, genes that are synthetic lethal with *recBC* defect identify a source of double strand breaks, for example, the *rep* mutant suffers double strand DNA breaks due to slower replication and fork stalling (4). According to the hypomorph compensation idea, one of the mutations of the co-lethal combination is a hypomorph for an essential function, while the second mutation is in a gene which somehow supports the weaker function of the first protein, making it adequate for survival. Such a relationship has been assigned, for example, for the *dut-1*(Ts) *phoU* co-lethality (88). Dut is an essential enzyme that converts dUTP to dUMP releasing PPi (a polyphosphate) (21). In the *phoU* background the concentration of polyphosphates increase (70), leading to further reduction in the already compromised Dut-1 activity, resulting in lethality.

We failed to detect any chromosomal fragmentation in the *dnaA recBC* strain. This result is consistent with our other two observations that (i) *recA dnaA* is not lethal and that (ii) restoration of recombinational repair without restoring linear DNA degradation does not improve viability of *dnaA recBC*. This weakens the possibility of an avoidance repair couple relationship between DnaA and RecBCD protein. With no evidence for chromosomal fragmentation, RecBCD could be contributing to the viability of *dnaA* mutant only via its DNA degradation activity – the only known RecA-independent function of RecBCD. This is further substantiated by the observation that combining *dnaA* with *recD1011* defect which has reduced capacity for DNA degradation compared to WT (73), due to the defective RecD protein, is also synthetic lethal. The

growth inhibition observed in *dnaA ruvA* and *dnaA ruvA recG* strains compared to the *dnaA* strain suggests that some branched DNA structure form in the *dnaA* strain which need resolution.

5.3.3 RecBCD function diverts DnaA46 for replication initiation.

Previous *in vitro* studies have reported that the DnaA protein aggregates if it does not bind to ATP , while the DnaA46 protein required incubation with chaperones DnaK and GrpE before disaggregating in the presence of ATP (31). Also, the *dnaA46* mutant has been shown to have asynchronous initiation at the permissive temperature of 29°C (85), demonstrating that DnaA46 is not available for timely initiation even at permissive temperatures. We propose that when the malfunctioning DnaA46 protein is not available for initiation, it aggregates and binds to other locations in the chromosome. There are 307 DnaA boxes spread around the *E. coli* chromosome (27), *datA* locus having the highest binding affinity followed by *oriC*. Our investigations in Δ*datA dnaA recBC* strain suggests that DnaA6 either doesn't bind to *datA* locus or DnaA46-*datA* complex is not a major threat to the moving replication fork. Another major role of *datA* site is the hydrolysis of DnaA-ATP to DnaA-ADP (27) and since DnaA46 has poor affinity for ATP at non-permissive temperatures, it likely doesn't interact with the *datA* locus.

The fact that DNA degradation activity of RecBCD is essential (Fig 4.8) suggests unscheduled pauses in the movement of replication forks followed by replication fork reversal due to bound DnaA46. But unlike the previously described cases of replication fork reversal, *dnaA recBC* does not experience RuvABC-dependent chromosomal fragmentation (Fig 4.11) and inactivating RuvABC complex does not improve the

viability of the *dnaA recBC* double mutant (Fig. 4.9A), arguing that the replication fork reversal is not dependent on RuvAB activity, possibly because the replisome is still associated with the regressed fork. Our preliminary investigations show that some branched DNA structures form at the *oriC* where DnaA binds, and these structures are susceptible to breakage (Fig. 4.14). We speculate that the degradation of regressed DNA at stalled forks by RecBCD allows restart of replication, while the auxiliary Rep helicase is utilized to remove the aggregated DnaA46 ahead of the forks, freeing DnaA46 for initiation function (Fig. 4.10). Thus an active RecBCD protein compensates for the deteriorating activity of a DnaA(Ts) protein as the temperature increases. Since *datA* site which has 7 DnaA boxes, has been ruled out as the possible site for DnaA46 binding and replication fork pausing in *dnaA recBC* mutant, the remaining 300 DnaA binding sites in the chromosome need to be examined for their contribution for replication fork pausing. In future whole genome ChIP with DnaA46 could identify such replication pause sites in the *E. coli* chromosome.

Current and previous work in the *dnaN recBC* mutant show that this mutant is prone to Ruv-dependent double strand breaks at 37°C (25), which suggests. DNA double strand breaks however may not be the cause of lethality in this mutant, as inactivation of the Ruv Holliday Junction resolution pathway does not rescue the mutant while still preventing chromosomal breaks (25). Also, at a higher temperature of 39°C this mutant is still inviable, despite no detectable fragmentation. Thus, the lethality in *dnaN recBC* mutant may also not fit into the category of lethality due to loss of avoidance-repair couple. The compensation idea still needs to be tested. The *dnaC recBC* experiences a minor amount of fragmentation but it needs further investigation before the lethality

could be characterized as due to a loss of avoidance-repair couple or hypomorph compensation.

5.4 Acknowledgements

We wish to thank Sharik Khan for his scientific assistance at the beginning of the project and several rotation students who helped in isolating suppressors for the synthetic lethal strains. The work was supported by # GM 073115 from the National Institutes of Health. The authors have no conflict of interest to declare.

5.5 Materials and Methods

5.5.1 Bacterial strains, growth conditions and chemical reagents

E. coli strains used in this study are K-12 derived and are described in Table1. The strains were grown in LB (per 1 liter: 10g of tryptone, 5g of yeast extract, 5g of NaCl, pH to 7.4 with 250 µl of 4 M NaOH; LB agar contained 15g of agar/liter of LB broth (65)) at 28°C unless mentioned otherwise. When required, the growth medium was supplemented with 100 µg/ml Ampicillin, 50 µg/ml kanamycin, 10 µg/ml tetracycline, 10 µg/ml chloroamphenicol or 1 mM IPTG.

5.5.2 Cloning

For the construction of pPR1 (*dnaA+ dnaN+*) plasmid, genomic DNA of MG1655 and pMTL20 were both digested with NcoI and ligated to create a plasmid library. The plasmid library was transformed into DH5α dnaA46 strain and plated at 42°C to select for suppressors of temperature sensitivity of DnaA46. One clone

containing insert was selected and called pPR1. pPR1 was digested with XhoI and religated to create a *dnaA*+ (*dnaN*–) plasmid (pPR7). pPR1 was digested with NcoI and re-ligated and transformed into DH5α *dnaA46* to create a plasmid with insert in the opposite orientation. Plasmid pPR2 was isolated from suppressors that grew and checked for inversion of orientation. pPR2 was digested with SphI and re-ligated to create the *dnaN*+ (*dnaA*–) plasmid (pPR8).

Cloning *dnaA* and *dnaA46* genes in pMTL20: Primers GCTATTCCATGGTACG GGCTGATG and GCTATCAAGCTTGTGCCACCATTTCCATCTCG were used to amplify the *dnaA*+ and *dnaA46* genes. Upon amplification the insert and vector were digested with NcoI and HindIII, ligated and transformed into DH5α *dnaA46* to select for suppressors. Plasmid was isolated from the suppressors and inserts were verified by sequencing.

Cloning of *hslUV*+ into pMTL20: Primers TCTCGGAATTCGCAGCTGGTTGA AGTTCCGT and CTGCCCATGGGATGAAAATGATTGAACGCG were used to amplify the wild type *hslUV* genes. The amplicon and the plasmid pMTL20 were digested with EcoRI and NcoI and ligated.

5.5.3 Spot test

Overnight cultures were diluted 100-fold to subculture and then grown at 28°C to OD = 0.1 – 0.15. Strains containing plasmids were sub-cultured in the presence of antibiotic to maintain the plasmid. Serial dilutions were made in 1% NaCl, and 10 µl were spotted on LB plates and incubated at appropriate temperatures for 24-48 hours.

5.5.4 Viability assay

Overnight cultures were diluted 100-fold and grown at 28°C to OD = 0.1 – 0.15. The cultures were shifted to 39°C either directly or were further diluted 30-fold, shaken at 28°C for 20 minutes to acclimatize to the diluted conditions and moved to 39°C. At appropriate times, aliquots were removed, serially diluted and spotted on LB plates. Colonies were counted after 18-24 hours of incubation of plates at room temperature.

5.5.5 Origin and terminus kinetics

Overnight cultures were sub-cultured 100-fold and grown at 28°C to OD = 0.1 – 0.15, when the cultures were further diluted 30-fold, shaken at 28°C for 20 minutes to acclimatize to the diluted conditions and moved to 39°C. 20 ml of *recBC dnaA* culture, 10 ml of *dnaA*, *recBC dnaA seqA*::pRL27 and *recBC dnaA hslUV*::pRL27, and 10, 8, 3, 3 and 3ml of *recBC* cultures were taken at, correspondingly, 0, 1, 2, 3, and 4 hours after shift to 39°C to isolate DNA in duplicate agarose plugs. The cells in plugs were lysed overnight at 65°C and denatured and processed further as described (72).

5.5.6 Pulse field gel electrophoresis

Overnight cultures were sub-cultured 100-fold and grown at 28°C to OD = 0.1 – 0.15 in the presence of ^{32}P label, as described in Khan and Kuzminov (40), then moved to 37°C or 39°C. 1- 0.25 ml aliquots were removed every hour to make agarose plugs using cell pellet. Pellets were re-suspended into 60 µl TE (10 mM Tris-HCl, 1 mM EDTA, pH 8.0), mixed with 5 µl of 5 mg/ml Proteinase K (Roche Applied Science, final concentration in plugs is 200 µg/ml) and 65 µl of molten agarose in lysis buffer (1.2%

agarose in 1 % laurylsarcosine, 50 mM Tris-HCl, 25 mM EDTA, pH 8.0) and poured into plug molds (Bio-Rad). The plugs were lysed for 16 hours at 65°C in the lysis buffer. The conditions for running pulsed-field gel electrophoresis and quantification of chromosomal fragmentation were exactly as before (48).

5.5.7 Rate of DNA synthesis

Overnight cultures were sub-cultured 100-fold and grown at 28°C to OD = 0.1 – 0.15, 200 µl aliquots were taken at each time and mixed with 1 µCi of ^{3}H-Thy and the reaction was incubated at 39°C for 2 minutes, when 5 ml of 5% TCA was added to stop further incorporation. The TCA precipitate was filtered on Fisherbrand G6 glass fiber filters, washed with 5 ml of 5% TCA, 5 ml of ethanol. 100 µl of 100 mM KOH was added to quench fluorescence. The filters were incubated with scintillation fluid and incorporated ^{3}H was measured using Beckman scintillation counter.

5.5.8 Detection of branched DNA structures

Overnight cultures were sub-cultured 100-fold and grown at 28°C to OD = 0.1 – 0.15, when the cultures were diluted 30-fold, shaken at 28°C for 20 minutes to acclimatize to the diluted conditions and moved to 39°C for 4 hours. DNA was isolated from 25 ml of *dnaA*, 50 ml of *dnaA recBC* and 1 ml of *recBC* strain by phenol-chloroform extraction. Briefly, cell pellet was suspended in 30% sucrose in TE, lysed with 2% SDS in TE, lysate was extracted first with 400 µl of phenol, then with 200 µl of phenol / 200 µl of chloroform mixture and, lastly, with 400 µl of chloroform. The aqueous phase was used to precipitate DNA by adding a final concentration of 100 mM

NaCl and two volumes of ethanol. The pellet was dissolved in 500 µl TE, and DNA was re-precipitated using NaCl and ethanol. 400 ng of DNA for each strain was digested with XmnI or StuI+NdeI, and the reaction was run of 0.7% agarose in 1X Tris-acetate-EDTA buffer. The gel was treated with 0.25 N HCl for 20 minutes, 0.5 M NaOH for 20 minutes and 1 M Tris-HCl pH=8.0, for 20 minutes, DNA was transferred to nylon membrane by capillary transfer and the membrane was hybridized with *oriC*-specific probe.

5.6 Figures

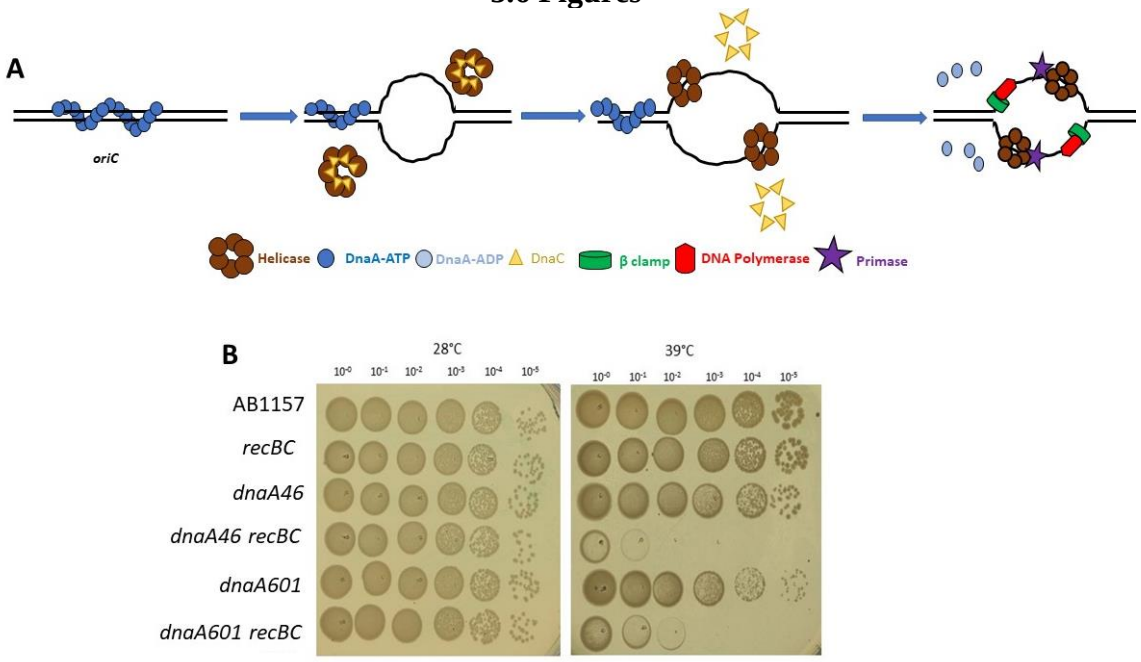

Figure 5.1. Scheme of *E. coli* replication initiation and synthetic lethality of *dnaA recBC* strain. Strains used are AB1157, *recBC*(Ts)(SK291), *dnaA46*(Ts)(SRK309-1), *dnaA46*(Ts) *recBC*(Ts)(SRK309), *dnaA601*(Ts) (RA77), *dnaA601*(Ts) *recBC*(Ts) (RA78) **A.** DnaA-ATP filament binds to *oriC* and unwinds the region. In the next step DnaC chaperones load the DnaB helicases which is followed by loading of the primase, β clamp and the DNA polymerase. The loading of β clamp converts the bound DnaA-ATP to DnaA-ADP which dissociates from the *oriC*. **B.** Strains are grown to OD600 = 0.1 and spotted on LB plates incubated at 28°C and 39°C.

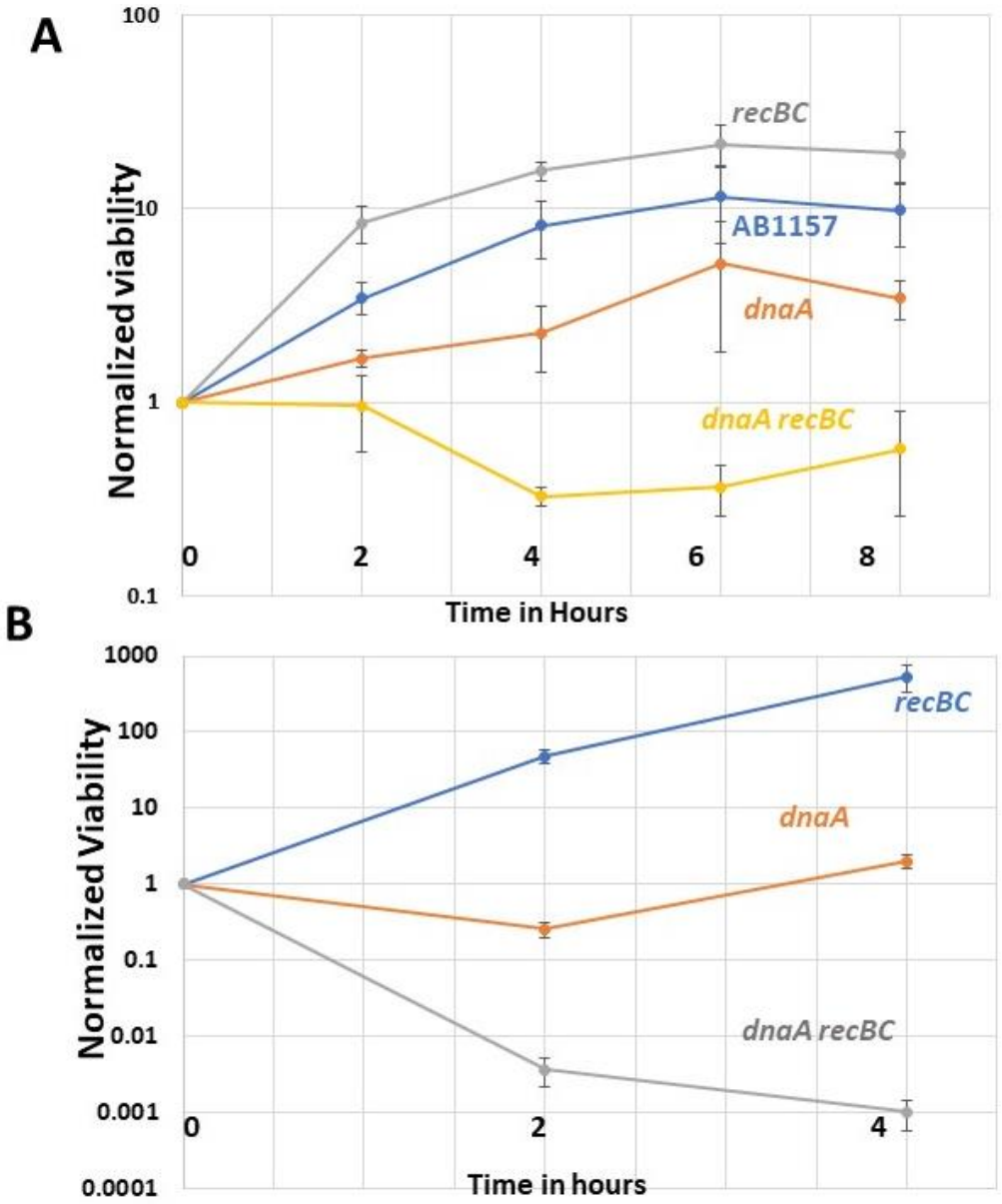

Figure 5.2. Viability of strains AB1157, *recBC*(Ts)(SK219), *dnaA46*(Ts)(SRK309-1), *dnaA46*(Ts) *recBC*(Ts)(SRK309) at 39°C. A. Cultures were grown 28°C to OD = 0.1 and moved to 39°C to measure viability. **B.** The cultures were grown to OD = 0.1 at 28°C, diluted 30-fold and then moved to 39°C to measure viability.

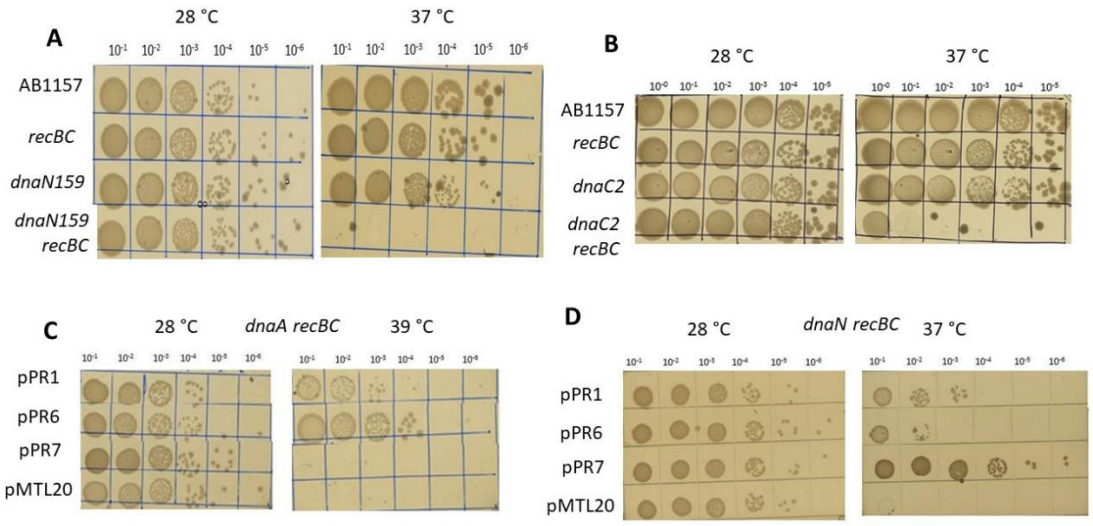

Figure 5.3. Synthetic lethality of *dnaN recBC, dnaC recBC* and independence of *dnaA recBC* and *dnaN recBC*. Strains used are AB1157, *recBC*(Ts) (SK219), *dnaA recBC* (SRK309) *dnaN159*(Ts) (RA70) and *dnaN159*(Ts) *recBC*(Ts) (RA71), *dnaC2*(Ts) (L392) and *dnaC2*(Ts) *recBC*(Ts) (RA72) **A, B.** Spotting of strains at 28°C and 37°C. **C.** Complementation of *dnaA recBC* with pPR1, pPR2, pPR7 and pMTL20. **D.** Complementation of *dnaN recBC* with pPR1, pPR2, pPR7 and pMTL20.

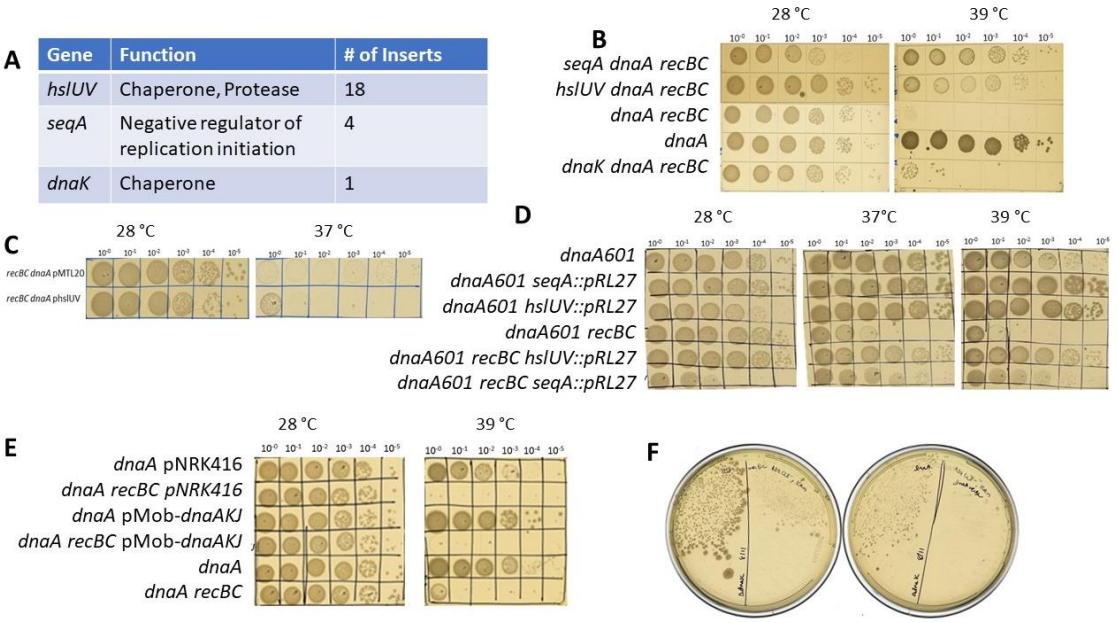

Figure 5.4. *dnaA recBC* (SRK309) lethality suppressor analysis. Strains used are *dnaA* (SRK309-1), *dnaA recBC* (SRK309), *seqA dnaA recBC* (RA74), *hslUV dnaA recBC* (RA73), *dnaK dnaA recBC* (RA109), *dnaA601 recBC* (RA77), *dnaA601 recBC hslUV*::pRL27 (RA79), *dnaA601 recBC seqA::*pRL27 (RA80) **A.** List of isolated suppressors for *dnaA recBC* lethality, their function and number of inserts. **B.** Verification of growth of suppressed *dnaA recBC* strains at 39°C. **C.** Over-expression of *hslUV* (pPR8) in *dnaA recBC* causes lethality at 37°C. **D.** Suppression of strain by the isolated suppressors. **E.** Over-expression of *dnaK*(pNRK416) or *dnaKJ* (pMob45) do not rescue *dnaA recBC* growth at 39°C. **F.** *dnaK* mutation couldn't be transduced into the *dnaA recBC* strain.

A

Gene	Function	# of Insert
lon	Protease/Chaperone	4
iscAUS	Fe-S cluster maintenance	6
diaA	Initiation factor	1
lcd, ubiC, pta	TCA cycle	2,1,1
mutH	Mismatch repair	1

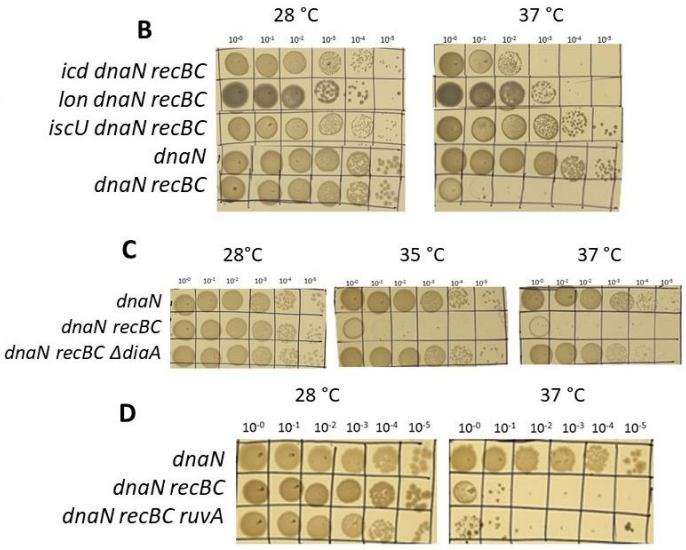

Figure 5.5. *dnaN recBC*(RA71) lethality suppressor analysis. Strains used are *dnaN recBC* (RA71), *dnaN recBC diaA* (RA92), *dnaN recBC icd* (RA88), *dnaN recBC lon* (RA89), *dnaN recBC iscU* (RA90), *dnaN recBC ruvA* (RA93). **A**. List of isolated suppressors for *dnaN recBC*, their cellular functions and number of inserts. **B, C.** Verification of growth of suppressed *dnaN recBC* strains at 37°C, **D.** *ruvA* inactivation doesn't suppress *dnaN recBC* lethality at 37°C.

A

Gene	Function	Inserts
diaA	Initiation function	3
recR	SS gap repair	1
recA	Homologous Recombination	1
yjjQ	Repressor of flagella biosynthesis	1
bssS	Biofilm synthesis regulation	1

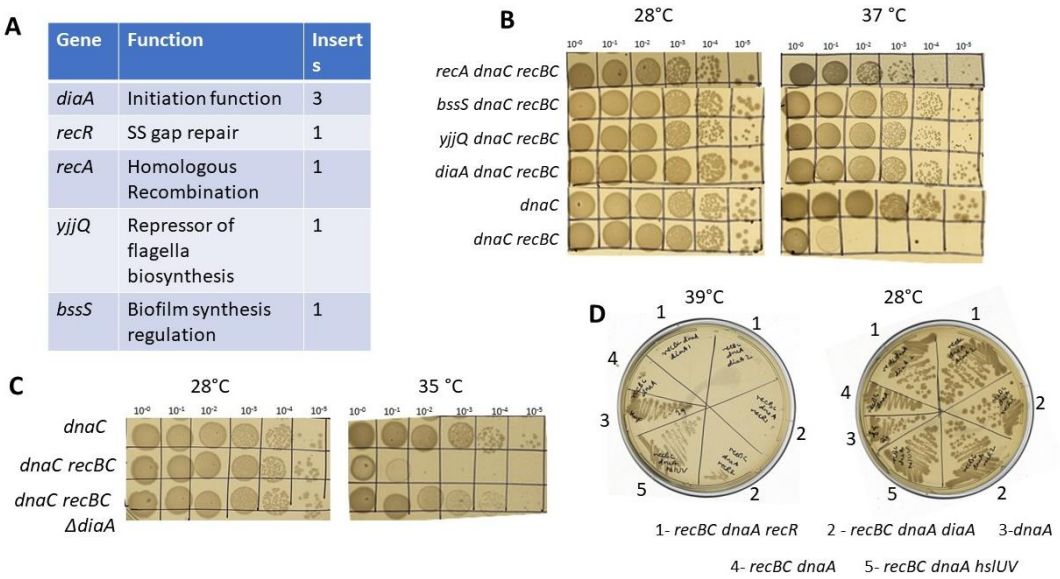

Figure 5.6. *dnaC recBC* (RA72) lethality suppressor analysis. Strains used are *dnaC recBC* (RA72) *dnaC recBC yjjQ* (RA97), *dnaC recBC bssS* (RA96), *dnaC recBC diaA* (RA98), *dnaC recBC recA* (RA95), *dnaC recBC ΔdiaA* (RA99), *dnaA recBC recR* (RA100), *dnaA recBC diaA* (RA102). **A.** List of isolated suppressors for *dnaC recBC*, their cellular functions and number of inserts. **B, C.** Verification of growth of suppressed *dnaC recBC* strains at 37°C *dnaC recBC yjjQ, dnaC recBC bssS, dnaC recBC diaA ,dnaC recBC recA , dnaC recBC ΔdiaA.* **D.** *dnaC recBC* suppressors *recR* and *diaA* do not rescue *dnaA recBC* lethality, *dnaA recBC recR, dnaA recBC diaA.*

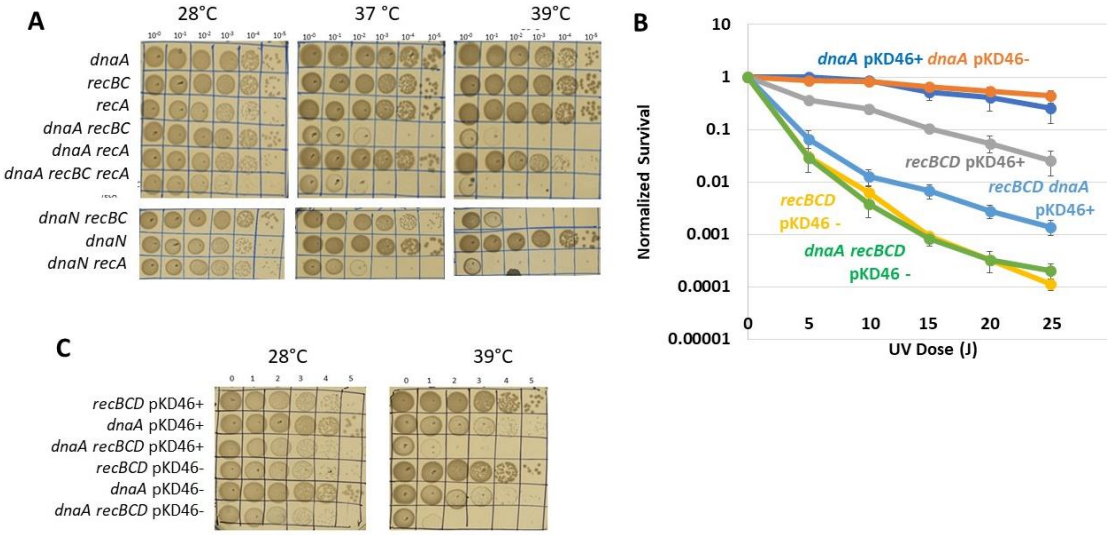

Figure 5.7. Recombinational repair is essential in *dnaN* mutants but not in *dnaA* mutants. Strains used are *dnaA recA* (RA76), *dnaN recA* (RA94), *dnaA* (SRK309-1), *dnaA recBC* (SRK309), *dnaA recA recBC* (RA107). **A.** Spot test showing *dnaA recA* (RA76) is growth inhibited but not lethal while *dnaN recA* (RA94) is synthetic lethal. **B.** Survival of pKD46+ (induction of λ recombination functions with 1mM arabinose) and pKD46- (repression of λ recombination functions with 1mM glucose) strains after UV radiation. **C.** Spot test of unirradiated strains used in B at 28°C and 39°C.

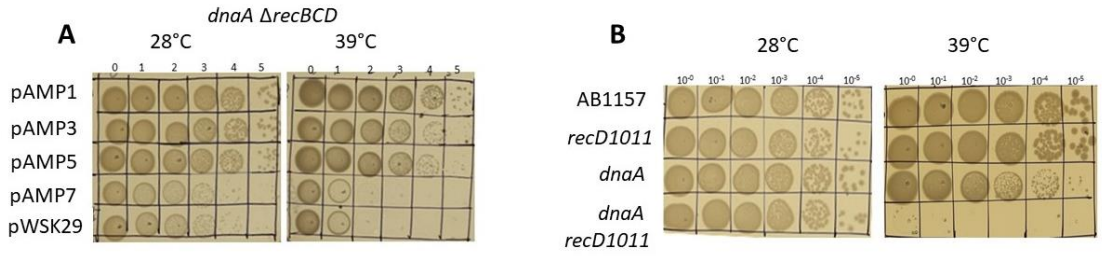

Figure 5.8. DNA degradation is essential in *dnaA* mutants. Strains used are AB1157, *recD1011*(BT125), *dnaA* (SRK309-1), *dnaA recD1011* (RA84), dnaA ΔrecBCD (RA75). complementation of *dnaA recBCD* strain with plasmids expressing complete or partial RecBCD function. **B.** *dnaA recD1011* is synthetic lethal.

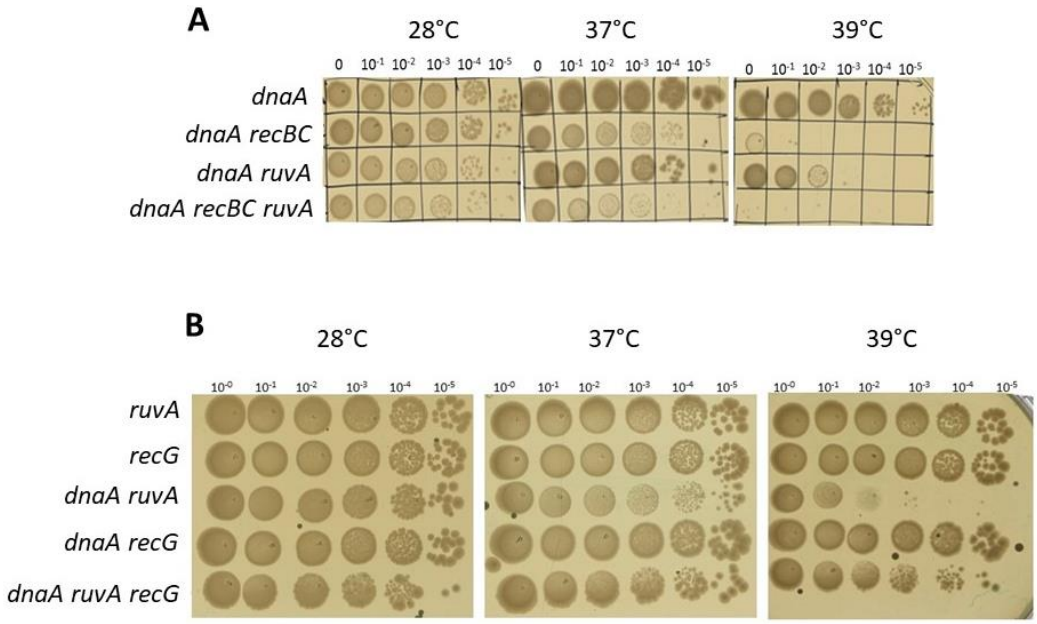

Figure 5.9. RecG function inhibits *dnaA ruvA* strain. Strains used are *dnaA* (SRK309-1), *dnaA recBC* (SRK309), *dnaA ruvA* (RA81), *dnaA recBC ruvA* (RA108), *dnaA recG* (RA82), *dnaA ruvA recG* (RA83) **A.** *ruvA* inactivation inhibits *dnaA* strain. **B.** *recG* suppresses *dnaA ruvA* strain.

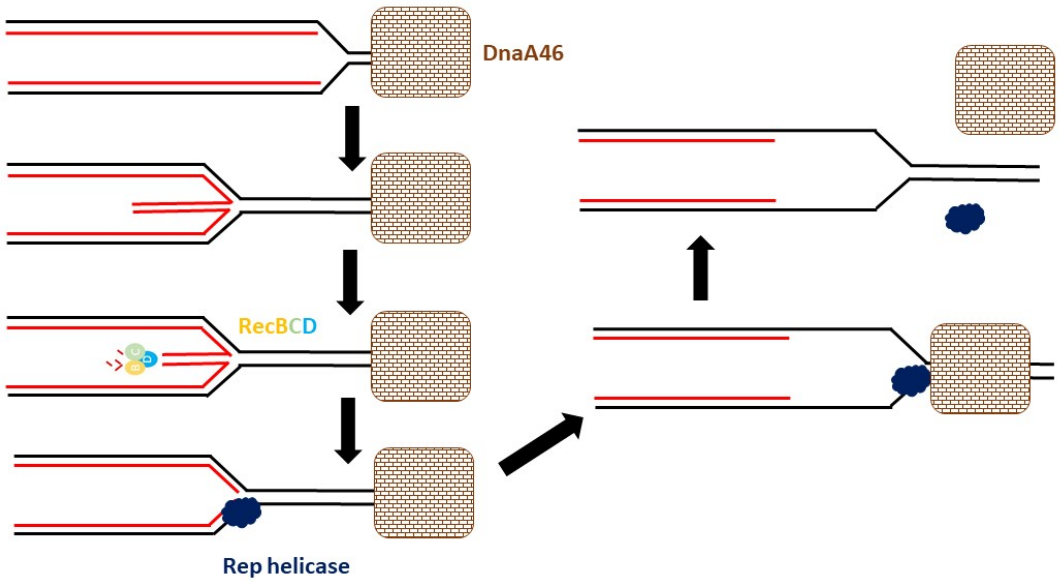

Figure 5.10. Hypothesis to explain lethality of *dnaA recBC* at semi permissive temperature. DnaA46 binds to DNA and inhibits the movement of replication forks. This cause fork regression. Regressed forks are reset by RecBCD and Rep helicase is recruited to remove the DnaA46 obstacle.

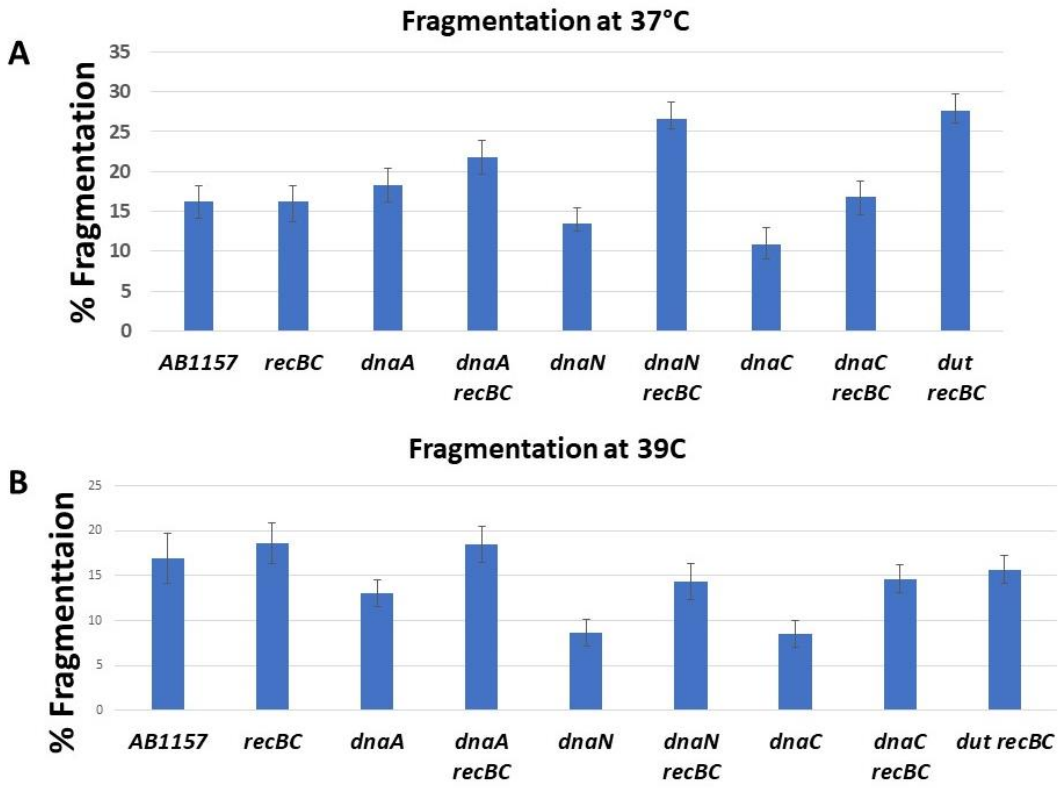

Figure 5.11. Quantification of linear DNA observed in Pulse Field Gel Electrophoresis analysis. Strains used are AB1157, *recBC* (SK219), *dnaA* (SRK309-1), *dnaA recBC* (SRK309), *dnaN* (RA69), *dnaAN recBC* (RA70), *dnaC* (L392), *dnaC recBC* (RA72), *dut recBC* (AK107) **A.** at 37°C. **B.** at 39°C.

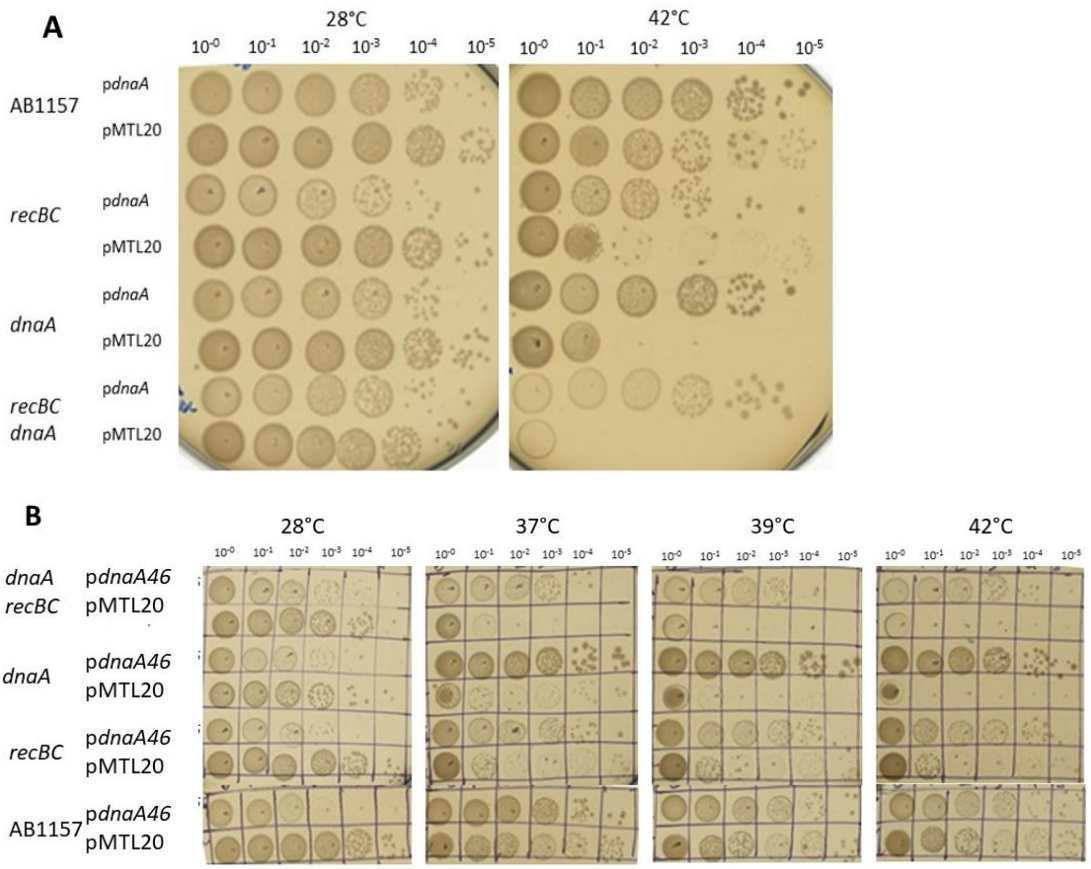

Figure 5.12. DnaA46 is dominant over DnaA. Strains used are *dnaA recBC* (SRK309), *dnaA* (SRK309-1), *recBC* (SK219) and AB1157 A. Strains are complemented with pMTL20-DnaA (pPR9) or pMTL20 at 28°C and 42°C. B. Strains are complemented with pMTL20-DnaA46 (pPR10) or pMTL20 and spotted at 28°C, 37°C, 39°C and 42°C.

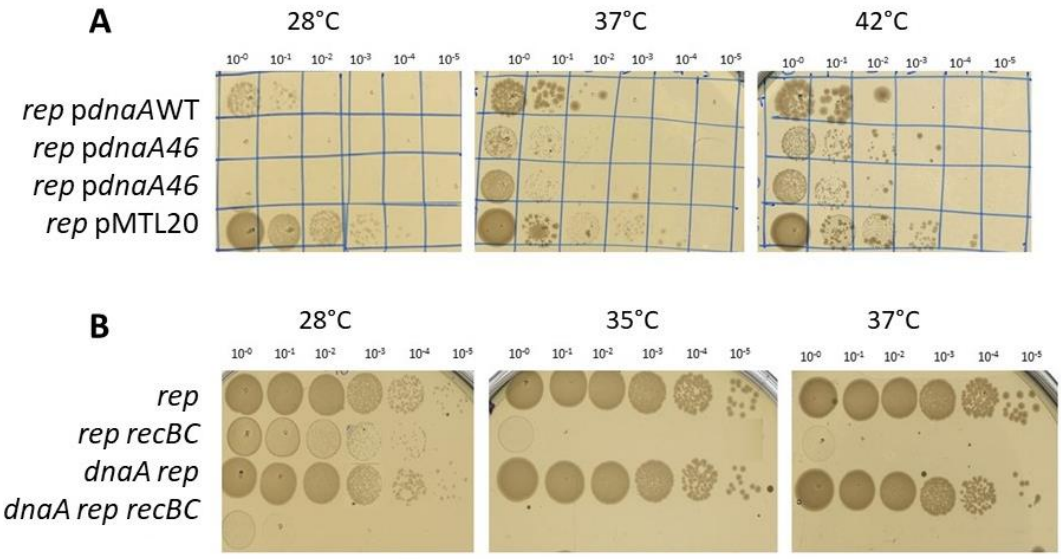

Figure 5.13. DnaA46 blocks replication fork movement in *rep* mutants. Strains used are *rep* (JJC213), *rep recBC* (RA85), *dnaA rep* (RA86) and *dnaA rep recBC* (RA87) **A.** Over-expression of DnaA46 (pPR10) and pMTL20 in *rep* mutants. **B.** Spot test of *rep*, *rep recBC*, *dnaA rep* and *dnaA rep recBC* at 28°C, 35°C and 37°C.

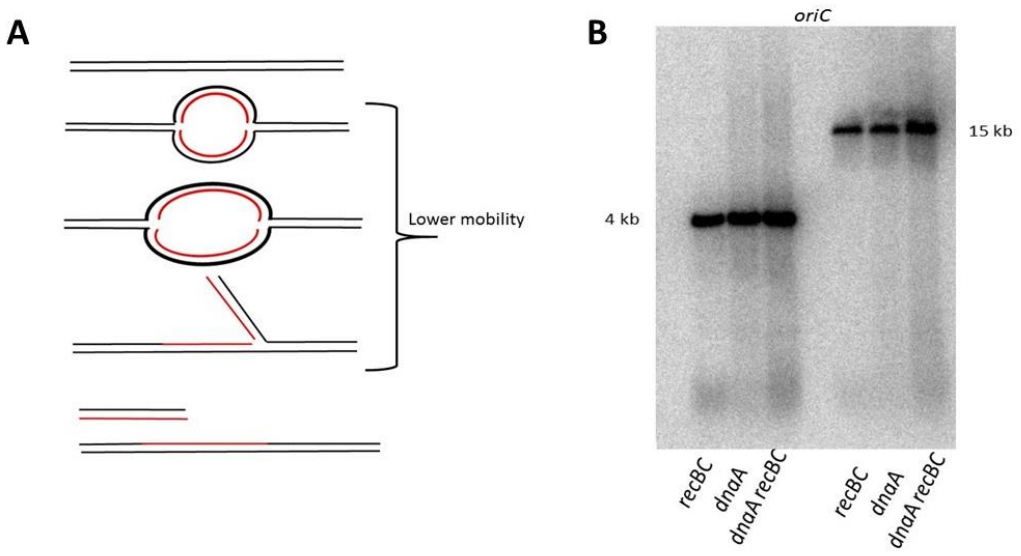

Figure 5.14. Detection of branched DNA structures at the *oriC* in *recBC* (SK219), *dnaA* (SRK309-1) and *dnaA recBC* (SRK309) at 39°C. A. Possible branched DNA structures around *oriC*. **B.** Southern hybridization with *oriC* specific probe of DNA isolated from strains *recBC*, *dnaA* and *dnaA recBC*.

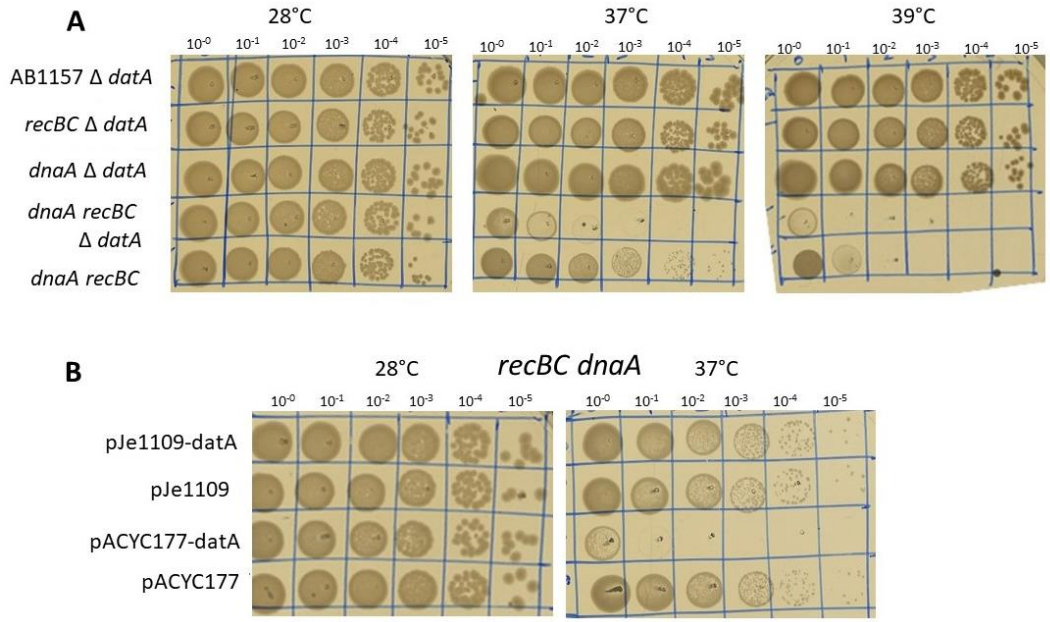

Figure 5.15. Role of *datA* in *dnaA recBC* lethality. Strains used are AB1157 *datA* (RA103), *dnaA datA* (RA105), *recBC datA* (RA104), *dnaA recBC datA* (RA106) **A.** Δ*datA* does not rescue *dnaA recBC* lethality at 39°C. **B.** Increasing the copy number of data exacerbates lethality of *dnaA recBC*.

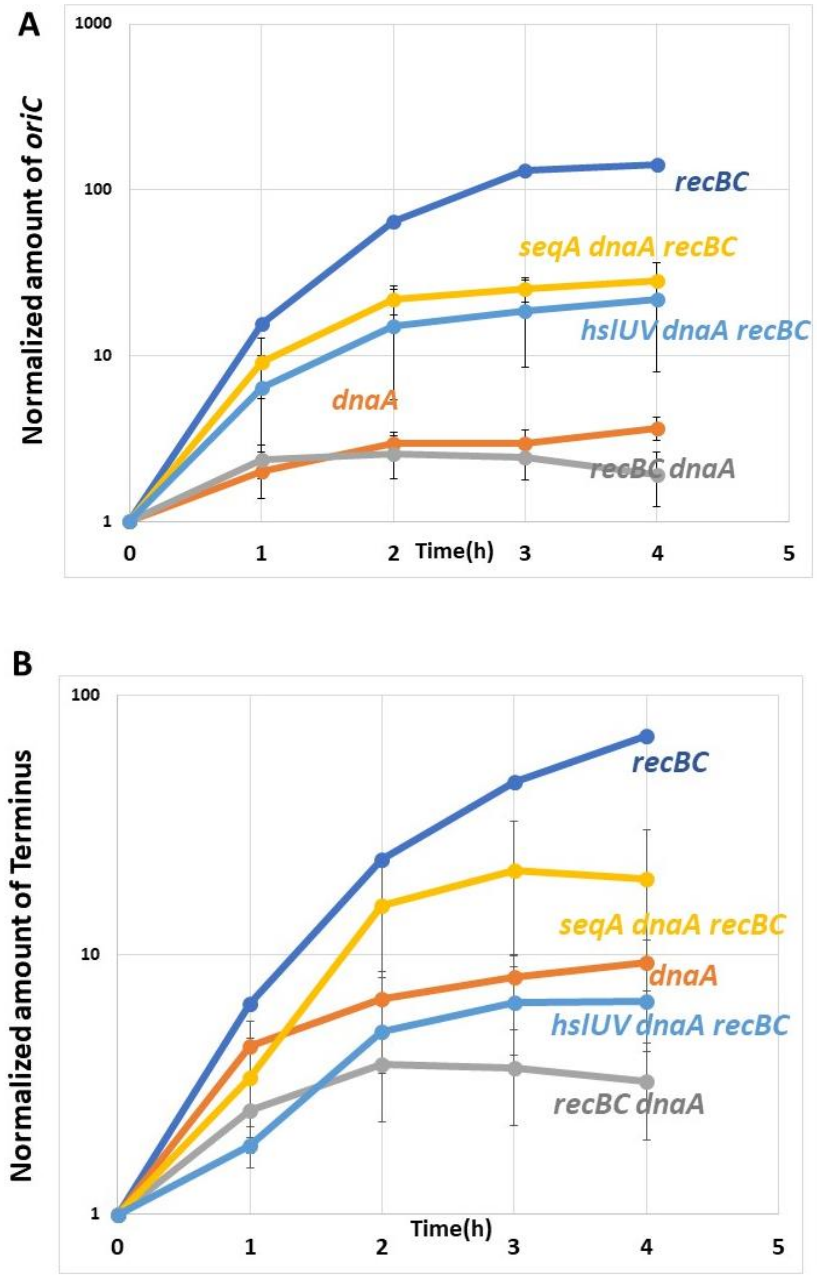

Figure 5.16. Origin and terminus evolution in strains *recBC* (SK219), *dnaA* (SRK309-1), *dnaA recBC* (SRK309), *dnaA recBC seqA* (RA74) and *dnaA recBC hslUV* (RA73) at 39°C.

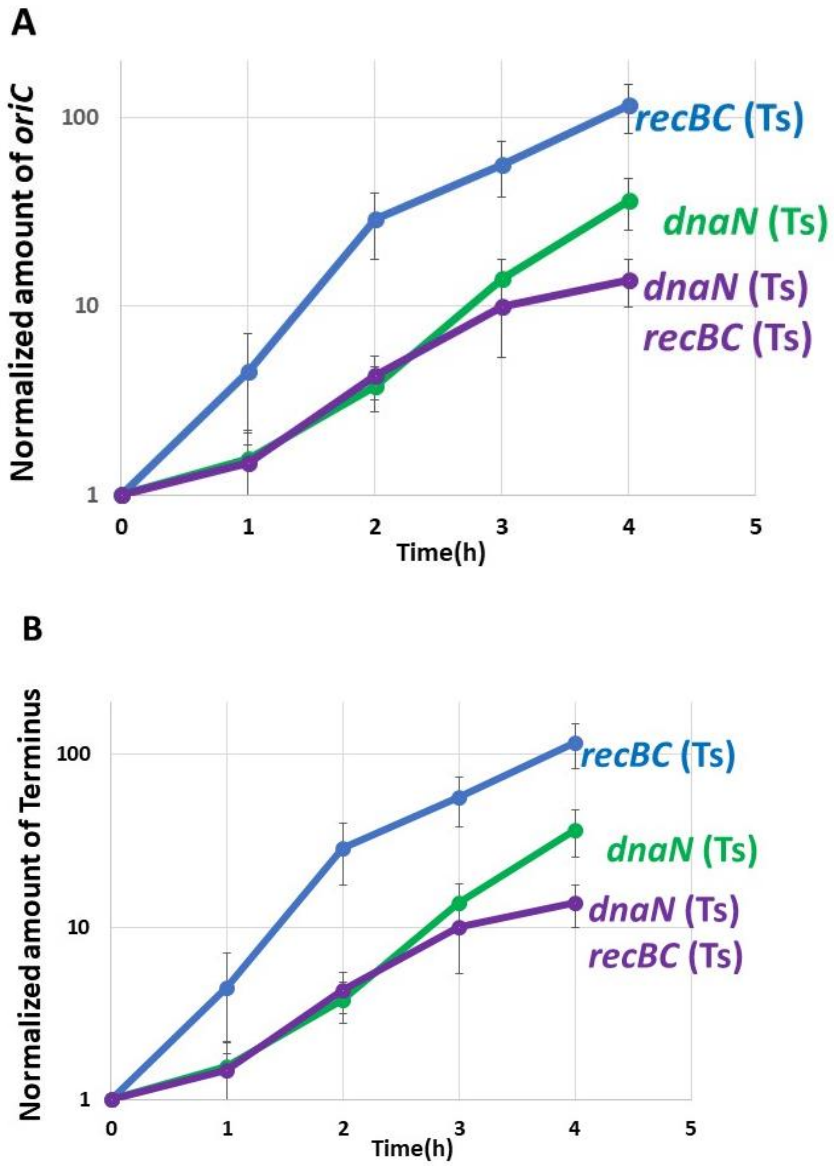

Figure 5.17. Origin and Termins accumulation in *recBC* (SK219), *dnaN* (RA70) and *dnaN recBC* (RA71) at 37°C.

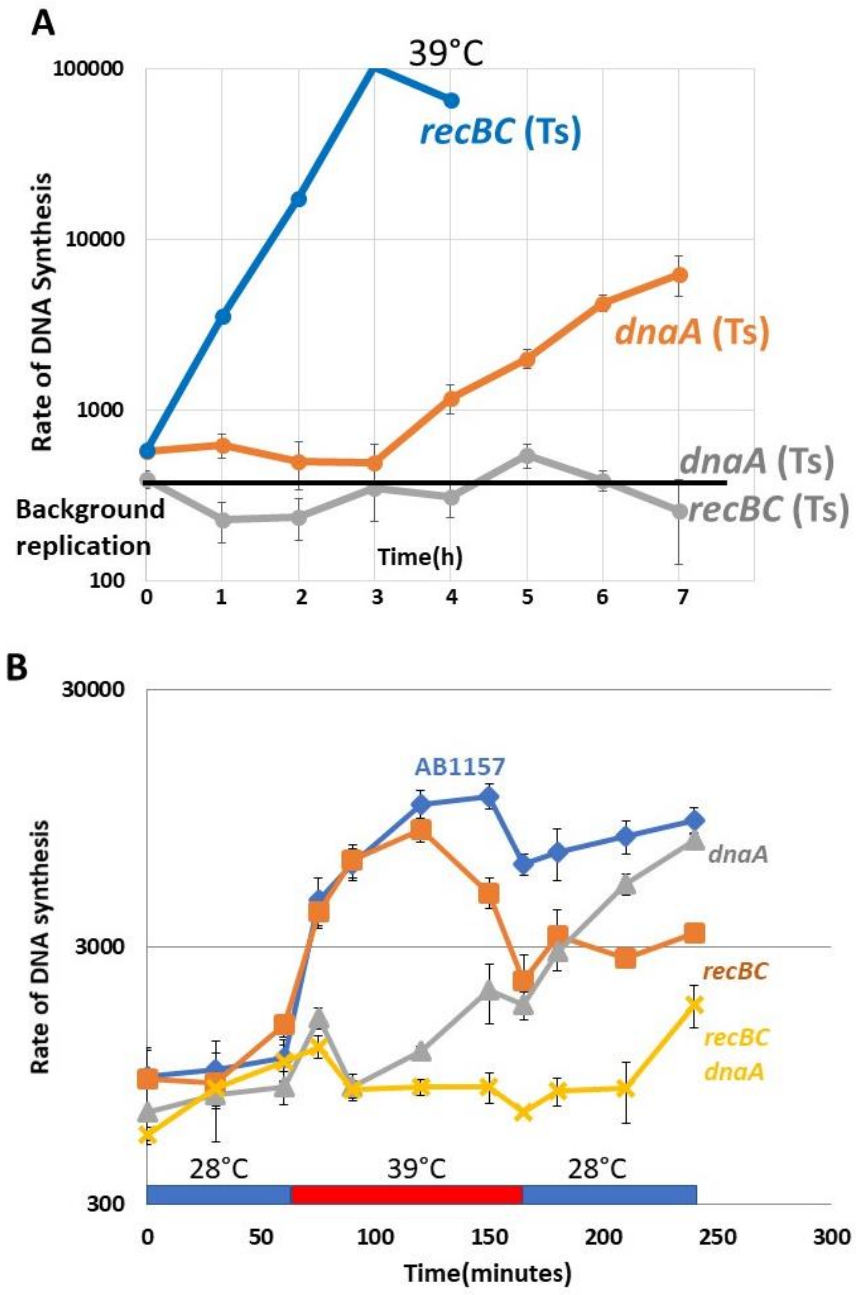

Figure 5.18. Replication stops in *dnaA recBC* at 39°C. Strains used are *recBC* (SK219), *dnaA* (SRK309-1), *dnaA recBC* (SRK309). Strains were grown to OD = 0.1 at 28°C and **A.** were 30-fold diluted and moved to 39°C. **B.** were continued at 28°C for 60 minutes, moved to 39°C for the next 90 minutes and brought back to 28°C for 90 minutes.

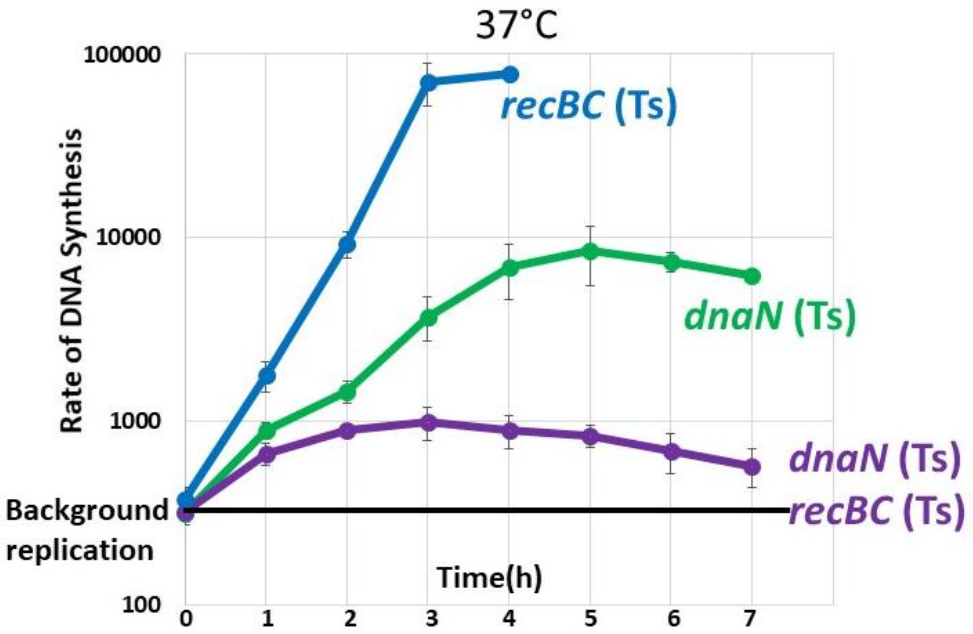

Figure 5.19. Replication is inhibted in dnaN recBC at 37°C. Strains used are *recBC* (SK219), *dnaN* (RA70) and *dnaN recBC* (RA71) at 37°C. Strains were grown to OD = 0.1 at 28°C, diluted 30 fold and moved to 37°C.

5.7 Tables

Table 5.1. List of strains used in this study.

Strain name	Genotype	Reference
AB1157	Wild Type	(5)
SRK309-1	AB1157 *dnaA46*(Ts)	Lab Collection
SK219	AB1157 *recB270*(Ts)*recC271*(Ts)	(48)
SRK309	AB1157 *dnaA46*(Ts) *recBC*(Ts)	SK129 x P1N9212 (94)
L392	AB1157 *dnaC2*(Ts)	Lab Collection
JB1 pSA122**	Δ*recBCD3*::*kan* pRecBC+	Lab Collection
CM2500**	*dnaA601*(Ts)	(26)
AK107	AB1157 *dut1 zic 4901::Tn10 recBC*(Ts)	(45)
GY9701**	*recA938::cam* miniF-kan *recA*+	R. Devoret via Benedicte Michel
JW1850-2**	*ΔruvA786::kan*	(4)
N2731**	*recG258::mini*-Tn*10kan*	(53)
NS373**	*dnaA46(Ts) tna::Tn10*	(79)
BT125	AB1157 *recD1011*	Lab Collection
JJC213	AB1157 *rep*::kan	(88)
JW3118-2**	*diaA::kan*	(4)
HC123**	*dnaN159*(Ts)	(77)
RA69	*dnaN159*(Ts) *yidX+ kan yidA+*	Precise insertion in HC123
RA70	AB1157 *dnaN159*(Ts) *yidX+ kan yidA+*	AB1157 x P1 RA69
RA71	AB1157 *dnaN159*(Ts) *recBC*(Ts)	SK219 x P1 RA69
RA72	AB1157 *dnaC2*(Ts) *recBC*(Ts)	SK219 x P1 L392
RA73	AB1157 *dnaA46*(Ts) *recBC*(Ts) *hslUV*::pRL27	SRK309 transformed with pRL27
RA74	AB1157 *dnaA46*(Ts) *recBC*(Ts) *seqA*::pRL27	SRK309 transformed with pRL27
RA75	AB1157 *dnaA46*(Ts) Δ*recBCD3::kan*	SRK309-1x P1 JB1
RA76	AB1157 *dnaA46*(Ts) *recA938::cat*	SRK309-1 x P1 GY9701
RA77	AB1157 *dnaA601*(Ts)	AB1157 x P1 CM2500
RA78	AB1157 *dnaA601*(Ts) *recBC*(Ts)	SK291 x P1 CM2500
RA79	AB1157 *dnaA601*(Ts) *recBC*(Ts) *hslUV*::pRL27	RA78 x P1 RA73

Table 5.1. (cont.)

RA80	AB1157 *dnaA601*(Ts) *recBC*(Ts) *seqA*::pRL27	RA78 X P1 RA74
RA81	AB1157 *dnaA46*(Ts) *ruvA786::kan*	SRK309-1 x P1JW1850-2
RA82	AB1157 *dnaA46*(Ts) *recG258::mini*-Tn*10 kan*	SRK309-1 x P1 N2731
RA83	AB1157 *dnaA46*(Ts) *ruvA786 recG258*	RA81 treated with pCP20 x P1N2731
RA84	AB1157 *dnaA46*(Ts) *recD1011*	BT125 x P1 NS373
RA85	AB1157 *rep recBC*(Ts)	SK219 x P1 JJC213
RA86	AB1157 *rep dnaA46*(Ts)	SRK309-1 x P1 JJC213
RA87	AB1157 *rep dnaA46*(Ts) *recBC*(Ts)	RA85 x P1 NS373
RA88	AB1157 *dnaN159*(Ts) *recBC*(Ts) *icd*::pRL27	RA71 transformed with pRL27
RA89	AB1157 *dnaN159*(Ts) *recBC*(Ts) *lon*::pRL27	RA71 transformed with pRL27
RA90	AB1157 *dnaN159*(Ts) *recBC*(Ts) *iscU*::pRL27	RA71 transformed with pRL27
RA91	AB1157 *dnaN159*(Ts) *recBC*(Ts)	RA71 treated with pCP20
RA92	AB1157 *dnaN159*(Ts) *recBC*(Ts) Δ*diaA::kan*	RA91 X P1 JW3118-2
RA93	AB1157 *dnaN159*(Ts) *recBC*(Ts) *ruvA786::kan*	RA91 x P1 JW1850-2
RA94	AB1157 *dnaN159*(Ts) *recA::938::cat*	RA70 x P1 GY9701
RA95	AB1157 *dnaC2*(Ts) *recBC*(Ts) *recA*::pRL27	RA72 transformed with pRL27
RA96	AB1157 *dnaC2*(Ts) *recBC*(Ts) *bssS*::pRL27	RA72 transformed with pRL27
RA97	AB1157 *dnaC2*(Ts) *recBC*(Ts) *yjjQ*::pRL27	RA72 transformed with pRL27
RA98	AB1157 *dnaC2*(Ts) *recBC*(Ts) *diaA*::pRL27	RA72 transformed with pRL27
RA99	AB1157 *dnaC2*(Ts) *recBC*(Ts) Δ*diaA::kan*	RA72 x P1JW3118-2
RA100	AB1157 *dnaA46*(Ts) *recBC*(Ts) *recR*::pRL27	RA72 transformed with pRL27
RA102	AB1157 *dnaA46*(Ts) *recBC*(Ts) *diaA*::pRL27	SRK309 x P1 RA99
RA103	AB1157 Δ*datA*::kan	Precise deletion of datA by Datsenko Wanner
RA104	AB1157 *recBC*(Ts) Δ*datA*::kan	SK219 x P1 RA103
RA105	AB1157 *dnaA46*(Ts) Δ*datA*::kan	SRK309-1 x P1 RA103

Table 5.1. (cont.)

RA106	AB1157 *dnaA46*(Ts) *recBC*(Ts) Δ*datA*::kan	SRK309 x P1 RA103
RA107	AB1157 *dnaA46*(Ts) *recBC*(Ts) recA938::cat	
RA108	AB1157 *dnaA46*(Ts) *recBC*(Ts) *ruvA786*	SRK309 x P1JW1850-2
RA109	AB1157 *dnaA46*(Ts) *recBC*(Ts) *dnaK*::pRL27	SRK309 transformed with pRL27

* other mutations include: F– λ– *rac– thi-1 hisG4* Δ*(gpt-proA)62 argE3 thr-1 leuB6 kdgK51 rfbD1 araC14 lacY1 galK2 xylA5 mtl-1 tsx-33 supE44*(glnV44) *rpsL31*(strR).

** A non AB1157 strain.

Table 5.2. Plasmids used in this study.

Plasmid	Replicon/Drug Resistance/Other Genes	Reference
pCP20	Rep^{ts} / *bla cat* / *flp*	(16)
pMTL20	pBR322 / *bla* / *lacZ alpha*	(13)
pACYC177	P15A/ *bla kan*	(14)
pJel109	R1/ *bla*	(68)
pKD46	Rep^{ts}/ *bla* / *exo gam bet araC*	(16)
pAMP1	pSC101/ *bla/ recC-ptr-recB-recD*	(65)
pAMP3	pSC101/ *bla / recC-ptr-recB*	(65)
pAMP5	pSC101/ *bla / recC-ptr-recB*-recD*	(65)
pAMP7	pSC101/ *bla / recC-ptr-recB^{1080}-recD*	(65)
pWSK29	pSC101/ *bla*	(65)
pNRK416	/ *bla* / *dnaK*	(7)
pMob45	pMob/ *bla* / *dnaK dnaJ*	(7)
pPR1	pBR322 / *bla* / *lacZ alpha dnaA-dnaN*	This study
pPR2	pBR322 / *bla* / *lacZ alpha dnaN-dnaA*	This study
pPR7	pBR322 / *bla* / *lacZ alpha dnaA*	This study
pPR8	pBR322 / *bla* / *lacZ alpha dnaN*	This study
pPR9	pBR322/ *bla* /*dnaA*	This study
pPR10	pBR322/ *bla* /*dnaA46*(Ts)	This study
pPR11	pBR322/ *bla* /hslUV	This study
pMOR1	pJel109/ *bla*/ datA	(68)
pMOR6	P15A/ *bla kan* /*datA*	(68)

5.8 References

1. Ahmer BMM. 2004. Cell-to-cell signalling in *Escherichia coli* and *Salmonella enterica*. *Mol. Microbiol.* 52(4):933–45.

2. Anderson DG, Kowalczykowski SC. 1997. The translocating RecBCD enzyme stimulates recombination by directing RecA protein onto ssDNA in a chi-regulated manner. *Cell*. 90(1):77–86.

3. Atlung T, Clausen ES, Hansen FG. 1985. Autoregulation of the *dnaA* gene of *Escherichia coli* K12. *Mol. Gen. Genet.* 200(3):442–50.

4. Baba T, Ara T, Hasegawa M, Takai Y, Okumura Y, et al. 2006. Construction of Escherichia coli K-12 in-frame, single-gene knockout mutants: The Keio collection. *Mol. Syst. Biol.* 2:2006.0008.

5. Bachmann BJ. 1996. Derivations and genotypes of some mutant derivatives of *Escherichia coli* K-12. *Escherichia coli Salmonella typhimurium Cell. Mol. Biol.*, pp. 2460–2488.

6. Braun RE, O'Day K, Wright A. 1985. Autoregulation of the DNA replication gene dnaA in *E. coli* K-12. *Cell*. 40(1):159–69.

7. Bredèche MF, Ehrlich SD, Michel B. 2001. Viability of *rep recA* mutants depends on their capacity to cope with spontaneous oxidative damage and on the DnaK chaperone protein. *J. Bacteriol.* 183(7):2165–71.

8. Brendler T, Abeles A, Austin S. 1995. A protein that binds to the P1 origin core and the oriC 13mer region in a methylation-specific fashion is the product of the host *seqA* gene. *EMBO J.* 14(16):4083–89.

9. Capaldo FN, Ramsey G, Barbour SD. 1974. Analysis of the growth of recombination-deficient strains of *Escherichia coli* K-12. *J. Bacteriol.* 118(1):242–49.

10. Carr KM, Kaguni JM. 1996. The A184V missense mutation of the *dnaA5* and *dnaA46* alleles confers a defect in ATP binding and thermolability in initiation of *Escherichia coli* DNA replication. *Mol. Microbiol.* 20(6):1307–18.

11. Carr KM, Kaguni JM. 2001. Stoichiometry of DnaA and DnaB protein in initiation at the Escherichia coli chromosomal origin. *J. Biol. Chem.* 276(48):44919–25.

12. Cassler MR, Grimwade JE, Leonard AC. 1995. Cell cycle-specific changes in nucleoprotein complexes at a chromosomal replication origin. *EMBO J.* 14(23):5833–41.

13. Chambers SP, Prior SE, Barstow DA, Minton NP. 1988. The pMTL nic- cloning vectors. I. Improved pUC polylinker regions to facilitate the use of sonicated DNA for nucleotide sequencing. *Gene*. 68(1):139–49.

14. Chang AC, Cohen SN. 1978. Construction and characterization of amplifiable multicopy DNA cloning vehicles derived from the P15A cryptic miniplasmid. *J. Bacteriol.* 134(3):1141–56.

15. Chuang SE, Burland V, Plunkett 3rd G, Daniels DL, Blattner FR. 1993. Sequence analysis of four new heat-shock genes constituting the *hslTS*/*ibpAB* and *hslVU* operons in *Escherichia coli*. *Gene.* 134(1):1–6.

16. Datsenko KA, Wanner BL. 2000. One-step inactivation of chromosomal genes in *Escherichia coli* K-12 using PCR products. *Proc. Natl. Acad. Sci. U. S. A.* 97(12):6640–45.

17. David Lane HE, Denhardt DT. 1975. The *rep* mutation. IV Slower movement of replication forks in *Escherichia coli rep* strains. *J. Mol. Biol.* 97(1):99–112.

18. Dillingham MS, Kowalczykowski SC. 2008. RecBCD enzyme and the repair of double-stranded DNA breaks. *Microbiol. Mol. Biol. Rev.* 72(4):642–71.

19. El-Hajj HH, Zhang H, Weiss B. 1988. Lethality of a *dut* (deoxyuridine triphosphatase) mutation in *Escherichia coli*. *J. Bacteriol.* 170(3):1069–75.

20. Flores MJ, Bierne H, Ehrlich SD, Michel B. 2001. Impairment of lagging strand synthesis triggers the formation of a RuvABC substrate at replication forks. *EMBO J.* 20(3):619–29.

21. Fuller RS, Funnell BE, Kornberg A. 1984. The dnaA protein complex with the *E. coli* chromosomal replication origin (*oriC*) and other DNA sites. *Cell*. 38(3):889–900.

22. Fuller RS, Kornberg A. 1983. Purified dnaA protein in initiation of replication at the *Escherichia coli* chromosomal origin of replication. *Proc. Natl. Acad. Sci. USA.* 80(October):5817–21.

23. Grompone G, Seigneur M, Ehrlich SD, Michel B. 2002. Replication fork reversal in DNA polymerase III mutants of *Escherichia coli*: a role for the beta clamp. *Mol. Microbiol.* 44:1331–39.

24. Guy C, Atkinson J, Gupta MK, Mahdi AA, Gwynn EJ, et al. 2009. Rep provides a second motor at the replisome to promote duplication of protein-bound DNA. *Mol Cell*. 36(4):654–66.

25. Hansen FG, Atlung T. 2018. The DnaA tale. *Front. Microbiol.* 9(FEB):1–19.

26. Hansen FG, Koefoed S, Atlung T. 1992. Cloning and nucleotide sequence determination of twelve mutant *dnaA* genes of *Escherichia coli*. *Mol. Gen. Genet.* 234(1):14–21.

27. Helmstetter CE. 1967. Rate of DNA synthesis during the division cycle of *Escherichia coli* B/r. *J. Mol. Biol.* 24(3):417–27.

28. Helmstetter CE, Cooper S. 1968. DNA synthesis during the division cycle of rapidly growing *Escherichia coli* B/r. *J. Mol. Biol.* 31(3):507–18.

29. Hupp TR, Kaguni JM. 1993. Activation of mutant forms of DnaA protein of *Escherichia coli* by DnaK and GrpE proteins occurs prior to DNA replication. *J. Biol. Chem.* 268(18):13143–50.

30. Hwang DS, Kaguni JM. 1988. Interaction of dnaA46 protein with a stimulatory protein in replication from the *Escherichia coli* chromosomal origin. *J. Biol. Chem.* 263(22):10633–40.

31. Ishida T, Akimitsu N, Kashioka T, Hatano M, Kubota T, et al. 2004. DiaA, a novel DnaA-binding protein, ensures the timely initiation of *Escherichia coli* chromosome replication. *J. Biol. Chem.* 279(44):45546–55.

32. Iwasaki H, Takahagi M, Shiba T, Nakata A, Shinagawa H. 1991. *Escherichia coli* RuvC protein is an endonuclease that resolves the Holliday structure. *EMBO J.* 10(13):4381–89.

33. Karu AE, MacKay V, Goldmark PJ, Linn S. 1973. The RecBC deoxyribonuclease of *Escherichia coli* K-12. Substrate specificity and reaction intermediates. *J. Biol .Chem.* 248(14):4874–84.

34. Katayama T, Kubota T, Kurokawa K, Crooke E, Sekimizu K. 1998. The initiator function of DnaA protein is negatively regulated by the sliding clamp of the *E. coli* chromosomal replicase. *Cell*. 94(1):61–71.

35. Katayama T, Kubota T, Takata M, Akimitsu N, Sekimizu K. 1996. Disruption of the *hslU* gene, which encodes an ATPase subunit of the eukaryotic 26S proteasome homolog in *Escherichia coli*, suppresses the temperature-sensitive *dnaA46* mutation. *Biochem. Biophys. Res. Commun.* 229(1):219–24.

36. Kato JI, Katayama T. 2001. Hda, a novel DnaA-related protein, regulates the replication cycle in *Escherichia coli*. *EMBO J.* 20(15):4253–62.

37. Kelman Z, O'Donnell M. 1995. DNA polymerase III holoenzyme: Structure and function of a chromosomal replicating machine. *Annu. Rev. Biochem.* 64:171–200.

38. Khan SR, Kuzminov A. 2012. Replication forks stalled at ultraviolet lesions are rescued via RecA and RuvABC protein-catalyzed disintegration in *Escherichia coli*. *J. Biol. Chem.* 287(9):6250–65.

39. Kitagawa R, Mitsuki H, Okazaki T, Ogawa T. 1996. A novel DnaA protein-binding site at 94.7 min on the *Escherichia coli* chromosome. *Mol. Microbiol.* 19(5):1137–47.

40. Kitagawa R, Ozaki T, Moriya S, Ogawa T. 1998. Negative control of replication initiation by a novel chromosomal locus exhibiting exceptional affinity for *Escherichia coli* DnaA protein. *Genes Dev.* 12(19):3032–43.

41. Klein HL, Bačinskaja G, Che J, Cheblal A, Elango R, et al. 2019. Guidelines for DNA recombination and repair studies: Cellular assays of DNA repair pathways. *Microb. Cell*. 6(1):1–64.

42. Konopa G, Szalewska-Palasz A, Schmidt A, Śrutkowska S, Messer W, Węgrzyn G. 1999. The presence of two DnaA-binding sequences is required for an efficient interaction of the *Escherichia coli* DnaA protein with each particular weak DnaA box region. *FEMS Microbiol. Lett.* 174(1):25–31.

43. Kouzminova E, Kuzminov A. 2006. Fragmentation of replicating chromosomes triggered by uracil in DNA. *J. Mol. Biol.* 355(1):20–33.

44. Kouzminova EA, Kadyrov FF, Kuzminov A. 2017. RNase HII saves *rnhA* mutant *Escherichia coli* from R-Loop-associated chromosomal fragmentation. *J. Mol. Biol.* 429(19):2873–94.

45. Kouzminova EA, Kuzminov A. 2004. Chromosomal fragmentation in dUTPase-deficient mutants of *Escherichia coli* and its recombinational repair. *Mol. Microbiol.* 51(5):1279–95.

46. Kouzminova EA, Rotman E, Macomber L, Zhang J, Kuzminov A. 2004. RecA-dependent mutants in *Escherichia coli* reveal strategies to avoid chromosomal fragmentation. *Proc. Natl. Acad. Sci. USA.* 101(46):16262–67.

47. Kuong KJ, Kuzminov A. 2012. Disintegration of nascent replication bubbles during thymine starvation triggers RecA- and RecBCD-dependent replication origin destruction. *J. Biol. Chem.* 287(28):23958–70.

48. Kushner SR. 1974. Differential thermolability of exonuclease and endonuclease activities of the recBC nuclease isolated from thermosensitive recB and *recC* mutants. *J. Bacteriol.* 120(3):1219–22.

49. Kuzminov A. 1999. Recombinational repair of DNA damage in *Escherichia coli* and bacteriophage lambda. *Microbiol. Mol. Biol. Rev.* 63(4):751–813.

50. Kuzminov A. 2011. Homologous Recombination—Experimental Systems, Analysis, and Significance. *EcoSal Plus*. 4(2):1–43.

51. Langer U, Richter S, Roth A, Weigel C, Messer W. 1996. A comprehensive set of DnaA-box mutations in the replication origin, oriC, of *Escherichia coli*. *Mol. Microbiol.* 21:301–11.

52. Larsen RA, Wilson MM, Guss AM, Metcalf WW. 2002. Genetic analysis of pigment biosynthesis in Xanthobacter autotrophicus Py2 using a new, highly efficient transposon mutagenesis system that is functional in a wide variety of bacteria. *Arch. Microbiol.* 178(3):193–201.

53. Lloyd RG, Buckman C. 1991. Genetic analysis of the *recG* locus of *Escherichia coli* K-12 and of its role in recombination and DNA repair. *J. Bacteriol.* 173(3):1004–11.

54. Lu M, Campbell JL, Boye E. 1994. SeqA: a negative modulator of replication initiation in *E. coli*. *Cell*. 77(3):413–26.

55. Lu YB, Ratnakar PV, Mohanty BK, Bastia D. 1996. Direct physical interaction between DnaG primase and DnaB helicase of *Escherichia coli* is necessary for optimal synthesis of primer RNA. *Proc. Natl. Acad. Sci. USA*. 93(23):12902–7.

56. Maaloe O, Hanawalt PC. 1961. Thymine deficiency and the normal DNA replication cycle. I. *J. Mol. Biol.* 3:144–55.

57. Margulies C, Kaguni JM. 1996. Ordered and sequential binding of DnaA protein to *oriC*, the chromosomal origin of *Escherichia coli*. *J. Biol. Chem.* 271(29):17035–40.

58. Marszalek J, Kaguni JM. 1994. DnaA protein directs the binding of DnaB protein in initiation of DNA replication in *Escherichia coli*. *J. Biol. Chem.* 269(7):4883–90.

59. Merrikh H, Zhang Y, Grossman AD, Wang JD. 2012. Replication-transcription conflicts in bacteria. *Nat. Rev. Microbiol.* 10(7):449–58.

60. Michel B, Boubakri H, Baharoglu Z, LeMasson M, Lestini R. 2007. Recombination proteins and rescue of arrested replication forks. *DNA Repair (Amst).* 6(7):967–80.

61. Michel B, Ehrlich SD, Uzest M. 1997. DNA double-strand breaks caused by replication arrest. *EMBO J.* 16(2):430–38.

62. Michel B, Sinha AK, Leach DRF. 2018. Replication fork breakage and restart in *Escherichia coli*. *Microbiol. Mol. Biol. Rev.* 82(3):1–19.

63. Miller D, Grimwade J, Betteridge T, Rozgaja T, Torque J, Leonard AC. 2009. Bacterial origin recognition complexes direct assembly of higher-order DnaA oligomeric structures. *Proc. Natl. Acad. Sci. USA*. 106(44):18479–84.

64. Miller JH. 1972. Experiments in Molecular Genetics. , p. 466. Cold Spring Harbor, NY: Cold Spring Harbor Laboratory Press.

65. Miranda A, Kuzminov A. 2003. Chromosomal lesion suppression and removal in Escherichia coli via linear DNA degradation. *Genetics*. 163(4):1255–71.

66. Missiakas D, Schwager F, Betton J, Georgopoulos C, Raina S. 1996. Identification and charecterization of HslV HslU (ClpQ ClpY) proteins involved in overall proteolysis of misfolded proteins in *Escherichia coli*. *EMBO J.* 15(24):6899–6909.

67. Molina F, Skarstad K. 2004. Replication fork and SeqA focus distributions in *Escherichia coli* suggest a replication hyperstructure dependent on nucleotide metabolism. *Mol. Microbiol.* 52(6):1597–1612.

68. Morigen, Boye E, Skarstad K, Lobner-Olesen A. 2001. Regulation of chromosomal replication by DnaA protein availability in *Escherichia coli*: Effects of the datA region. *Biochim. Biophys. Acta - Gene Struct. Expr.* 1521(1–3):73–80.

69. Morohoshi T, Maruo T, Shiari Y, Kato J, Ikeda T, et al. 2002. Accumulation of inorganic polyphosphate in *phoU* mutants of *Escherichia coli* and *Synechocystis sp.* strain PCC6803. *Appl. Environ. Microbiol.* 68(8):4107–10.

70. Ohmori H, Kimura M, Nagata T, Sakakibara Y. 1984. Structural analysis of the *dnaA* and *dnaN* genes of *Escherichia coli*. *Gene*. 28:159–70.

71. Rao TVP, Kuzminov A. 2019. Sources of thymidine and analogs fueling futile damage-repair cycles and ss-gap accumulation during thymine starvation in *Escherichia coli*. *DNA Repair (Amst).* 75:1–17.

72. Rinken R, Thoms B, Wackernagel W. 1992. Evidence that *recBC*-dependent degradation of duplex DNA in *Escherichia coli recD* mutants involves DNA unwinding. *J. Bacteriol.* 174(16):5424–29.

73. Rizzitello A, Harper JR, Silhavy TJ. 2001. Genetic evidence for parallel pathways of chaperone activity in the periplasm of Escherichia coli. *J. Bacteriol.* 183(23):6794–6800.

74. Rothstein R, Michel B, Gangloff S. 2000. Replication fork pausing and recombination or “gimme a break”. *Genes Dev.* 14:1–10.

75. Rotman E, Khan SR, Kouzminova EA, Kuzminov A. 2014. Replication fork inhibition in *seqA* mutants of *Escherichia coli* triggers replication fork breakage. *Mol. Microbiol.* 93(1):50–64.

76. Rudolph CJ, Upton AL, Stockum A, Nieduszynski CA, Lloyd RG. 2013. Avoiding chromosome pathology when replication forks collide. *Nature*. 500:608–11.

77. Sakakibara Y, Mizukami T. 1980. A temperature-sensitive *Escherichia coli* mutant defective in DNA replication: *dnaN*, a new gene adjacent to the *dnaA* gene. *Mol. Gen. Genet.* 178(3):541–53.

78. Samitt CE, Hansen FG, Miller JF, Schaechter M. 1989. In vivo studies of DnaA binding to the origin of replication of *Escherichia coli*. *EMBO J.* 8(3):989–93.

79. Schaus N, O'Day K, Peters W, Wright A. 1981. Isolation and characterization of amber mutations in gene *dnaA* of *Escherichia coli* K-12. *J. Bacteriol.* 145(2):904–13.

80. Schmidt R, Bukau B, Mogk A. 2009. Principles of general and regulatory proteolysis by AAA+ proteases in *Escherichia coli*. *Res. Microbiol.* 160(9):629–36.

81. Sekimizu K, Bramhill D, Kornberg A. 1987. ATP activates DnaA protein in initiating replication of plasmids bearing the origin of the *E. coli* chromosome. *Cell*. 50(2):259–65.

82. Simmons LA, Felczak M, Kaguni JM. 2003. DnaA Protein of *Escherichia coli*: Oligomerization at the *E. coli* chromosomal origin is required for initiation and involves specific N-terminal amino acids. *Mol. Microbiol.* 49(3):849–58.

83. Sinha AK, Durand A, Desfontaines J-M, Iuechenko I, Auger H, et al. 2017. Division-induced DNA double strand breaks in the chromosome terminus region of *Escherichia coli* lacking RecBCD DNA repair enzyme. *PLoS Genet.* 13(10):e1006895.

84. Skarstad K, Boye E, Steen HB. 2001. Timing of inititaion of chromosome replication in individual *Escherichia coli* cells. *EMBO J.* 183(15):4543–50.

85. Slominska M, Wahl A, Wegrzyn G, Skarstad K. 2003. Degradation of mutant initiator protein DnaA204 by proteases ClpP, ClpQ and Lon is prevented when DNA is SeqA-free. *Biochem J.* 871:867–71.

86. Soltis D, Lehman I. 1983. RecA protein-promoted DNA strand exchange. Stable complexes of RecA protein and single-stranded DNA formed in the presence of ATP and single-stranded DNA binding protein. *J. Biol. Chem.* 257(14):8523–32.

87. Ting H, Kouzminova EA, Kuzminov A. 2008. Synthetic lethality with the *dut* defect in Escherichia coli reveals layers of DNA damage of increasing complexity due to uracil incorporation. *J. Bacteriol.* 190(17):5841–54.

88. Uzest M, Ehrlich SD, Michel B. 1995. Lethality of *rep recB* and *rep recC* double mutants of *Escherichia coli*. *Mol. Microbiol.* 17:1177–88.

89. Vinella D, Brochier-Armanet C, Loiseau L, Talla E, Barras F. 2009. Iron-sulfur (Fe/S) protein biogenesis: Phylogenomic and genetic studies of A-type carriers. *PLoS Genet.* 5(5):e1000497.

90. von Freiesleben U, Krekling M, Hansen F, Lobner-Olesen A. 2000. The eclipse period of *Escherichia coli*. *EMBO J.* 19(22):6240–48.

91. Wahle E, Lasken RS, Kornberg A. 1989. The dnaB-dnaC replication protein complex of *Escherichia coli*. II. Role of the complex in mobilizing dnaB functions. *J. Biol. Chem.* 264(5):2469–75.

92. Waldminghaus T, Weigel C, Skarstad K. 2012. Replication fork movement and methylation govern SeqA binding to the *Escherichia coli* chromosome. *Nucleic Acids Res.* 40(12):5465–76.

93. Wang J, Chen R, Julin DA. 2000. A single nuclease active site of the *Escherichia Coli* RecBCD enzyme catalyzes single-stranded DNA degradation in both directions. *J. Biol. Chem.* 275(1):507–13.

94. Wechsler JA, Gross JD. 1971. Escherichia coli mutants temperature sensitive for DNA synthesis. *Mol. Gen. Genet.* 113:273–84.

95. Weigel C, Schmidt A, Ruckert B, Lurz R, Messer W. 1997. DnaA protein binding to individual DnaA boxes in the *Escherichia coli* replication origin, *oriC*. *EMBO J.* 16(21):6574–83.

96. Whitby MC, Vincent SD, Lloyd RG. 1994. Branch migration of Holliday junctions: identification of RecG protein as a junction specific DNA helicase. *EMBO J.* 13(21):5220–28.

97. Wickner S, Hurwitz J. 1975. Interaction of *Escherichia coli dnaB* and *dnaC(D)* gene products in vitro. *Proc. Natl. Acad. Sci. USA*. 72(3):921–25.

98. Yu M, Souaya J, Julin DA. 1998. Identification of the nuclease active site in the multifunctional RecBCD enzyme by creation of a chimeric enzyme. *J. Mol. Biol.* 283(4):797–808.

99. Yuzhakov A, Kelman Z, O'Donnell M. 1999. Trading places on DNA-a three-point switch underlies primer handoff from primase to the replicative DNA polymerase. *Cell*. 96(1):153–63.

CHAPTER 6: CONCLUSION AND FUTURE DIRECTIONS

6.1 Summary of My Findings

6.1.1 BER is not a major cause of lethality for T-starved strains

Death due to T-starvation has been observed in all forms of life; in fact, several popular anticancer and antibacterial drugs utilize this conserved killing pathway. Interestingly, a lethal response to starvation for an essential nutrient is quite rare in prokaryotes. In *E. coli*, T-starvation begins with a transient stasis (the resistance period), followed by a sudden shift to exponential death, which lasts several hours. The most favored idea to explain this viability loss upon T-starvation has been the futile cycle of repeated uracil incorporation and excision events (1, 10, 14, 18). Surprisingly, this idea was not tested formally in *E. coli* before our work. Contrary to its expectations, we find that repeated uracil incorporation and excision is not a major cause of death, as inactivation of uracil excision in *ung thyA* strain still leads to TLD. Even if we allow a massive and stable uracil incorporation, as seen in the *dut ung thyA* strain, TLD still occurs, although it does become shallower. Thus, it seems that — unless there is an expanded pool of dUTP in the cell and it is allowed stable incorporation – both of which do not happen in *thyA* mutants, TLD kinetics is unperturbed. We also find that stable uracil incorporation does not prevent DNA degradation associated with TLD and only delays it by a couple of hours. We also show that ribouracil incorporation-excision events don't contribute to TLD. Finally, we demonstrate that SSG accumulation correlates with the exponential death phase of TLD.

6.1.2 Internal sources of dT useful during TLD

We hypothesized that the resistance phase of TLD is due to an internal reserve of dT, and once this source is used up, *E. coli* begins losing its viability. We suspected the stable RNA species, tRNA and rRNA, which, respectively, contain either 1 or 2 ribothymidines in their structures as possible sources. We found that both these species of RNA are indeed a source of T late in exponential death phase, but they do not contribute to the maintenance of the resistance phase. T-starvation leads to massive chromosomal fragmentation during the resistance phase, and dT for the maintenance of the resistance phase could be derived by degradation of such broken chromosomal DNA pieces. By inactivating the main DNA degradation pathways, we found that chromosomal DNA degradation does support viability late in the exponential death phase, but not in the resistance phase of TLD. Finally, we identified the dTDP-sugar complexes, which are intermediates in exopolysaccharide capsule synthesis, as the source of dT essential for the resistance phase. Strains that do not produce this intermediate, have the resistance phase reduced, while strains that cannot retrieve dT from these dTDP-sugar conjugates, have no resistance phase, experience hyper-TLD, an immediate and catastrophic chromosomal DNA loss and eventual cell lysis.

6.1.3 DNA degradation is essential in a *dnaA*(Ts) mutant

Our investigation of the synthetic lethal *dnaA*(Ts) *recBC*(Ts), suggests that under nonpermissive conditions this mutant permanently halts its replication activity, while the *dnaA*(Ts) (RecBCD+) mutant pauses replication for a while, but then resumes it and survives under the same conditions. The isolated suppressors of *dnaA*(Ts) *recBC*(Ts)

restored the replication activity. We identified that it is the DNA degradation activity of RecBCD complex that restores viability (and replication) in *dnaA*(Ts) mutant at higher temperatures. Based on our results, we hypothesize that, as temperature increases, the DnaA(Ts) protein binds to DNA tightly and blocks the progress of replication forks, causing their regression. We further hypothesize that regressed forks are restored by the RecBCD activity and recharged by the Rep helicase, which removes the DnaA(Ts) block. The block removal frees DnaA(Ts) from the chromosomal DNA and makes more of it available for interactions with *oriC*, improving replication initiation.

6.2 Future Directions

6.2.1 Measure dUTP levels in the cell

Our genetic studies suggest that repeated uracil incorporation excision events is not the major driver of TLD. One argument cited in support of the futile uracil incorporation-excision cycle is that limited dTTP concentrations cause an increase in the cellular dUTP levels, as the enzyme Dcd (deoxycytidine deaminase), which is the main source of dUTP in *E. coli*, is not inhibited by dTTP anymore (2). dUTP levels are undetectable in normal conditions (3, 4) and it is not known whether dUTP accumulates to a significant level in T-starved bacteria. Although stable uracil incorporation doesn't prevent TLD in *thyA* mutants, we detect an increased density of uracil in DNA during TLD. Is this increase due to increased dUTP levels in the cell? Or lack of dTTP promotes dUTP incorporation even when its levels are undetectable by physical techniques?

6.2.2 Detection of DNA lesions on T-starved chromosomes

The distinct roles of the two recombinational repair pathways during TLD is now well established by several recent studies on the kinetics of TLD in various DNA repair mutants (7, 8, 16, 17). They found that double strand break repair is essential to maintain the resistance phase, while single-strand gap repair exacerbates the RED phase. In our study, we further show that double strand breaks can be detected only during the resistance phase, while accumulation of persistent single strand gaps correlates with the exponential death phase (23). The steeper death in the *recBCD thyA* mutant suggests additional DNA breaks during the RED phase, but our measurements of chromosomal fragmentation by pulsed field gel electrophoresis (PFGE) failed to revel additional fragmentation in the *recBCD thyA* strain. This is truly puzzling and does not help to explain why the *recBCD thyA* mutant dies faster and deeper than *thyA* mutant.

One reason for our inability to detect additional chromosomal fragmentation in the *recBCD thyA* mutant is a possibility that the DNA lesions are not simple breaks in the chromosome, which produce sub-chromosomal DNA fragments, making them detectable by PFGE (15). Instead, there could be accumulation of σ replicating chromosome structures. Careful isolation of DNA from cells undergoing T-starvation could be used to visualize σ-replicating structures in plasmids isolated from *recBCD thyA* mutant via electron microscopy but their quantification may prove difficult. Since PFGE allows detection of only linear broken DNA, digesting DNA with enzymes that specifically attacks the branched DNA of σ-replicating structures or linked chromosome may detect additional "linear" DNA. Also, ss-gaps accumulating in the *thyA* strain apparently are not converted into DNA breaks detectable by PFGE. The toxic

recombination structures created by RecF on such ss-gaps needs visual examination or probing by branched DNA-targeting enzymes, as suggested above.

6.2.3 Development of other assays to detect SSG

Genetic studies predicted the existence of persistent ss-gaps in the chromosome of T-starved cells, and we developed an assay based upon the ratio of signals obtained from Southern hybridization of non-denatured versus denatured DNA with whole genome probe, to detect and quantify such gapped intermediates. Development of other assays that can detect SSG will help verify our findings. For example, treatment of DNA isolated from T-starved strains in agarose plugs with enzymes that specifically attack ss-DNA (like S1 nuclease), with subsequent separation in PFGE could be another useful way to estimate the single-strandedness of the genome.

6.2.4 Loss of the terminus region

Another reason contributing to the poor survival of *recBCD thyA* mutants is the greater loss of the terminus compared to the *thyA* strain, as observed in the marker-frequency analysis (17, 23). The terminus have the lowest copy number in growing cells (close to 1), so any DNA lesion or loss of this region is irreparable by homologous recombination. The loss of the terminus in *recBCD* mutants is also seen in Thy+ conditions, and the chromosome segregation studies suggest that the division septum chops the tail of the unresolved sigma-structure that is being segregated away from the circular chromosome into one of the new daughter cells (25). This terminus loss is avoided by blocking cell division. Cell division is completely inactivated during TLD, so

the source of additional DNA loss in the terminus is unclear. The complex of Tus protein with the *ter* sites (present on both arms of the chromosome) allow passage of replication forks only in one direction and not the reverse direction, restricting the two replisomes to meet in the broad chromosomal region flanked by the oppositely oriented *ter* sites (6, 21). To investigate terminus DNA loss during TLD, one can start with inactivating Tus and measuring the terminus loss without replication fork termination. This can be tested by looking at deep sequencing profiles in *tus thyA* and *recBCD tus thyA* strains. Also, terminus DNA loss should be tested for its replication-dependence.

6.2.5 Detection of stalled replication forks during TLD

The rate of replication is reduced to 10% of the normal rate within 30 minutes of T-starvation and continues to go down later on (17). At the same time, there is over-initiation at the origin, which is especially conspicuous in the *thyA recA* mutants (17). The reduced replication rates in combination with over-initiation predicts accumulation of stalled replication forks around *oriC*, which was indeed detected by 2D agarose gel electrophoresis (19). However, DNA repair mutants have not been examined using this method, which may provide additional insights into the deeper death of *recBCD thyA* strain and the shallow deaths of *recA thyA* and *recF thyA* strains compared to the parent *thyA* strain. Using plasmids with *oriC* we may find that the *recA thyA* and *recF thyA* mutants show a strong signal corresponding to a preserved (multi-fork) replication bubble around the origin while the *recBCD thyA* strain shows signals corresponding to sigma replicating structures.

6.2.6 Mapping RecA and RecF interaction sites on the chromosome

Sequencing the genomes of T-starved cultures have shown progressive loss of *oriC* and the region around it in the *thyA* strain (17, 24). Apart from this, measuring the amounts of total DNA and amounts of specific regions like *oriC* and *ter* in the population have made it clear that there might be genome-wide DNA loss during T-starvation (23). The mechanism of this DNA loss is unclear at present, although complete preservation of *oriC* in *recA* (17) mutants and higher accumulation of DNA in *recF* mutants (23) before DNA degradation sets in, points to the action of RecA and RecF in DNA destabilization. Mapping RecA's interaction by ChIP-seq method on the chromosome during TLD, in *thyA* versus *thyA recF* mutants, could be crucial in identifying the spots where RecF initiates, and RecA promotes, the toxic recombination.

6.2.7 What is the source of SOS in non-replicating strains?

Persistent SOS induction promoted by RecF action is one of proposed mechanisms of TLD (7). Slow but continuous replication during TLD is thought to be the source of ss-gaps which RecF utilizes to induce SOS continuously. But recent work presented in this report shows SOS induction and chromosome destabilization happen even in the absence of replication in T-starved cultures (Chapter 3). Is the SOS induction in non-replicating cells generated by spontaneous DNA breaks, which are then processed by RecBCD? Does RecF have an independent role in inducing SOS in non-replicating cells? These questions can be answered by measuring SOS levels in *recBCD thyA* and *recF thyA* strain in non-replicating cells.

DNA degradation is also observed (in fact, it is increased) in non-replicating cells, which suggests replication-independent mechanism for triggering DNA breaks in the cell. This may also be responsible for the loss of terminus seen in replicating T-starved strains, one of the least replicated regions of the chromosomes. Deep sequencing may be able to tell the precise chromosomal locations where this DNA loss is initiated.

6.2.8 Isolation of suppressors

The replication-independence of TLD has come as a great surprise to the researchers in the field, as all current models to explain TLD have replication as the basis of lethal DNA lesion (1, 13, 14). This however does not mean that replication does not contribute to the pathology of TLD, — only that it is not sufficient for the killing. The role of replication is still worth pursuing in replicating cells, but it is more important now to explore TLD mechanisms in non-replicating cells.

Our study shows that the LMW dTDP-sugars of the exopolysaccharide capsule synthesis pathway are the reserve of much-needed dT during T-starvation. Moreover, we identified two classes of mutants that affect the dTDP-sugar pool size and the viability of cells during T-starvation: a) mutants which do not synthesize dTDP-sugars and experience the same or slightly deeper TLD (*rfbA rffH thyA* mutants); b) mutants that cannot retrieve dT from the dTDP-sugar conjugates and show hyper TLD (*rffC thyA* and *rffT thyA* mutants). Since TLD can happen in the absence of replication, is there another essential process that requires dT?

The *rffC thyA* (and *rffHC thyA*) mutant described in this report has one of the most severe TLD kinetics along with the previously known hyper-TLD of *recBCD thyA*.

One could isolate suppressors of this severe lethality, to try and identify replication-independent functions that contribute to TLD. For example, the *rffC thyA* mutant lyses and rapidly degrades its DNA, and the reason for both events is unknown. An effort to isolate suppressors of "standard" TLD in *thyA* mutant is also underway in this lab.

6.2.9 Role of non-metabolized dTDP-sugar intermediate in TLD

Theoretically, both classes of mutants mentioned above should have similar sensitivity to T-starvation because they are both either missing or are unable to access an additional source of dT. But the differential effects in these two classes suggest that the irretrievable form of dT, accumulating in class 'b', could be toxic for the cell. Formally, in class ‘b’ mutants, either the interrupted antigen synthesis (arrest at the ECA lipid II intermediate) or the presence of non-metabolizable dTDP-sugar could be problematic for the cell. Plating of the strains on LB + dT shows that both classes of mutants grow without any defect in the presence of dT. In other words, both the interrupted antigen synthesis, as well as accumulation of non-metabolizable dTDP-sugar intermediates, are well-tolerated if dT is available. Since class ‘a’ mutant also have interrupted antigen synthesis, it seems that the presence of unusable dTDP-sugar is toxic for the cell. We haven’t specifically identified the composition of this toxic dTDP-sugar complex, though the literature suggests it is dTDP-4-amino-4,6-dideoxy-α-D-galactose (), and it is not known why this metabolite should be toxic in T-starved strains. It would be informative to catalogue the various dTDP-sugar species in the cell and identify the toxic ones.

6.2.10 Role of ECA lipid II and loss of antigen layer in TLD

Mutants that accumulate the ECA lipid II intermediate, have cell shape defects, — apparently because they hoard the UndP handle in the inner membrane in a non-productive state when it is required for synthesis of other cell envelope structures (12). Accumulation of the ECA lipid II intermediate may also be responsible for the cell lysis we encounter in *rffHC thyA* mutant. This has been partially tested by preventing initiation of ECA synthesis, as described above by using *rfe thyA* mutant in which UndP is not trapped, and we see that hyper TLD is averted (Chapter 3, Fig. 3.14C). But a more definitive test will be to see if *rfe* inactivation suppresses the extreme phenotypes of *rffC thyA* by preventing build-up of ECA intermediates. Additionally, UndP overexpression in hyper-TLD mutants may restore the normal TLD kinetics. Since in the presence of dT we do not see any effect of either ECA interruption or dTDP-sugar intermediate accumulation, it can be argued that either dT inhibits the activity of the enzymes that generates the ECA intermediate, or dT itself plays a role in the cell envelope maintenance. We have noticed that the *thyA* strains are more sensitive to SDS in the absence of dT, suggesting an additional role of dT in the cell envelope maintenance.

The cell membrane has always been assumed to be in contact with the chromosomal DNA at specific sites during the cell cycle – for example, hemi-methylated *oriC* sequence binds to membrane in *E. coli* (22). There is growing evidence that several bacteria including *E. coli* routinely release vesicles containing DNA from their cell surface (26) (Fig. 4.2.). If this mechanism is still active during T-starvation and is known to be more frequent in bacteria with fragile envelopes (26), then this may explain how DNA breaks can happen in the absence of replication. Since there is limited opportunity

to repair chromosomal breaks in the absence of dTTP, this can lead to the gradual chromosomal loss we observe. It can also be imagined that if the nucleoid is held by several protein anchors in the inner membrane, then during filamentation of cells increasing the distance between protein anchors could stretch and eventually break the DNA (proposed in Chapter 3). Currently there is no evidence for the second scenario.

6.2.11 Link between the chromosome damage and the envelope integrity

SOS response causes the cells to filament, while the T-starvation causes inadequate synthesis of exopolysaccharide capsule in such elongating cells, exacerbating their envelope problems. The exopolysaccharide capsule increases the strength of the cell envelope against external insults (5), and its loss may be contributing to lethality. In our visualization of cells using light microscopy and TEM, we find that the *thyA* mutant cells after extended periods of T-starvation develop cellular voids, and TEM images show masses of what looks like the exopolysaccharide capsule layer, separated from cells. Dynamic cellular voids due to retraction and expansion of the cytoplasm were previously observed in *E. coli* mutants with impaired link between the inner and the outer membranes (20). It is possible that the cell filamentation and loss of the exopolysaccharide capsule contributes to the cytoplasm instability leading to the dynamic voids we detect in our images.

The loss of the exopolysaccharide capsule layer may be an artifact of TEM sample preparation procedure, but it does indicate that this layer has become detachable in the absence of dT, as we have not observed such loss in dT-supplemented cells. However, these phenotypes need more systematic investigation using antibodies to detect

the loss of antigen in dT-starved cultures over time. The structures consistent with loss of the exopolysaccharide capsule were also observed in cells treated with nalidixic acid that inhibits DNA gyrase and induces DNA damage through a mechanism different from TLD. This suggests that there may be a general cellular response of envelope deterioration whenever DNA is irreversibly damaged. Other microscopic techniques, like SEM or AFM may give additional information about the cell surface changes during T-starvation.

One key question that arises from these imaging studies is how could DNA damage lead to envelope disintegration?

6.2.12 The role of ROS in TLD

Recent investigations have implicated reactive oxygen species (ROS)-mediated damage in the mechanism of TLD in *thyA* mutants and in the sensitivity of *E. coli* strains treated with trimethoprim (Tmp) (9, 11). We are currently testing these assertions. Our preliminary studies show that inactivation of catalases KatG and KatE, individually or together, fails to make *thyA* strains more susceptible to TLD. Additionally, adding hydrogen peroxide (the ultimate source of ROS) at the beginning of T-starvation extends the resistance phase instead of hastening TLD, as predicted by the above studies. In the future, it would be interesting to see if regular addition of peroxide to dT-starved strains continues to protect the *thyA* strain and maybe even prevent hyper-TLD mutants, like *recBCD thyA* and *rffC thyA*, from losing viability. The study implicating ROS in Tmp sensitivity in *E. coli* was a qualitative comparison of inhibition, done by exposing the bacteria chronically to Tmp on plates (9). It would be more informative to perform a

quantitative study, comparing Tmp-sensitivities of various *E. coli* strains to establish the role of ROS in Tmp action. Since we show that ECA- strains are more sensitive to T-starvation, in the future it would be interesting to verify whether they are also more sensitive to Tmp.

6.2.13 Identify DnaA binding sites on the chromosome

Our work on the *dnaA*(Ts) *recBC*(Ts) lethality suggests that DnaA(Ts) protein binds tighter to its chromosomal sites and blocks the progress of replication forks. However, deleting the *datA* site on the *E. coli* chromosome, which has the highest affinity for DnaA-ATP complex did not exacerbate the viability of the double mutant. The proposed tighter binding could be detected by DnaA(Ts) ChIP-sequencing technique, since DnaA is known to bind hundreds of sites around the chromosome.

6.2.14 Why is DnaA(Ts) lethal?

We find that the damage caused of DnaA(Ts) is reversible at 39°C, due to RecBCD functions, but at 42°C its effect is not reversible even in the presence of RecBCD, and the cells eventually die. Since *dnaA* mutants cannot initiate replication, it is unclear why the mutation is not bacteriostatic, but instead kills at the non-permissive temperatures. In the future, it will be interesting to monitor the stability of the chromosomal DNA in the *dnaA*(Ts) mutants at 42°C.

6.3 The Final Word

A cell can be killed in three basic ways: by disrupting its envelope (cell lysis), by stopping its metabolism (metabolic death) or by inactivating its chromosome (genetic death). In contrast to the first two, genetic death has unclear mechanisms and is still underemployed as a target for antibiotics or anti-cancer treatments. Our work contributes to rectifying this situation.

We have presented our investigations in two cases of genetic death – TLD and *dnaA*(Ts) *recBC*(Ts) in this thesis. Our work has identified double strand breaks, ss-gaps and significant DNA loss as the chromosomal problems during TLD. We have not identified any chromosomal lesions in *dnaA recBC* strain, but it seems that a protein bound to DNA could also be a chromosomal lesion, if DNA repair is unavailable. Development of sequencing technology brought a much-required impetus in the TLD field (17, 24). Similarly, new methods and technologies will be useful in probing some new phenotypes associated with TLD, like the misplaced nucleoid in *rffHC thyA* mutants, the link between DNA integrity and cell envelope integrity, and the unexplained DNA loss in the absence of DNA replication.

6.4 References

1. Ahmad SI, Kirk SH, Eisenstark A. 1998. Thymine metabolism and thymineless death in prokaryotes and eukaryotes. *Annu. Rev. Microbiol.* 52:591–625.

2. Beck CF, Eisenhardt AR, Neuhard J. 1975. Deoxycytidine triphosphate deaminase of *Salmonella typhimurium*. *J. Biol. Chem.* 250(2):609–16.

3. Bochner BR, Ames BN. 1982. Complete analysis of cellular nucleotides by two-dimensional thin layer chromatography. *J. Biol. Chem.* 257(16):9759–69.

4. Buckstein MH, He J, Rubin H. 2008. Characterization of nucleotide pools as a function of physiological state in *Escherichia coli*. *J. Bacteriol.* 190(2):718–26.

5. Danese PN, Oliver GR, Barr K, Bowman GD, Rick PD, Silhavy TJ. 1998. Accumulation of the enterobacterial common antigen lipid II biosynthetic intermediate stimulates *degP* transcription in *Escherichia coli*. *J. Bacteriol.* 180(22):5875–84.

6. Duggin IG, Wake RG, Bell SD, Hill TM. 2008. The replication fork trap and termination of chromosome replication. *Mol. Microbiol.* 70:1323–33.

7. Fonville NC, Bates D, Hastings PJ, Hanawalt PC, Rosenberg SM. 2010. Role of RecA and the SOS response in thymineless death in *Escherichia coli*. *PLoS Genet.* 6(3):e1000865.

8. Fonville NC, Vaksman Z, Denapoli J, Hastings PJ, Rosenberg SM. 2011. Pathways of resistance to thymineless death in *Escherichia coli* and the function of UvrD. *Genetics*. 189(1):23–36.

9. Giroux X, Su WL, Bredeche MF, Matic I. 2017. Maladaptive DNA repair is the ultimate contributor to the death of trimethoprim-treated cells under aerobic and anaerobic conditions. *Proc. Natl. Acad. Sci. U. S. A.* 114(43):11512–17.

10. Goulian M, Bleile B, Tseng BY. 1980. The effect of methotrexate on levels of dUTP in animal cells. *J. Biol. Chem.* 255(22):10630–37.

11. Hong Y, Li L, Luan G, Drlica K, Zhao X. 2017. Contribution of reactive oxygen species to thymineless death in *Escherichia coli*. *Nat. Microbiol.* 2(12):1667–75.

12. Jorgenson MA, Kannan S, Laubacher ME, Young KD. 2016. Dead-end intermediates in the enterobacterial common antigen pathway induce morphological defects in *Escherichia coli* by competing for undecaprenyl phosphate. *Mol. Microbiol.* 100(1):1–14.

13. Khan SR, Kuzminov A. 2019. Thymineless death in *Escherichia coli* is unaffected by the chromosomal replication complexity. *J. Bacteriol.* 201(9):1–16.

14. Khodursky A, Guzmán EC, Hanawalt PC. 2015. Thymineless death lives on: New insights into a classic phenomenon. *Annu. Rev. Microbiol.* 69(1):247–63.

15. Klein HL, Bačinskaja G, Che J, Cheblal A, Elango R, et al. 2019. Guidelines for DNA recombination and repair studies: Cellular assays of DNA repair pathways. *Microb. Cell*. 6(1):1–64.

16. Kuong KJ, Kuzminov A. 2010. Stalled replication fork repair and misrepair during thymineless death in *Escherichia coli*. *Genes to Cells*. 15(6):619–34.

17. Kuong KJ, Kuzminov A. 2012. Disintegration of nascent replication bubbles during thymine starvation triggers RecA- and RecBCD-dependent replication origin destruction. *J. Biol. Chem.* 287(28):23958–70.

18. Ladner R. 2001. The role of dUTPase and uracil-DNA repair in cancer chemotherapy. *Curr Protein Pept Sci.* 2(4):361–70.

19. Martín CM, Viguera E, Guzmán EC. 2014. Rifampicin suppresses thymineless death by blocking the transcription-dependent step of chromosome initiation. *DNA Repair (Amst).* 18(1):10–17.

20. Mychack A, Amrutha RN, Chung C, Cardenas Arevalo K, Reddy M, Janakiraman A. 2019. A synergistic role for two predicted inner membrane proteins of *Escherichia coli* in cell envelope integrity. *Mol. Microbiol.* 111(2):317–37.

21. Neylon C, Kralicek AV, Hill TM, Dixon NE. 2005. Replication termination in Escherichia coli: Structure and antihelicase activity of the Tus-Ter complex. *Microbiol. Mol. Biol. Rev.* 69:501–26.

22. Ogden GB, Pratt MJ, Schaechter M. 1988. The replicative origin of the *E. coli* chromosome binds to cell membranes only when hemimethylated. *Cell*. 54(1):127–35.

23. Rao TVP, Kuzminov A. 2019. Sources of thymidine and analogs fueling futile damage-repair cycles and ss-gap accumulation during thymine starvation in *Escherichia coli*. *DNA Repair (Amst).* 75:1–17.

24. Sangurdekar DP, Hamann BL, Smirnov D, Srienc F, Hanawalt PC, Khodursky AB. 2010. Thymineless death is associated with loss of essential genetic information from the replication origin. *Mol. Microbiol.* 75(6):1455–67.

25. Sinha AK, Durand A, Desfontaines J-M, Iuechenko I, Auger H, et al. 2017. Division-induced DNA double strand breaks in the chromosome terminus region of *Escherichia coli* lacking RecBCD DNA repair enzyme. *PLoS Genet.* 13(10):e1006895.

26. Toyofuku M, Nomura N, Eberl L. 2019. Types and origins of bacterial membrane vesicles. *Nat. Rev. Microbiol.* 17(1):13–24.